Handover Mechanisms in 3GPP Long Term Evolution (LTE)

A Thesis
submitted to
University of Technology, Sydney
by

Cheng-Chung Lin

In accordance with
the requirements for the Degree of

Doctor of Philosophy

Faculty of Engineering and Information Technology
University of Technology, Sydney
New South Wales, Australia
August 2013

CERTIFICATE OF AUTHORSHIP/ORIGINALITY

I certify that the work in this thesis has not previously been submitted for a degree nor has it been submitted as part of requirements for a degree except as fully acknowledged with the text.

I also certify that the thesis has been written by me. Any help that I have received in my research work and the preparation of the thesis itself has been acknowledged. In addition, I certify that all information sources and literature used are indicated in the thesis.

Signature of Candidate

_____

ACKNOWLEDGMENT

My Ph.D. supervisor, Assoc. Prof. Dr. Kumbesan Sandrasegaran. I would be lost without his guidance.

Members of my advisory committee: Assoc. Prof. Dr Xinning Zhu and Dr Xiaoying Kong.

Centre for Real-time Information Networks (CRIN) for the facilities and services that were made available during my Ph.D. study.

My close friends and all CRIN members for their friendly support and caring.

My family for the encouragement, it would have been impossible for me to complete this research work without their encouragement.

And most importantly, my girlfriend, Wen-Yu Liao, for the support, patience, and understanding I needed to get through this experience.

Last, but not least, my joy in our family: Bun and Dumpling.

ABSTRACT

The Long-Term Evolution (LTE) network is a new radio access technology (RAT) proposed by the Third Generation Partnership Project (3GPP) to provide a smooth migration towards the fourth generation (4G) network. Long Term Evolution-Advanced (LTE-A) is a major enhancement of the LTE standard proposed by the 3GPP to meet the 4G mobile communication standards.

Handover is one of the key components in cellular network mobility management. Handover is a mechanism that transfers an on-going call or data session from one base station (BS) to another BS or one sector to another sector within the same BS. Hard handover has been adopted in LTE and LTE-A systems by 3GPP due to the flat IP-based architecture and the lack of a centralized controller. The use of hard handovers reduces the complexity of the handover mechanism and minimizes the handover delay. However, the hard handover approach causes call drops that may result in lost data during a session. The objective of this thesis is to provide the basis for improving handover performance in the LTE and LTE-A systems.

A C++ system level simulator that can dynamically model the large and complex downlink LTE and LTE-A was developed as part of this research work followed by a proposed handover parameters optimization method. The simulation results show that the handover parameters optimization method can effectively minimize the unnecessary number of handovers while maximizing the system throughput.

Under an initial assumption of an ideal mobile cellular channel (i.e. the mobile cellular channel is not subject to any impairment), this thesis proposes a new handover algorithm in the LTE system and three new Coordinated Multiple Transmission and Reception (CoMP) handover algorithms in the LTE-A system. The simulation results show that the proposed handover algorithm outperforms well-known handover algorithms in the LTE system by having less number of handovers, shorten total system delay whilst maintaining a higher total system throughput. The performance of the proposed CoMP handover algorithms are evaluated and compared with open literature CoMP handover algorithm via simulation. It is shown via simulation that the proposed

CoMP handover algorithms can improve the system throughput and minimize the system delay in a saturated system scenario in the LTE-A system.

A more practical LTE-A system where the mobile cellular channels are subject to impairments is considered for performance testing of selected CoMP handover algorithms. The impairments for a practical LTE-A system are assumed to be in two scenarios: outdated feedback and missing feedback. It is shown via computer simulations that the system throughput and system delay are very sensitive against outdated Channel Quality Information (CQI) feedback and missing CQI feedback. Furthermore, a handover failure caused by an inappropriate feedback increases the number of unnecessary handovers which require additional resources in the network and may significantly degrade the system performance.

TABLE OF CONTENTS

LIST OF FIGURES

LIST OF TABLES

LIST OF ACRONYMS

1G	First Generation
2G	Second Generation
3G	Third Generation
3GPP	Third Generation Partnership Project
4G	Fourth Generation
ACK	Acknowledgement
AMC	Adaptive Modulation and Coding
AMPS	Analogue Mobile Phone System
BBC	Break-Before-Connect
BER	Bit Error Rate
BLER	Block Error Rate
BS	Base Station
CA	Carrier Aggregation
CBB	Connect-Before-Break
CBR	Constant Bit Rate
CBTC	Communication Based Train Control
CC	Chase Combining
CCS	CoMP Coordinating Set
CCSn	Central Control Station
CS	Cell Selection
CS/CB	Coordinated Scheduling / Beamforming
CSI	Channel State Information
CTS	Cooperative Transmission Set
CTP	CoMP Transmission Point
CDF	Cumulative Distribution Function
CDMA	Code Division Multiple Access
CoMP	Coordinated Multiple Point
CP	Cyclic Prefix
CQI	Channel Quality Information

CRC	Cyclic Redundancy Check
DL	Downlink
DSSS	Direct Sequence Spread Spectrum
EDGE	Enhanced Data Rates for GSM Evolution
E-UTRAN	Evolved Universal Terrestrial Radio Access Network
eNB/eNodeB	Enhanced Node B
EPC	Evolved Packet Core
EPS	Evolved Packet System
FIFO	First-In-First-Out
FDD	Frequency Division Duplex
FDMA	Frequency Division Multiple Access
GBR	Guaranteed Bit Rate
GPRS	General Packet Radio Services
GSM	Global System for Mobile Communication
GTP	GPRS Tunnelling Protocol
HARQ	Hybrid Automatic Repeat Request
Hata	Okumura-Hata
HOA	Handover Algorithm
HOL	Head-of-Line
HSDPA	High-Speed Downlink Packet Access
HSPA+	High-Speed Packet Access+
HSUPA	High-Speed Uplink Packet Access
IEEE	Institute of Electrical and Electronics Engineers
IMT-Advanced	International Mobile Telecommunications Advanced
IP	Internet Protocol
IR	Incremental Redundancy
ISI	Inter-Symbol Interference
ITU	International Telecommunication Union
ITU-R	International Telecommunication Union – Radiocommunication
JP	Joint Processing
JTACS	Japanese Total Access Communications System
LHHAARC	LTE Hard Handover Algorithm with Average RSRP Constraint

LTE	Long Term Evolution
LTE-A	Long Term Evolution - Advanced
MAC	Medium Access Control
Max-Rate	Maximum Rate
MCS	Modulation and Coding Scheme
MIMO	Multiple-Input Multiple-Output
MME	Mobility Management Entity
MRS	Mobile Relay Station
MS	Mobile Station
MSE	Mean Square Error
NACK	Negative Acknowledgement
NMT	Nordic Mobile Telephone
NRT	Non Real-Time
OFDM	Orthogonal Frequency Division Multiplex
OFDMA	Orthogonal Frequency Division Multiple Access
P-GW	Packet Gateway
PAPR	Peak-to-Average Power Ratio
PDC	Personal Digital Communications
PDF	Probability Distribution Function
PDSCH	Physical Downlink Shared Channel
PDN	Packet Data Network
PF	Proportional Fair
PHS	Personal Handy-phone System
PHY	Physical
PLR	Packet Loss Ratio
PRB	Physical Resource Block
QAM	Quadrature Amplitude Modulation
QCI	QoS Class Identifier
QoS	Quality of Service
QPSK	Quadrature Phase Shift Keying
RACH	Random Access Channel
RAT	Radio Access Technology

RB	Resource Block
RE	Resource Element
RLC	Radio Link Control
RLF	Radio Link Failure
RNC	Radio Network Controller
RR	Round Robin
RRC	Radio Resource Control
RRM	Radio Resource Management
RSRP	Reference Signal Received Power
RSS	Received Signal Strength
RT	Real-Time
S-GW	Serving Gateway
SAW	Stop-and-Wait
SC-FDMA	Single Carrier-Frequency Division Multiple Access
SINR	Signal-to-Interference-plus-Noise-Ratio
SSDT	Site Selection Diversity Technique
SSHO	Semi-Soft Handover
TACS	Total Access Communications System
TAU	Tracking Area Update
TB	Transport Block
TDD	Time Division Duplex
TDMA	Time Division Multiple Access
TPS	Transmission Point Selection
TSN	Transmission Sequence Number
TTI	Transmission Time Interval
UE	User Equipment
UL	Uplink
UMTS	Universal Mobile Telecommunications System
UTRAN	Universal Terrestrial Radio Access Network
VoIP	Voice over IP
WCDMA	Wideband Code Division Multiple Access
WiMAX	Worldwide Interoperability for Microwave Access

LIST OF SYMBOLS

α	Proposed parameter in LTE Integrator Handover Algorithm
β	Forgetting factor proposed in RSS Based TTT Window Handover Algorithm
γ	A decimal constant factor proposed in Capacity Integrated CoMP Handover Algorithm
σ	Shadow fading standard deviation
$\sigma_{\mu 0}$	Variance (mean power)
$\mu\_ap_i(t)$	Approximated uncorrelated filtered white Gaussian noise with zero mean of process i at time t
$\mu_i(t)$	Priority of user i at scheduling interval t
μ_n	Uncorrelated filtered white Gaussian noise with zero mean of of the nth sinusoid
$\rho_i(t)$	Shadow fading autocorrelation function,
$\gamma_{i,j}(t)$	Instantaneous SINR of user i on PRB j at time t
$\theta_{i,n}$	Doppler phase of process i of the nth sinusoid
$\zeta(t)$	Frequency flat Rayleigh fading at time t
$\xi_i(t)$	Shadow fading gain of user i at time t
$a(h_m)$	Mobile antenna correction factor
$c_{i,n}$	Doppler coefficient (which represents a real weighting factor) of process i of the nth sinusoid
$Capacity_C(t)$	Capacity indicator of cell c at time t
Capacity Threshold	Decimal constant factor proposed in Capacity Integrated CoMP Handover Algorithm
d_0	Shadow fading correlation distance
$dir_i(t)$	Direction of user i at time t
$\|dis_i(t)\|$	Magnitude of distance of user i from eNB at time t
D_{pc}	Web browsing reading time
$DIFs\_i(t)$	The RSRP difference of the user i at serving cell at time t

$DP_{l,i}(t)$	Delay of the *l*th packet of user *i* at time *t*
$Efficiency_{i,j}(t)$	Efficiency (in bits/RE) of PRB *j* of user *i* at time *t*
f	Frequency of the transmission
$f_{i,n}$	Discrete Doppler frequency of process *i* of the *n*th sinusoid
f_{max}	Maximum Doppler frequency
$FDIFs\_i(t)$	Filtered RSRP difference value of user *i* at serving cell *s* at time *t*
$G(t)$	Gaussian random variable of user *i* at time *t*
$gain_{i,j}(t)$	Channel gain of user *i* on PRB *j* at time *t*
h_b	Height of the eNB
h_m	Height of the user terminal
$HisRButilize_c(t)$	Historical RB utilize value of cell *c* at time *t*
Hys	Hysteresis parameter for handover event
HO_{t_i}	Number of handovers of user *i* at time *t*
ICI	Inter-cell interference
$I_i(t+1)$	Indicator function of the event that packets of user *i* are selected for transmission at scheduling interval *t+1*
J	Total number of PRBs
$loc_i(t)$	Location of user *i* at time *t*
Mn	Measurement result of the neighbouring cell
$mpath_{i,j}(t)$	Multi-path fading gain of user *i* on PRB *j* at time *t*
Ms	Measurement result of the serving cell
N	Total number of users
N_o	Thermal noise
N_d	Number of embedded objects in a web browsing packet call
N_i	Number of sinusoids of process *i*
$N_{service}$	Total number of users of a service
Np	Total number of periods
Ocn	Cell specific offset of the neighbour cell
Ocs	Cell specific offset of the serving cell
Ofn	Frequency specific offset of the neighbour cell frequency
Off	Offset parameter for handover event
Ofs	Frequency specific offset of the serving cell frequency

$pdiscard_{c\_i}(t)$	Total discarded packet size of cell *c* whichever earlier received by UE *i* at time *t*
$pdiscard\_service_i(t)$	Total size of discarded packets (in bits) of user *i* of a service at time *t*
$pl_i(t)$	Path loss of user *i* at time *t*
$prx_i(t)$	Total size of correctly received packets (in bits) of user *i* at time *t*
$psize_{c\_i}(t)$	Total packet size of cell *c* whichever earlier received by UE *i* at time *t*
$psize\_service_i(t)$	Total size of all packets that have arrived into the eNB buffer of user *i* of a service at time *t*
$ptransmit_{c\_i}(t)$	Number of transmitted bits of cell *c* received by UE *i* at time *t*
P_{total}	Total eNB transmit power
$PRBmax_c$	Total PRBs in cell *c*
$PRBuse_c(t)$	Total PRBs being used in cell *c* at time *t*
$r_i(t)$	Instantaneous data rate (across the whole bandwidth) of user *i* at scheduling interval *t*
$R_i(t)$	Average throughput of user *i* at scheduling interval *t*
RB_{max}	Maximum available number of PRBs
$RButilize_c(t)$	RB utilize value of cell *c* at time *t*
RE_{data}	Total number of REs specified for downlink data transmission
$RSRP_{avgS\_i}$	Average RSRP received by user *i* from serving cell *S*
$RSRP_{i,j}(t)$	RSRP of user *i* on PRB *j* at time *t*
$\overline{RSRP}_i(t)$	Average RSRP of user *i* among all PRBs at time *t*
$RSRP_{S\_i}(nTm)$	RSRP received by user *i* from serving cell *S* at *n*th *Tm*
$RSRP_S$	RSRP received from the serving cell
$RSRP_T$	RSRP received from the target cell
$RSRP_{T\_CCS}$	RSRP received from the target cell in the CCS
$RSRP_{T\_CTP}$	RSRP received from the target cell in the CTP
$\overline{RSS}$	Filtered RSS measurement
$\overline{RSS}(nTu)_S$	Filtered RSS of the serving cell at *n*th *Tu*
$\overline{RSS}(nTu)_T$	Filtered RSS of the target cell at *n*th *Tu*

service PLR	PLR of a type of service (either RT or NRT service)
S_E	Web browsing embedded object size
S_M	Web browsing main object size
T	Total simulation time
T_p	Web browsing parsing time
Tm	Handover measurement period
Tu	An integer multiple of Tm
THO	Total number of handovers
$TOA_{l,i}$	Time of arrival of the lth packet of user i in the eNB buffer
$v_i(t)$	Speed of user i at time t
$W_i(t)$	Delay of the HOL packet of user i at time t
X	Resolution in pixel
Y	Resolution in pixel

Chapter 1

INTRODUCTION

The number of the mobile cellular subscribers has explosively grown in the last decade. The International Telecommunication Union (ITU) Statistics shows that there were six billion global mobile cellular subscribers in 2011 and is expected to be more than six billion global mobile cellular subscribers in 2013 as shown in Figure 1.1.

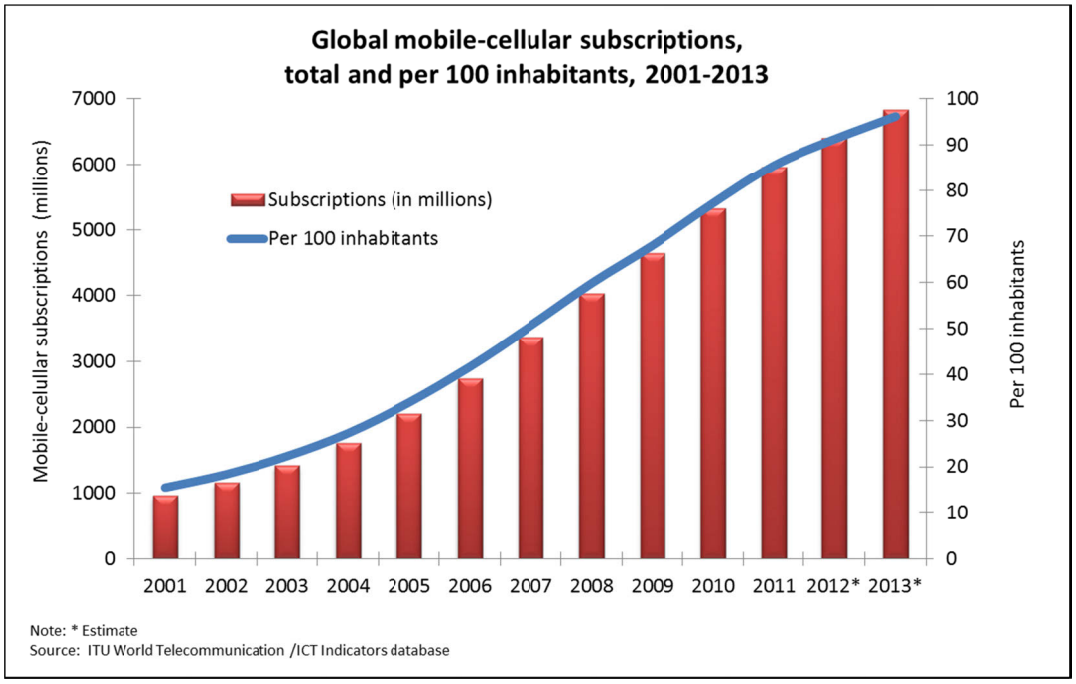

Figure 1.1: Global mobile-cellular subscriptions (2001-2013) [1]

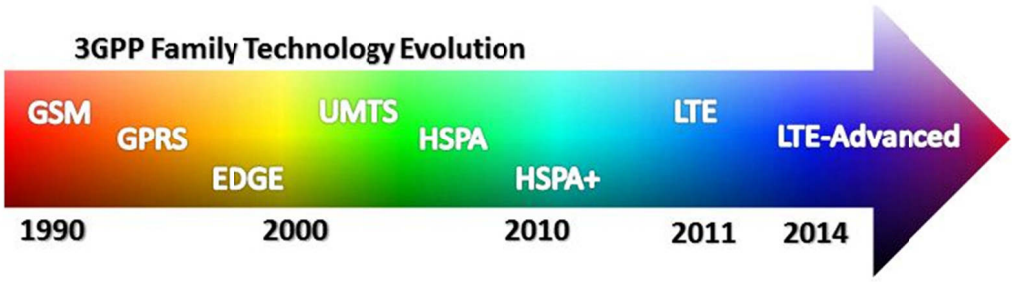

Figure 1.2: 3GPP Family Technology Evolution (1990-2014) [2]

Figure 1.2 shows LTE and LTE-Advanced are parts of the technology evolutionary path beyond third generation (3G) technology, following GSM, GPRS, EDGE, UMTS, HSPA (HSDPA and HSUPA combined) and HSPA Evolution (HSPA+).

The first generation (1G) mobile system based on circuit switch technology was developed in early 1980s. The 1G mobile cellular systems was designed for voice telephony using analogue technology. Frequency Division Multiple Access (FDMA) technology was adopted to combine different telephony channels. There were several different systems in the 1G cellular systems, such as Analogue Mobile Phone System (AMPS) in North America, Nordic Mobile Telephone (NMT) in Scandinavia and some European countries, Japanese Total Access Communications System (JTACS) in Japan, and Total Access Communication System (TACS) used worldwide [3]. The common limitations of 1G cellular systems were inconsistency in voice quality, frequent dropped calls, and inefficient usage of radio spectrum [4].

The second generation (2G) mobile cellular systems based on digital technology was developed in the early 1990s. The 2G mobile cellular systems was designed for better call quality, security and more efficient usage of radio spectrum compared with the 1G systems. A number of multiple access methods were introduced including Time Division Multiple Access (TDMA) and Code Division Multiple Access (CDMA) technologies. Global System for Mobile communications (GSM), Personal Digital Communications (PDC), cdmaOne, and Personal Handy-phone System (PHS) are examples of 2G mobile cellular systems [5].

GSM is by far the most successful commercial mobile cellular system with 80.42% mobile cellular subscribers worldwide in September 2008 [6]. However, due to the increasing demand of the Internet access, these 2G mobile cellular systems, including GSM, could not satisfy the quality of service (QoS) of high-speed multimedia services due to their low data rate (i.e. up to 9.6 kbps) of circuit switched services. Therefore several mobile cellular system enhancements were standardized to overcome the limitations of 2G systems. General Packet Radio Services (GPRS) is a packet-switch based system which was known as 2.5G and it provides significant improvement in data rates compared with 2G mobile cellular systems.

The third generation (3G) mobile cellular system standardized by 3GPP is Universal Mobile Telecommunication System (UMTS). UMTS uses Wideband CDMA (WCDMA) technology based on Direct Sequence Spread Spectrum (DSSS) [7], and it was standardized in 3GPP Release 99 standard. UMTS was designed and deployed to be backward compatible with existing GSM and GPRS systems. A 3G mobile cellular system known as CDMA2000 was introduced by the 3GPP2 organisation and it was backward compatible with the existing cdmaOne system.

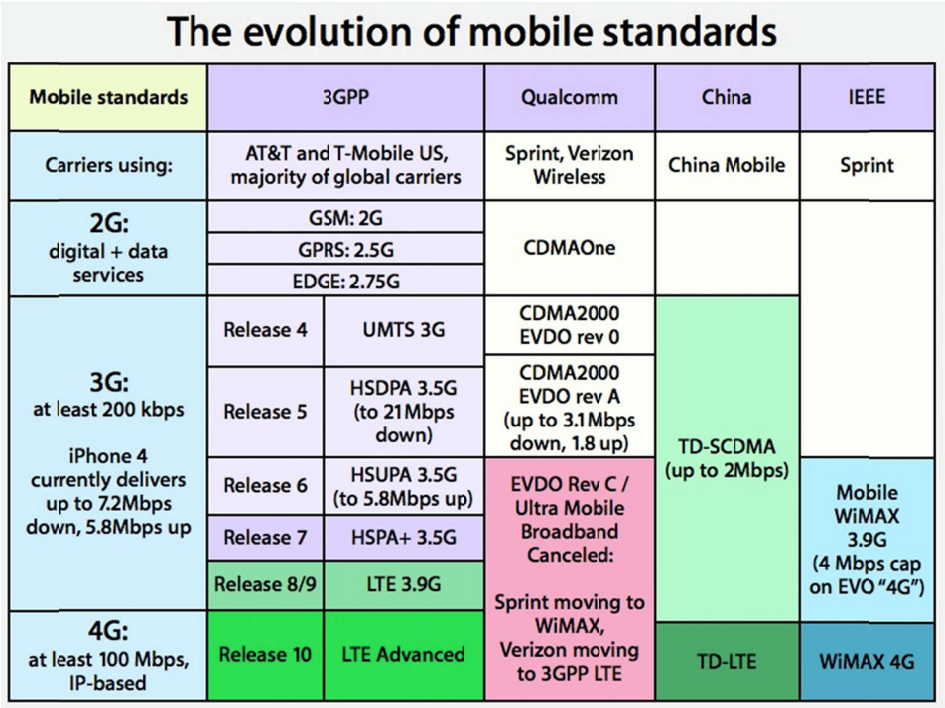

Figure 1.3: Evolution of the mobile cellular systems families [8]

A further step in the 3G mobile cellular system evolution was introduced as High-Speed Downlink Packet Access (HSDPA) system. HSDPA was able to provide a more efficient and reliable quality of communications using Adaptive Modulation and Coding (AMC), packet scheduling and Hybrid Automatic Repeat Request (HARQ). Further enhancement of the HSDPA system was made for the uplink. High-Speed Uplink Packet Access (HSUPA) was standardized in the 3GPP Release 6 standard, High-Speed Packet Access + (HSPA+) was standardized in the 3GPP Release 7 and Release 8 standards.

Figure 1.3 shows the evolution from 2G towards Fourth Generation (4G) mobile cellular systems. Three different organisations: 3GPP, 3GPP2 / Qualcomm, and Institute of Electrical and Electronics Engineers (IEEE) dominate the evolution of the mobile cellular systems shown in Figure 1.3. In the evolution of the mobile cellular systems, 3GPP plays the role of upgrading the mobile cellular systems based on the 2G GSM networks whereas 3GPP2 upgrades the mobile cellular systems based on the 2G cdmaOne networks. IEEE joined the evolution of the mobile cellular systems with introduction of the Worldwide Interoperability for Microwave Access (WiMAX) standard that provides the delivery of last mile wireless broadband access as an alternative to cable and DSL for high-speed multimedia services. Based on GSM network achievement as the most commercially successful 2G mobile cellular system in the world, 3GPP family is consider as the world's leading mobile cellular systems.

The 3G Universal Terrestrial Radio Access Network (UTRAN) network has evolved into the Long-Term Evolution (LTE) network, also known as Evolved UTRAN (EUTRAN). This is a new radio access technology (RAT) proposed by the 3GPP to provide a smooth migration towards fourth generation (4G) network. The first LTE network was launched by TeliaSonera in Oslo and Stockholm on December 14, 2009 [9]. Several key requirements of the LTE standardization include:

1. Ensure competitiveness of the 3GPP family over a long time frame [3]
2. Improve performance and radio spectrum efficiency [10]
3. Reduce the cost of deployment and multimedia delivery [11]

[12] reports that in May 10, 2013, there are 175 LTE commercial networks in 70 countries and 424 operators investing in LTE in 126 countries including 371 operator commitments in 116 countries and 53 pre-commitment trials in 10 more countries worldwide. Figure 1.4 shows that it is forecasted that there will be 248 commercial LTE network launches by the end of 2013. Furthermore, there will be over 32 million worldwide subscriptions of the LTE services by 2013 [13]. However, LTE as specified in the 3GPP Release 8 and 9 document series does not satisfy the technical requirements which were originally set by the International Telecommunication Union – Radiocommunication sector (ITU-R) organization in its International Mobile Telecommunications Advanced (IMT-Advanced) specification [14].

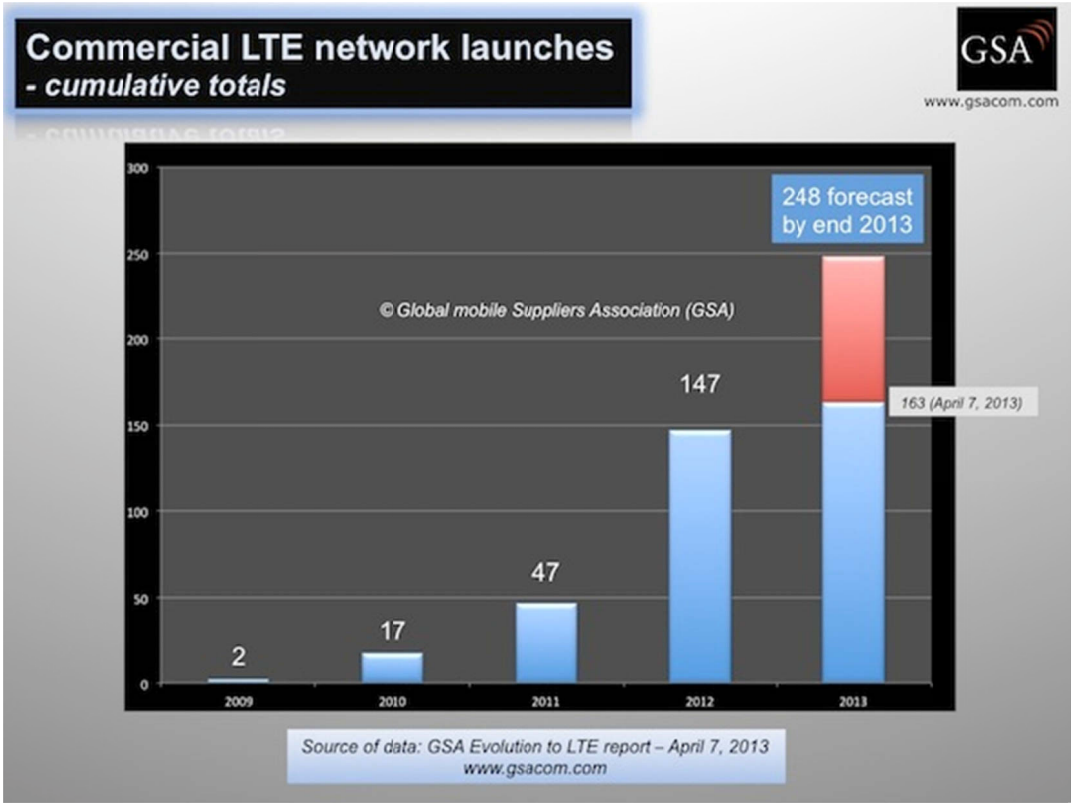

Figure 1.4: Commercial LTE network launches – Cumulative Totals [15]

Long Term Evolution-Advanced (also known as LTE-Advanced, LTE-A or LTE Release 10) is a mobile communication standard proposed by the 3GPP in September 2009 as a major enhancement of the LTE standard. LTE-A was formally accepted as a candidate 4G system to improve LTE system to meet the IMT-Advanced requirements

issued by the ITU-R. The first commercial implementation of LTE-A was launched in October 2012 by Russian network Yota [16]. Currently LTE-A and LTE systems are one of the latest commercial 3GPP standards available in the market.

1.1 LTE and LTE-A Overview

Both LTE and LTE-A are purely packet switched radio access technologies that focus on providing a better quality of mobile services. LTE specification was designed to provide downlink peak rates of 100 Mbps, an uplink peak rates of 50 Mbps, and increase the capacity, coverage, and speed of mobile wireless networks compared to previous 3G technologies [17-21]. LTE-A supports even higher capacity, coverage, and data rates (i.e. up to 1 Gbps in downlink and up to 500 Mbps in uplink) than LTE system [22]. The key features provided by LTE and LTE-A systems are discussed in the following sub-sections.

1.1.1 Air-Interface (Spectrum Flexibility)

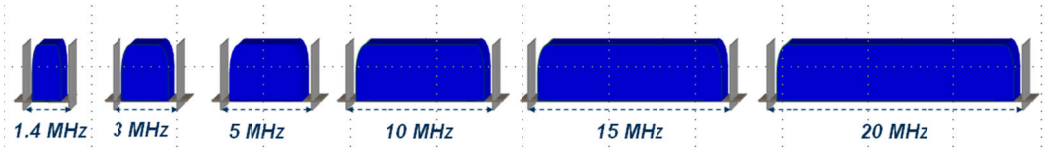

Figure 1.5: Scalable bandwidth in LTE [23]

LTE and LTE-A are designed to support spectrum flexibility in the following three ways:

a) LTE and LTE-A can be deployed with different duplexity: Frequency Division Duplexing (FDD), Time Division Duplexing (TDD), and half-duplex FDD [24]. FDD mode allows downlink and uplink transmissions simultaneously working in different frequency bands while TDD mode allows downlink and uplink transmissions working in the same frequency band with different time slots. FDD are commonly deployed in a paired spectrum, while TDD is commonly deployed in an un-paired spectrum.
b) LTE and LTE-A support flexible standardized bandwidth in 1.25 MHz, 2.5 MHz, 5 MHz, 10 MHz, 15 MHz and 20 MHz as shown in Figure 1.5. Depending on the

available bandwidth, the transmission bandwidth can be chosen by operators [17]. A smaller bandwidth is suitable for LTE deployment using legacy mobile cellular bands whereas a larger bandwidth aims to provide higher data rates.

c) LTE and LTE-A support operation on different frequency bands and are compatible with any systems deployed within 900 MHz, 2.1 GHz and 2.6 GHz spectrums.

1.1.2 Network Architecture

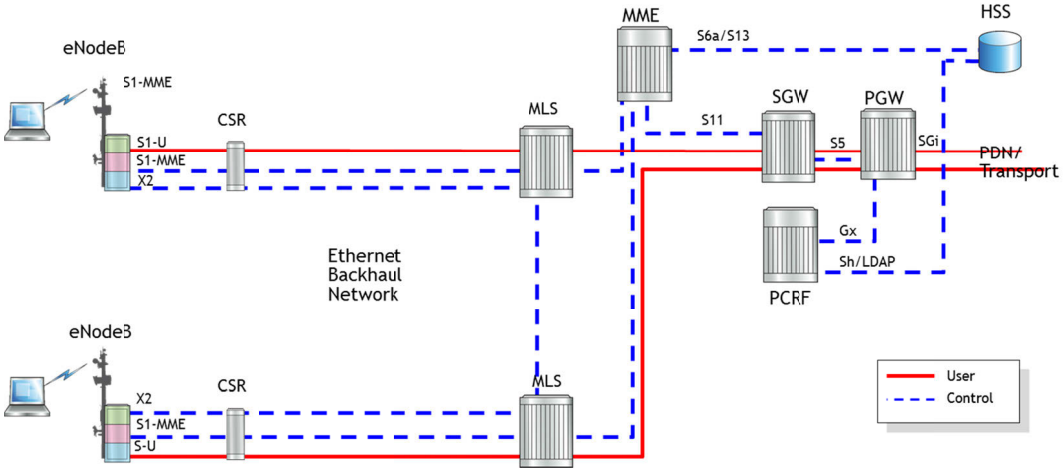

Figure 1.6: LTE overall architecture [25]

Figure 1.6 shows the LTE overall architecture which consists of the Evolved Packet Core (EPC) and the evolved-UMTS Terrestrial Radio Access Network (E-UTRAN or eUTRAN) The EPC and eUTRAN are collectively referred to as Evolved Packet System (EPS). There is only one node known as evolved-NodeB (eNodeB / eNB) in E-UTRAN [26]. The eNodeB is directly connected to LTE user equipment (UE) and the packet core network via EPC. There are two main interfaces in LTE architecture: X2 and S1 interfaces. X2 interface is the interconnection between eNodeBs in E-UTRAN while S1 interfaces are responsible for connection to EPC components, such as mobile management entity (MME), serving gateway (S-GW) [27-29]. Due to the simplification of the LTE network, all the radio resource management functionalities which also include packet scheduling and handover mechanism are implemented in eNodeBs. The MME is the control plane element that manages network access and mobility. The MME controls how UEs interact with the network. The S1-MME reference point

between MME-eNodeB is used by MME to exchange information to control and set up user data sessions. The S-GW serves as the local mobility anchor for UE and terminates the packet data network interface towards the eUTRAN and supports user-plane mobility. It performs IP routing and forwarding functions and maintains data paths between eNodeBs and the PGW. The P-GW function provides the UE with an IP address and connects a user to PDN (packet data network, or IP network).

1.1.3 Access Schemes (OFDMA)

LTE and LTE-A use Orthogonal Frequency Division Multiple Access (OFDMA) which is a variant of OFDM (Orthogonal Frequency Division Multiplex) as a downlink access technology, while Single Carrier Frequency Division Multiple Access (SC-FDMA) is adopted as the uplink access technology. The OFDMA is robust to Inter-Symbol Interference (ISI) and has immunity to frequency-selective fading of the mobile cellular channels [30]. Figure 1.7 shows the difference between OFDMA and SC-FDMA when a series of Quadrature Phase Shift Keying (QPSK) data symbols are being transmitted.

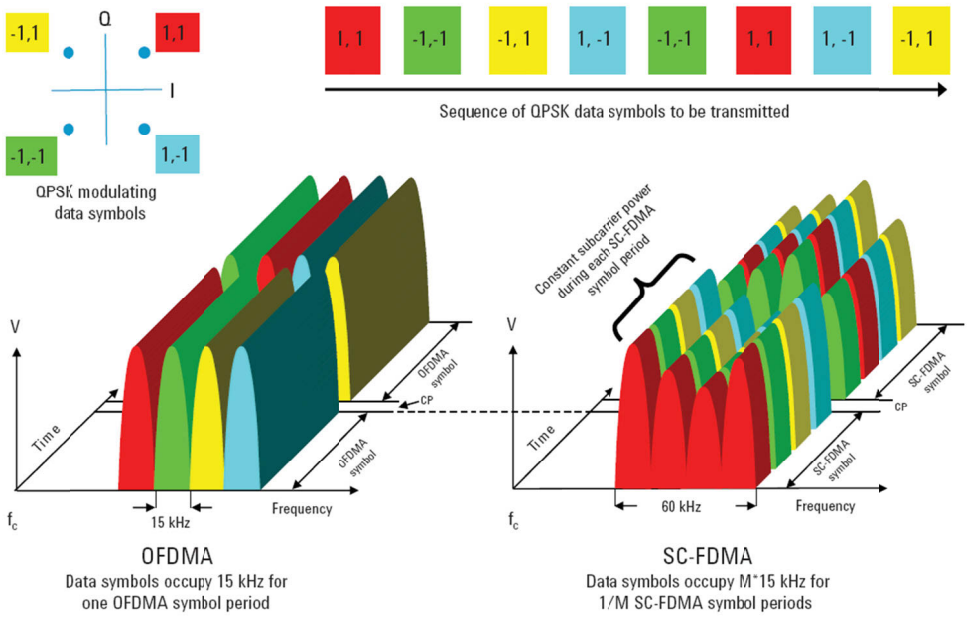

Figure 1.7: The difference between OFDMA and SC-FDMA Transmitting a Series of QPSK Data Symbols [31]

OFDMA divides the available bandwidth into multiple narrow-band equally spaced and mutually orthogonal sub-carriers as shown in Figure 1.8. Each sub carrier has a zero value at the sampling point of all other subcarriers. All sub-carriers in LTE have 15 kHz spacing regardless of the total bandwidth.

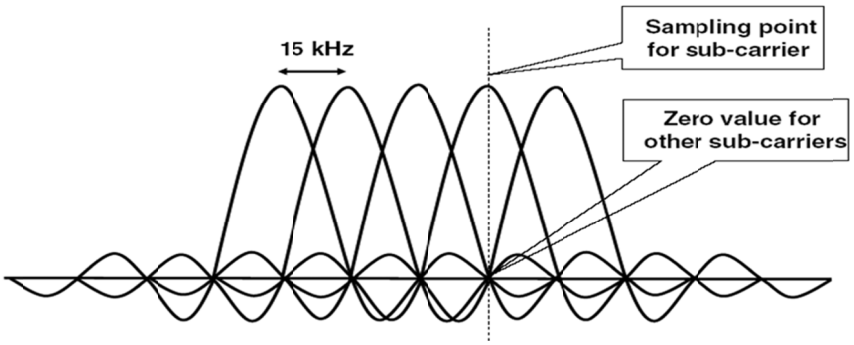

Figure 1.8: Sub-carriers orthogonally [23]

In the time domain, a guard interval known as Cyclic Prefix (CP) is inserted between each OFDMA symbol in order to combat the ISI due to channel delay spread. Each time slot consists of seven OFDM symbols with short/normal CP or six OFDM symbols with long/extended CP [32]. The frequency and time domain of an OFDM signal is represented in Figure 1.9. Note that OFDMA signal in the time domain and frequency domain refers to OFDMA symbol and sub-carrier, respectively.

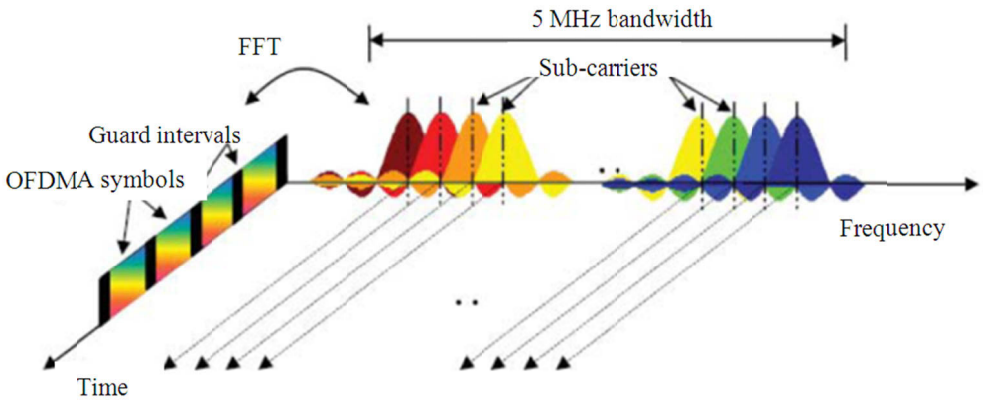

Figure 1.9: Time and frequency domains representation of the OFDMA signals [33]

In mobile cellular systems, the UE is always power-limited. OFDMA has a high peak-to-average power (PAPR) ratio which leads to power-amplifier in-efficiency [21]. This

condition needs to be avoided in the UE side. Therefore, SC-FDMA technology was selected because it provides a more efficient usage of the battery in the UE is better suited for the uplink LTE.

1.1.4 Resource Block (RB)

The smallest transmission unit in the downlink LTE-A system is known as a physical resource block (PRB) which consist of a pair resource blocks (RB) [34]. A PRB has a bandwidth of 180 kHz (12 sub-carriers) and a duration of 1ms (TTI) and a RB has a bandwidth of 180 kHz and a duration of 0.5ms. A downlink time slot has a duration of 0.5 ms and contains either 6 or 7 OFDM symbols depending on the usage of long or short CP, respectively. A Resource element is the basic unit of Physical Resource in LTE [35]. Each RB contains 72 resource elements (REs) when long CP is used, while 84 RE when normal CP is used. The graphical representation of the downlink RB in LTE and available downlink bandwidth with associated number of RBs in LTE is shown in Figure 1.10 and Table 1.1, respectively.

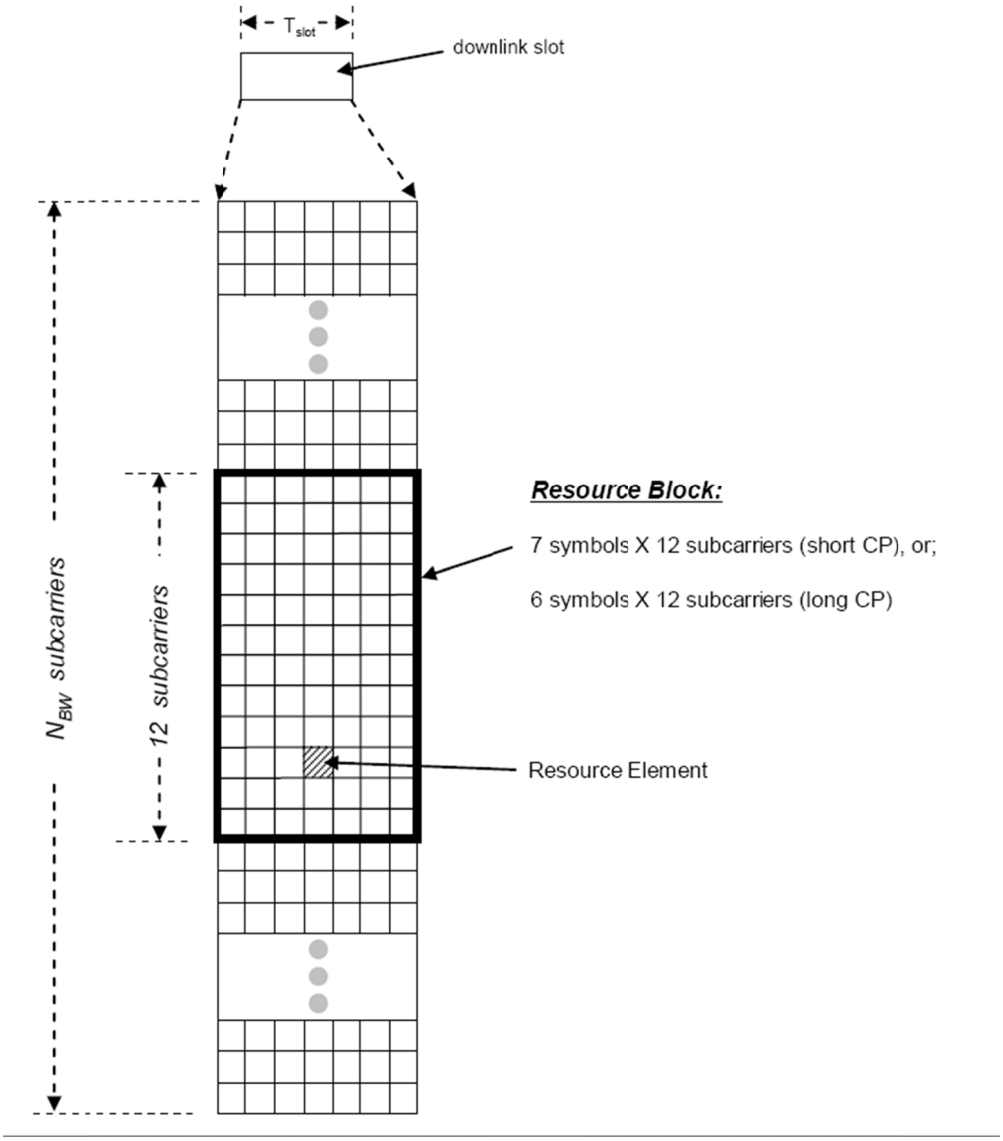

Figure 1.10: Downlink Resource Block in LTE [36]

Table 1.1: Available Downlink Bandwidth with Associated Number of RBs in LTE [31]

Bandwidth (MHz)	1.25	3	5.0	10	15.0	20.0
Number of available RBs	6	15	25	50	75	100
Sub-carrier bandwidth (kHz)	15					
RB bandwidth (kHz)	180					

1.1.5 Quality of Service (QoS)

The QoS differentiation in the LTE is provided in the EPS bearer introduced by the 3GPP organisation [10]. An EPS bearer can either be Guaranteed Bit Rate (GBR) or Non-GBR bearer based on its QoS requirements. Each EPS bearer contains bearer level QoS parameters with QoS Class Identifiers (QCIs), allocation retention priority, the GBR and the maximum data rate [37]. The complete list of the QCI configuration and the QoS parameters for LTE is shown in Table 1.2.

Table 1.2: Standardised QCIs for LTE [38]

QCI	***Service type***	***Priority***	***Packet delay budget (ms)***	***Packet error loss rate***	***Example applications***
1	GBR	2	100	10^{-2}	Conversational voice
2		4	150	10^{-3}	Conversational video (live streaming)
3		5	300	10^{-6}	Non-conversational video (buffered streaming)
4		3	50	10^{-3}	Real time gaming
5	Non-GBR	1	100	10^{-6}	IMS signalling
6		7	100	10^{-3}	Voice, video (live streaming), interactive gaming
7		6	300	10^{-6}	Video (buffered streaming), TCP-based i.e. www, e-mail, chat, ftp, p2p file sharing, progressive video, etc.)
8		8			
9		9			

1.1.6 LTE-A Key Features

There are a number of key features introduced in LTE-A, including carrier aggregation, downlink and uplink spatial multiplexing enhancement, coordinated multipoint point (CoMP) transmission and reception, relaying nodes, and heterogeneous networks compatibility [39].

Carrier aggregation permits an eNodeB to group several distinct channels into one logical channel [40]. This results in a high peak data rate of 1 Gbps in downlink and 500 Mbps in uplink being achieved with bandwidth extension from 20 MHz to 100 MHz in

LTE-Advanced [41]. Figure 1.11 shows the contiguous intra-band carrier aggregation, non-contiguous intra-band carrier aggregation, and non-contiguous inter-band carrier aggregation in LTE-A.

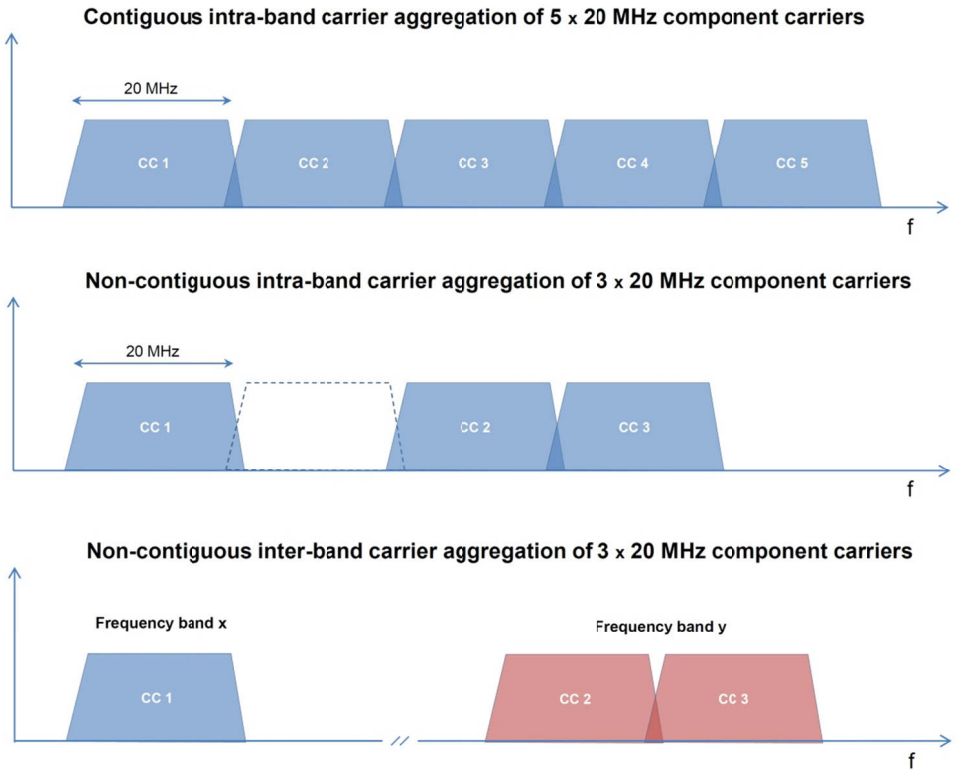

Figure 1.11: Carrier Aggregation in LTE-A [42]

LTE supports four multiple-input multiple-output (MIMO) antenna schemes in the downlink while one MIMO antenna scheme in the uplink direction. LTE-A extends the MIMO capabilities of LTE Release 8 to support up to eight downlink antennas and up to four uplink antennas for MIMO. Eight-layer and four-layer MIMO spatial multiplexing in downlink and uplink increase average and peak data rate and the cell edge throughput [41]. Figure 1.12 shows the number of antenna ports and spatial layers used in LTE-A.

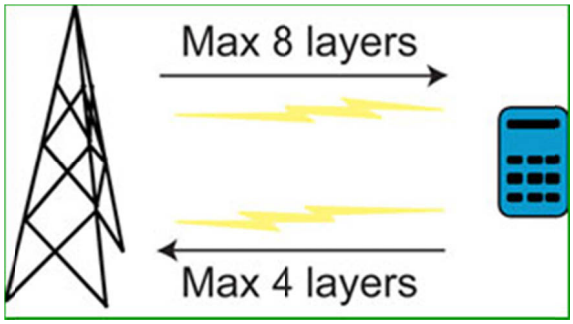

Figure 1.12: Number of Antenna Ports and Spatial Layers in LTE-A [43]

CoMP transmission and reception improves the cell-edge throughput and/or system throughput in LTE-A with multiple data transmissions. Figure 1.13 shows the fundamental CoMP scheme in LTE-A.

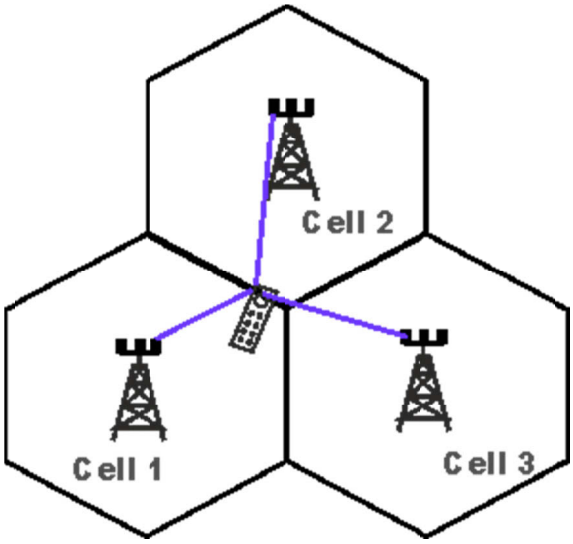

Figure 1.13: CoMP in LTE-A [44]

The support for relaying in LTE-A is to enhance the coverage and the capacity of the network [22]. In a relaying scenario, the UE communicates with the relay node which communicates with an anchor eNodeB (also known as donor eNodeB). The eNodeB may communicate other non-relayed UEs directly as shown in Figure 1.14.

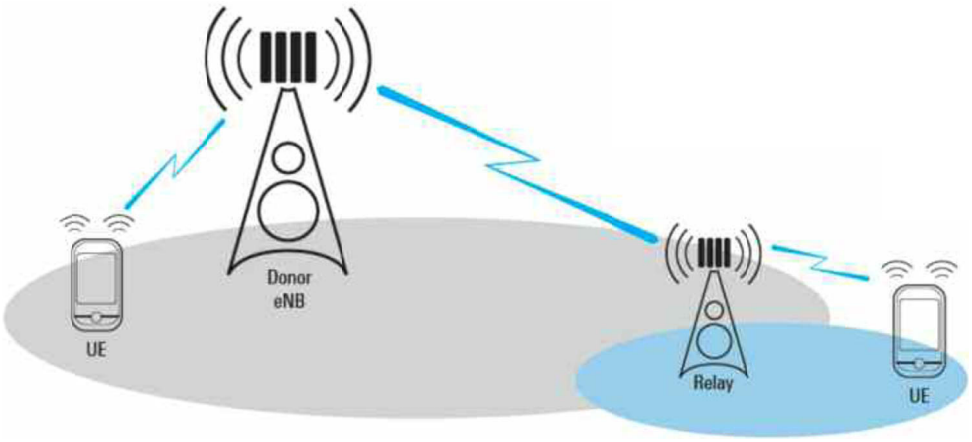

Figure 1.14: Relaying in LTE-A [22]

Heterogeneous networks compatibility provides coverage and capacity in areas difficult or expensive to reach using the traditional approach [39].

1.2 Packet Scheduling

Packet scheduling is a key LTE mechanism that is responsible for efficient allocation PRB at every TTI for transmission of user packets on the uplink and downlink for active users based on certain scheduling criteria. Packet scheduling decisions have to take into account of QoS satisfaction, guaranteeing fairness, and optimizing the system performance [45].

The downlink packets destined for each user arrive from the core network and are queued at the eNodeB buffer to be transmitted. The packet scheduler, which is located at the Medium Access Control (MAC) Layer, is responsible for assigning the most appropriate PRBs for each competing users in each 1 ms Transmission Time Interval (TTI). The selected packets are segmented at the Radio Link Control (RLC) Layer and transmitted [46].

The packet scheduling algorithm in the downlink LTE is responsible for selecting the user whose packets need to be transmitted on every PRB. This algorithm takes several input information into consideration, such as Channel Quality Information (CQI), packet delay information, buffer status, RB usage …etc. [47-49].

The CQI is reported by each active UE to the eNodeB to estimate its channel quality. A channel-aware packet scheduler is permitted by this CQI report to schedule a user on its favourable RB based on the user's channel quality [50-54].

A simple illustration demonstrating the idea of a general packet scheduling model for downlink LTE system is in Figure 1.15. Figure 1.15 shows that the packet scheduler makes the decision of the downlink packets queued at the eNodeB buffer to be transmitted by assigning the most appropriate PRBs for each competing users based on the CQI report and the packet scheduling algorithm.

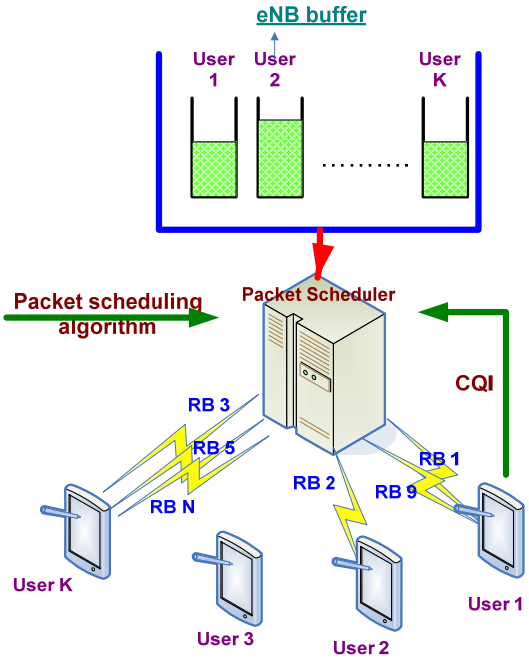

Figure 1.15: A generalised model of downlink LTE packet scheduling [55]

A Transport Block (TB) is a group of packets that are transmitted to a user in one TTI. The data rate for packets transmission which is determined by the size of the TB depends upon the Modulation and Coding Scheme (MCS) on each RB that is assigned to the user. Figure 1.16 shows a transport block in a sub frame of 10 ms radio frame in LTE.

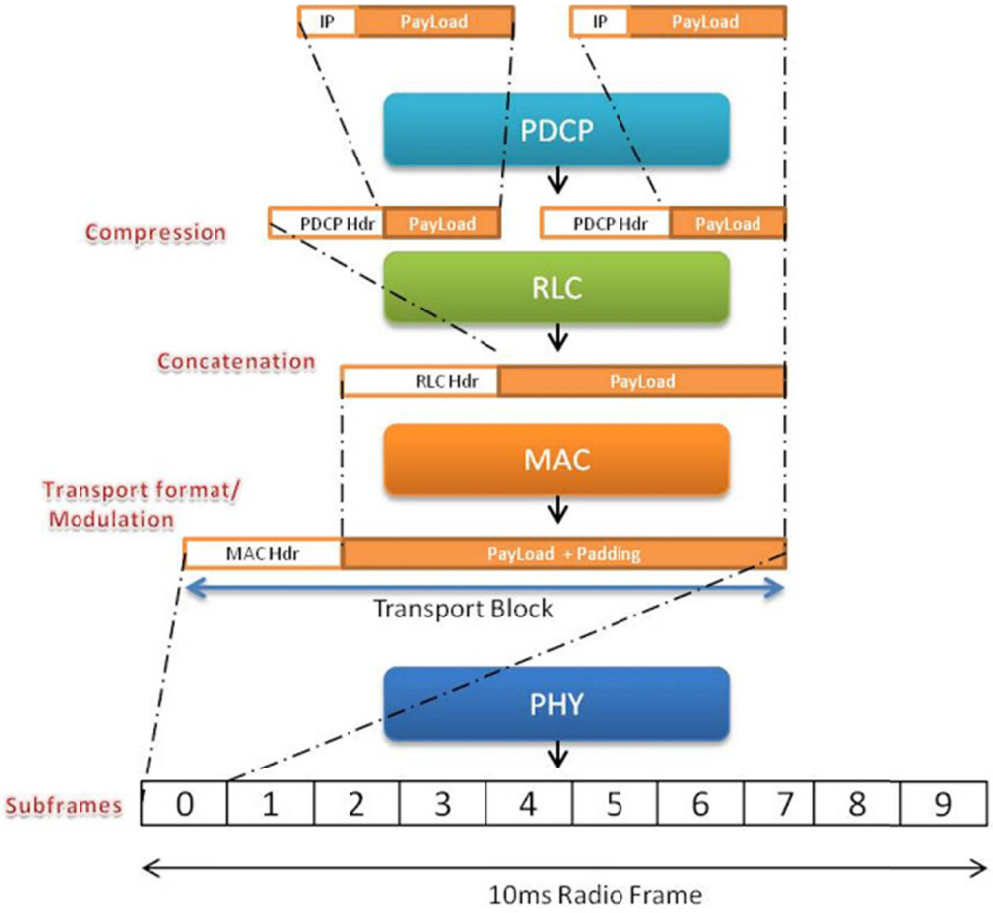

Figure 1.16: A Transport Block in LTE [56]

1.3 Handover

Handover is a mechanism that transfers an on-going call or data session from one base station (BS) to another BS or one sector to another sector within the same BS. Figure 1.17 shows an illustrative figure of handover behaviour. When a mobile station is moving from one BS to another, the received signal level of the serving BS (BS1 in Figure 1.17) starts decreasing while the received signal level of the target BS (BS2 in Figure 1.17) starts increasing. A handover is triggered if the received signal of the serving BS is lower than the received signal of a target BS minus a signal level threshold (Hysteresis in Figure 1.17).

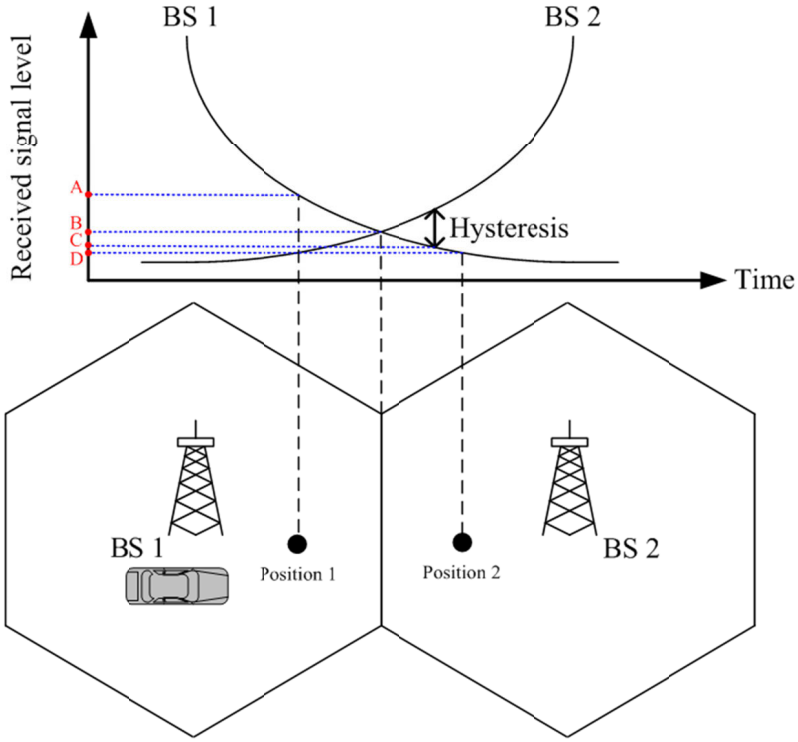

Figure 1.17: An Illustrative Figure of Handover [57]

Handover is one of the key components in cellular network mobility management [58]. Vertical handovers and horizontal handovers are the two categories in handovers [59]. Vertical handovers are the handovers of transferring a UE from one BS to another BS crossing different radio access technologies (RATs). Vertical handovers can be performed within the same family technologies, such as LTE to WCDMA or LTE to GSM, or different family technologies such as LTE to WiMAX or LTE to Ultra Mobile Broadband [58, 60-62]. Horizontal handovers refer to the handover process which is performed within the same network technology. Given that the horizontal handovers are standardized in the 3GPP standardization, the focus of this thesis is based on the horizontal handovers in LTE system.

1.4 Motivation and Objectives

Handover mechanisms in LTE and LTE-A systems are relatively new area of research in future wireless networks. The scarcity of the radio resources, the dynamic nature of propagation environment, the variety of user mobility as well as maximizing the possible system throughput and minimizing the system delay are the major challenges that need to be addressed when researching the handover mechanisms in LTE and LTE-A systems. Given that a LTE-A system is a major enhancement of the LTE system, the feasibility of the LTE handover mechanisms on LTE-A system needs to be studied.

CoMP technology is expected to improve the cell-edge throughput and/or system throughput with multiple data transmissions in LTE-A compared with the LTE system. In coordinated multipoint networks, multiple base stations send information in a coordinated manner to the mobile station, the current existing handover algorithms in LTE network are not applicable for CoMP networks [63]. Furthermore, existing CoMP technologies in LTE-A system could lead to system capacity overload and saturated system throughput issues within a highly congested network. Therefore, new handover algorithms which can support CoMP technology and take system capacity into consideration in the LTE-A system is focused in this thesis.

The mobile cellular channels are subject to various impairments due to interference, multi-path fading, shadowing, and imperfect channel feedback reports. These impairments may cause severe performance degradation especially for handover algorithms that rely on an accurate RSRP report. The mobile cellular channel impairments of the CoMP handover algorithms due to impairment environments in a practical LTE-A cellular network are taken into considerations in our performance analysis.

Given the challenges, five questions to be highlighted in this research are:

1. Given the current handover algorithms in multi-carrier systems, can one improve the performance of the current algorithms by minimizing system delay and maximizing the system throughput in a multi-cell scenario?

2. Given a set of handover algorithms in LTE, can one evaluate these algorithms based on the simulation performance analysis?
3. How suitable are LTE handover mechanisms for LTE Advanced?
4. Given that current existed handover algorithms in LTE network are not applicable for CoMP networks, can one design a handover algorithm that support CoMP technology and take system capacity into consideration in LTE-A system?
5. Given that handover algorithms rely on an accurate RSRP report to perform optimized performance, what is the performance impact of CoMP handover algorithms due to impairment environments in a practical LTE-A cellular network?

1.5 Thesis Overview

A number of contributions are made in this thesis to address the LTE and LTE-A handover challenges outlined in Section 1.4. The contributions and brief descriptions of remaining chapters of this thesis are given below:

Chapter 2: Modelling and Simulation of LTE and LTE-A

This chapter describes a general downlink LTE and LTE-A system model including topology model, mobility model, radio propagation model, and traffic model. The modelling of the CQI, Reference Signal Received Power (RSRP), handover mechanism, packet scheduling and Hybrid Automatic Repeat Request (HARQ) are discussed. The traffic characteristics and performance metrics that are used to evaluate the system performance are introduced. Moreover, relevant underlying assumptions that are used throughout the thesis are summarized in this chapter.

Chapter 3: Handover Algorithms

This chapter studies the fundamental handover mechanism, the standard handover procedure in LTE, and a number of handover algorithms developed for LTE system. An optimization method is introduced to minimize the number of handovers and maximize the system throughput in a multi-cell scenario. Furthermore, a handover algorithm in LTE is proposed to minimize unnecessary handovers while maintaining the same

channel quality. The performance of selected handover algorithms in LTE are optimized and compared in this chapter.

Chapter 4: Advanced LTE-A CoMP Handover Algorithms

The CoMP technology is expected to enhance the LTE-A system throughput and reduce the packet loss ratio (PLR) compared with the LTE system. However, this could lead to system capacity overload and saturated system throughput issues within a highly congested network. To address this situation, this chapter describes three proposed CoMP handover algorithms for the LTE-A system. These algorithms take one or more decision information (i.e. instantaneous RSRP, instant/historical PRB usage) into consideration so as to increase system capacity. System performance of each proposed CoMP handover algorithm is evaluated and compared with open literature handover algorithm via simulation.

Chapter 5: Performance Testing of CoMP Handover Algorithms with Various Traffics in LTE-A

A performance testing of selected CoMP handover algorithms with various traffics in LTE-A system is discussed in this chapter. The simulation results are provided including the handover parameters optimization of each CoMP handover algorithm under different speed scenarios and followed by the discussion of the performance testing for real-time (RT) traffic, non real-time (NRT) traffic, and mixed RT and NRT traffic in the LTE-A system.

Chapter 6: Performance Testing of CoMP Handover Algorithms for Practical LTE-A Cellular System

A practical LTE-A cellular system with mobile cellular channel impairments is considered in this chapter for performance testing of CoMP handover algorithms. The impairments for a practical LTE-A system are assumed to be in two scenarios: outdated feedback and missing feedback. A constantly feedback delayed channel is assumed in the outdated feedback scenario while a missing feedback environment is assumed in the missing feedback scenario. The performances of each CoMP handover algorithm for

perfect feedback scenario, outdated feedback scenario, and missing feedback scenario in a practical LTE-A system are individually evaluated and discussed in this chapter.

Chapter 7: Conclusions and Future Research Directions

This chapter summarises the thesis contributions and recommends some studies relevant for future research.

1.6 Contributions

Majority of the contributions included in this thesis appear in peer reviewed journal and conference papers. They are outlined as following:

Journal Articles

C.-C. Lin, K. Sandrasegaran, H.A.M. Ramli, and R. Basukala, "Optimized Performance Evaluation of LTE Hard Handover Algorithm with Average RSRP Constraint" in *International Journal of Wireless and Mobile Networks (IJWMN),* vol. 3, no. 2, April 2011, pp. 1-16.

C.-C. Lin, K. Sandrasegaran, X. Zhu, and Z. Xu, "Limited CoMP Handover Algorithm For LTE-Advanced," *Journal of Engineering,* vol. 2013, p. 9, 2013.

Z. Xu, K. Sandrasegaran, B. Hu, and **C.-C. Lin**, "A Study of WLAN RSSI Based Distance Measurement Using EEMD," *International Journal of Advanced Research in Computer Science and Software Engineering*, vol. 3, p. 6, 2013.

Y. Wang, K. Sandrasegaran, X. Zhu, **C.-C. Lin**, A. Daeinabi, "Packet Scheduling in LTE with Imperfect CQI," *International Journal of Advanced Research in Computer Science and Software Engineering*, vol. 3, issue 6, July 2013.

Conference Papers

C.-C. Lin, K. Sandrasegaran, H. A. M. Ramli, and M. Xue, "Requirement of Handover Modeling in the Downlink 3GPP Long Term Evolution System," in IEEE 24th

International Conference on Advanced Information Networking and Applications Workshops (WAINA) 2010, pp. 305-310.

M. Xue, K. Sandrasegaran, H. A. M. Ramli, and **C.-C. Lin**, "Performance Analysis of Two Packet Scheduling Algorithms in Downlink 3GPP LTE System," in the IEEE 24th International Conference on Advanced Information Networking and Applications Workshops, Perth, Australia, 2010.

L. Wu, K. Sandrasegaran, M. Elkashlan, and **C.-C. Lin**, "Performance Evaluation on Common Radio Resource Management Algorithms," presented in the IEEE 24th International Conference on Advanced Information Networking and Applications Workshops, Perth, Australia, 2010.

H.A.M. Ramli, K. Sandrasegaran, R. Basukala, R. Patachaianand, M. Xue, and **C.-C.Lin**, "Resource Allocation Technique for Video Streaming Applications in the LTE System", in Proceeding of the 19th Annual Wireless and Optical Communications Conference (WOCC), Shanghai, China, May 2010, pp. 1-5.

L. Chen, K. Sandrasegaran, R. Basukala, F. M. Madani, and **C.-C. Lin**, "Impact of soft handover and pilot pollution on video telephony in a commercial network," in 16th Asia-Pacific Conference on Communications (APCC) 2010, pp. 481-486.

K. Sandrasegaran, R. Patachaianand, F. M. Madani, and **C.-C. Lin**, "Analysis of opportunistic contention-based feedback protocol for downlink OFDMA," in Australasian Telecommunication Networks and Applications Conference (ATNAC) 2010, pp. 72-77.

C.-C. Lin, K.Sandrasegaran, H.A.M. Ramli, R. Basukala, R. Patachaianand, L. Chen and T.S. Afrin, "Optimization of Handover Algorithms in 3GPP Long Term Evolution System", in Proceeding of the International Conference on Modeling, Simulation and Applied Optimization (ICMSAO 2011), April 2011, pp. 1-5.

C.-C. Lin, K. Sandrasegaran, and S. Reeves, "Handover algorithm with joint processing in LTE-advanced," in 9th International Conference on Electrical

Engineering/Electronics, Computer, Telecommunications and Information Technology (ECTI-CON) 2012, pp. 1-4.

C.-C. Lin, K. Sandrasegaran, X. Zhu, and Z. Xu, "Performance evaluation of capacity based CoMP handover algorithm for LTE-Advanced," in 15th International Symposium on Wireless Personal Multimedia Communications (WPMC) 2012, pp. 236-240.

C.-C. Lin, K. Sandrasegaran, X. Zhu, and Z. Xu, "On the performance of capacity integrated CoMP handover algorithm in LTE-Advanced," in 18th Asia-Pacific Conference on Communications (APCC) 2012, pp. 871-876.

Chapter 2

MODELLING AND SIMULATION OF DOWNLINK LTE AND LTE-A

There are a number of methods that can be used for evaluating the performance of a mobile cellular network. These methods include test bed, theoretical analysis, and computer simulation.

A test bed is a platform for experimentation of development projects and researches. A typical test bed could include software, hardware, and networking components [64]. Emulab offers researchers a wide range of environments in which to develop, debug, and evaluate their systems [64]. Considerable financial, labour, and hardware resources are required for test bed methods [65, 66]. Test bed results are difficult to analyse because they are heavily influenced by the test environment [67].

Theoretical analysis is an approach that identifies the origins of a theory, examines the meaning of the theory, analyses the logical adequacy of the theory, determines the usefulness of the theory, define the degree of generalizability and the parsimony of the theory, and determines the testability of the theory [68]. Theoretical analysis is a complex method that depends on the model being built and it is a time consuming method for evaluating accurate result due to the steps involved.

Computer simulation is a less expensive and complex method that makes modelling and studying a large scale mobile cellular system more practical [69]. Researchers can design and analyse a number of mobile cellular scenarios easily by using computer simulation. A computer simulation of a cellular network was used for performance evaluation in this thesis because it is less expensive and less complex to study when compared to theoretical analysis and test bed methods.

A number of LTE simulators are available in the literature: a MATLAB-based downlink physical-layer simulator for LTE [70], an OFDMA wireless system using WM-SIM platform [71], 4G Evolution Lab - LTE and LTE-Advanced Toolbox and Blockset for MathWorks MATLAB® and Simulink® [72], LTE eNodeB Software Framework [73], a MATLAB computationally efficient LTE system level simulator [74] [70-76], and LTE-Sim [75]. However, these simulators do not support handover protocols. A MATLAB-based downlink physical-layer simulator for LTE [70], an OFDMA wireless system using WM-SIM platform [71] and 4G Evolution Lab – LTE and LTE-Advanced Toolbox and Blockset for MathWorks MATLAB® and Simulink® [72] focus more on the Physical (PHY) Layer aspects. LTE eNodeB Software Framework [73] is not accessible for public research communities. LTE-Sim [75] is an open source framework which supports well-known packet scheduling strategies such as Proportional Fair (PF), Modified Largest Weighted Delay First (MLWDF), and Exponential Proportional Fair (EPF), frequency reuse techniques, and PHY layer models. However, LTE-Sim does not support handovers. Therefore, a C++ system level simulator based on [77] that can dynamically models the large and complex downlink LTE was developed as part of this research work. The simulator consists of the following models:

1. System Model
2. Topology Model
3. User mobility model
4. Radio propagation model including Path Loss, Shadow Fading, Multi-path Fading, and Signal-to-Interference-plus-Noise-Ratio (SINR) computation
5. CQI reporting
6. Reference Signal Received Power (RSRP) computation
7. Handover Model
8. Packet Scheduling Model
9. Hybrid Automatic Repeat Request (HARQ) Model
10. Traffic Model

The system model of the C++ system level simulator is inherited from [77]. The Topology is expanded from single cell in [77] to seven hexagonal cells. The wrapped-around function in the user mobility model in this thesis was redesigned and enhanced

based on the work in [77] in order to overcome an unrealistic outcome. The radio propagation model (including Path Loss, Shadow Fading, Multi-path Fading, and SINR) and CQI reporting were inherited from [77] with six more computations for six more cells in the simulation. The RSRP computation and handover model were newly implemented for handover protocols. The packet scheduling model and HARQ model were inherited from [77]. However, the HARQ model in each cell was enhanced for the CoMP requirements in LTE-A system. The constant stream traffic in traffic model in this thesis was newly implemented for modelling various type of traffic.

This chapter is structured as follows: Section 2.1 describes a general downlink LTE and LTE-A system model implemented within the system level simulator. A topology model, a mobility model, and a radio propagation model will be discussed in Section 2.2, Section 2.3, and Section 2.4, respectively. Section 2.5 describes the modelling of the CQI while Section 2.6 presents the modelling of the RSRP. Section 2.7, Section 2.8, and Section 2.9 present the modelling of handover, packet scheduling, and HARQ, respectively. A description of RT and NRT traffic characteristics is discussed in Section 2.10 followed by the performance metrics discussion in LTE and LTE-A in Section 2.11. Section 2.12 summarises all assumptions listed in previous sections and Section 2.13 gives a summary of this chapter.

2.1 System Modelling

A system bandwidth of 5 MHz with 25 PRBs and 2 GHz carrier frequency with normal cyclic prefix (7 OFDM symbols over a slot of 0.5 ms duration) is used in this thesis. Each eNodeB transmits at 43.01 dBm [11] and each PRB is assumed to be transmitted with equal power. The total amount of 25 PRBs are available to be shared among all the users within a cell. Table 2.1 summarises the simulation parameters and these parameters are compatible with the LTE specifications 3GPP Technical Report 25.814 [30]. The number of sub-carriers per PRB is 12 which gives a bandwidth of (12 x 15 kHz) 180 kHz for each PRB.

Table 2.1: Main downlink LTE system parameters

System Parameters	***Values***	***Reference***
Cellular layout	Hexagonal grid, wrap around (reflect), 7 cells	NA
Radius	100	NA
Bandwidth	5 MHz	[30]
Carrier frequency	2 GHz	[30]
Mode of operation	FDD	[30]
Number of PRBs	25	[30]
Number of sub-carriers per PRB	12	[30]
Total Number of Sub-carriers	300	25 x 12
Sub-carrier spacing	15 kHz	[30]
Scheduling interval (TTI)	1 ms	[11]
Number of OFDMA symbols per TTI	14 (Normal CP)	[30]
Total number of REs	168	14 x 12
Total eNB transmit power	43.01 dBm	[11]

2.2 Topology Modelling

The simulation topology consists of 7 hexagonal cells of radius 100m and with an eNodeB located at the centre of each cell. Users are uniformly distributed within the system boundary where the blue rectangle area as shown in Figure 2.1.

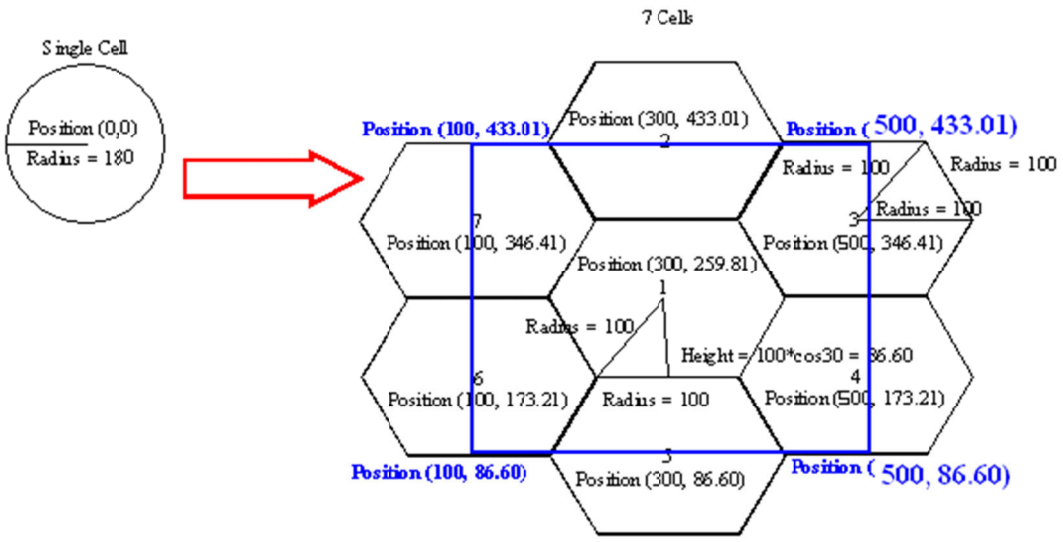

Figure 2.1: Multi-cell and multi-user simulation environment

2.3 Mobility Modelling

In a multi-cell/multi-user mobility model, each user is assigned a random direction at the beginning of its data session and moves within the cell at a constant speed in a constant direction. The constant speed can be chosen from 3, 30, or 120 km/hr. The location of user *i* at time *t* is determined using a complex number (z = x + iy) as described in Equation (2.1).

$$loc_i(t) = loc_i(t-1) + (v_i(t-1) * dir_i(t-1)) \tag{2.1}$$

where $loc_i(t)$ is the location (complex number) of user *i* at time *t*, $v_i(t-1)$ is the speed of user *i* at time *t-1* and $dir_i(t-1)$ is the direction of user *i* at time *t-1*.

A wrap around method is applied when each UE reaches the system boundary [78]. The reflected location of user *i* at time *t* is determined using a complex number (z= x +iy) as described in Equation (2.2).

$$loc_i(t) = loc_i(t-1) + (v_i(t-1) * (dir_i(t-1) * -1)) \quad (2.2)$$

where $loc_i(t)$ is the location (complex number) of user i at time t, $v_i(t\text{-}1)$ is the speed of user i at time $t\text{-}1$ and $dir_i(t\text{-}1)$ is the direction of user i at time $t\text{-}1$.

Figure 2.2 and Figure 2.3 show two implementations of the wrap-around function implemented in a multi-cell scenario.

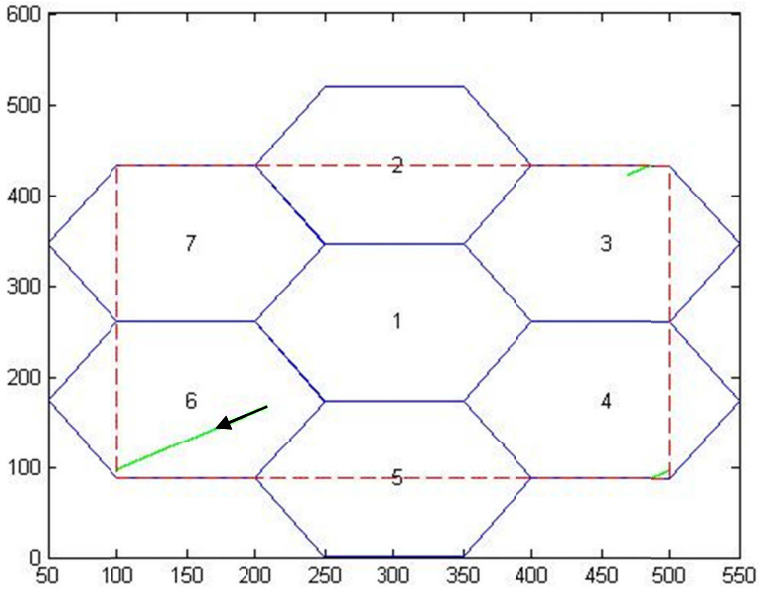

Figure 2.2: A sample of a wrapped-around process in multi-cell scenario

In Figure 2.2, when a user moves from Cell 6 and reaches the red rectangle boundary, the user will enter from the opposite side which is the right top side of the red rectangle boundary. The wrap-around function ensures that all users remain within the simulation topology. However, a sudden change of the X and Y coordinates of a user directly affects the received radio signal strength of a user and forces this user to handover to the target cell (Cell 3) which results in an unrealistic outcome. In order to overcome these issues, a redesigned wrap-around function with a reflect mechanism was implemented as shown in Figure 2.3.

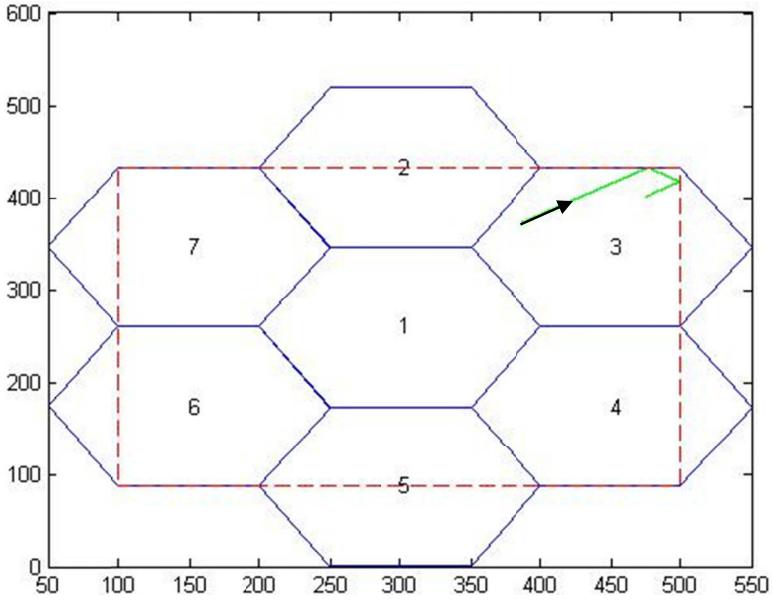

Figure 2.3: A sample of a reflect wrap-around process in multi-cell scenario

In Figure 2.3, when a user moves from Cell 3 towards the right top corner and reaches the red rectangle boundary, the user will be reflected and kept within Cell 3 at this point.

2.4 Radio Propagation Modelling

Radio propagation refers to the behaviour of electromagnetic waves when they propagate from a transmitter to a receiver. It affects the received signal strength at a receiver [79]. Channel gain can be expressed as the ratio of received signal strength to transmitted signal. The channel gain consists of three components: path loss, shadow fading and multi-path fading gains, each of these factors will be described below in details.

2.4.1 Path Loss

Path loss is the reduction in the power density of an electromagnetic wave as it propagates through free space caused by the natural expansion of the radio wave front. Okumura-Hata (Hata) model [80] is used to calculate the path loss in this thesis. Hata model is one of the most widely used empirical propagation prediction models [81]. Hata model is based on the results of extensive experimental measurements and is

considered as one of the most accurate path loss model in mobile communications. Hata model can be expressed in the following equations:

$$pl_i(t) = 46.3 + 33.9 * \log_{10}(f) - 13.82 * \log_{10}(h_b) - a(h_m) + (44.9 - 6.55 * \log_{10}(h_b)) * \log_{10}(|dis_i(t)|) \quad (2.3)$$

$$a(h_m) = (1.1 * \log_{10}(f) - 0.7) * h_m - (1.56 * \log_{10}(f) - 0.8) \quad (2.4)$$

$$dis_i(t) = loc_i(t) - loc_i(t-1) \quad (2.5)$$

where $pl_i(t)$ is the path loss (in dB) of user i at time t, $|dis_i(t)|$ is the distance (in meter) of user i from eNB at time t, $loc_i(t)$ is the location (complex number) of user i at time t, f is the frequency of the transmission (in MHz), h_b is the height of the eNB (in meter), h_m is the height of the user terminal (in meter), and $a(h_m)$ is the mobile antenna correction factor.

2.4.2 Shadow Fading

Shadow fading refers to the variation in the field strength of a radio signal that is caused by reflection, diffraction and shielding phenomenon from obstructions such as building, trees and rocks [82]. The shadow fading gain in this thesis was modelled and computed using a Gaussian lognormal distribution with a 0 dB mean and a 8 dB standard deviation [83]. Two equations expressed below are used to determine the shadow fading gain:

$$\xi_i(t) = \rho_i(t-1) \cdot * \xi_i(t-1) + \sigma * \left(\sqrt{1 - \rho_i(t-1)^2 \cdot}\right) * G(t-1) \quad (2.6)$$

$$\rho_i(t-1) = \exp\left(\frac{-v_i(t-1)}{d_0}\right) \quad (2.7)$$

where $G(t-1)$ is a Gaussian random variable of user i at time $t-1$, $\rho_i(t-1)$ is the shadow fading autocorrelation function, $v_i(t-1)$ is the speed of user i at time $t-1$, σ is the shadow fading standard deviation, and d_0 is the shadow fading correlation distance.

2.4.3 Multi-path Fading

Multi-path fading is caused by reflection and/or scattering of an electromagnetic signal. It results in the addition of electromagnetic signals received from multiple paths. In this thesis, the multi-path fading was modelled based on a frequency flat Rayleigh Fading Model [84]. The statistical based frequency flat Rayleigh fading is modelled by a complex Gaussian random process and widely used for signal propagation modelling and has the following equation:

$$\mu\_ap_i(t) = \sum_{n=1}^{N_i} c_{i,n} \cos(2\pi f_{i,n} t + \theta_{i,n}) \quad i = 1,2,3 \tag{2.8}$$

$$c_{i,n} = \sigma_{\mu 0} \sqrt{\frac{2}{N_i}} \tag{2.9}$$

$$f_{i,n} = f_{\max} \sin(\frac{\pi}{2} \mu_n) \tag{2.10}$$

where $\theta_{i,n}$ is the Doppler phase of process i of the nth sinusoid, $f_{i,n}$ is the discrete Doppler frequency of process i of the nth sinusoid, $c_{i,n}$ is the Doppler coefficient of process i of the nth sinusoid, N_i is the number of sinusoids of process i, $\mu\_ap_i(t)$ is the approximated uncorrelated filtered white Gaussian noise with zero mean of process i at time t, $\sigma_{\mu 0}$ is the variance (mean power), μ_n is uncorrelated filtered white Gaussian noise with zero mean of the nth sinusoid, and f_{max} is the maximum Doppler frequency.

Figure 2.4 shows a block diagram representation of the frequency flat Rayleigh fading ($\zeta(t)$) at time t based on Equation (2.8), Equation (2.9), and Equation (2.10).

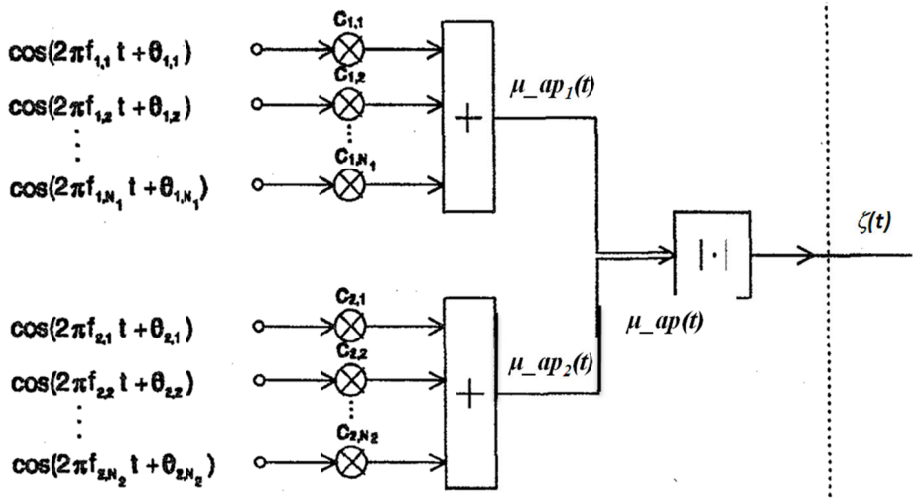

Figure 2.4: Frequency flat Rayleigh fading structure [84]

2.4.4 Signal to Interference-plus-Noise Ratio (SINR)

Signal to Interference-plus-Noise Ratio (SINR) is commonly used in wireless communication as a representation to measure the quality of wireless connections. SINR experienced by a UE varies with time and on each RB in the OFDMA system because of the time-selective fading nature of the radio signals in a cellular network [85]. In this thesis, it is assumed that there is a minimum variation of multi-path fading among all sub-carriers within a PRB. The instantaneous SINR ($\gamma_{i,j}(t)$) of user i on PRB j at time t in this thesis is computed based on the center subcarrier frequency of the PRB [77] as expressed below [86]:

$$\gamma_{i,j}(t) = \frac{P_{total} * gain_{i,j}(t)}{PRB_{\max}(ICI + N_o)} \tag{2.11}$$

$$gain_{i,j}(t) = 10^{\left(\frac{pl_i(t)}{10}\right)} * 10^{\left(\frac{\xi_i(t)}{10}\right)} * 10^{\left(\frac{mpath_{i,j}(t)}{10}\right)} \tag{2.12}$$

where $\gamma_{i,j}(t)$ is the instantaneous SINR (in dB) of user i on PRB j at time t, $mpath_{i,j}(t)$ is the multi-path fading gain (in dB) of user i on PRB j at time t, $pl_i(t)$ is the path loss(in dB) of user i at time t, $\xi_i(t)$ is the shadow fading gain (in dB) of user i at time t, P_{total} is the total eNB transmit power (in dBm), RB_{max} is the total available number of PRBs, N_o is the thermal noise (in watts), and ICI is the inter-cell interference (in watts).

In this thesis it is assumed that there is a constant inter-cell interference throughout the simulation.

2.5 Channel Quality Information (CQI)

The instantaneous SINR computed from Equation (2.11) is mapped into a CQI value (SINR-to-CQI mapping) at the UE and the UE feeds the CQI value back to the eNB through the uplink channel. Every CQI value corresponds to a MCS value which is a threshold value for block error rate (BLER) not to exceed [11]. In this thesis, the BLER threshold was set to 10% which is a recommended threshold in [70]. Figure 2.5 shows that when a fixed value of BLER is set, a higher SINR implies a higher MCS. Figure 2.6 shows the SINR-to-CQI mapping for a 10% BLER threshold.

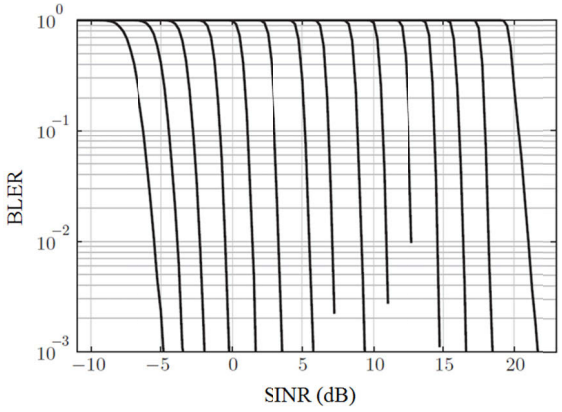

Figure 2.5: BLER curves [70]

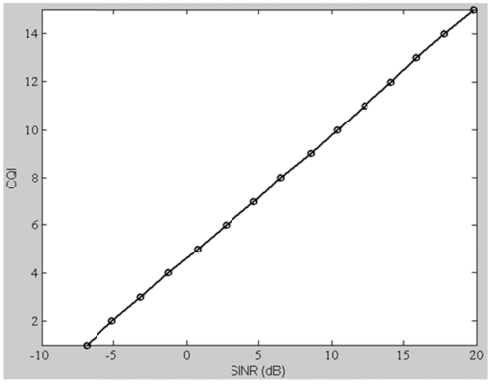

Figure 2.6: SINR-to-CQI mapping for 10% BLER threshold

In this thesis, it is assumed that the CQI is reported to the eNB on each PRB by a UE. A practical downlink LTE and LTE-A is considered to have a 10% BLER threshold [87]. The practical downlink system is assumed that:

1. All eNBs in the system constantly use the latest correctly received CQI whenever the last CQI report is not available.

2. All eNBs in the system are able to detect any error within the CQI report.

3. The erroneous CQI report is discarded and the latest correctly received CQI is used for packet scheduling [88-90].

4. All eNBs use an outdated CQI reported by UEs directly.

CQI report is used for making a scheduling decision at eNB and the Modulation and Coding (MCS) scheme used for UE data transmission. Table 2.2 presents the efficiency of bits per RE in CQI table for 10% BLER threshold. It can be observed in Table 2.2 that a higher order MCS results in a higher efficiency.

Table 2.2: CQI table (10% BLER threshold) [87]

CQI	***Minimum SINR (dB)***	***MCS***		***Efficiency (Bits/RE)***
		Modulation	***Approximate code rate***	
0	<-6.936	Out of range	--	--
1	-6.936	QPSK	0.0762	0.1523
2	-5.147	QPSK	0.1172	0.2344
3	-3.18	QPSK	0.1885	0.3770
4	-1.253	QPSK	0.3008	0.6016
5	0.761	QPSK	0.4385	0.8770
6	2.699	QPSK	0.5879	1.1758
7	4.694	16 QAM	0.3691	1.4766
8	6.525	16 QAM	0.4785	1.9141
9	8.573	16 QAM	0.6016	2.4063
10	10.366	64 QAM	0.4551	2.7305
11	12.289	64 QAM	0.5537	3.3223
12	14.173	64 QAM	0.6504	3.9023
13	15.888	64 QAM	0.7539	4.5234
14	17.814	64 QAM	0.8525	5.1152
15	19.829	64 QAM	0.9258	5.5547

It is assumed in this thesis that the total REs within an PRB in a practical LTE and LTE-A are limited to 148 for the 10% BLER threshold due to the fact that REs are used for control and signalling purposes [11]. Given the CQI table in Table 2.2 and the total number of REs specified for downlink data transmission, the instantaneous data rate of user *i* on PRB *j* at time *t* ($r_{i,j}(t)$) can be calculated as follows:

$$r_{i,j}(t) = Efficiency_{i,j}(t) * \frac{RE_{data}}{TTI} \tag{2.13}$$

where $Efficiency_{i,j}(t)$ is the efficiency (in bits/RE) of PRB *j* of user *i* at time *t* and RE_{data} is the total number of REs specified for downlink data transmission.

2.6 Reference Signal Received Power (RSRP)

RSRP is expressed as the received signal strength without the sum of thermal noise and inter-cell interference. Similar to SINR, RSRP experienced by a UE varies in each timeslot and on each PRB. The RSRP on a PRB was computed on a sub-carrier located at the center frequency of the PRB. Furthermore, an average RSRP among total number of PRBs can be further obtained from the sum of the RSRP on each PRB divided by the total number of PRBs in the simulation. In this thesis, an average RSRP is used for determine the most appropriate target eNB. The RSRP ($RSRP_{i,j}(t)$) experienced by user *i* on PRB *j* at time *t* and the average RSRP ($\overline{RSRP}_i(t)$) experienced by user *i* at time *t* is computed as follows respectively [91]:

$$RSRP_{i,j}(t) = P_{total} * gain_{i,j}(t) \tag{2.14}$$

$$\overline{RSRP}_i(t) = \frac{\sum_{j=1}^{J} RSRP_{i,j}(t)}{J} \tag{2.15}$$

Where $RSRP_{i,j}(t)$ is the RSRP (in dBm) of user *i* on PRB *j* at time *t*, $gain_{i,j}(t)$ is the channel gain from Equation (2.12) of user *i* on PRB *j* at time *t*, P_{total} is the total eNB transmit power (in dBm), $\overline{RSRP}_i(t)$ is the average RSRP (in dBm) of user *i* among all PRBs at time *t*, and *J* is the total number of PRBs.

2.7 Handover

The handover mechanism such as handover algorithm and/or decision maker has to be implemented in the downlink LTE model in multi-cell scenario for users travelling between eNBs. Two components are involved: handover processor and MME/Gateway need to be added into eNodeBs and the simulation environment, respectively. Figure 2.7 shows a downlink LTE model in a multi-cell scenario.

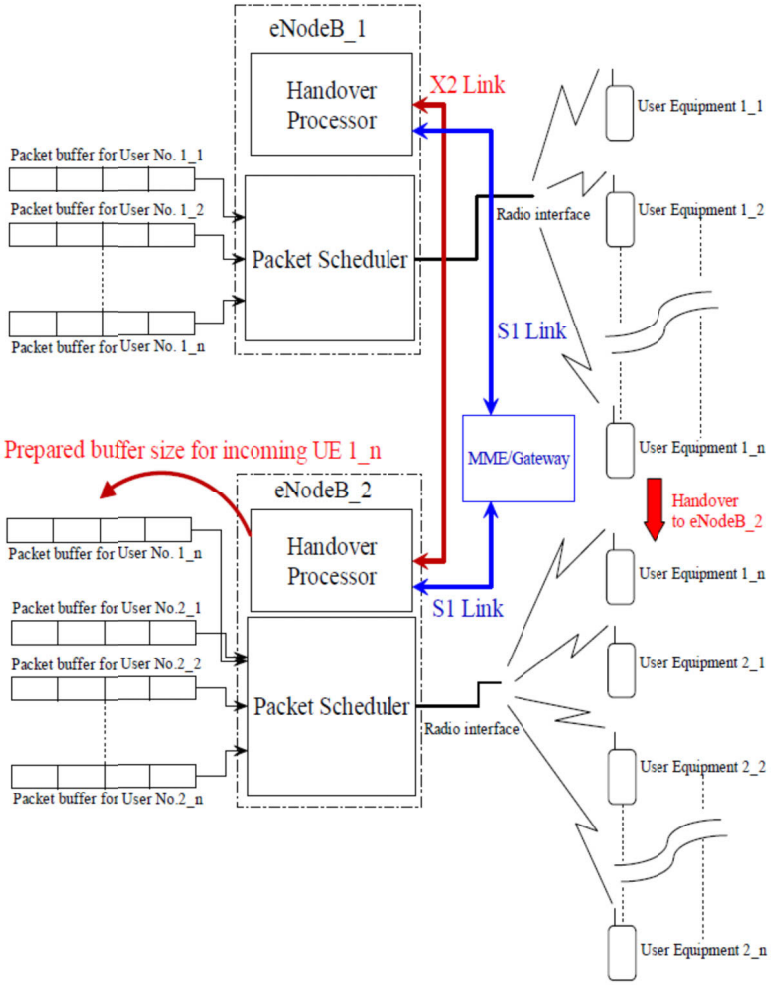

Figure 2.7: The downlink LTE model in a multi-cell scenario

The requirement of handover modelling in the downlink LTE model in multi-cell scenario were divided in to three parts; user equipment (UE), eNodeB, and

gateway/mobile management entity (MME). Each part consists of three phrases as this is the standard format of handover procedure in LTE [92].

A. User Equipment (UE)

In preparation phase, the measurement report sent from the UE is a major basis for the eNodeB to make a decision. It consists of three input values, and three output values to the serving eNodeB as shown in Figure 2.8. Figure 2.8 shows the basic concept of the input/output of a measurement report.

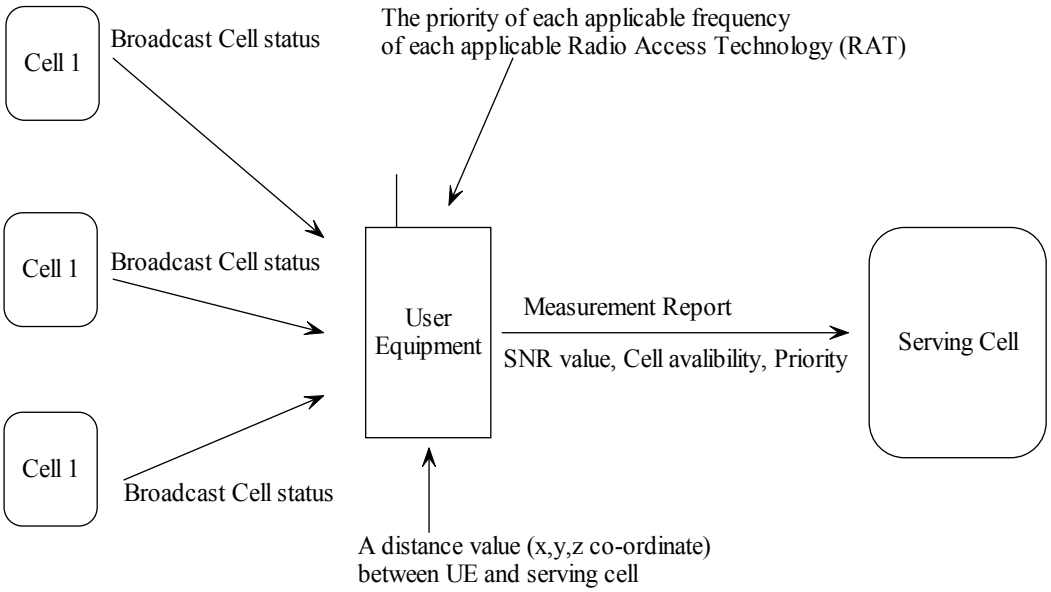

Figure 2.8: The input/output of a measurement report

Inputs:

1. The priority of each applicable frequency of each applicable RAT.

2. Neighbouring cell status (i.e. whether neighbouring cell is congested or reserved).

3. A distance value (x,y, and z co-ordinate) between a UE and source eNodeB.

Outputs in the measurement report:

1. The SINR value calculated by the UE.
2. Cell availability.
3. The priority of each applicable frequency of each applicable RAT.

In the execution phase,

1. The UE needs to perform a random access procedure on the Random Access Channel (RACH) in the target cell. In order to simulate the handover behavior, it is assumed in this thesis that this RACH selection will be successful each time the UE connects to the target eNodeB.
2. The UE needs to get uplink time alignment assigned for target eNodeB.
3. The UE needs to get UL / DL resources scheduled in order to be able to commence user data transmission.
4. The UE needs to send a HANDOVER COMPLETE message in the target cell.

In the completion phase, there is only one step involved in the UE side; the UE needs to be performed the tracking area update (TAU) back to the MME.

B. eNodeB

In preparation phase,

1. A hysteresis value of RSRP in source eNodeB should be setup for triggering the handover procedure. The formula of the handover triggering is as follow [93],

$$Mn + Ofn + Ocn - Hys > Ms + Ofs + Ocs + Off \tag{2.16}$$

where *Mn* is the measurement result of the neighbouring cell, *Ofn* is the frequency specific offset of the neighbour cell frequency, *Ocn* is the cell specific offset of the neighbour cell, *Hys* is the hysteresis parameter for a handover event, *Ms* is the measurement result of the serving cell, *Ofs* is the frequency specific offset of the serving cell frequency, *Ocs* is the cell specific offset of the serving cell, and *Off* is the offset parameter for this event.

2. A HANDOVER REQUEST message sent from source to target eNodeB is required. Two modes can be selected by the source eNodeB in this request, either lossless or seamless mode.

3. Target eNodeB has the rights to accept or deny this handover request by self-checking the capacity of its own.

4. Target eNodeB starts preparing buffer and paging for the incoming UE.

5. A HANDOVER REQUEST ACK message sent from target to source eNodeB is required. Two modes can be accepted in this ACK, either lossless or seamless mode. If the target eNodeB accepts the handover request in Step 2, do Step 5. Otherwise ignore Step 5.

6. A HANDOVER COMMAND message sends to the UE from source eNodeB, if the source eNodeB receives the HANDOVER REQUEST ACK message from Step 5, do Step 6, otherwise ignore Step 6.

In execution phase,

1. The source eNodeB starts sending user plan data to target eNodeB by X2 interface, the data forwarding process.

2. The target eNodeB has to measure on the UL transmission of the UE (on the RACH).

3. Determine the timing advance that the UE has to use for its UL transmissions. This timing advance is used for arrival time synchronization of multiple UEs at the target eNB.

4. When target eNodeB receives the HANDOVER COMPLETE message from the UE, it needs to trigger the variation procedure to check the identifier of this UE has the rights to access this cell or not.

5. The target eNodeB starts sending DL data to the UE.

In completion phase,

1. The target eNodeB needs to send the PATH SWITCH REQUEST message to the MME/GW.

2. Target eNodeB sends out the RELEASE RESOURCE message to the source eNodeB.

2.8 Packet Scheduling

Packet Scheduling schedules the user data packets arriving at the eNB by segmenting them into fixed smaller packet size, time-stamped and place them in the user buffer at the eNB queued for transmission based on a First-In-First-Out (FIFO) basis. In this thesis, each user's packet in the eNB was assumed as fully buffered throughout the simulation. The packet delay is the total waiting time of each user packet stays in the eNB buffer until it has been transmitted. There is no packet delay computation considered in this thesis if the packets that have been discarded by the eNB or correctly received by the UEs in the simulation. The packet delay is mathematically expressed as:

$$DP_{l,i}(t) = t - TOA_{l,i} \quad l \in \textit{packets in eNB buffer / transmission buffer} \tag{2.17}$$

where $DP_{l,i}(t)$ is the delay of the *lth* packet of user *i* at time *t* and $TOA_{l,i}$ is the time of arrival of the *l*th packet of user *i* in the eNB buffer.

A packet is discarded if it has been staying in the eNB buffer for a period of time which exceeds a buffer delay threshold. In this thesis, a buffer delay threshold is defined as the maximum time that a packet can stay in the eNB buffer. This threshold varies depending upon the types of traffic and/or applications.

The packet scheduler selects the user with highest priority (depend on varies requirements) and transmits this user's data packets in each TTI on each PRB. A PRB in the downlink LTE and LTE-A can be assigned once only to a user in one TTI, however multiple PRBs can be assigned to the same user in each TTI. Once a user is selected, the packet scheduler always schedules the retransmission packets (if any) ahead of the first transmission packets.

A TB is a group of packets that is transmitted to a user in a TTI. Each TB has a unique Transmission Sequence Number (TSN) which is used to identify the sequence delivery of packets towards the Application Layer [46]. The Cyclic Redundancy Check (CRC) bits are builded in TSN for error detection. A user can only have one TB of first transmission or retransmission at each TTI. The size of a TB varies by the channel quality and depends on the MCS on each RB which was assigned to the user. Figure 2.9 shows a TB diagram with number of packets and CRC bits.

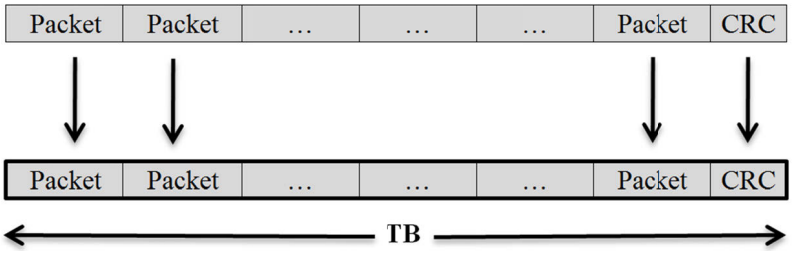

Figure 2.9: A TB diagram with number of packets and CRC bits [55]

A user feeds back an ACK Acknowledgement indicates a TB that is correctly received while a Negative Acknowledgement (NACK) indicates a TB failed in decoding. The

packets belong to a TB are removed from the transmission buffer in the eNB if any of these requirements below is satisfied:

1. An ACK Acknowledgement feedback associated with the TB is received.
2. The associated TB reaches the maximum number of retransmissions.
3. A radio link control (RLC) message indicating the expiry timer is received.

Otherwise all user data packets are stored into a transmission buffer in the eNB up on transmission [94-96]. Furthermore, all user data packets of a TB are removed from the transmission buffer if the delays of the user data packets exceed the buffer delay threshold. Three packet scheduling algorithms are modelled in this thesis: Maximum Rate (Max-Rate) algorithm, Round Robin (RR) algorithm, and Proportional Fair (PF) Algorithm. Each of these algorithms will be described below in details.

2.8.1 Maximum Rate (Max-Rate) Scheduling Algorithm

Maximum Rate (Max-Rate) [97] algorithm always selects the user with the best channel quality for transmission the packets on a radio resource. This algorithm maximises system throughput as it transmits packets to the users with the best channel quality at that time. However, it is less likely to have any transmission opportunity to a user with a poor channel quality. The users with a poor channel quality are always ignored in the favour of the users in better channel conditions. The users with a poor channel quality will not be scheduled unless their channel conditions are improved. Therefore Max-Rate is not capable of guaranteeing fairness among the users. Max-Rate algorithm can be expressed in the following:

$$\mu_i(t) = r_i(t) \tag{2.18}$$

where $\mu_i(t)$ is the priority of user i at scheduling interval t and $r_i(t)$ is the instantaneous data rate (across the whole bandwidth) of user i at scheduling interval t.

2.8.2 Round Robin (RR) Algorithm

Round Robin (RR) algorithm allocates equal segment of packet transmission time and resource to each user in a cyclic fashion. RR algorithm achieves the best fairness

performance without taking the channel quality of each user into consideration. Since RR does not consider the channel condition for each user as a factor in the algorithm, it results in a comparatively lower throughput performance than other packet scheduling algorithms.

2.8.3 Proportional Fair (PF) Algorithm

Proportional Fair (PF) algorithm [98] provides a better trade-off between throughput maximization and fairness guarantee. PF algorithm schedules packets of a user in each scheduling interval as expressed below:

$$\mu_i(t) = \frac{r_i(t)}{R_i(t)} \tag{2.19}$$

$$R_i(t+1) = \left(1 - \frac{1}{t_c}\right) R_i(t) + I_i(t+1) * \frac{1}{t_c} * r_i(t+1) \tag{2.20}$$

$$I_i(t+1) = \begin{cases} 1 & \text{if packets of user i are scheduled at scheduling interval } t+1 \\ 0 & \text{if packets of user i are not scheduled at scheduling interval } t+1 \end{cases} \tag{2.21}$$

where $\mu_i(t)$ is the priority of user i at scheduling interval t, $r_i(t)$ is the instantaneous data rate (across the whole bandwidth) of user i at scheduling interval t, $R_i(t)$ is the average throughput of user i at scheduling interval t, $I_i(t+1)$ is the indicator function of the event that packets of user i are selected for transmission at scheduling interval $t+1$ and t_c is a time constant.

The t_c value provides a control between throughput maximisation and fairness guarantee in the PF algorithm. The PF performance is comparable to the Max-Rate at a higher t_c and comparable to the RR algorithm at a lower t_c. A t_c value of 1000 ms [98] is used in this thesis to provide a better trade-off between throughput and guaranteed fairness.

2.9 Hybrid Automatic Repeat Request (HARQ)

Each TB in LTE and LTE-A is encoded prior to transmission or retransmission [99]. Three kinds of bits are included in an encoded TB: information bits, parity bits, and CRC bits. The CRC bits are used for checking the correctness of the encoded TB received by a user. The user feeds back an ACK or NACK indicating a TB is correctly decoded or not (i.e. not all packets are correctly decoded), respectively. While a NACK

is received, the eNB needs to schedule a retransmission for this TB. The erroneous TB received by the user is either discarded or buffered and combined the later subsequent retransmission as referred to Type I or Type II HARQ, respectively.

In this thesis, two well-known existed Type II HARQ techniques are considered: Chase Combining (CC) [100] and Incremental Redundancy (IR) [101]. CC retransmits an identical TB with the same attributes as in the first transmission such as the same MCS, the same number of RBs used, and the same TSN. The identical retransmitted TB is later combined with previously received TB at the user.

The IR technique generates various multiple versions of a TB. A number of combination of information bits, parity bits, and CRC bits are used in each version of a TB. A different version of the TB was sent in each retransmission. The user receiving each retransmission TB is provided additional information for increasing the probability of successful decoding the TB.

In this thesis, a HARQ protocol namely Stop-and-Wait (SAW) was used. A 8 ms duration is needed for the SAW protocol to complete a cycle in LTE and LTE-A [102]. A complete SAW HARQ cycle is shown in Figure 2.10. While the first 1 ms is used to send a TB from the eNB to the user, a following 3 ms duration is used by the user to decode the received TB and perform a CRC check. Then the user encodes and sends a HARQ feedback (ACK or NACK) back to the eNB within the next 1 ms. Lastly, the eNB decodes the HARQ feedback and constructs a new encoded TB based on the feedback within the following 3 ms.

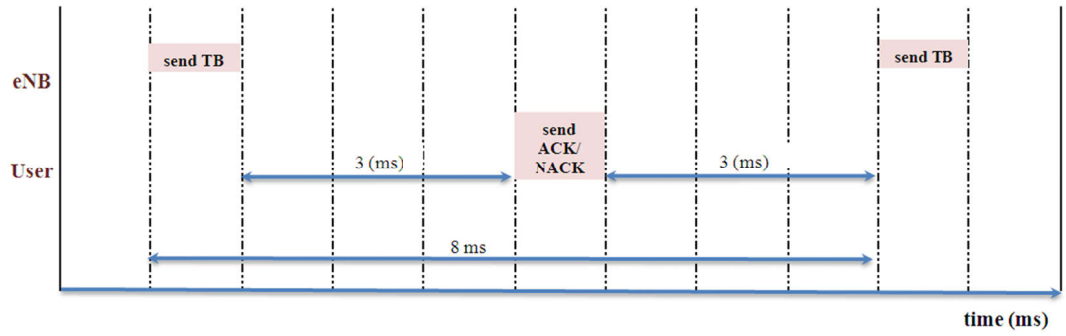

Figure 2.10: A complete SAW HARQ cycle [103]

2.10 Traffic Characteristics

It was assumed in this thesis that a user with an active data session is running either RT or NRT applications. The web browsing is a NRT application while constant streaming is a RT application. The web browsing and the constant streaming are discussed in the following sub-sections.

2.10.1 Web Browsing Traffic Model

Figure 2.11 shows a typical web browsing session as a sequence of packet calls. There is a combination of one main object and multiple embedded objects in a packet call as shown in Figure 2.11.

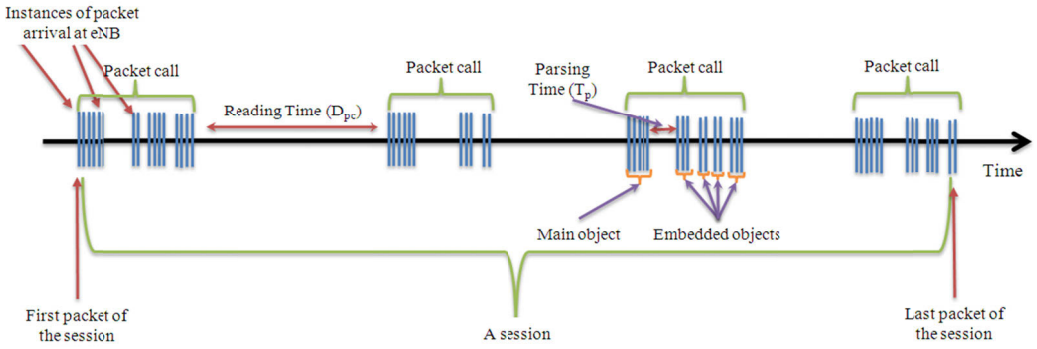

Figure 2.11: A typical web browsing session [33]

The main object represents the body of the web page while the embedded objects are the banners, icons, multimedia files…etc. embedded in the web page. The sizes of the main object (S_M) and the embedded object (S_E) are modelled using a truncated lognormal distribution. The number of embedded objects in a packet call (N_d) is modelled using a truncated Pareto distribution. The parsing time (T_p) and the reading time (D_{pc}) are the inter-arrival time between the main object and the first embedded object and the inter-arrival time between two consecutive packet calls, respectively. Both of the T_p and the D_{pc} followed an exponential distribution. Table 2.3 summarises the parameters of a web browsing application.

Table 2.3: Web browsing parameters [33]

Information types	***Distribution and parameters***	***PDF***
Main object size (S_M)	*Truncated lognormal* Mean = 10710 bytes Standard deviation (std. dev.) = 25032 bytes Minimum = 100 bytes Maximum = 2 Mbytes	$f_x = \frac{1}{\sqrt{2\pi}\sigma x}\exp\left[\frac{-(\ln x-\mu)^2}{2\sigma^2}\right] \quad x \geq 0$ σ=1.37,μ=8.35
Embedded object size (S_E)	*Truncated lognormal* Mean = 7758 bytes Std. dev. = 126168 bytes (Minimum =50 bytes Maximum =2 Mbytes	$f_x = \frac{1}{\sqrt{2\pi}\sigma x}\exp\left[\frac{-(\ln x-\mu)^2}{2\sigma^2}\right] \quad x \geq 0$ σ=2.36,μ=6.17
Number of embedded objects per page (N_d)	*Truncated Pareto* Mean=5.64 Max= 53	$f_x = \left[\frac{\alpha k^\alpha}{x^{\alpha+1}}\right] \quad k \leq x < m$ $f_x = \left[\frac{k}{m}\right]^\alpha \quad x = m$ α=1.1, k=2, m=55 Note: subtract k from the generated random value to obtain N_d.
Reading time (D_{pc})	*Exponential* Mean= 30 sec	$f_x = \lambda e^{-\lambda x} \quad x \geq 0$ χ=0.033
Parsing time (T_p)	*Exponential* Mean= 0.13 sec	$f_x = \lambda e^{-\lambda x} \quad x \geq 0$ χ =7.69

2.10.2 Constant Stream Model

Constant streaming can be modelled as a sequence of packets that are constantly received by users and each packet arrives at a regular time interval. The constant stream traffic provides Constant Bit Rate (CBR) to the users for the entire simulation. Generally, the packet size and the data rate remains constant at all time. In this thesis, a constant 1 Mbps data rate stream is considered for the constant stream model. A sample of constant stream packet arrivals for 1 Mbps data rate for 1000 ms simulation is shown in Figure 2.12.

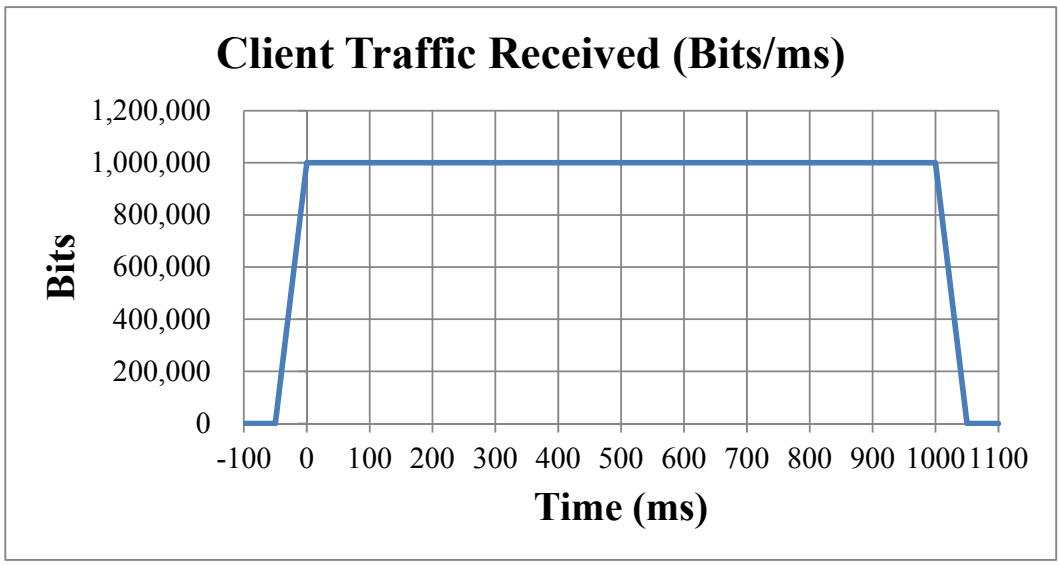

Figure 2.12: A sample of constant stream for 1 Mbps data rate for 1000 ms simulation

2.11 Performance Metrics

A number of metrics such as system throughput, service PLR (Packet Loss Ratio), system delay, RB utilisation and number of handovers are used in this thesis to evaluate packet scheduling and handover performance. These metrics can be divided into three categories: LTE, LTE-A, and both LTE and LTE-A defined as follows.

2.11.1 LTE

System throughput in bits per second is an indication of the size of the transmission pipe between eNB and UE. It is defined as the total size of successfully transmitted packets at all users in the downlink divided by the simulation time. It can be mathematically expressed as:

$$system \;\; throughput = \frac{1}{T}\sum_{i=1}^{N}\sum_{t=1}^{T} prx_i(t) \tag{2.22}$$

where $prx_i(t)$ is the total size of correctly received packets (in bits) of user i at time t, T is the total simulation time and N is the total number of users.

PLR is an indication of the percentage of correctly received data (in bits) at receiver. It is defined as the ratio of total size of discarded packets to the total size of all packets arriving into the eNodeB buffer. The PLR has to be maintained below a threshold

during the simulation in order to satisfy the QoS requirement of a service. The PLR value should be as low as possible to ensure to a better performance. The expression for PLR is given in the following equation:

$$service\ PLR = \frac{\sum_{i=1}^{N_{service}} \sum_{t=1}^{T} pdiscard\_service_i(t)}{\sum_{i=1}^{N_{service}} \sum_{t=1}^{T} psize\_service_i(t)} \tag{2.23}$$

where *service PLR* indicates the PLR of a certain type of service (either RT or Non-RT service), $pdiscard\_service_i(t)$ is the total size of discarded packets (in bits) of user i of a service at time t, $psize\_service_i(t)$ is the total size of all packets (in bits) that have arrived into the eNB buffer of user i of a service at time t, $N_{service}$ is the total number of users of a service and T is the total simulation time in millisecond.

System delay is an indication of the average waiting time of packet before transmission. It is defined as average system Head-of-Line (HOL) delay or queuing delay. A HOL delay is defined as the time duration from the time of arrival of the HOL packet at the eNodeB buffer to current time. The system delay needs to always be kept at a minimum value. The HOL packet of a user is the packet that has stayed in its buffer at the eNB for the longest time.

$$W_i(t) = \max\left\{DP_{l,i}(t)\right\} \quad l \in packets\ in\ eNB\ buffer \tag{2.24}$$

where $W_i(t)$ is the delay of the HOL packet of user i at time t and $DP_{l,i}(t)$ is the delay of the *lth* packet of user i at time t. Both $W_i(t)$ and $DP_{l,i}(t)$ are in millisecond.

The average system delay is mathematically expressed as follows:

$$average\ system\ delay = \frac{1}{T}\sum_{t=1}^{T}\frac{1}{N}\sum_{i=1}^{N}W_i(t) \tag{2.25}$$

where $W_i(t)$ is the delay of the HOL packet of user i at time t (Equation (2.24)), N is the total number of users and T is the total simulation time.

2.11.2 LTE-A

The LTE-A system throughput is defined as the total transmitted packets per second and can be mathematically expressed as:

$$system\ throughput = \frac{1}{T}\sum_{t=1}^{T}\sum_{i=1}^{N} ptransmit_{c\_i}(t) \quad c \forall CTP_i \tag{2.26}$$

where N is the total number of UEs, T represents the total simulation time, and $ptransmit_{c\_i}(t)$ denotes the number of transmitted bits of cell c whichever earlier received by UE i at time t. Cell c belongs to CoMP Transmission Point (CTP) of UE i.

PLR gives the percentage of discarded packets. A packet is discarded once the delay of the packet goes beyond the delay deadline. PLR can be mathematically expressed as:

$$PLR = \sum_{t=1}^{T}\sum_{i=1}^{N} pdiscard_{c\_i}(t) \Big/ \sum_{t=1}^{T}\sum_{i=1}^{N} psize_{c\_i}(t) \quad c \forall CTP_i \tag{2.27}$$

where N is the total number of UEs, T represents the total simulation time, and $pdiscard_{c\_i}(t)$ and $psize_{c\_i}(t)$ denotes the total discarded packet size and total packet size of cell c whichever earlier received by UE i at time t, respectively. Cell c belongs to CTP of UE i.

The average system delay is mathematically expressed as follows:

$$average\ system\ delay = \frac{1}{T}\sum_{t=1}^{T}\frac{1}{N}\sum_{i=1}^{N} W_{c\_i}(t) \quad c \forall CTP_i \tag{2.28}$$

where $W_i(t)$ is the delay of the HOL packet of cell c for the earliest received packet by UE i at time t (Equation (2.24)), N is the total number of users and T is the total simulation time. Cell c belongs to CTP of UE i.

2.11.3 Both LTE and LTE-A

RB utilization is an indication of how well the available PRBs are used in a LTE system. It is defined as time average of the proportion of total used PRBs to total PRBs in each cell. It can be expressed as:

$$AverageRB\ utilisation_c = \frac{1}{T}\sum_{t=1}^{T}\frac{PRBuse_c(t)}{PRB\max_c} \tag{2.29}$$

where $PRBuse_c(t)$ denotes the total PRBs being used in cell c at time t and $PRBmax_c$ denotes the total PRBs in cell c. A high RB utilization value indicates the cell is in a highly saturated state at current time instant. When UEs are going to be handed over to a cell with high RB utilization, handover requests have to be rejected. On the other hand, when the cell is having a low RB utilization value, it seems the cell is more capable of accommodating more incoming UEs.

The total number of handovers is defined as the number of handovers of all users during the simulation interval and can be mathematically expressed as:

$$THO = \sum_{t=1}^{T}\sum_{i=1}^{N} HO_{t\_i} \tag{2.30}$$

where N is the total number of users, T represents the total simulation time, HO_{t_i} denotes the number of handovers of user i at time t, and THO represents total number of handovers.

2.12 Summary of Assumptions

All the assumptions that were used in the thesis are summarised in this section. These assumptions are:

1. The instantaneous SINR on a PRB is computed based on the center frequency of the PRB located on a sub-carrier and there are minimum variations of multi-path fading among the sub-carriers of a PRB.
2. Inter-cell interference is assumed to be constant.
3. The CQI is reported to the eNodeB on each PRB.
4. Each UE's packet is buffered without lost in the eNodeB throughout the simulation.

2.13 Summary

This chapter described a general downlink LTE and LTE-A system model implemented within the system level simulator. The modelling of the downlink LTE and LTE-A topology (seven cells model), mobility, radio propagation (Hata model, Gaussian distribution, and Rayleigh fading model), CQI reporting, RSRP, handover, packet scheduling, and HARQ were discussed. The traffic characteristics of the real time and non-real time services are presented. The performance metrics (system throughput, PLR, system delay, RB utilisation, and number of handovers) that were used to evaluate handover performance and the assumptions that are used in the thesis were defined.

Chapter 3

HANDOVER ALGORITHMS

An algorithm is an effective method for solving a problem expressed as a finite sequence of instructions. It is usually a high-level description of a procedure which manipulates well-defined input data to produce other data [104]. An algorithm can be used to solve a given problem, implement a solution, and communicate about your problem/solution to people. A handover algorithm is used for making a handover decision and it consists of one or more conditions associated with radio propagation related handover parameters. A handover will be triggered only if conditions specified in the handover algorithm are satisfied. The environmental conditions used in a handover algorithm could vary over time depending on a user's mobility.

This chapter studies the basic cell selection and handover schemes for cellular networks followed by a number of well-known handover algorithms. Thereafter, a proposed handover algorithm in LTE system is presented. The handover parameters of selected handover algorithms for LTE are optimized by applying a proposed optimization method. It is necessary to determine optimized handover parameters to ensure efficiency and reliability of a handover algorithm. The performance of selected handover algorithms is evaluated and compared using the optimized parameters. The performance study aims to identify the strength and the weakness of each selected handover algorithm with optimized handover parameters.

This chapter is organised as follows: Section 3.1 and Section 3.2 thoroughly describe the fundamental cell selection and basic handover schemes, respectively. Section 3.3 studies the two handover mechanisms in LTE system. Section 3.4 discusses several well-known handover algorithms and Section 3.5 discusses a proposed handover algorithm in LTE system. Section 3.6 discussed the performance of the selected handover algorithms in LTE with optimized handover parameters followed by the performance comparison. Finally, a summary of the chapter is given in Section 3.7.

3.1 Cell Selection

Cell Selection (CS) is a mechanism that is used to select the most appropriate cell for a UE to camp on as it moves within a cellular network. The major difference between CS and handover is differentiated by the on-going call or data session of the UE. CS takes place without an on-going call or data session whereas a handover only happens when a UE has an on-going call or data session. CS can be either using a distance-based or received signal strength-based process. Three basic CS schemes will be introduced in the following subsections: distance-based CS scheme, ideal CS scheme and normal CS scheme.

3.1.1 Distance-based Cell Selection (CS) Scheme

In the distance-based CS scheme, the mobile always camps on the nearest BS [105]. Figure 3.1 shows the basic concept of a distance-based CS scheme that r_1, r_2, and r_3 are the distance from the mobile to the three nearest base stations, BS_1, BS_2, and BS_3, respectively. Based on the distance-based CS scheme, the mobile station will choose and camp on the base station $_{BS}1$ in this example.

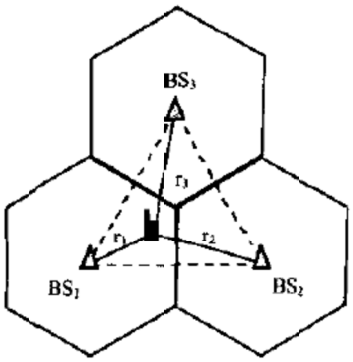

Figure 3.1: Distance-based Cell Selection Scheme [105]

3.1.2 Ideal Cell Selection (CS) Scheme

In the Ideal CS scheme [105], the mobile always chooses and camps on the BS which has the strongest received signal strength. Due to the rapid variation of the received signal strength, the BS with the minimum distance might not be the best BS. The Ideal CS scheme starts from gathering the received signal strength from different base stations followed by a maximum selection to select the best BS. Figure 3.2 shows the principle of the ideal CS scheme where E_{P1}, E_{P2}, and E_{P3} represent the received signal strength from BS_1, BS_2, and BS_3, respectively.

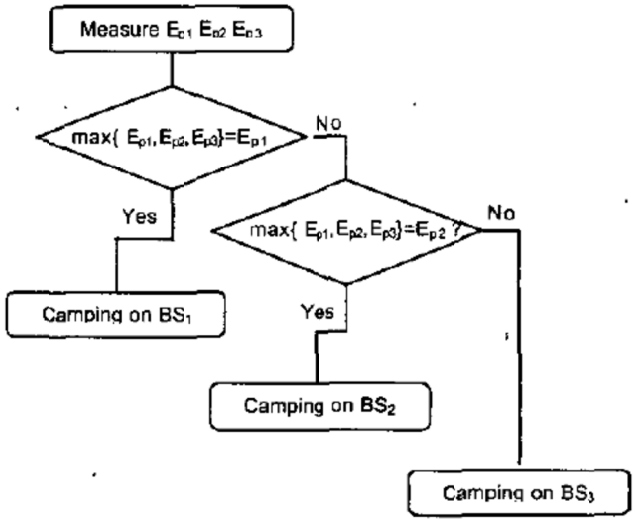

Figure 3.2: Flowchart of the Ideal Cell Selection Scheme [105]

3.1.3 Normal Cell Selection (CS) Scheme

However, the mobile may not be always camping on the best BS due to the mobility, radio propagation, or other reasons. A more realistic CS scheme is needed to include the real world scenarios. The basic principle of the Normal CS Scheme [105] is to have the mobile camp on the nearest BS unless the difference between the received signal strength from the source and target BS is above a certain threshold.

Figure 3.3 shows the flowchart of the Normal CS Scheme. The received signal strength difference between E_{P2} and E_{P1}, E_{P3} and E_{P1}, and E_{P3} and E_{P2} are computed and compared with CS_th (threshold) in the Normal CS Scheme. Moreover, when the

threshold CS_th equals to zero dB, the Normal CS scheme corresponds to the Ideal CS scheme due to the simplified comparison of choosing the maximum received signal strength between three base stations.

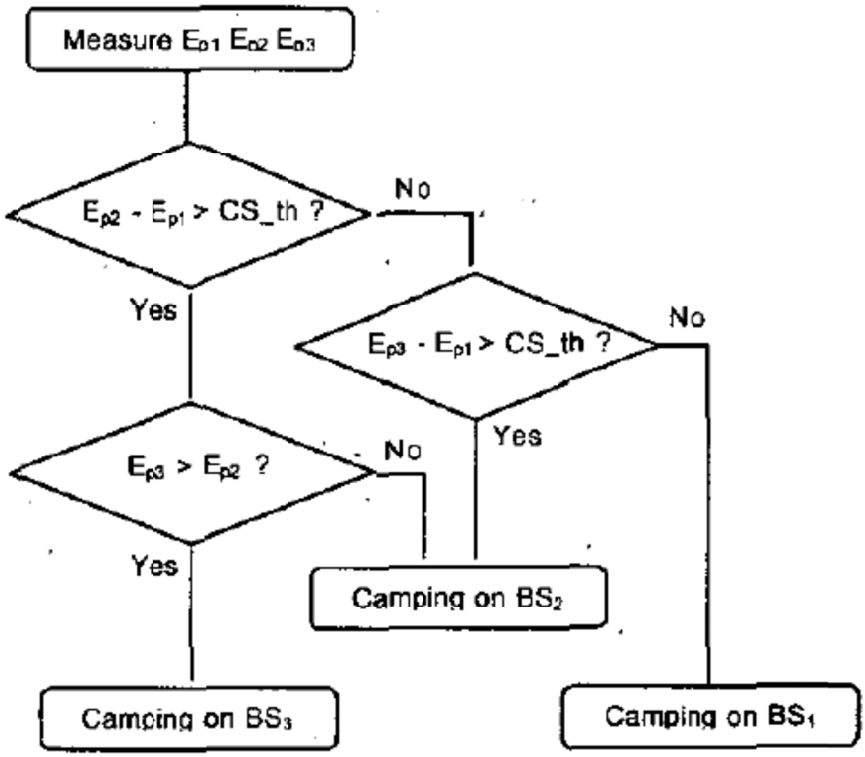

Figure 3.3: Flowchart of the Normal Cell Selection Scheme [105]

3.2 Handover Mechanisms

There are two types of handover mechanism in general: (a) hard handover [106] also known as Break-Before-Connect (BBC) handover and (b) soft handover [107] or Connect-Before-Break (CBB) handover. Hard and soft handover are discussed in the following subsections.

3.2.1 Hard Handover

In the legacy wireless systems, hard handover is the commonly used handover method. The hard handover requires a UE to break an existing connection with the current cell (source cell) and then make a new connection with a target cell [108]. Hard handover has been adopted in LTE system by 3GPP due to the flat IP-based architecture and the lack of a centralized controller. The use of hard handovers reduces the complexity of the handover mechanism and minimizes the handover delay. However, the hard handover approach causes call drop that may result in lost data during a session. Therefore, a mechanism to avoid data loss is needed for hard handovers.

3.2.2 Soft Handover

Soft handover is a category of handover mechanism where radio links are added and removed in such manner that the UE always keeps at least one radio link active to the mobile network [108]. Soft and softer handover were introduced in WCDMA/UTRAN architecture. Radio Network Controller (RNC) is the centralized device to perform handover control for each UE in the UMTS network. It is possible for a UE to be simultaneously connected to two or more cells (or cell sectors) during a call [109]. If the multiple connections from a UE are within the same physical site, it is referred to a softer handover. From a handover perspective, soft handover is better suited than hard handover for maintaining an active session without voice or packet call drop. However, the soft handover requires more signalling procedures in the WCDMA network. Figure 3.4 and Figure 3.5 show a soft handover with different NodeBs and softer handover within the same NodeB, respectively.

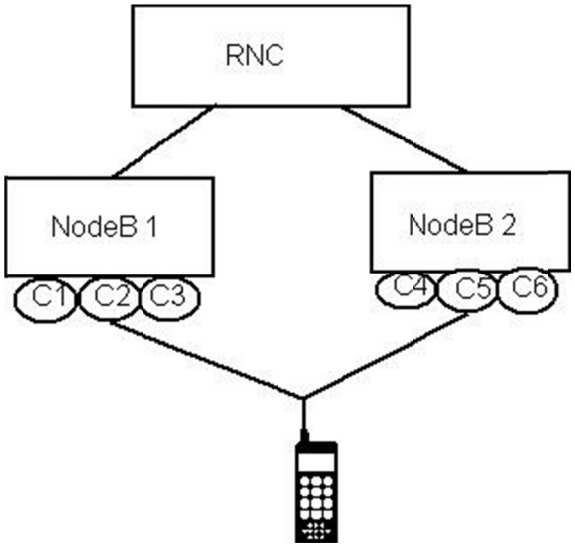

Figure 3.4: Soft handover with different NodeBs [110]

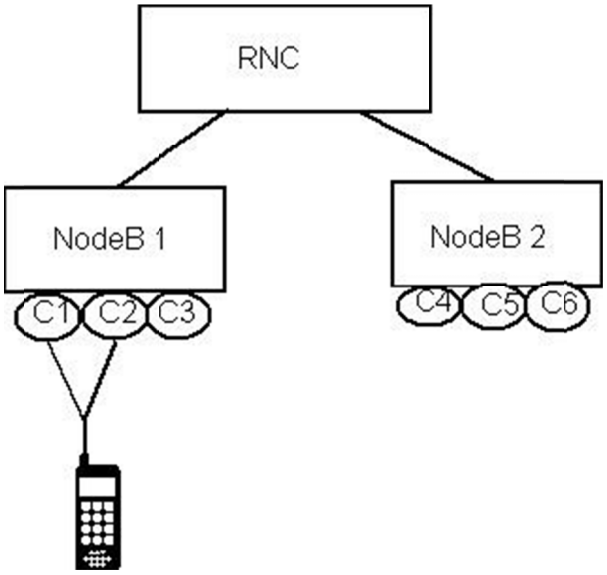

Figure 3.5: Softer handover within the same NodeB [110]

3.3 Handover in LTE

Handovers in 3GPP-LTE system are all hard handovers. There are two types of handover procedure in downlink LTE for UEs in active mode: S1 and X2 handover procedures. (Active mode means that the UE is transmitting or receiving packets to or from the core network.) Each of the handover procedures is discussed in the following subsections.

3.3.1 X2-based Handover

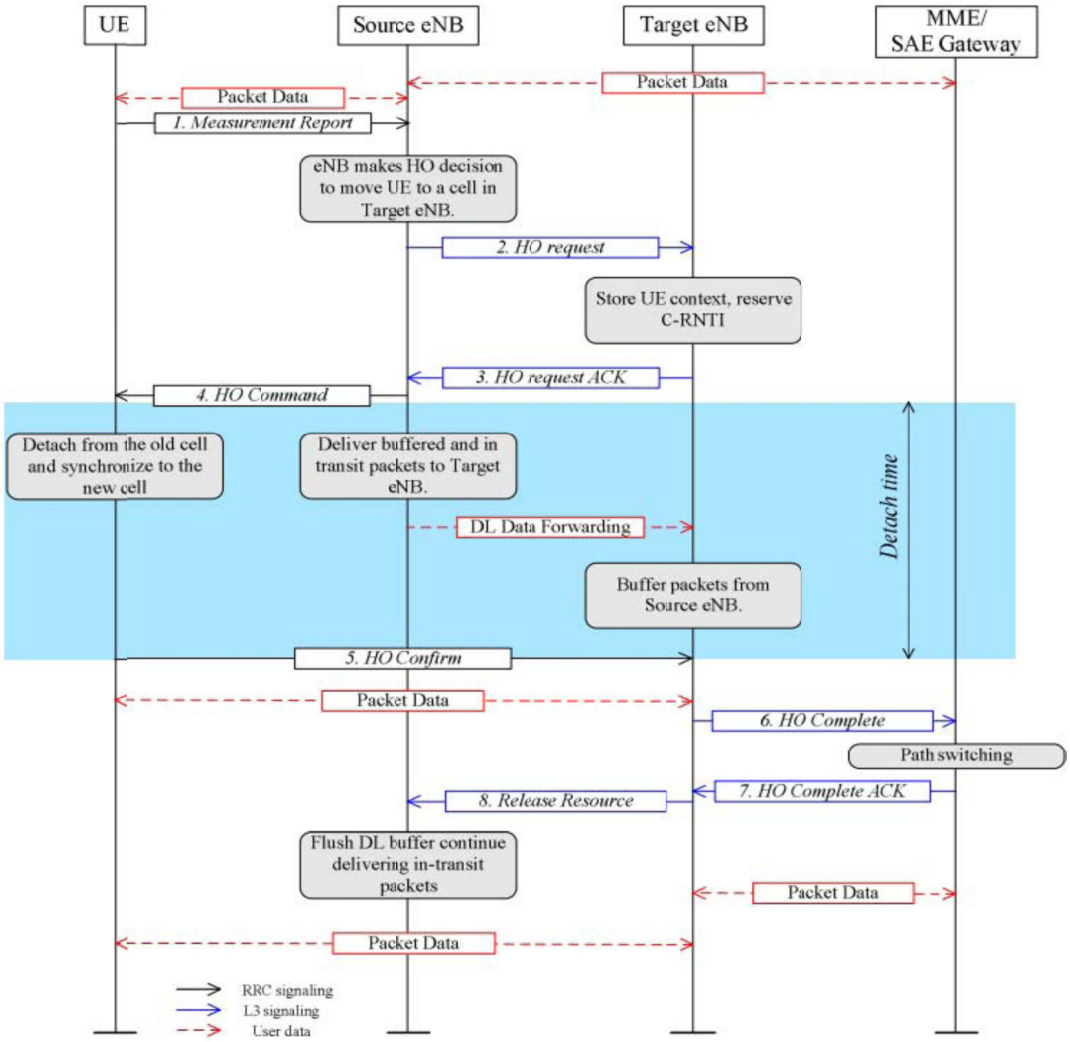

Figure 3.6: LTE X2-based handover procedure [111]

The X2-handover procedure is used for inter-eNodeB handover as well as balancing network load and hence minimizing interference. However, when an X2 interface is not present between two eNodeBs or if the source eNodeB has been configured to perform handover towards a particular target eNodeB via the S1 interface, then an S1-handover procedure will be triggered [112]. There are three phases involved in the S1 and X2 handover procedures namely preparation phase, execution phase, and completion phase [113, 114].

Figure 3.6 shows a simplified signal exchange diagram of the X2-based handover in LTE. The preparation phase starts from Step 1 to Step 4 when the source eNodeB initiates a handover decision to handover a UE to a target eNodeB based on the measurement report sent by the UE on a periodic basis. If the handover decision is made, the source eNodeB sends out a HANDOVER REQUEST message to the target eNodeB.

In LTE there are two modes (seamless and lossless modes) that can be used for seamless connectivity during handover. If the seamless mode is selected by the source eNodeB, it proposes the seamless mode to the target eNodeB in the HANDOVER REQUEST message (Step 2 in Figure 3.6). This request establishes a GPRS Tunnelling Protocol (GTP) tunnel between the source and target eNodeB for data forwarding. If the target eNodeB accepts the HANDOVER REQUEST message, the target eNodeB will first allocate an appropriate buffer size for the incoming UE and then inform the source eNodeB the tunnel endpoint where the forwarded data is expected to be received in the HANDOVER REQUEST ACK message (Step 3 in Figure 3.6). Similar to the seamless mode, if the source eNodeB selects lossless mode then the source eNodeB proposes to the target eNodeB in the HANDOVER REQUEST message (Step 2 in Figure 3.6). If the target eNodeB accepts it, the target eNodeB will first allolcate appropriate the buffer size for the incoming UE and then indicate in the HANDOVER REQUEST ACK message (Step 3 in Figure 3.6) to the source eNodeB. Additionally source eNodeB forwards those user plane downlink packets over X2 interface to the target eNodeB. These packets and a GTP extension header field are sent over X2 prior to the newly arriving packets from the source S1 path. The same GTP tunnel mechanism is used in the seamless handover mode. In addition, the target eNodeB must ensure that all the packets are delivered in-sequence at the target side. Once the source eNodeB receives the HANDOVER REQUEST ACK message (Step 3 in Figure 3.6), it now can send out the HANDOVER COMMAND message to the UE (Step 4 in Figure 3.6) requesting it to perform a handover action.

In the execution phase (Step 4 and Step 5 in Figure 3.6), the UE detaches from the source eNodeB and attempts to connect to the target eNodeB. The source eNodeB forwards the buffered and newly arrived packets to the target eNodeB instead of the UE (since the UE is not attached in the network) and the target eNodeB buffers all

forwarded packets from the source eNodeB for the UE. Meanwhile the UE starts to attach to the target eNodeB using a random access procedure on the RACH. The UE also needs to have uplink time alignment assigned by the target eNodeB by measuring the uplink transmission of the UE (on the RACH) [115]. After the UE attached to the target eNodeB, a HANDOVER COMFIRM message has to be sent to the target eNodeB (Step 5 in Figure 3.6) to complete the execution phase.

A completion phase begins after Step 5 in Figure 3.6 when the target eNodeB forwards the buffered packets to the UE. The target eNodeB informs the MME/Gateway to switch path from the source eNodeB to the target eNodeB by sending a HANDOVER COMPLETE message (Step 6 in Figure 3.6). The MME/Gateway will then update its path to the corresponding UE and send back a HANDOVER COMPLETE ACK message in responding the HANDOVER COMPLETE message (Step 7 in Figure 3.6). Target eNodeB sends out a RELEASE RESOURCE message to source eNodeB to flush the buffer in source eNodeB (Step 8 in Figure 3.6). Source eNodeB flushes the downlink buffer after receiving RELEASE RESOURCE message from target eNodeB.

According to [115], it is important to ensure the correct delivery order of packets while forwarding from the source to the target eNodeB in order to achieve high TCP throughput performance. Reference [116] purposed one possible solution that could be considered to avoid out of sequence problem during forwarding buffered packets.

3.3.2 S1-based Handover

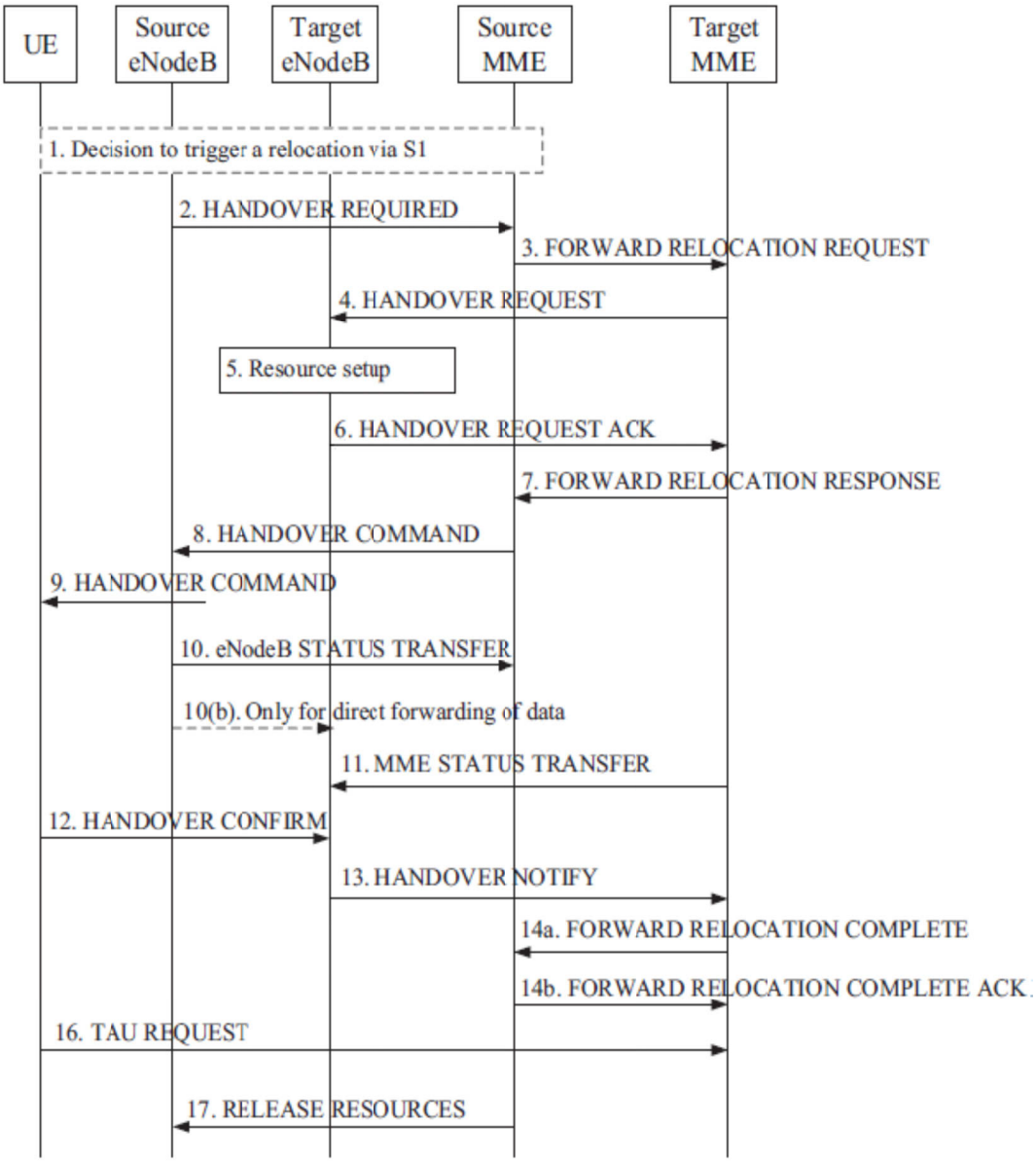

Figure 3.7: LTE S1-based handover procedure modified [102]

The S1-based handover procedure in LTE is shown in Figure 3.7. S1-based handover procedure is more complex than X2-based handover due to the fact that there does not exist a direct X2 link between two eNodeBs. The S1-based handover procedure also enables LTE to perform handover with other RATs such as CDMA2000/HRPD [61] due to its compatibility with other non-3GPP specific access technologies. There are

three phases involved in S1-based handover (a) preparation phase involving the core network where the resources are first prepared at the target eNodeB (from Steps 2 to Step 9 in Figure 3.7), (b) an execution phase (from Step 10 to Step 12 in Figure 3.7) and (c) a completion phase (from Step 13 to Step 17 in Figure 3.7) to complete the entire handover procedure.

In the preparation phase, the source eNodeB makes a handover decision and send out a HANDOVER REQUEST message to the source MME via the S1 interface. Source MME forwards the RELOCATION REQUEST message to the target MME. Target MME sends out the HANDOVER REQUEST message to the target eNodeB via the S1 interface. If the target eNodeB accepts this HANDOVER REQUEST message, the target eNodeB performs a resource setup for the incoming UE and then sends out a HANDOVER REQUEST ACK message back to the target MME via the S1 interface. A RELOCATION REQUEST message will be forwarded from the target MME to the source MME. A HANDOVER COMMAND message will be sent out from the source MME to the UE via the source eNodeB and indicates that the network is ready for the UE to perform this handover. The UE upon receiving the HANDOVER COMMAND message starts performing the handover action and the handover procedure moves to the execution phase.

In the execution phase, the source eNodeB sends out a eNodeB STATUS TRANSFER message to the source MME and the source MME in turn sends out a MME STATUS TRANSFER message to the target eNodeB via target MME. The source eNodeB directly forwards the buffered packets to the target eNodeB. The execution phase is completed after the UE attaches to the target eNodeB and sends out a HANDOVER CONFIRM message to the target eNodeB.

In the completion phase, target eNodeB sends out a HANDOVER NOTIFY message to the target MME (Step 13 in Figure 3.7) and a FORWARD RELOCATION COMPLETE message is sent by the target MME and acknowledged by the source MME (Step 14a and Step 14b in Figure 3.7). Lastly, a TRACKING AREA UPDATE (TAU) request will be directly sent from the UE to the target MME for updating local area information and the source MME will send out a RELEASE RESOURCE message

to the source eNodeB to release all the resources that were used for this handover process.

3.4 Handover Algorithms in LTE

In this section, several LTE based handover algorithms are introduced in the following sub-sections. One of the major problems with handover is the ping-pong effect which occurs when a mobile is continuously handed over between target and serving cells due to the rapid variation of received signal strengths. Ping-pong effect results in a wastage of network resources such as signalling overhead, extra resources allocation and data traffic delay increases. Therefore effectively preventing unnecessary handovers are essential.

A handover measurement period (*Tm*) is a time interval that is used for checking the handover condition periodically. Figure 3.8 shows a handover measurement period and the LTE Hard Handover Algorithm.

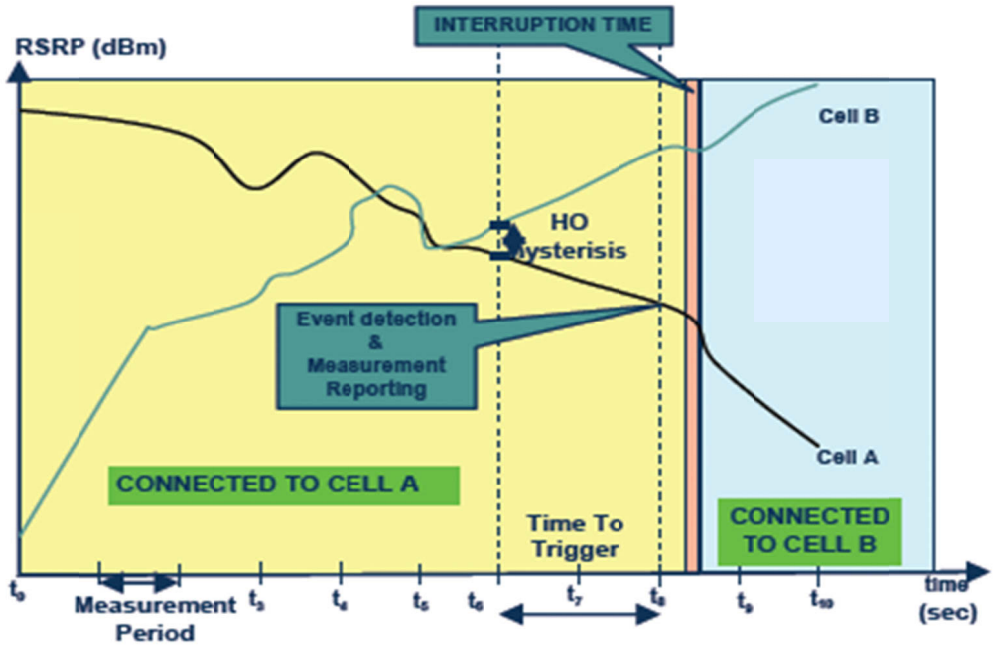

Figure 3.8: Handover Measurement Period in the LTE Hard Handover Algorithm [117]

3.4.1 LTE Hard Handover Algorithm [117]

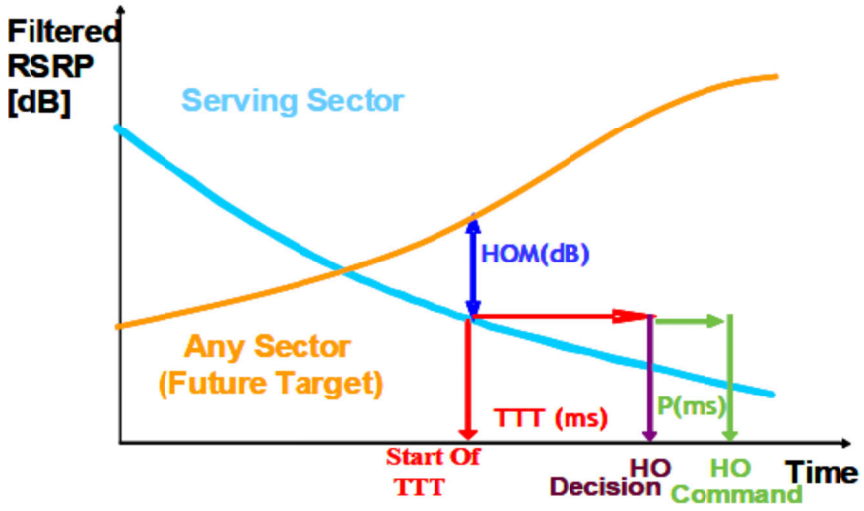

Figure 3.9: LTE hard handover algorithm [118]

LTE Hard Handover Algorithm also known as Power Budget Handover Algorithm is a simple basic effective handover algorithm that consists of two variables: Handover Margin (HOM) and Time to Trigger (TTT) value. A HOM is a parameter that represents a threshold value of difference in received signal strength between the serving cell and the target cell and is used to ensure the target cell is the most appropriate cell during handover. A TTT value is the time interval which the HOM condition is satisfied. A combination of TTT and HOM can prevent unnecessary handovers. A handover action can only be performed after the HOM and TTT condition are satisfied. Figure 3.9 shows the basic concept of LTE Hard Handover Algorithm.

When a mobile is moving away from the serving cell, the RSRP which the mobile received from the serving cell degrades with time. A handover decision has to be made if the equation expressed below is satisfied for the entire TTT duration:

$$RSRP_T > RSRP_S + HOM \tag{3.1}$$

where $RSRP_T$ is the RSRP received from the target cell and $RSRP_S$ is the RSRP received from the serving cell. A TTT observation is triggered when the Equation (3.1) is satisfied. During the TTT observation time slot, if the $RSRP_S$ gets higher than the $RSRP_T$

or the difference between $RSRP_T$ and $RSRP_S$ is less than the HOM, the TTT observation trigger will be reset. Otherwise a handover will be executed.

The number of handovers that occur are basically depending on the TTT value and the HOM value: the smaller the HOM and TTT value, the more the number of handovers.

3.4.2 Received Signal Strength (RSS) Based TTT Window Handover Algorithm [119]

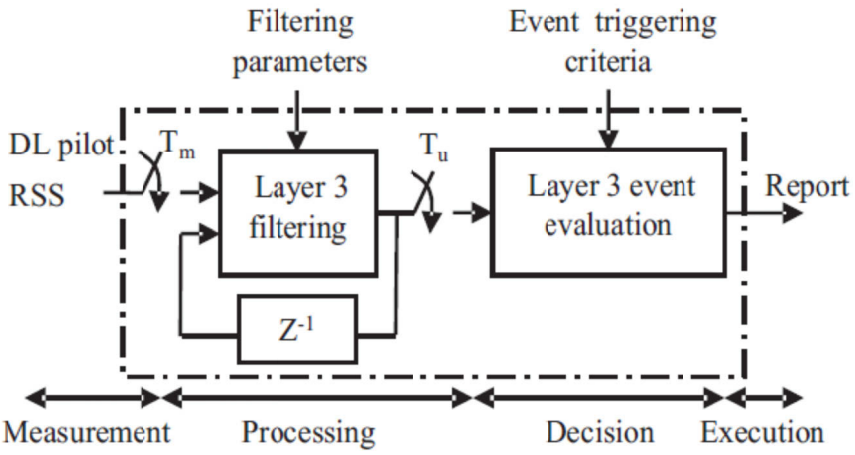

Figure 3.10: RSS Based TTT Window Handover Algorithm [119]

Figure 3.10 shows that RSS Based TTT Window Handover Algorithm consists of four steps: measurement, processing, decision, and execution. At the measurement step, the instantaneous RSRP value is stored at each and historical data is used at the processing step. A comparison based on this historical data at the processing step is performed at the decision step followed by the handover decision at the execution step.

The algorithm is separated into two parts: signal strength gathering and signal strength comparison. The formula used in the signal strength gathering part is expressed below:

$$\overline{RSS}(nTm) = \beta RSS(nTm) + (1-\beta)\overline{RSS}((n-1)Tm) \tag{3.2}$$

where $\overline{RSS}$ is the filtered RSS measured every Tm where n is the n-th interval. β is called "forgetting factor" and is defined as a fraction between 0 and 1 as shown below:

$$\beta = \frac{Tm}{Tu} \tag{3.3}$$

where *Tu* is an integer multiple of *Tm*. After the filtered RSS and the forgetting factor are computed from Equation (3.2) and Equation (3.3), the signal strength comparison is performed using the formula below:

$$\overline{RSS}(nTu)_T > \overline{RSS}(nTu)_S + HOM \tag{3.4}$$

where $\overline{RSS}(nTu)_T$ and $\overline{RSS}(nTu)_S$ are the filtered RSS of the target cell and serving cell at n-th *Tu* interval, respectively.

In the RSS Based TTT Window Handover Algorithm, as β gets closer to 0, the current $\overline{RSS}(nTm)$ is more dependent on the historical $\overline{RSS}((n-1)Tm)$. On the other hand, as β gets closer to 1, the current $\overline{RSS}(nTm)$ is more dependent on the current *RSS(nTm)*.

Unlike in LTE Hard Handover Algorithm, the TTT (*Tu*) is an integer multiple of *Tm*. The TTT observation has to be triggered whenever the filtered received signal strength of the target sector is greater than the filtered received signal strength of the serving sector plus HOM. If the filtered received signal strength of the target sector is less than the filtered received signal strength of the serving sector plus HOM at any time instant within a *Tu* window, the TTT observation will be stopped and reset. Otherwise the handover decision will be made after Equation (3.4) is satisfied for the *Tu* duration.

3.4.3 LTE Integrator Handover Algorithm [120]

The main concept of LTE Integrator Handover Algorithm is to make a handover decision using historical signal strength differences. The idea of historical data is similar to RSS Based TTT Window Handover Algorithm discussed in Section 3.4.2. There are three parts consist in LTE Integrator Handover Algorithm: RSRP difference calculation, filtered RSRP difference computation, and handover decision. The RSRP difference calculation can be expressed as follow:

$$DIFs\_i(t) = RSRP_T(t) - RSRP_S(t) \tag{3.5}$$

where $RSRP_T(t)$ and $RSRP_S(t)$ is the RSRP received by the UE from the target and the serving cell at time *t*, respectively. *DIFs_i(t)* is the RSRP difference of the user *i* at time *t*. The filtered RSRP difference computation can be expressed as follows:

$$FDIFs\_i(t) = (1-\alpha) * FDIFs\_i(t-1) + \alpha * DIFs\_i(t) \tag{3.6}$$

where α is a proposed variable and is defined as a fraction between 0 and 1, *FDIFs_i(t)* is the filtered RSRP difference value of user *i* at serving cell *s* at time *t*, and *DIFs_i(t)* is the RSRP difference value calculated in Equation (3.5).

The *FDIFs_i(t)* value depends on the proportion between current RSRP difference and historical filtered RSRP difference based on α. As α gets closer to 1, the *FDIFs_i(t)* is more dependent on the current *DIFs_i(t)*. On the other hand, as α goes closer to 0, the *FDIFs_i(t)* is more dependent on the *FDIFs_j(t-1)*. A handover decision will be made based on the following condition after the filtered difference has been computed:

$$FDIF_{s\_i}(t) > HOM \tag{3.7}$$

If the *FDIFs_i(t)* between any of target cell and serving cell is greater than HOM, a handover decision will be triggered immediately. Please note that the ping-pong effect may occur due to lack of TTT mechanism involved in this algorithm.

3.4.4 Semi-Soft Handover(SSHO) Algorithm [121]

Semi-soft Handover (SSHO) algorithm for multicarrier systems is proposed based on Site Selection Diversity Technique (SSDT) in [121]. SSDT is a macro-diversity method used in soft handover mode in the WCDMA network [122]. The main objective of SSHO algorithm is to reduce the inter-cell interference caused by multiple transmissions in a soft handover mode while transmitting on the downlink of the best (serving) cell.

Semisoft handover algorithm divides the frequency bandwidth into two different bands: control band and data band. Figure 3.11 shows the concept of the frequency bandwidth divided into control and data bands in a seven cells scenario.

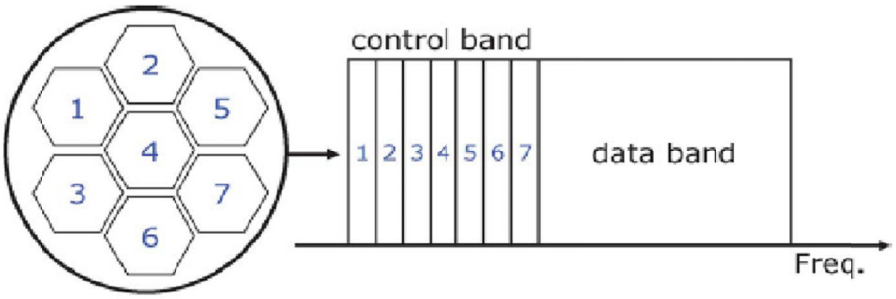

Figure 3.11: Bandwidth divided into data and control bands [121]

In Figure 3.11, the control band with a frequency reuse factor of seven is partitioned into seven sub-bands and sub-band is allocated to one of cells. The data band with frequency factor of one is transmitted on all seven cells. A UE can simultaneously receive information from neighbouring cells through the control channel and selects the cell with the highest RSRP to transmit packets via SSDT.

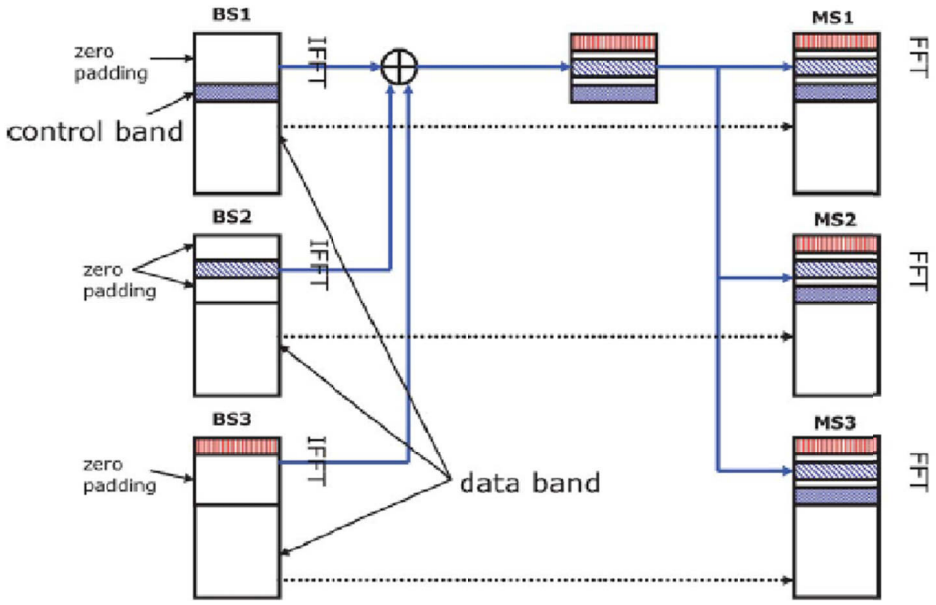

Figure 3.12: Multi-cell detection using zero padding [121]

Figure 3.12 shows the multi-cell detection using zero padding in SSHO algorithm. Assuming BS1, BS2, and BS3 in Figure 3.12 are the serving cell of Mobile Station 1 (MS1), MS2, and MS3, respectively. Each MS receives all neighbouring cells information by filling the zero padding in the control band (as shown in Figure 3.12) and receives the user data directly from the corresponding serving BS in the data band.

SSHO algorithm not only enables each MS keeping multiple control signals of the cells but also minimizes the inter-cell interference by using channel division and zero padding technique. However, a signalling overhead issue may occur due to receiving the multiple control signals from all neighbouring BSs.

3.4.5 A Soft Handover Algorithm for TD-LTE in high-speed railway scenario [123]

A soft handover algorithm for TD-LTE was proposed in [123] to deal with a high-speed (350 km/hr to 500 km/hr) railway scenario. The soft handover algorithm for TD-LTE in a high-speed railway scenario was aimed to reduce the number of radio link failure (RLF) and ping-pong effect, minimize interrupt delay caused by the high-speed, and provide a satisfactory user experience. Figure 3.13 shows that the environment of the high-speed railway scenario used in [123]. All eNodeBs are built along the railway.

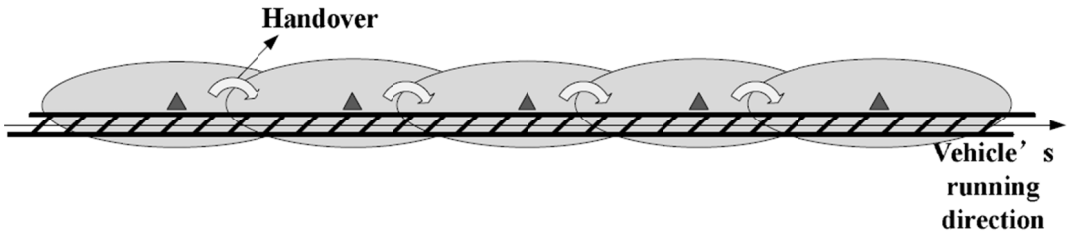

Figure 3.13: The environment of the high-speed railway scenario [123]

The soft handover algorithm for TD-LTE in high-speed railway scenario provides a handover list for every UE in the scenario. Each handover list contains the DL control information of two neighbouring eNodeBs. The UE connects with both eNodeBs while both eNodeBs also admit the UE and have this UE's information. The radio resources in both eNodeBs are allocated to the UE. However there is only one DL transmission in every single frame from the eNodeB with the highest RSRP. The eNodeB provides the DL transmission for the UE is called anchor eNodeB.

$$Better\_eNB - Test\_eNB < Threshold \tag{3.8}$$

$$Better\_eNB - Test\_eNB > HOM \tag{3.9}$$

Two steps were introduced to control the eNodeBs in the handover list: add and remove eNodeBs. A tested eNodeB would be added into the list and removed from the list is based on the Equation (3.8) and Equation (3.9), respectively. When the signal strength of the tested eNodeB satisfies a threshold (named "adding threshold"), the tested eNodeB would be added in to the list. On the other hand, the test eNodeB would be removed from the list when the signal strength of the tested eNodeB is less than the better eNodeB with a HOM.

By applying the soft handover algorithm for TD-LTE in high-speed railway scenario, the signal quality of the UEs in the high-speed railway scenario has a much smaller deterioration. Furthermore, the soft handover algorithm for TD-LTE in high-speed railway scenario results less frequent interruption delay during the handover process which provides a better user experience as well as system throughput.

3.5 Proposed Handover Algorithm in LTE

Hard handover mechanism is adopted to be used in 3GPP LTE in order to reduce the complexity of the LTE network architecture. This mechanism comes with degradation in system throughput as well as a higher system delay. A new handover algorithm in LTE known as LTE Hard Handover Algorithm with Average RSRP Constraint (LHHAARC) is proposed in this thesis in order to minimize the number of handovers and the system delay as well as maximizing the system throughput.

LHHAARC [124] is proposed based on LTE Hard Handover Algorithm with an average RSRP condition for more efficient handover performance. The average RSRP can be calculated as following:

$$RSRP_{avgS\_i} = \frac{\sum_{n=1}^{Np} RSRP_{S\_i}(nT_m)}{Np} \tag{3.10}$$

where $RSRP_{S\_i}(nTm)$ is the RSRP received by user i from serving cell S at n-th Tm and Np is the total number of periods. An average RSRP constraint can be expressed as following:

$$RSRP_T(t) > RSRP_{avgS\_i} \tag{3.11}$$

where $RSRP_T(t)$ is the current RSRP received from target cell T and $RSRP_{avgS\_i}$ is the average RSRP computed from Equation (3.10). The handover decision will be made by satisfying Equation (3.11) followed by two conditions listed below:

$$RSRP_T > RSRP_S + HOM \tag{3.12}$$

$$HOTrigger \geq TTT \tag{3.13}$$

A handover will be triggered if and only if Equation (3.11), Equation (3.12), and Equation (3.13) are all satisfied. Please note that $RSRP_{avgS\_i}$ will be reset to 0 each time due to serving cell changes when a handover is successfully performed.

The concept of LHHAARC is to narrow down the possibility of handovers to minimize unnecessary handovers; this algorithm aims to minimize unnecessary handovers by limiting UE to be handed over to a target cell whose current RSRP is higher enough to be satisfying the handover condition and also higher than the historical RSRP of the serving cell from the first handover measurement period till the last.

3.6 Performance Evaluation

The performance of LTE Hard Handover Algorithm, RSS Based TTT Window Handover Algorithm, LTE Integrator Handover Algorithm, and LHHAARC is evaluated in this section. SSHO algorithm and the soft handover algorithm for TD-LTE in high-speed railway scenario are not selected for performance evaluation because the soft handover mechanism involved in both handover algorithms is not standardized in the LTE system. The performance evaluation is separated into two subsections: parameter optimization and performance comparison. The parameter optimization is performed to ensure that all selected handover algorithms operated with the optimized performance in the subsequent performance comparison.

The performance of four handover algorithms are optimized, evaluated, and compared using the computer simulation tool discussed in Chapter 2 with 100 UEs in the downlink LTE system. UEs are uniformly distributed within a rectangle area as shown in Figure 3.14. It is assumed in this chapter that the CQI reporting is performed in each

TTI of 1 millisecond and on each PRB. A total of 16 CQI levels are used. The HARQ technique in [125] was adopted to recover wireless transmission errors. The CQI and HARQ reporting are assumed to be error free with 3 ms CQI delay and 4 ms HARQ (ACK/NACK) delay. The maximum number of error packet retransmissions is limited to 3. The Round Robin (RR) packet scheduling algorithm was chosen for a fair transmission opportunity for all users and a 50 millisecond interval was set for the handover measurement period.

A simulation time of 1000 milliseconds and 10000 milliseconds (which is the limitation of the simulator) were used for performance optimization and handover algorithms performance comparison. System parameters used in the simulation for optimization and performance comparison are given in Table 3.1.

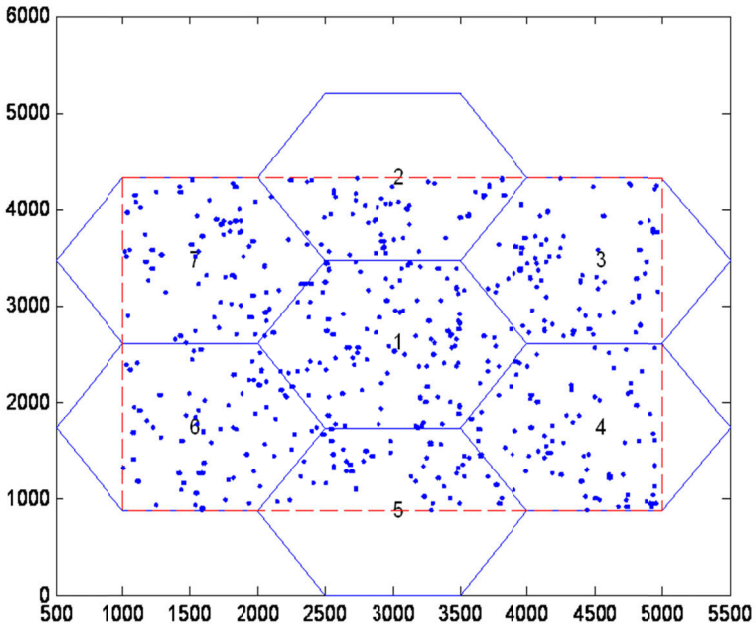

Figure 3.14: Simulation Environment [124]

Table 3.1: Simulation Parameters for Optimization and Performance Comparison

Parameters	Values
Cellular layout	Hexagonal grid, wrap around (reflect), 7 cells
Carrier Frequency	2 GHz
Bandwidth	5 MHz
Number of PRBs	25
Number of sub-carriers per PRB	12
Sub-carrier Spacing	15 kHz
Path Loss	Cost 231 Hata model
Shadow fading	Gaussian distribution
Multi-path	Rayleigh fading
Packet Scheduler	Round Robin
Scheduling Time (TTI)	1 ms
Data Traffic	1 Mbps Constant Rate
User	100
User's position	Uniform distributed
User's direction	Randomly choose from [0,2π], constantly at all time
Simulation time	1000 ms for optimization 10000 ms for performance evaluation
Handover measurement period	50 ms

3.6.1 Parameters Optimization

Parameters optimization of the four handover algorithms is discussed in this section under three speed scenarios. The results in [126] show that an optimized handover algorithm can effectively minimize the unnecessary number of handovers while maximizing system throughput. The optimized parameters are determined by comparing a new parameter called *OptimizeRatio* value which is a ratio of total system throughput to the average number of handovers. *OptimizeRatio* can be computed as follows:

$$OptimizeRatio_{(HOA,Speed)} = \frac{ST_{(HOM,TTT)}}{ANOH_{(HOM,TTT)}} \tag{3.14}$$

where *HOA* indicates the handover algorithm, *Speed* is the corresponding speed in each scenario. *ST* and *ANOH* are the total system throughput of the 7 cells and the average number of handovers per UE per second, respectively. *TTT* will be replaced by α or β factor when the LTE Integrator Handover Algorithm or RSS Based TTT Window Algorithm is selected, respectively.

Table 3.2 outlines LTE Hard Handover Algorithm, RSS Based TTT Window Algorithm, LTE Integrator Handover Algorithm, and LHHAARC are referred as HOA 1, HOA 2, HOA 3, and HOA 4 respectively, in the following discussions. The range of the HOM and α or β factor follows the values that are given in [120, 127]. The highest *OptimizeRatio* value leads to a set of optimized parameters of the selected handover algorithm for a specific speed by maximizing the total system throughput and minimizing the average number of handovers per UE per second.

Table 3.2: Simulation Parameters for Optimization

Parameters	**Values**
Handover Algorithm (HOA)	1: LTE Hard Handover Algorithm 2: RSS Based TTT Window Algorithm 3: LTE Integrator Handover Algorithm 4: LHHAARC
TTT	(0, 1, 2, 3, 4, 5) millisecond
HOM	(0, 1, 2, 3, 4, 5, 6, 7, 8, 9, 10) dB
UE Speed	(3, 30, 120) km/hr
α / β	(0.25, 0.5, 0.75, 1)

The *OptimizeRatio* results in Figure 3.15 are determined using input sets as HOA 1 and UE speeds equal to 3, 30, and 120 km/hr with changing HOM value from 0 to 10 and TTT value from 0 to 5.

The highest bar graph in each speed scenario in Figure 3.15 indicates the highest *OptimizeRatio* value in each simulation and it refers to HOM and TTT equal to 10 and 5 in 3 km/hr scenario, HOM and TTT equal to 6 and 5 in 30 km/hr scenario, and HOM and TTT equal to 7 and 5 in 120 km/hr scenario, respectively.

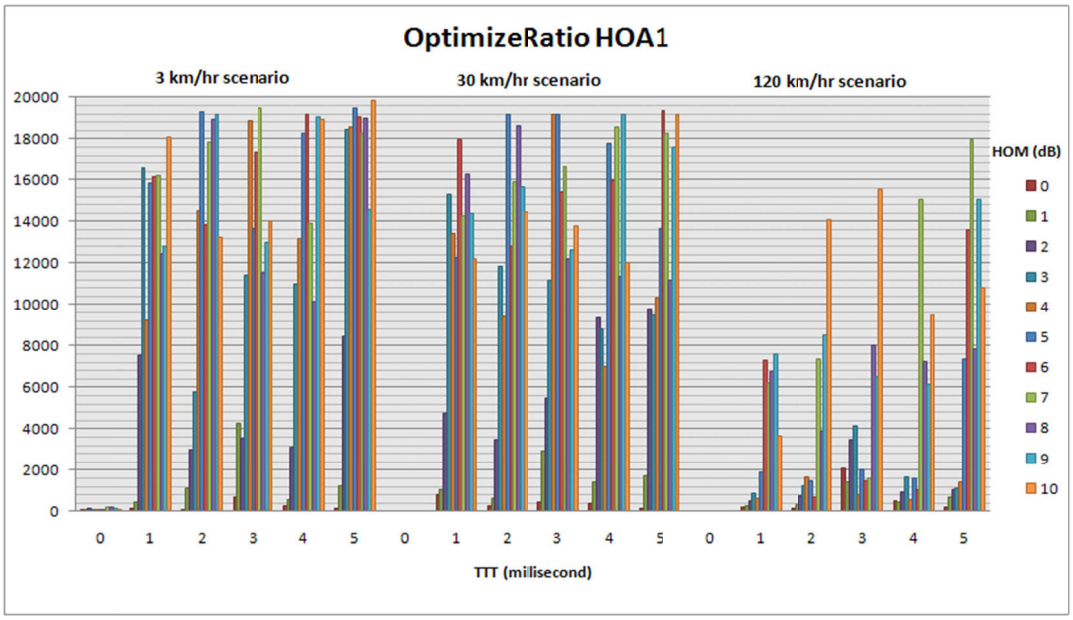

Figure 3.15: *OptimizeRatio* in HOA 1

Figure 3.16 shows the *OptimizeRatio* in HOA 2 with three speed scenarios. The set of β and HOM results the highest *OptimizeRatio* value in 3 km/hr scenario, 30 km/hr scenario, and 120 km/hr scenario, are 0.25 and 6, 1 and 6, and 0.25 and 9, respectively.

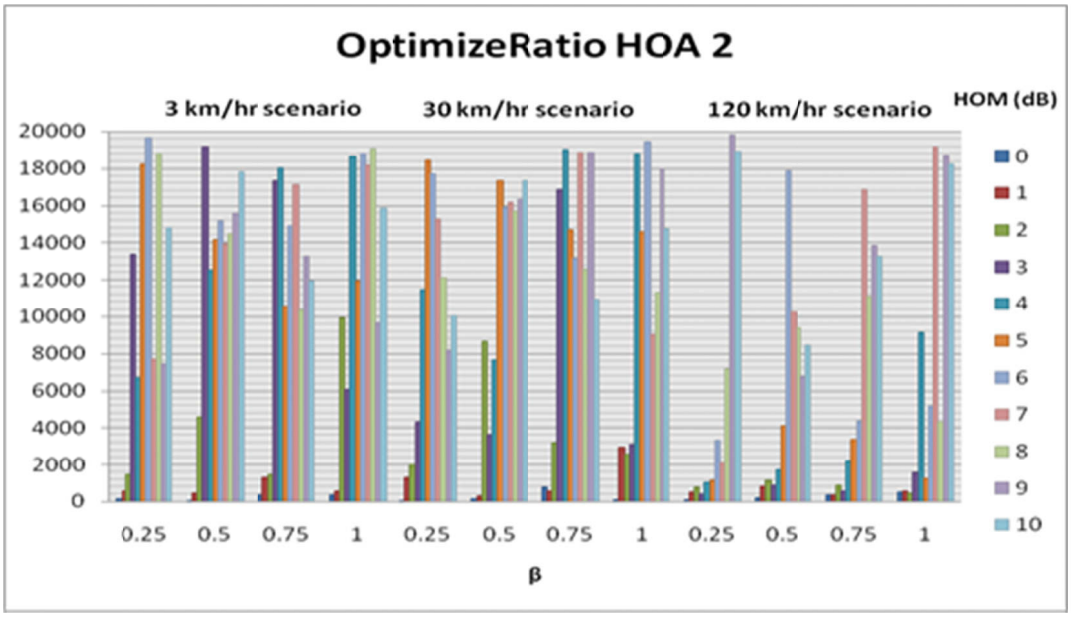

Figure 3.16: *OptimizeRatio* in HOA 2

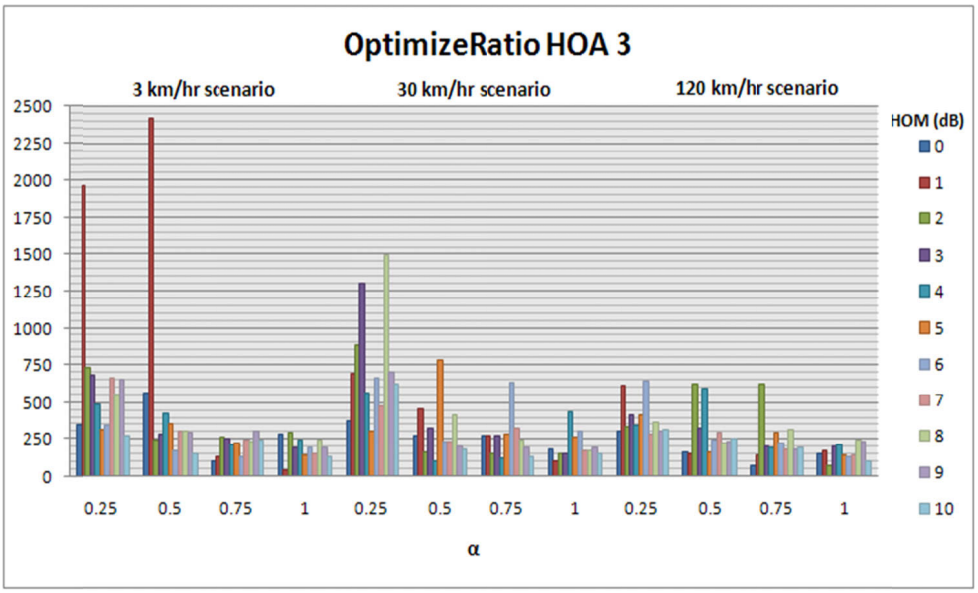

Figure 3.17: *OptimizeRatio* in HOA 3

The highest *OptimizeRatio* value in HOA 3 can be seen in Figure 3.17 as α and HOM equal 0.5 and 1, 0.25 and 8, and 0.25 and 6 in 3 km/hr, 30 km/hr, and 120 km/hr speed scenario, respectively.

A set of optimized parameters of HOA 4 is determined in Figure 3.18 as HOM and TTT equal 10 and 2, 8 and 4, and 10 and 1 in 3 km/hr, 30 km/hr, and 120 km/hr speed scenario, respectively.

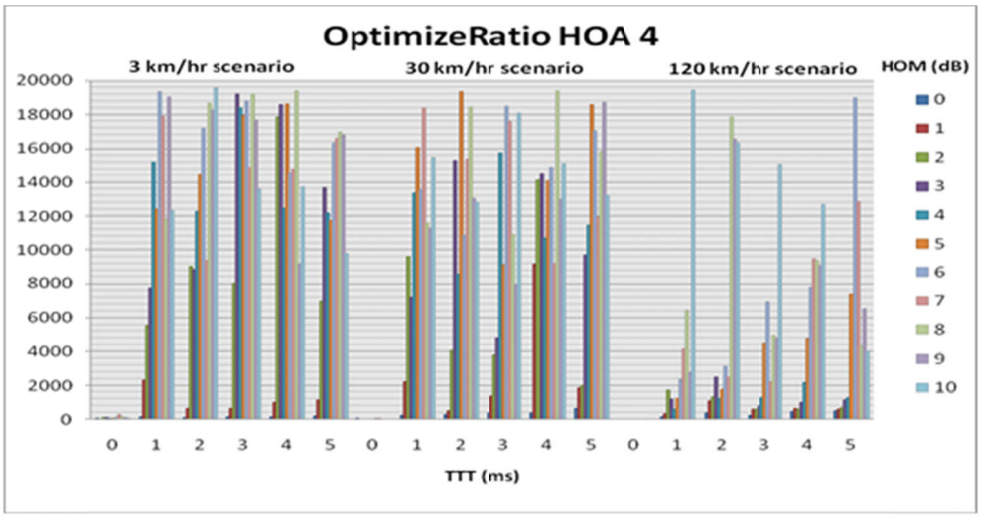

Figure 3.18: *OptimizeRatio* in HOA 4

Table 3.3 shows a summarized result of the optimized parameters for each handover algorithm for the three speed scenarios. The results of the performance comparison in the following section are based on the optimized parameters as listed in Table 3.3.

Table 3.3: Optimized Parameters

Speed [km/hr]	HOA 1: LTE Hard Handover Algorithm	HOA 2: RSS Based TTT Window Handover Algorithm	HOA 3: LTE Integrator Handover Algorithm	HOA 4: LHHAARC
3	[HOM, TTT] = [10, 5]	[HOM, β] = [6, 0.25]	[HOM, α] = [1, 0.5]	[HOM, TTT] = [10, 2]
30	[HOM, TTT] = [6, 5]	[HOM, β] = [6, 1]	[HOM, α] = [8, 0.25]	[HOM, TTT] = [8, 4]
120	[HOM, TTT] = [7, 5]	[HOM, β] = [9, 0.25]	[HOM, α] = [6, 0.25]	[HOM, TTT] = [10, 1]

3.6.2 Performance Comparison

Figure 3.19 shows the average number of handovers per UE per second of four handover algorithms with increasing UE speeds. It can be seen that, the average number of handovers in HOA 3 is significantly higher when compared with the other three handover algorithms for all speed scenarios possibly due to the lack of the TTT mechanism. All three handover algorithms (i.e. HOA 1, HOA 2, and HOA 4) achieve a similar average number of handovers at 3 km/hr and 30 km/hr speed scenarios.

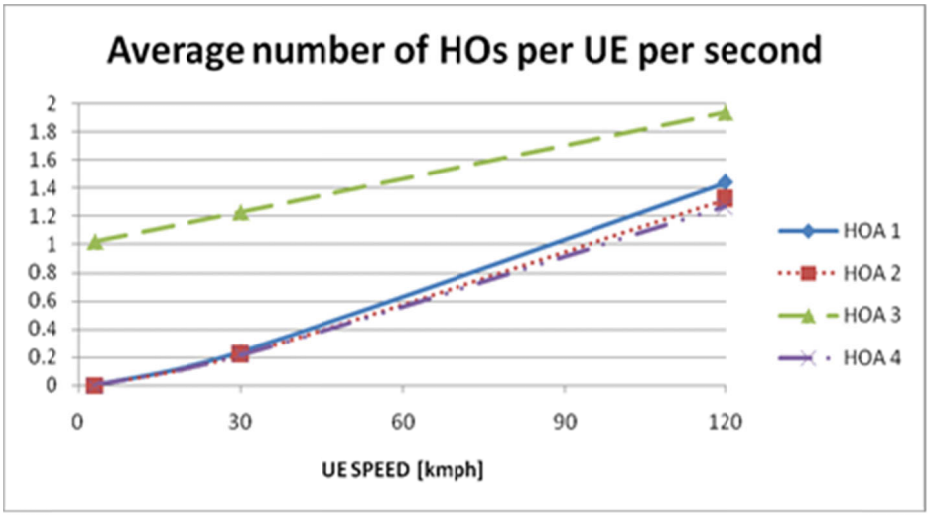

Figure 3.19: Average number of handovers of four handover algorithms

The result shows that HOA 4 has the lowest average number of handovers of 0, 0.21, and 1.28 at 3 km/hr, 30 km/hr, and 120 km/hr speed scenarios, respectively. Furthermore, the proposed HOA 4 has reduced (up to 35.56%) the average number of handovers per UE per second when compared with the HOA 3.

Figure 3.20 shows the total system throughput of four handover algorithms with increasing UE speeds. A higher total system throughput value implies a higher system performance for a handover algorithm. Figure 3.20 shows that HOA 3 has the highest total system throughput of 77.2496 Mbps at 3 km/hr due to users frequently performing handover between cells which allows users to switch to a cell with a better channel quality. However, the total system throughput drops gradually to 55.9141 Mbps and 41.976 Mbps at speed 30 and 120 km/hr respectively by having higher number of handovers.

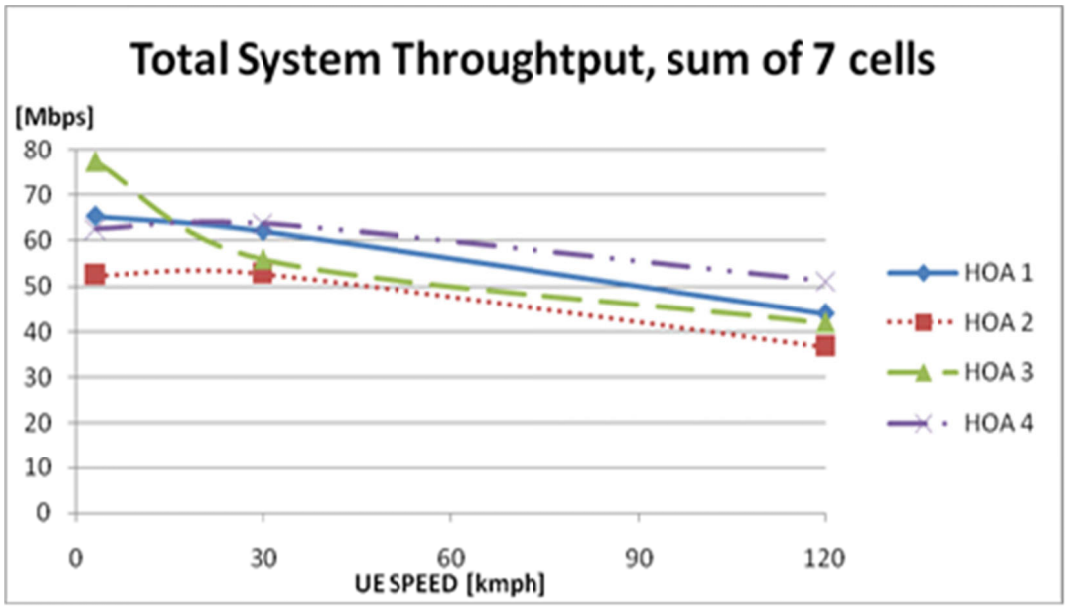

Figure 3.20: Total System Throughput, sum of seven cells of four handover algorithms

A long TTT window in HOA 2 (T_u = 100 ms) delays the time to execute a handover which delays a UE to be handed over to a cell with better signal quality, and therefore HOA 2 has the lowest total system throughput in all speed scenarios. The total system throughput of HOA 4 in all speed scenarios has a highest value of 177.4205 Mbps when compared to HOA 1 (171.3447 Mbps), HOA 2 (141.8809 Mbps), and HOA 3 (175.1397

Mbps). Furthermore, the sum of total system throughput of HOA 4 has a 3.55%, 25%, and 1.302% performance improvement over HOA 1, HOA 2, and HOA 3, respectively.

Figure 3.21 shows the total system delay of four handover algorithms in three speed scenarios. HOA 3 has a slightly higher delay possibly due to lack of the TTT mechanism at all speed scenarios as compared with the other three handover algorithms. HOA 4 has the smallest total system delay at all speed scenarios (63.1917 ms, 742.917 ms, and 7082.12 ms at 3 km/hr, 30 km/hr, and 120 km/hr, respectively). The total system delay of HOA 1, HOA 2, HOA 3, and HOA 4 in all speed scenarios are 9611.00 ms, 10214.45 ms, 15048.69 ms, and 7888.23 ms, respectively. This result shows that HOA 4 provides less than the total system delay of HOA 1, HOA 2, and HOA 3 in all speed scenarios by 17.93%, 22.77%, and 47.58% less delay, respectively.

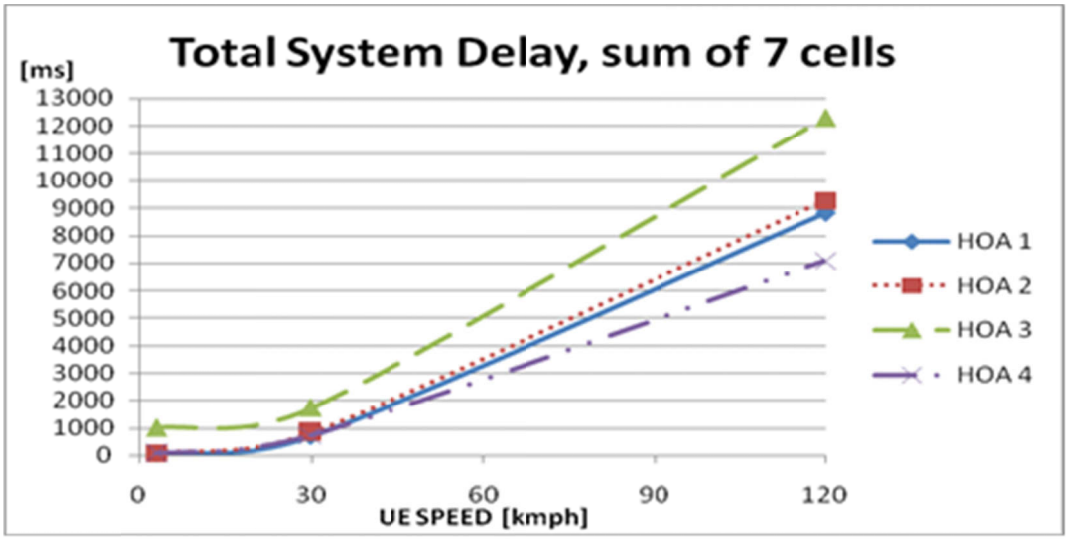

Figure 3.21: Total System Delay, sum of seven cells of four handover algorithms

3.7 Summary

This chapter studied the basic cell selections and handover schemes for the LTE cellular networks followed by a number of well-known handover algorithms and a proposed handover algorithm in LTE system. The performance of the proposed LHHAARC is optimized and compared with three well-known handover algorithms (LTE Hard Handover Algorithm, RSS Based TTT Window Algorithm, and LTE Integrator Handover Algorithm) under three different UE speed scenarios. It is shown via

computer simulation that the proposed handover algorithm has reduced (up to 35.56%) the average number of handovers when compared to LTE Integrator Handover Algorithm. Moreover, the total system throughput under the proposed handover algorithm is 3.55%, 25%, and 1.302% higher as compared to the LTE Hard Handover Algorithm, RSS Based TTT Window Algorithm and LTE Integrator Handover Algorithms, respectively. The proposed handover algorithm is able to maintain a lower system delay when compared with the other three well known handover algorithms (i.e. 17.93%, 22.77%, and 47.58% reductions when compared with LTE Hard Handover Algorithm, RSS Based TTT Window Algorithm and LTE Integrator Handover Algorithms, respectively). Moreover, the results obtained are in line with results in the literature and hence validated the system level simulator described in Chapter 2.

Given that the downlink LTE is a complex multi-carrier mobile cellular system that performs handover in both time and frequency domains, it was concluded that the mathematical analysis is impractical for use in this research work.

Chapter 4

ADVANCED LTE-A COMP HANDOVER ALGORITHMS

Many proposals in the literature have been studied as candidates for LTE-Advanced technologies. The concept of cooperated multiple point (CoMP) transmission and reception is a promising research topic. CoMP transmission and reception was initially proposed in the 3GPP Release 10 in 2010 [128, 129] and remains as an open topic to be continuously enhanced for real-life scenarios at the Workshop on LTE Release 12 and Beyond [130, 131]. CoMP transmission and reception improves the cell-edge data rate and average data rate, and is suitable to increase spectral efficiency (and hence capacity) for much more dense network deployments in urban areas and capacity hotspots.

Network coordination provided by the CoMP transmission and reception in 3GPP LTE-Advanced networks results in spectrally efficient and high capacity communication with enhanced cell edge user throughput [132]. In coordinated multipoint networks, multiple base stations send information in a coordinated manner to the mobile station. Due to the information exchanged in a coordinated manner and the data synchronization among multiple base stations, the current existing handover algorithms in LTE network are not applicable for CoMP networks [63]. Therefore new CoMP handover algorithms are needed to be designed in a coordinated multipoint LTE-A network.

A CoMP Handover Algorithm in LTE-A system is introduced in [133]. Based on the research work, the CoMP Handover Algorithm enhances the LTE-A system throughput and reduces the PLR when compared with the LTE system. However, this algorithm could lead to system capacity overload and saturated system throughput issues within a highly congested network. Improved user and cell throughput due to CoMP may be limited by the capacity. A handover algorithm could mitigate this limitation by

considering the capacity and the load [134]. Hence, a new handover algorithm that supports CoMP and takes system capacity into consideration in LTE-A system is necessary. Three CoMP handover algorithms are proposed in this chapter: Limited CoMP Handover Algorithm, Capacity Based CoMP Handover Algorithm, and Capacity Integrated CoMP Handover Algorithm. The Limited CoMP Handover Algorithm comes with the concept of accommodating as many UEs as possible. The Capacity based CoMP handover algorithm aims to emphasis the quality of target cells in both capacity and channel quality domains and ensures the radio resources are efficiently used in the system. The Capacity Integrated CoMP Handover Algorithm inherits the concept of the Capacity Based CoMP Handover Algorithm and is further improved with an additional mechanism whereby instantaneous and historical RB utilization values are taken into consideration when making the handover decision.

The performance of each of the proposed CoMP handover algorithm is evaluated and compared with the CoMP Handover Algorithm using the simulation tool discussed in Chapter 2. It is shown via simulation that the Limited CoMP Handover Algorithm can improve the system throughput when compared to the CoMP Handover Algorithm in a saturated system. The Limited CoMP Handover Algorithm is able to maintain a lower system delay when compared with the CoMP Handover Algorithm. Simulation results show that both the Capacity Based CoMP Handover Algorithm and the Capacity Integrated CoMP Handover Algorithm can improve the system throughput and minimize the system delay when compared to the CoMP Handover Algorithm. However, the Capacity Based CoMP Handover Algorithm has a side effect of having higher total numbers of handovers. The Capacity Integrated CoMP Handover Algorithm eliminates the side effect (lower or equivalent total number of handovers) and achieves a lower PLR when compared to the CoMP Handover Algorithm.

This chapter is organised as follows: Section 4.1 thoroughly describes the related CoMP technology and studies existing CoMP handover algorithms. Section 4.2 introduces three proposed CoMP handover algorithms for LTE-A and the performance of each proposed CoMP handover algorithm is evaluated and compared with the CoMP Handover Algorithm in this subsection. Section 4.3 concludes this chapter.

4.1 Related Works

CoMP transmission and reception is the key technique in LTE-A to improve the cell-edge throughput and/or system throughput. There are two types of CoMP schemes for LTE-A system: Coordinated Scheduling / Beamforming (CS/CB) and Joint Processing (JP). A further variant of JP is introduced as transmission point selection (TPS) in [135]. CS/CB shares the channel state information (CSI) for multiple UE terminals by multiple coordinated eNodeBs while transmits the UE's packets only at one eNodeB. JP provides multiple data transmissions which contain the same packets for each UE among multiple cooperated eNodeBs. The data transmission of each UE in TPS is available at multiple coordinated eNodeBs, however the transmission of beamformed data for a given UE terminal is performed at a single TP at each time instance [135]. Figure 4.1 shows an example of CoMP with CS/CB and JP transmission in a distributed network architecture.

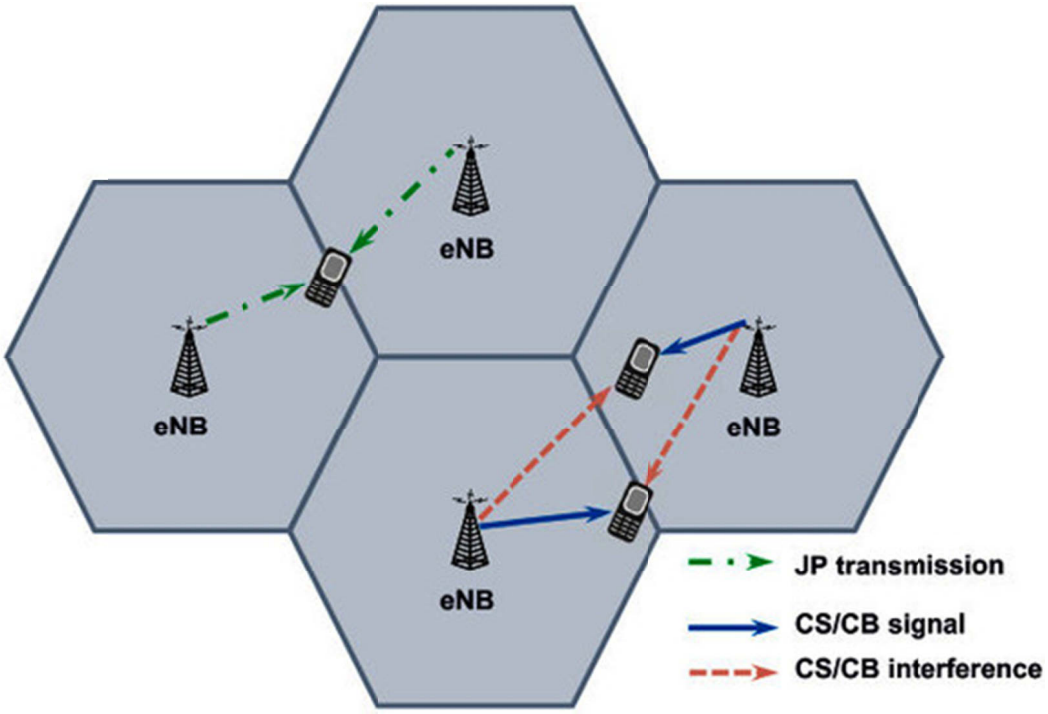

Figure 4.1: Example of CoMP in a distributed network architecture [136]

Handovers in LTE-A are all hard handovers [58]. A single connection for each UE connected with the source eNodeB at any time instant is restricted by the nature of hard

handover mechanism. The concept of JP in CoMP technology supports multiple data transmissions for each UE in the LTE-A system. Existing hard handover algorithms in LTE network are not applicable for CoMP networks in the LTE-A system. This is especially the case when the same data streams from multiple cells are received by a UE for JP transmission. (The same technique is used for soft handover in UMTS [137].) Therefore a new CoMP handover algorithm is required for a coordinated multipoint LTE-A network.

Several handover algorithms proposed in the literature for CoMP LTE-A system are introduced in the following subsections.

4.1.1 A Fractional Soft Handover Scheme for 3GPP LTE-Advanced System [138]

A fractional soft handover (FSHO) scheme for 3GPP LTE-Advanced system in [138] starts with utilizing carrier aggregation which is the one of the key features introduced involved in LTE-Advanced. Figure 4.2 shows an example of carrier aggregation in LTE-A.

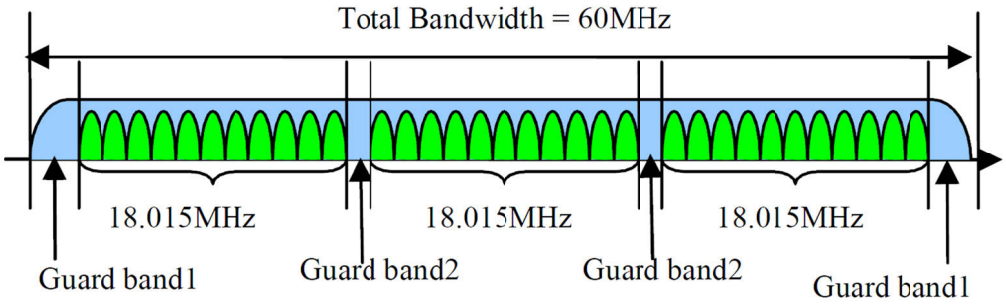

Figure 4.2: Example of Carrier Aggregation in LTE-A [138]

There are two requirements when using the carrier aggregation if the bandwidth of Guard band 2 in Figure 4.2 is not multiples of the sub-carrier spacing or if the discontinuous spectrum aggregation is used to generate the total bandwidth:

1. Three 20MHz IFFT (Inverse Fast Fourier transform) modules are needed in the eNodeB transmitter

2. Three 20MHz FFT (Fast Fourier transform) modules are needed in the receiver of UE

Based on these assumptions, UE can simultaneously receive the signal from multiple eNodeBs using different FFT modules. This mechanism is the basis of the proposed FSHO scheme in the LTE-Advanced system. Furthermore, all component carriers in [138] are assumed to be used by the eNodeB and UEs and data transmissions are assumed to be transmitted from all component carriers. Therefore the source eNodeB needs to negotiate with the target eNodeB by selecting one of these component carriers such as the FSHO carrier during the handover preparation phase. Figure 4.3 shows the signal exchange diagram of the FSHO in the LTE-A system. Note that solid arrow lines and dashed arrow lines indicate the flows of the control plane messages and the user plane packets, respectively.

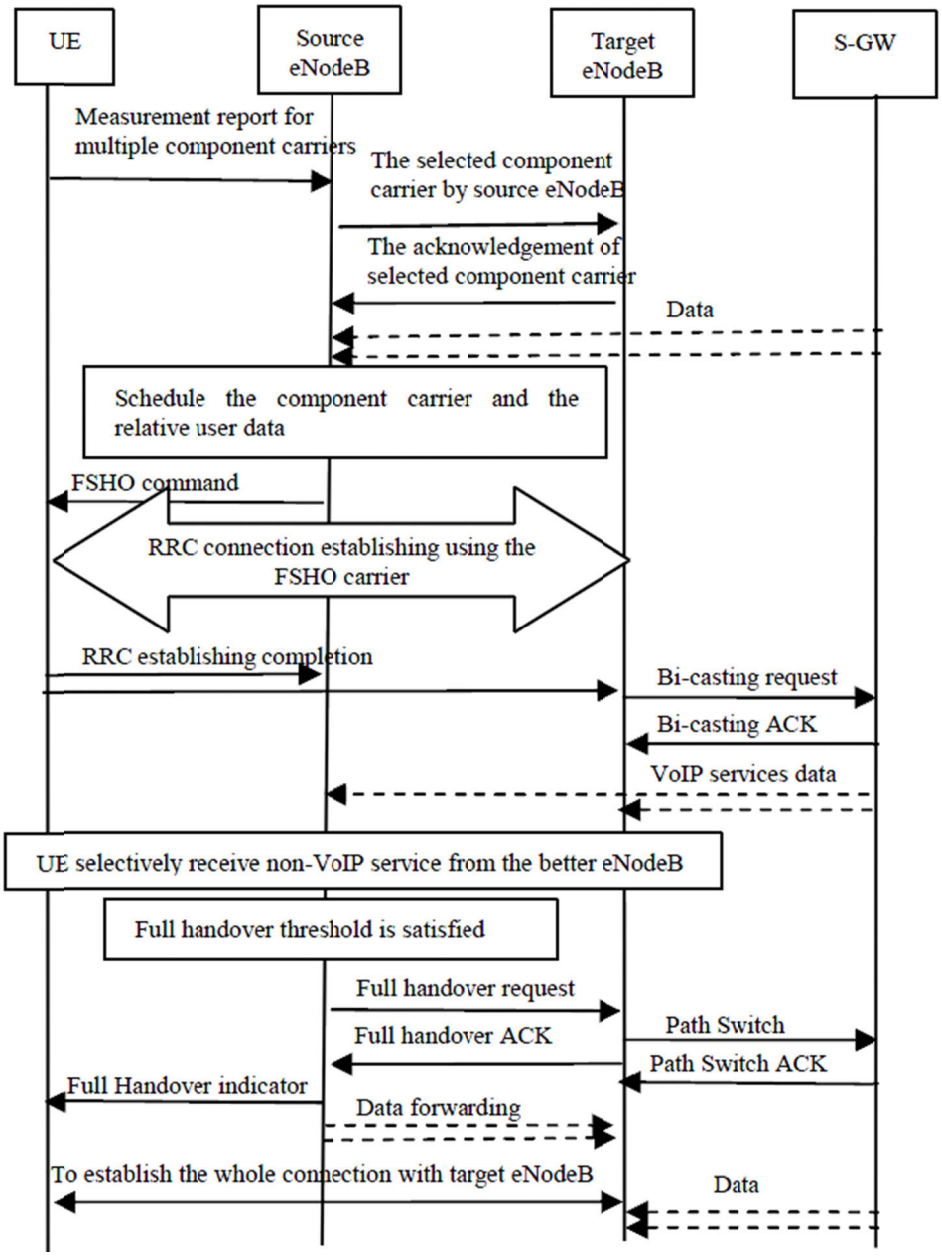

Figure 4.3: Message Chart of the FSHO in LTE-A [138]

In the handover preparation, UE sends the measurement report to the source eNodeB for multiple component carriers. Based on the support of carrier aggregation in LTE-A system and different FFT modules built in each UE terminal, UE can measure the pilot signal strength of each component carrier of neighbouring eNodeBs. The source eNodeB selects the appropriate target eNodeB and component carrier based on the measurement report sent by the UE. Then, the source eNodeB sends the handover

request message to require the preparation of a FSHO at the target eNodeB. The target eNodeB checks the authorization of the UE and the availability of the selected component carrier. An acknowledgement of selected FSHO component carrier is sent from the target eNodeB to the source eNodeB if the UE can be accommodated in the target eNodeB. Otherwise, it shall send the NACK to the source eNodeB. Upon acknowledging the FSHO carrier by the target eNodeB, the source eNodeB sends out the FSHO command to the UE. Meanwhile, the data transmission on the FSHO component carrier is scheduled to the other component carrier by the source eNodeB in order to satisfy the QoS of the current on-going session.

After receiving the FSHO command, the radio resource control (RRC) connection is established using the FSHO carrier by the UE with the target eNodeB. After the RRC establishment has been completed, the UE sends out an RRC ESTABLISHING COMPLETION message to the source eNodeB and the target eNodeB. A bi-casting request message is sent to S-GW by the target eNodeB after receiving the RRC ESTABLISHING COMPLETION message. S-GW replies the ACK message to the target eNodeB while bi-casting the Voice over IP (VoIP) packets to the source eNodeB and target eNodeB at the same time. The VoIP packets are simultaneously transmitted to the UE from the target eNodeB and source eNodeB, while non-VoIP packets are only transmitted to the UE from the eNodeB with better signal quality.

In addition, a traditional hard handover mechanism is applied when the signal quality of the source eNodeB is below a predefined threshold. A FULL HANDOVER REQUEST message is sent from the source eNodeB to the target eNodeB indicating a handover occurred. The target eNodeB sends the ACK back to the source eNodeB and the target eNodeB sends the path switch command to the S-GW. After receiving the full handover ACK message, the source eNodeB sends a FULL HANDOVER INDICATOR message to the UE to perform the hard handover procedure. The FSHO procedure is completed when the UE is fully served by the target eNodeB after the detaching time.

A fractional soft handover (FSHO) scheme is proposed based on the carrier aggregation for the 3GPP LTE-Advanced system. Due to the absence of CoMP technique in the FSHO scheme, it is not selected for performance comparison in this chapter.

4.1.2 A CoMP Soft Handover Scheme for LTE Systems in High Speed Railway [139]

Due to the higher data rate and lower system latency, long-term evolution (LTE) has been chosen as the next generation's evolution of railway mobile communication system by the International Union of Railways. A CoMP soft handover scheme for LTE systems in high speed railway scenario is proposed in [139] to improve the traditional hard handover of LTE.

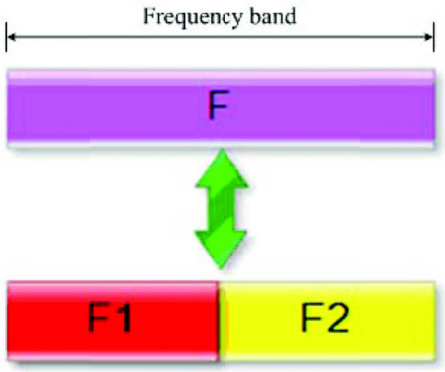

Figure 4.4: The Frequency Allocation Approach for Railway Scenario [139]

An interference-avoid co-channel deployment approach for railway scenario is proposed in Figure 4.4. The whole frequency band is divided into two parts which are called F1 and F2, respectively as shown in Figure 4.4. F1 and F2 are assigned to the up-direction trains (the trains are going to the metropolis) and to the down-direction trains (contrary to up-direction), respectively as shown in Figure 4.5.

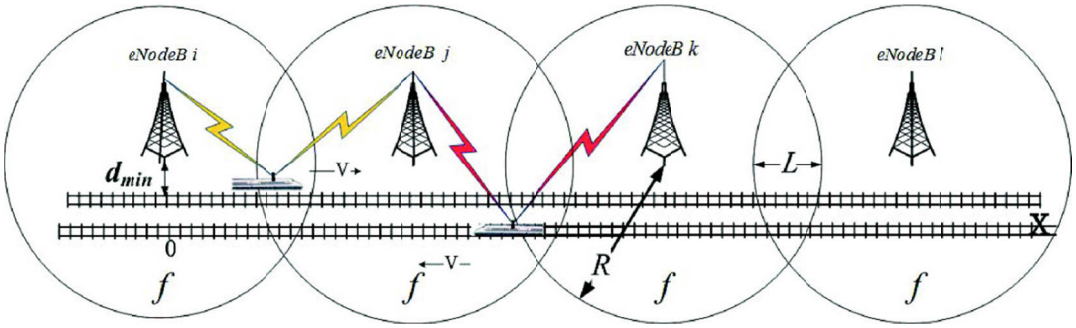

Figure 4.5: Co-channel Network Approach for Railway Communication [139]

The proposed co-channel deployment approach maximizes the spectrum efficiency and minimizes the inter-cell interference of adjacent eNBs when compare to the Global System for Mobile Communications – Railway (GSM-R) network.

A dual on-vehicle stations cooperation scheme is proposed in [139]. The mobile relay stations (MRSs) in the front and the rear of the train are mounted and controlled by a central control station (CCSn). Figure 4.6 shows the dual on-vehicle stations solution.

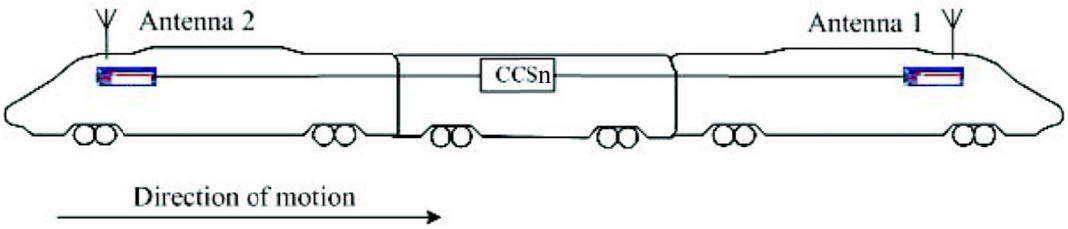

Figure 4.6: Dual On-vehicle Stations Solution [139]

The downlink and the uplink data of the users in the vehicle are transmitted to the eNodeBs along the track via the CCSn. The downlink data received by the two on-vehicle stations from the eNodeBs along the track are gathered to the CCSn which forwards the collected data to the pico-base stations inside the train. The uplink data of the users inside the train are gathered to the CCSn by pico-base stations deployed on-vehicle and the gathered data are transmitted to the eNodeBs along the track under the control of the CCSn via the front and the rear stations.

A seamless soft handover scheme utilizing CoMP joint processing and transmission technology is proposed and shown from Figure 4.7 to Figure 4.9.

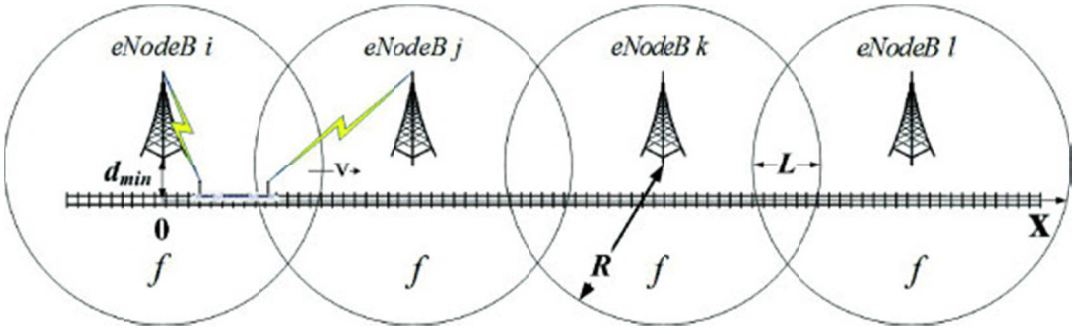

Figure 4.7: Target eNodeB Joins The Cooperative Set [139]

When the front on-vehicle station enters into the overlapping area, the source eNodeB *i* activates the cooperative transmission set (CTS) composed of eNodeB *i* and eNodeB *j*. Based on the measurement information reported by the moving train, the position information supplied by the communication based train control system (CBTC) and the CTS activation control message is received by the target eNodeB. After the CTS is activated, the user plane data of users inside the train are shared between the source eNodeB *i* and the target eNodeB *j* via X2 interfaces. The two adjacent eNodeBs use the same frequency resource to communicate with the train. It should be noted that two eNodeBs are always included in CoMP CTS in the linear coverage topology of the high-speed railway. Figure 4.7 shows target eNodeB *j* joins the cooperative set.

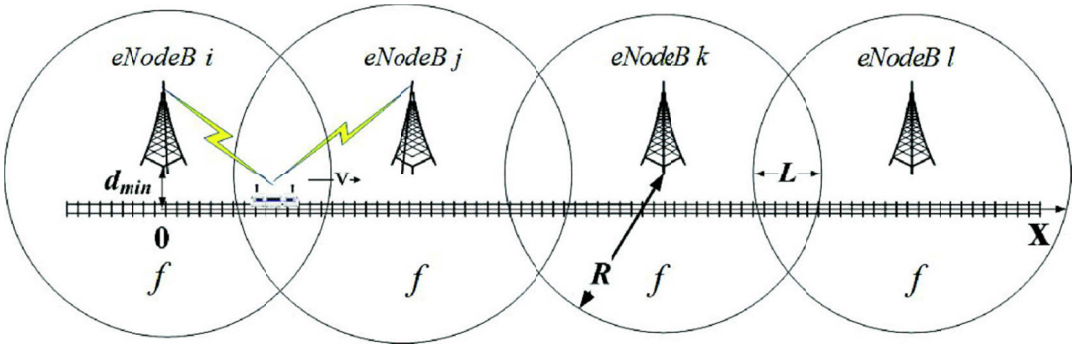

Figure 4.8: Two Adjacent eNodeBs Serve The Train Simultaneously in The Overlapping Area [139]

eNodeB *i* and eNodeB *j* keep the cooperative relation and communicate with the train simultaneously as shown in Figure 4.8 when the train body entirely enters into the overlapping area. The front and the rear on-vehicle stations can receive signals from the two cooperative eNodeBs, but the measurement information is only forwarded to the source eNodeB *i*. The handover decision is made by the source eNodeB *i* based on the measurement information reported by the moving train and the RRM information of the target eNodeB *j*. The data transmission in user plane will not be interrupted.

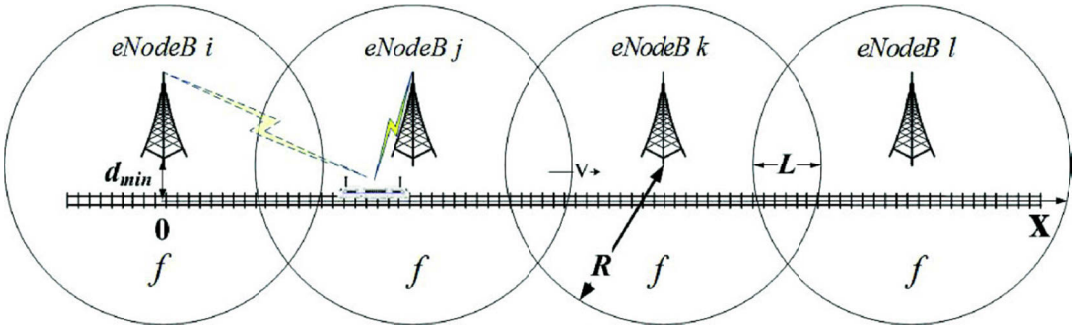

Figure 4.9: The Former Source eNodeB Interrupts Sending Data [139]

When the signal strength of the target eNodeB is greater than the source eNodeB plus a certain threshold, a handover is triggered. This is caused by the train moving away from the source eNodeB *i*, as shown in Figure 4.9. This process follows the current hard handover scheme. Meanwhile, the target eNodeB *j* continuously transmits the user plane data to users inside the train with the same frequency resource by Physical Downlink Shared Channel (PDSCH), which avoids the interrupt latency caused by the current hard handover scheme. After the handover procedure has completed, the former source eNodeB *i* was eliminated from the cooperative set by the current source eNodeB *j*.

The optimized handover scheme based on CoMP can degrade the outage probability and improve the handover performance by the communication between the train with two adjacent eNodeBs in the overlapping area. This mechanism achieves a seamless hard handover as soft handover scheme. However, this CoMP handover algorithm is only proposed for high speed railway scenarios which are not suitable for random UE directions. As a consequence, the CoMP soft handover scheme for LTE systems in high speed railway is not implemented in this chapter.

4.1.3 CoMP Handover Algorithm [133]

The handover algorithm that supports JP introduced in [133] is discussed in this section. Figure 4.10 shows an example of CoMP in the LTE-A system model.

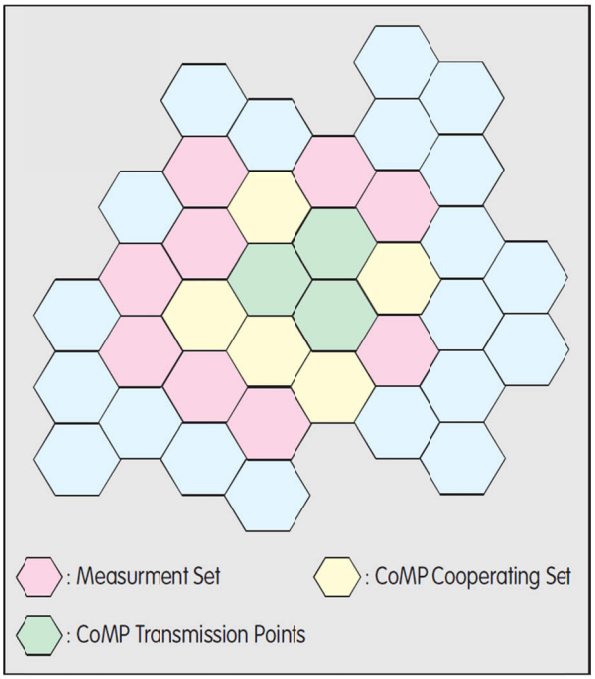

Figure 4.10: CoMP in LTE-A system [133]

There are four elements considered when making a handover decision: serving cell, measurement set, CoMP coordinating set (CCS), and CoMP transmission points (CTP). A serving cell is the cell which takes the responsibility of making handover decision and maintains the connection of each UE to the network. An UE can only attach to one serving cell at each time instant. A measurement set is a set of cells whose RSRPs can be received and reported by the UE to the serving cell for making the selection of CCS. A CCS is a set of cells which are selected by the serving cell from the measurement set. Furthermore, A CTP is a set of cells chosen from the CCS by the serving cell for sending downlink data directly to an UE. A flowchart of the CoMP Handover algorithm is given in Figure 4.11.

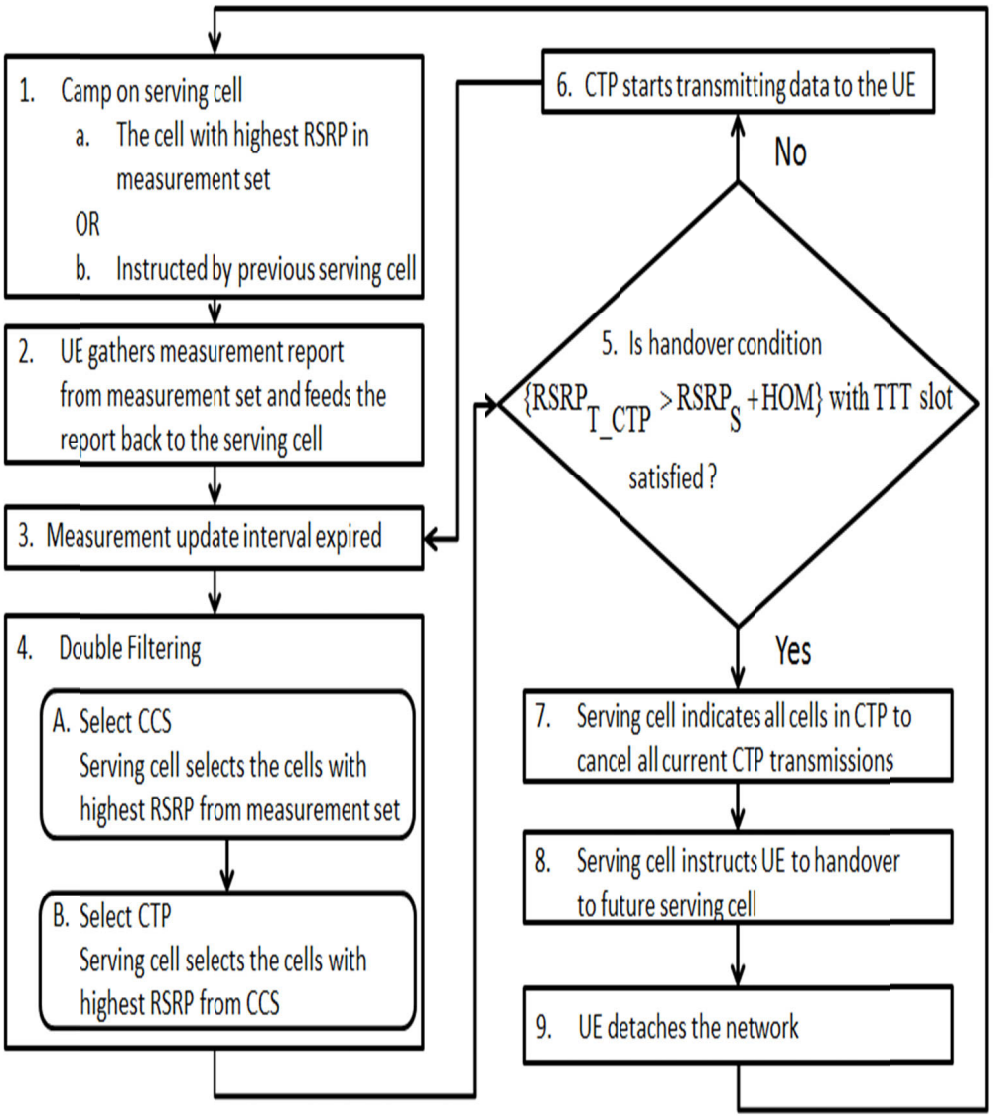

Figure 4.11: Flowchart of CoMP Handover Algorithm in LTE-A

The handover algorithm starts when the UE joins the network by camping on the cell whose RSRP is the highest or the cell which was instructed by its previous serving cell. Then UE starts to feedback the serving cell with the measurement set which is the RSRP measurements received from all cells in the network. Serving cell selects a set of cells with the highest RSRP in the measurement set as a CCS. Similarly, a set of cells with the highest RSRP in CCS will be selected by the serving cell as the CTP. After the CTP selection is finalized, the serving cell will request all cells in the CTP to start transmitting packets to the UE. A regular measurement update is required during the

transmission in LTE and LTE-A standards. When the regular measurement update is required during the transmission, the selection of CCS and CTP for each UE will be repeated by the serving cell to search for updated target cells. A handover is triggered when the condition is satisfied for the TTT time duration expressed as following:

$$RSRP_{T\_CTP} > RSRP_S + HOM \tag{4.1}$$

where $RSRP_{T\_CTP}$ and $RSRP_S$ are the RSRP received by an UE from the target cell in the CTP and the serving cell, respectively.

Once the handover is triggered, the serving cell sends a cancellation message to each of the cell in CTP to cancel the current transmissions. A handover command is triggered to instruct the UE to handover to the future serving cell..

The concept of this algorithm is to emphasize the opportunity of attaching to a future target cell which has the best channel quality for each UE by double filtering the measurement set into CCS and CTP. This reduces the signalling overhead between the UE and serving cell by narrowing down the RSRP observation from a full measurement set to the CTP while checking the handover constraint.

The performance of the CoMP Handover Algorithm in LTE-A is evaluated and compared with standard hard handover in LTE in terms of system throughput, PLR, and RB utilization metrics. The simulation environment and the performance metrics are discussed in Chapter 2. The complete system parameters used in the simulation are listed in Table 4.1. The Hybrid Automatic Repeat Request (HARQ) technique in [125] was used to recover from wireless transmission errors. The maximum number of error packet retransmissions is limited to 3.

Table 4.1: Downlink 3GPP LTE and LTE-A System Parameters

Parameters	**Values**
Cellular layout	Hexagonal grid, wrap around (reflect), 7 cells
Radius	100 m
Carrier Frequency	2 GHz
Bandwidth	5 MHz
Number of RBs	25
Number of sub-carriers per RB	12
Sub-carrier Spacing	15 kHz
Slot Duration	0.5 ms
Number of OFDM Symbols / Slot	7
Path Loss	Cost 231 Hata model
Shadow fading	Gaussian log-normal distribution
Multi-path	Non-frequency selective Rayleigh fading
Modulation and Coding Scheme	QPSK, 16QAM, and 64QAM
HARQ / Retransmission	Enable / 3 times
Packet Scheduler	Round Robin
Scheduling Time (TTI)	1 ms
Data Traffic	1 Mbps Constant Rate
User	30, 50, 80, 100
User's position	Fixed uniform distributed
User's direction	Randomly choose from [0,2π], constantly at all time
User's velocity	120 km/hr
Simulation time	5000 ms
RSRP sampling timer interval	50 ms
Handover Margin	5 dB
Time to Trigger (TTT)	5 ms
Size of CCS and CTP	2

The simulation results of the handover algorithm with JP in LTE-A are presented and compared with the standard handover algorithm in the LTE. Note that the number of handovers in the LTE system is the same as in the LTE-A system due to the fixed positions, directions, and velocity of each UE in the two simulations. Figure 4.12 shows the system throughput comparison in LTE-A and LTE system. LTE-A provides a higher system throughput than LTE due to the benefit of having multiple transmissions for each UE in the network. The system throughput improvements of LTE-A over LTE in 30, 50, 80, and 100 UEs are 42%, 47%, 49%, and 27%, respectively.

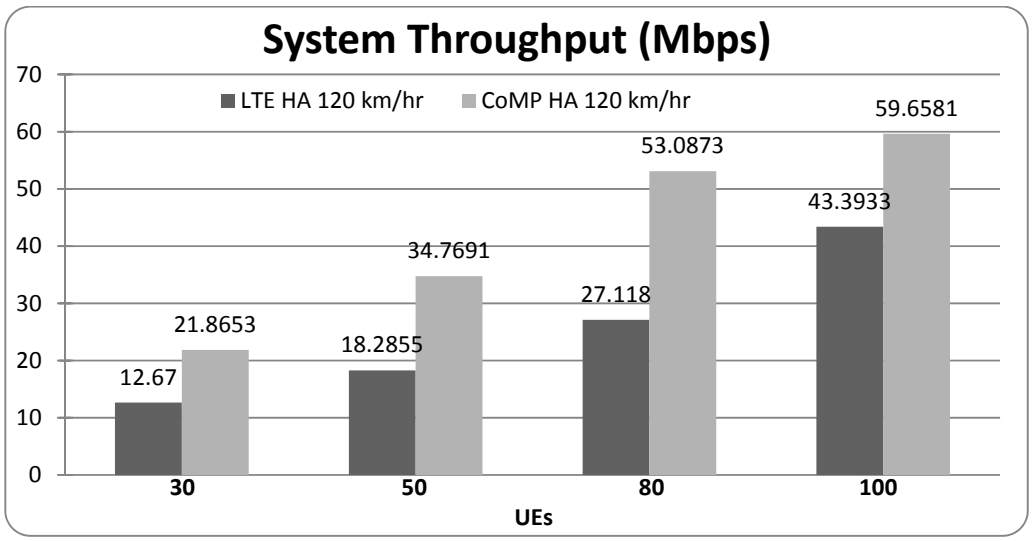

Figure 4.12: System Throughput of CoMP Handover Algorithm in LTE-A vs Hard Handover Algorithm in LTE

Figure 4.13 shows the PLR comparison in LTE-A and LTE systems. In contrast, LTE-A provides 36%, 31%, and 26% lower PLRs than LTE in first 3 scenarios (30, 50, and 80 UEs, respectively). This is because UEs in LTE-A receive redundant packets coming from multiple transmissions which can effectively reduce the PLRs for each packet. However, LTE-A has a slightly higher PLRs (0.2% higher than LTE system) in the case of 100 UEs.

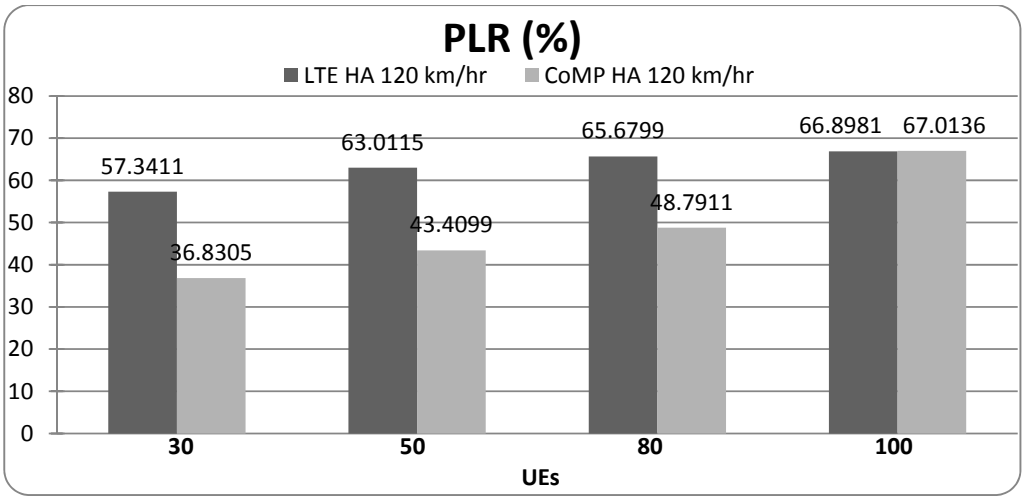

Figure 4.13: PLR of CoMP Handover Algorithm in LTE-A vs Hard Handover Algorithm in LTE

Figure 4.14 shows the RB utilization comparison in LTE-A and LTE systems. The higher the RB utilization value indicates a higher system load. LTE-A achieves higher system loads when compared to LTE in all scenarios due to the fact that it has multiple transmissions for each UE. The RB utilization in the LTE-A system shows 26.12%, 35.77%, 40.69%, and 37.32% above the LTE system in each scenario. Furthermore, the system capacity reaches 95% with 100 UEs in LTE-A, which leads to system throughput saturation and higher PLR issues. It is because that there are not enough resources in the eNodeBs for buffering each UE's incoming packets when the system is close to its full capacity. The CoMP Handover Algorithm aims to satisfy the requirements of JP in CoMP transmission and reception in the LTE-A system.

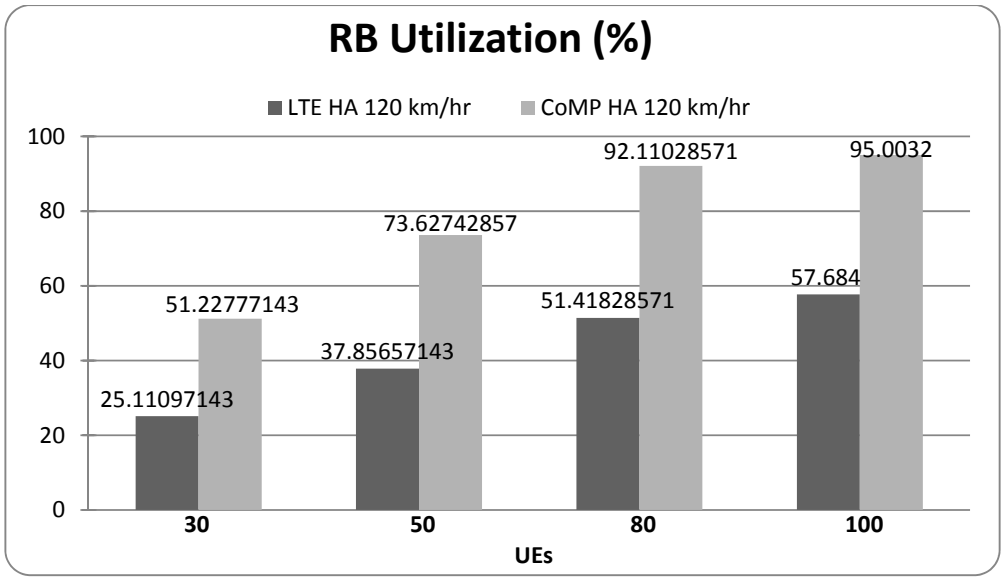

Figure 4.14: RB Utilization of CoMP Handover Algorithm in LTE-A vs Hard Handover Algorithm in LTE

Simulation results show that, when compared to the standard hard handover algorithm in the LTE system, the CoMP Handover Algorithm in LTE-A is able to improve system throughput and minimize PLR effectively. However, this algorithm could lead to system capacity overload and saturated system throughput issues within a highly congested network.

4.2 Proposed CoMP Handover Algorithms

Three CoMP handover algorithms have been proposed (Limited CoMP Handover Algorithm, Capacity Based CoMP Handover Algorithm, and Capacity Integrated CoMP Handover Algorithm) in order to overcome the system capacity overload and saturated system throughput issues while maintaining the system performance efficiency. Each proposed CoMP handover algorithm is described in detail, followed by a performance evaluation and comparison with the CoMP Handover Algorithm discussed in Section 4.1.3.

4.2.1 Limited CoMP Handover Algorithm

Limited CoMP Handover Algorithm consists of the same four concepts as in the CoMP Handover Algorithm: serving cell, measurement set, CoMP coordinating set (CCS), and CoMP transmission points (CTP). A serving cell takes the responsibility of making handover decision for each UE in the network. A measurement set is a set of cells whose RSRPs can be received and reported by the UE and fed back to the serving cell for making the selection of CCS. A CCS is a subset of the measurement set and a CTP is a subset of CCS. Three handover parameters are involved in Limited CoMP Handover Algorithm: measurement period, handover margin (HOM), and time to trigger (TTT) timer. A measurement period is a time interval that is used for checking the handover condition periodically. A HOM is a constant variable that represents the threshold for the difference in RSRP between the serving and the target cells. A TTT value is the time interval that is required for satisfying HOM condition.

A flowchart of the Limited CoMP Handover Algorithm is given in Figure 4.15. Note that the red solid line in Figure 4.15 indicates the time instant of a measurement period, the blue dash line in Figure 4.15 indicates the time instant other than the measurement period, and the black long dash dot line in Figure 4.15 indicates every time instant.

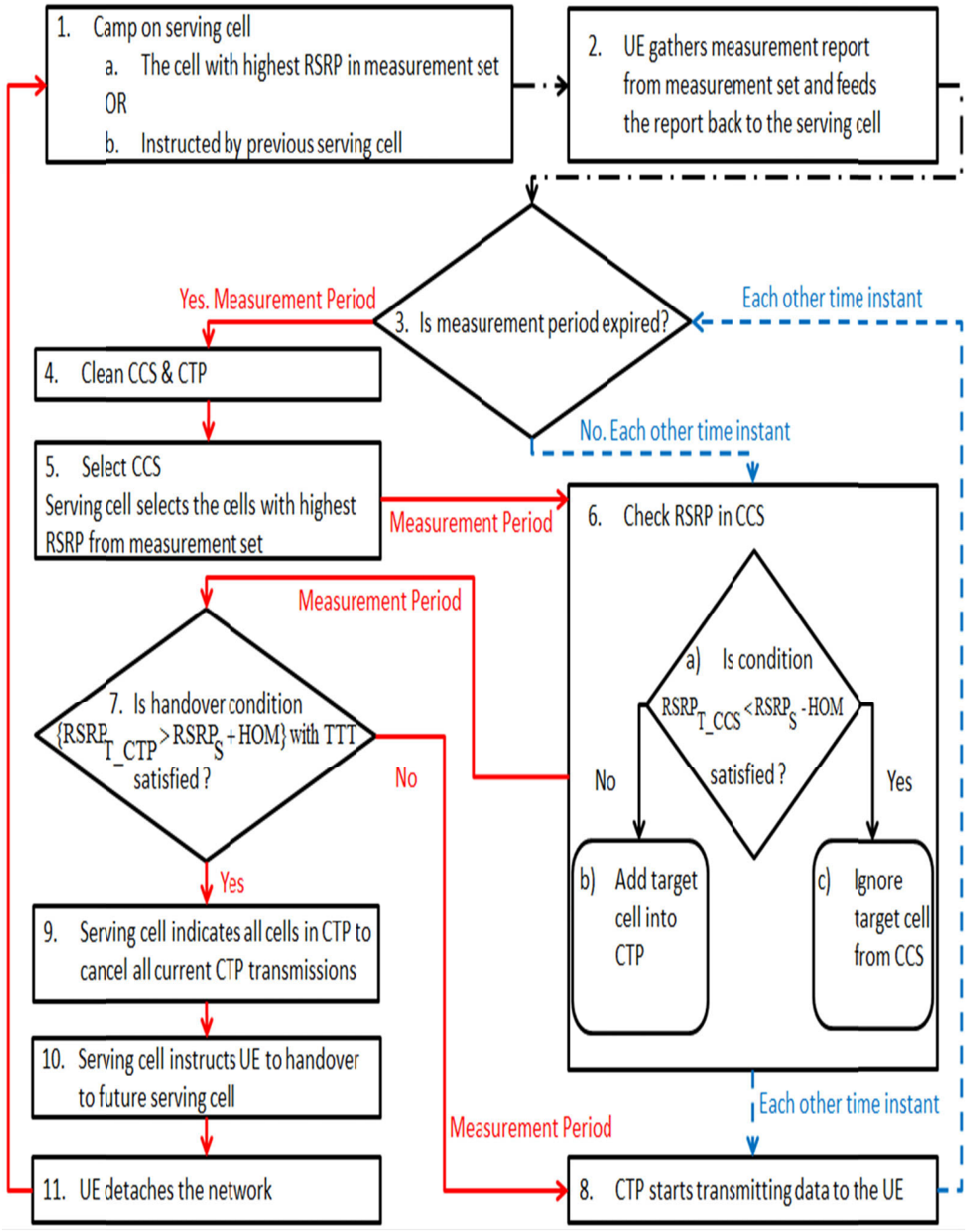

Figure 4.15: Flowchart of Limited CoMP Handover Algorithm in LTE-A

The Limited CoMP Handover Algorithm starts the cell selection/reselection when the UE joins the network by camping on the cell with the highest RSRP or the cell which was instructed by the previous serving cell. The UE gathers measurement reports which are the RSRP measurements received from the measurement set and feeds the reports

back to the serving cell. The first measurement period expires immediately due to an update required for the new incoming UE. The serving cell recursively selects the cell with the highest RSRP to be the CCS until reaching the end of measurement set. Moreover, the CTP selection will be recursively executed by the serving cell until reaching the end of CCS based on:

$$RSRP_{T\_CCS} < RSRP_S - HOM \tag{4.2}$$

where $RSRP_{T\_CCS}$ and $RSRP_S$ are the RSRPs received by an UE from the target cell in the CCS and the serving cell, respectively.

The target cell in the CCS will be ignored if Equation (4.2) is satisfied, otherwise the target cell in the CCS will be added into the CTP. After the CTP selection is finalized, serving cell performs handover condition check in the CTP based on Equation (4.3):

$$RSRP_{T\_CTP} > RSRP_S + HOM \tag{4.3}$$

where $RSRP_{T\_CTP}$ and $RSRP_S$ are the RSRPs received by an UE from the target cell in the CTP and the serving cell, respectively.

A handover is triggered if Equation (4.3) is satisfied within the TTT duration. The serving cell sends out a handover command to instruct the UE to handover to the future serving cell. Lastly, the UE detaches from the network and camps on a new serving cell after the interruption time (the time period which UE disconnects from the network). The CTP starts transmitting data to the UE and wait for the next incoming measurement period expired if Equation (4.2) is not satisfied at any point during the TTT duration. When the measurement period is not expired, the serving cell directly performs the CTP selection (Step 6 in Figure 4.15). The CTP continues transmitting data to the UE and repeat this process until the next measurement period expires.

The CoMP Handover Algorithm compares the highest RSRP of the target cells in measurement set and CCS for the candidate target cells in CTP (Step 4.A and 4.B in Figure 4.11). The CoMP Handover Algorithm improves the system throughput by giving multiple connections to each UE at any time instant regardless their channel conditions. This mechanism accelerates the current system capacity multiple times to

reach its maximum capacity due to multiple connections needed to be maintained for each UE in the network. Therefore the CoMP Handover Algorithm leads to system capacity overload and saturated system throughput issues within a high congested network.

The Limited CoMP Handover Algorithm comes with the concept of accommodating as many UEs as possible. The Limited CoMP Handover Algorithm utilizes the available radio resources by differentiating a cell-center UE (the UE with good/fair channel conditions) or a cell-edge UE (the UE with fair/bad channel conditions). Multiple data transmissions are given to a cell-edge UE while a single data transmission is given to a cell-center UE in order to save the available radio resources for accommodating more incoming UE.

The major difference between CoMP Handover Algorithm and Limited CoMP Handover Algorithm is shown in Step 6 in Figure 4.15. The Limited CoMP Handover Algorithm tracks the channel quality of each target cell in CCS at any time instant by using the HOM in Equation (4.2). If the RSRP of a target cell in the CTP received by a UE is significantly lower than the RSRP of the serving cell with a HOM, this UE is categorized as a cell-center UE. Thus the multiple data transmissions for cell-center UEs should be avoided in order to prevent the radio resources overused in other target cells in CTP based on the concept of the Limited CoMP Handover Algorithm. On the other hand, if the RSRP of a target cell in the CTP received by a UE is within the range of the HOM from the RSRP of the serving cell, this UE is categorized as a cell-edge UE. Thus the Limited CoMP Handover Algorithm has to provide multiple data transmissions for cell-edge UEs to maintain their qualities of connections while they stay in cell-edge areas. This mechanism (Step 6 in Figure 4.15) helps eliminating inefficient data transmissions at any time instant in the network, therefore the Limited CoMP Handover Algorithm is able to maintain the available radio resources more efficiently.

The Limited CoMP Handover Algorithm and the CoMP Handover Algorithm share most of the steps other than Step 6 in Figure 4.15 as following:

•The cell (re)selection when the UE joins the network in Step 1 in Figure 4.11 and Figure 4.15.

•UE gathers measurement reports and feeds them back to the serving cell in Step 2 in Figure 4.11 and Figure 4.15.

•A periodic measurement check in Step 3 in Figure 4.11 and Figure 4.15.

•CCS selection in Step 4.A in Figure 4.11 and Step 5 in Figure 4.15.

•Handover condition check in Step 5 in Figure 4.11 and Step 7 in Figure 4.15.

•CTP starts transmitting data to UEs in Step 6 in Figure 4.11 and Step 8 in Figure 4.15.

•Serving cell indicates all cells in CTP to cancel all current CTP connections in Step 7 in Figure 4.11 and Step 9 in Figure 4.15.

•Serving cell instructs UE to handover to the future serving cell in Step 8 in Figure 4.11 and Step 10 in Figure 4.15.

• UE detaches the network in Step 9 in Figure 4.11 and Step 11 in Figure 4.15.

Step 1 and Step 2 in the two algorithms are information gathering procedures. Similarly, Step 3 performs a standard periodical measurement check in both algorithms. Step 4.A in Figure 4.11 and Step 5 in Figure 4.15 share the concept of CCS selection based on the target cells with the highest RSRP in the measurement set. However, the CCS selection in Step 5 in Figure 4.15 can be used dynamically based on different requirements (such as delay constraint) rather than RSRP. Step 5 in Figure 4.11 and Step 7 in Figure 4.15 function as the standard handover condition check within CTP. Step 6 to Step 9 in Figure 4.11 and Step 8 to Step 11 in Figure 4.15 are the same in that both algorithms transmit data from CTP to UEs if the handover condition check (Step 5 in Figure 4.11 and Step 7 in Figure 4.15) is not satisfied, otherwise the serving cell sends out handover control messages in CTP for the UE to be handed over to the future serving cell. Lastly, the UE detaches the network and repeats the cell (re)selection (Step 1 in Figure 4.11 and Figure 4.15) in both algorithms.

The performance of CoMP Handover Algorithm and Limited CoMP Handover algorithm are evaluated and compared on the basis of RB utilization, system throughput, and system delay using the simulation tool described in Chapter 2. The system parameters used in the simulation are listed in Table 4.2. A simulation time between 0 ms and 10000 ms is needed for performance comparison for the proposed CoMP handover algorithms. However, 1000 ms and 10000 ms were intentionally used for optimization and performance evaluation as shown in Table 3.1. Therefore a 5000 ms (a mid-value of 10000 ms) simulation time was considered in Table 4.2.

Table 4.2: Simulation Parameters for Limited CoMP Handover Algorithm and CoMP Handover Algorithm

Parameters	**Values**
Cellular layout	Hexagonal grid, wrap around (reflect), 7 cells
Radius	100 m
Carrier Frequency	2 GHz
Bandwidth	5 MHz
Number of PRBs	25
Number of sub-carriers per PRB	12
Sub-carrier Spacing	15 kHz
Slot Duration	0.5 ms
Number of OFDM Symbols / Slot	7
Path Loss	Cost 231 Hata model
Shadow fading	Gaussian distribution
Multi-path	Rayleigh fading
Modulation and Coding Scheme	QPSK, 16QAM, and 64QAM
HARQ / Retransmission	Enable / 3 times
Packet Scheduler	Round Robin
Scheduling Time (TTI)	1 ms
Data Traffic	1 Mbps Constant Rate
User	30, 50, 100, 150, 200, 250, 300
User's position	Fixed uniform distributed
User's direction	Randomly choose from [0,2π], constantly at all time
User's velocity	120 km/hr
Simulation time	5000 ms
RSRP sampling timer interval	10 ms
Handover Margin	[1 ,2, 3, 4, 5] dB
Time to Trigger (TTT)	5 ms
Size of CCS	3
Size of CTP	2

Figure 4.16 shows the RB Utilization of the CoMP Handover Algorithm and Limited CoMP Handover Algorithm in LTE-A. The RB Utilization increases when the number of UEs increases in both algorithms because the more UEs coming in the simulation, the more PRBs have to be used for the users to transmit packets; therefore the RB Utilization will eventually reach 100% in the simulation when the number of users increases in both algorithms. The CoMP Handover Algorithm has a higher RB Utilization over Limited CoMP Handover Algorithm in all UEs scenarios. This is because the CoMP Handover Algorithm has two transmissions at all times, which requires at most twice as many PRBs as the Limited CoMP Handover Algorithm.

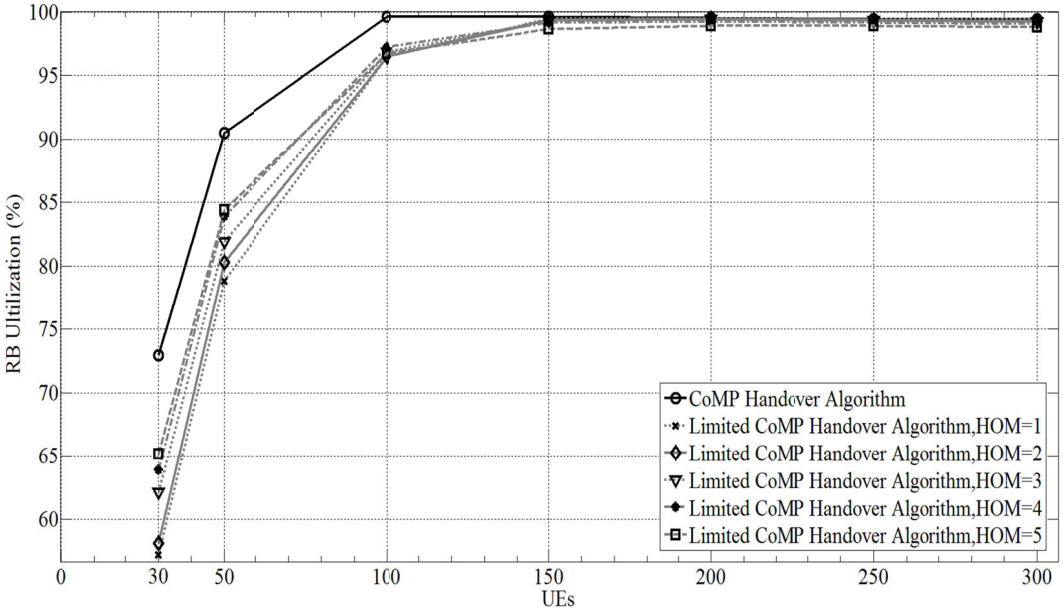

Figure 4.16: RB Utilization of CoMP Handover Algorithm and Limited CoMP Handover Algorithm in LTE-A

In the case of 30 UEs in the simulation, the CoMP Handover Algorithm reaches 72.94% RB Utilization, whereas the Limited CoMP Handover Algorithm reaches 57.18%, 58.11%, 62.11%, 63.90%, and 65.18% RB Utilizations for HOM of 1, 2, 3, 4, and 5 dB, respectively. Furthermore, a 100% RB Utilization state shown in Figure 4.16 is the system saturation point for both CoMP handover algorithms. The CoMP Handover Algorithm reaches the system saturation point with 100 UEs in the simulation while the Limited CoMP Handover Algorithm reaches the system saturation point with 150 UEs

in the simulation. A HOM of 1 dB gives the lowest RB Utilization which overcomes other HOM values in Limited CoMP Handover Algorithm. The system becomes saturated after the number of UEs reaches 150 in both algorithms.

Figure 4.17 shows the system throughput comparison of the CoMP Handover Algorithm and the Limited CoMP Handover Algorithm in LTE-A. The overall trend of system throughput increases in both handover algorithms with increasing the number of UEs because the more UEs coming in the simulation, the more packets were successfully transmitted in the system. Based on Equation (2.26), a higher number of transmitted bits in the system results a higher system throughput.

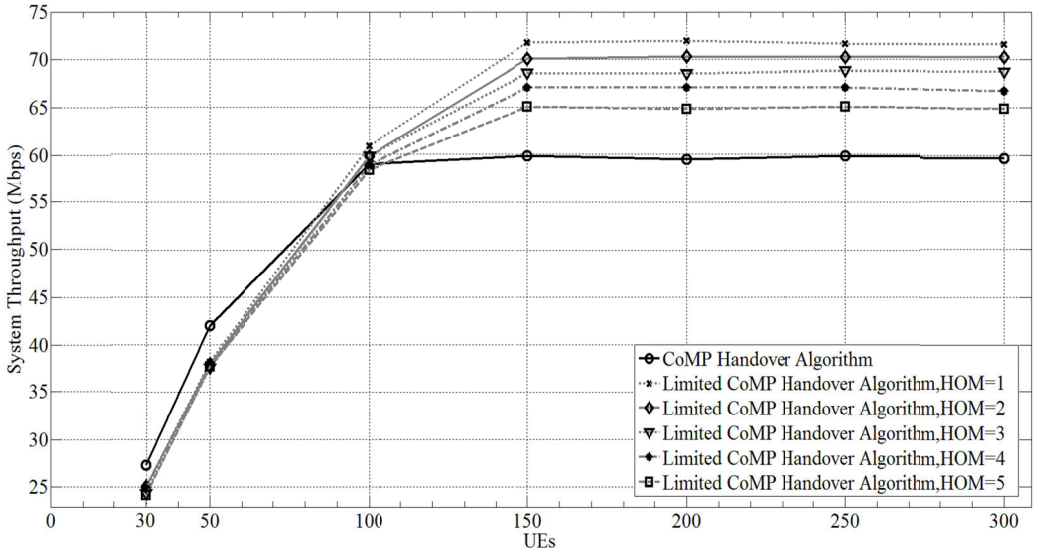

Figure 4.17: System Throughput of CoMP Handover Algorithm and Limited CoMP Handover Algorithm in LTE-A

The CoMP Handover Algorithm provides better system throughputs of 27.28 Mbps and 42.02 Mbps when compared to the Limited CoMP Handover Algorithm in the scenarios of 30 and 50 UEs, respectively. This is because when the number of UEs is low, the RB Utilization of the CoMP Handover Algorithm has not reached the saturated state (from Figure 4.16); hence the UEs in CoMP Handover Algorithm can fully utilize all the available PRBs in the network, which directly improves the system throughput. On the other hand, the Limited CoMP Handover Algorithm restricts the number of data connections for each UE at any time in the system based on their channel conditions.

Even when there are still plenty of available PRBs remain in the system, the Limited CoMP Handover Algorithm only support one single data connection at a time for UEs in a fair/good channel condition, which limits the number of transmitted bits in the system, and in turn directly limits the system throughput. Therefore the CoMP Handover Algorithm can reach a higher system throughput over the Limited CoMP Handover Algorithm in a light loaded system.

However when there are 150 UEs, the Limited CoMP Handover Algorithm outperforms the CoMP Handover Algorithm with the system throughput improvements of 19.91%, 17.09%, 14.64%, 12.02%, and 8.65% when the HOM of 1, 2, 3, 4, and 5 dB, respectively. The Limited CoMP Handover Algorithm takes the advantage of supporting single data connection for cell-center UEs in the system. A cell-center UE in the CoMP Handover Algorithm will be allocated by two data transmissions at any time, while in the Limited CoMP Handover Algorithm, a cell-center UE can only be allocated by one single data transmission. This restriction frees the available PRBs of the second data connection from the cell-center UE and the freed PRBs can be further used for other new incoming UEs which increase transmitted packets in the system, therefore enhancing the system throughput. When the system becomes fully loaded, the system throughput stops increasing due to insufficient radio resources (PRBs) to be allocated to the UEs in the system. The system throughput of the CoMP Handover Algorithm stops increasing and stays fixed around 60 Mbps at 150, 200, 250, and 300 UEs scenarios. When the system becomes saturated in 150, 200, 250, and 300 UEs scenarios, the system throughputs of the Limited CoMP Handover Algorithm stops increasing and stays fixed at 72 Mbps, 70 Mbps, 68 Mbps, 67 Mbps, and 65 Mbps when the HOM is 1, 2, 3, 4, and 5 dB, respectively. When the HOM is 5 dB, the Limited CoMP Handover Algorithm has the lowest system throughput due to the fact of having the largest HOM value which delays the handover triggering timing.

Figure 4.18 shows the system delay comparison of the CoMP Handover Algorithm and limited CoMP handover algorithm in LTE-A. The overall trend of system delay increases in both handover algorithms with increasing the number of UEs. This is because the queuing delay of the buffered packets in the eNodeBs increases due to the increased transmission requests by the higher number of UEs in the simulation.

The CoMP Handover Algorithm has a lower system delay of 4341.33 ms when compared to the Limited CoMP Handover Algorithm of 4597.8 ms when the HOM is 1 dB. It is because the available PRBs in the simulation are not yet fully utilized; thus the time packets spend in the eNodeB buffer is minimized. Hence, the CoMP Handover Algorithm has a lower system delay.

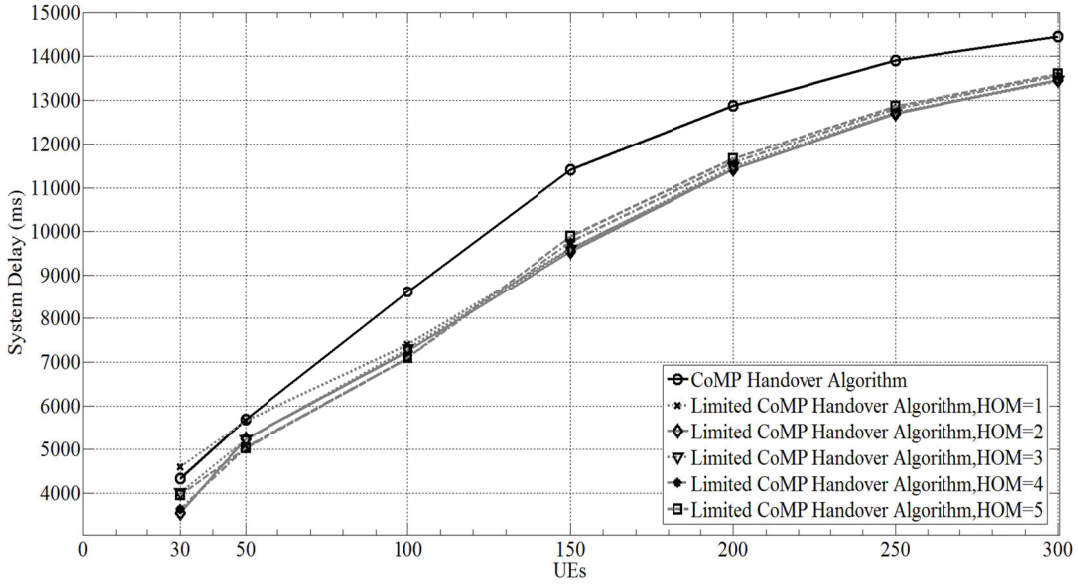

Figure 4.18: System Delay of CoMP Handover Algorithm and Limited CoMP Handover Algorithm in LTE-A

The CoMP Handover Algorithm has higher system delay of 5691.81 ms, 8615.15 ms, 11416.7 ms, 12874.8 ms, 13904.8 ms, and 14455 ms when compared to the Limited CoMP Handover Algorithm in the scenario of 50, 100, 150, 200, 250, and 300 UEs, respectively. This is because every UE's packet in serving cell and/or target cell in CTP has to be buffered and queued to be transmitted in the system. In the CoMP Handover Algorithm, two data connections are used at any time instant for each UE in the simulation. The packets belonging to the UE need to be buffered in the serving cell and the target cell in CTP. This behaviour increases the loading and the queuing delay of both serving cell and the target cell in CTP which leads to a higher system delay. In the Limited CoMP Handover Algorithm, when a cell-edge UE only can be offered a single data connection, this UE will not have the chance to have the second data connection from the target cell in CTP. Thus there will be no packet to be buffered and queued in

the target cell in CTP for this particular UE. Therefore this UE will not increase the loading and the queuing delay of the target cell in CTP which leads to a lower system delay result.

It is shown via simulation that the proposed handover algorithm can improve the system throughput when compared to the CoMP Handover Algorithm in a saturated system when the number of UEs is 150, 200, 250, and 300. The proposed handover algorithm is able to maintain a lower system delay when compared with the CoMP Handover Algorithm. Moreover, the system throughput and system delay of the proposed handover algorithm can be further improved by optimizing the HOM variable.

4.2.2 Capacity Based CoMP Handover Algorithm

The Capacity Based CoMP Handover Algorithm aims to select the appropriate target cells (in terms of capacity and channel quality) and ensures that the radio resources are efficiently used in the system.

The Capacity Based CoMP Handover Algorithm uses the same four concepts in the CoMP Handover Algorithm and/or Limited CoMP Handover Algorithm: serving cell, measurement set, CoMP coordinating set (CCS), and CoMP transmission points (CTP). There are four parameters involved in the Capacity Based CoMP Handover Algorithm: HOM, TTT, measurement period, and RB utilization value. HOM, TTT, and measurement period were described in the LTE hard handover algorithm in Section 3.4.1. An instantaneous RB utilization value evaluates the proportion of total used PRBs to total PRBs in each cell and describes the current state of the cell's capacity. It can be expressed as:

$$RButilize_c = PRBuse_c(t) / PRB\max_c(t) \tag{4.4}$$

The Capacity Based CoMP Handover Algorithm computes the instantaneous RB utilization value in real time to evaluate the system capacity of each eNB immediately to make a handover decision. A higher RB utilization value indicates that the cell becomes overloaded; therefore a cell reselection needs to be considered when more UEs are going to be handed over to this cell. On the other hand, when the cell has a lower RB utilization value, it is capable of accommodating more incoming UEs.

The Capacity Based CoMP Handover Algorithm starts the cell selection/reselection when the UE joins the network by camping on the cell with the highest RSRP in the measurement set or the cell which was instructed by the previous serving cell. The UE then gathers measurement reports which are the RSRP measurements received from the measurement set and feeds the reports back to the serving cell. The first measurement period expires immediately due to an update required for the new incoming UE. Moreover, the serving cell selects a set of cells with the lowest RB utilization value from the measurement set as CCS. The CTP selection will be done by the serving cell based on selecting a set of cells with the highest RSRP from CCS. The size of CCS can be adjusted but the size of CTP cannot be greater than the size of CCS. A handover will be triggered when the triggering condition Equation (4.5) is satisfied during the entire TTT duration, otherwise the CTP starts transmitting data to the UE and waits for the next measurement period expiration.

$$RSRP_{T\_CTP} > RSRP_S + HOM \tag{4.5}$$

where $RSRP_{T\_CTP}$ and $RSRP_S$ are the RSRPs received by a UE from the target cell in the CTP and the serving cell, respectively. Once a handover is triggered, the serving cell indicates all cells in the CTP to cancel all current CTP transmissions. A handover command is sent to instruct the UE to be handovered to the future serving cell. Lastly, the UE detaches the network and camps on a new serving cell after the interruption time. A flowchart of the Capacity Based CoMP Handover Algorithm is given in Figure 4.19.

The difference between the CoMP Handover Algorithm and Capacity Based CoMP Handover Algorithm starts from Step 4 in Figure 4.19. An instantaneous system capacity is computed by each eNB in the network and the Capacity Based CoMP Handover Algorithm prioritizes the target eNB based on its instantaneous RB utilization value. Whenever a target eNB has the lowest instantaneous RB utilization value, this target eNB is added into CCS as a candidate of the CTP. This is because when the cell has a lower RB utilization value, it is capable of accommodating more incoming UEs. Checking RB utilization value in CCS selection (Step 4 in Figure 4.19) reduces unnecessary feedback from the UE to the serving cell and ensures that the radio resources are efficiently used in the system. Thus, when the process moves to Step 5 in

Figure 4.19, the Capacity Based CoMP Handover Algorithm ensures that the target cells in CCS all have the lowest instantaneous RB utilization values and it ensures that the signal quality of target cells when selecting the target cells in CTP. Therefore, the overall system capacity can be optimized.

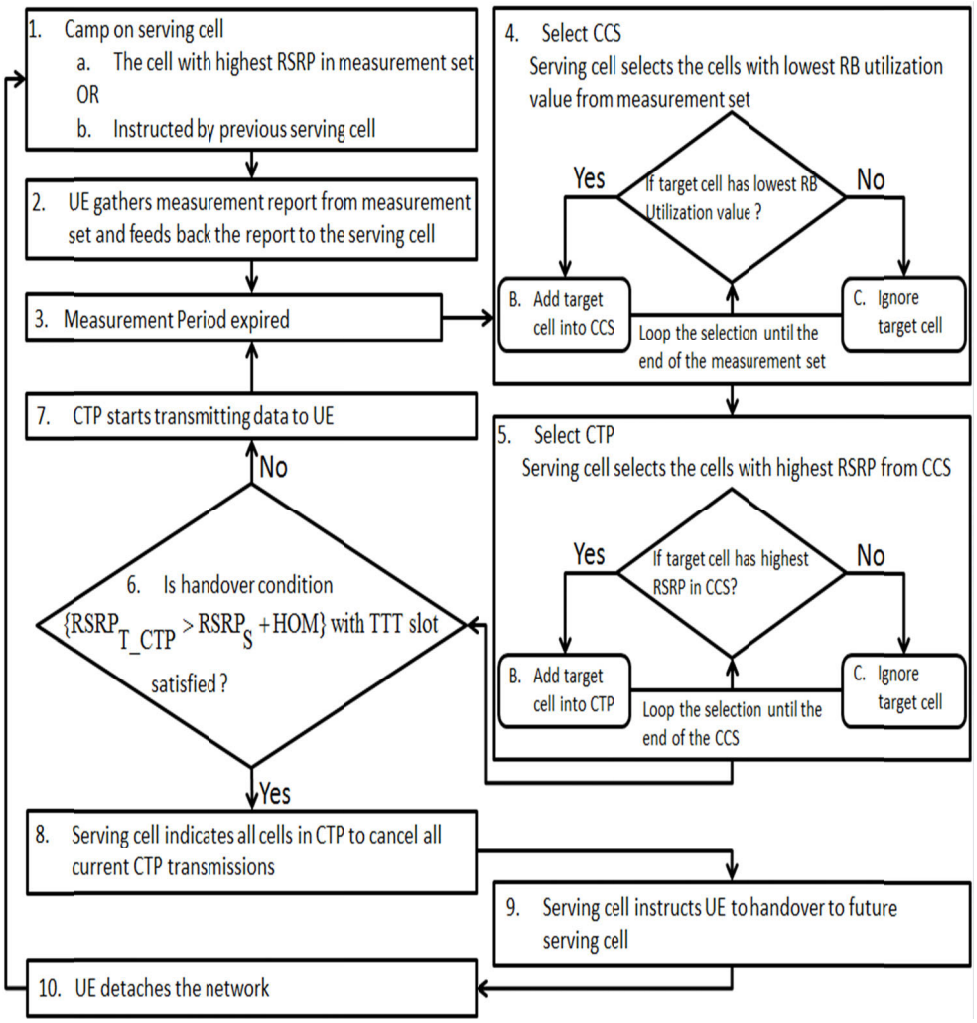

Figure 4.19: Flowchart of Capacity Based CoMP Handover Algorithm in LTE-A

The performance of the Capacity Based CoMP Handover Algorithm and the CoMP Handover Algorithm in LTE-A is evaluated based on three metrics: system throughput, system delay, and the total number of handovers. The simulation tool described in Chapter 2 is used. The system parameters used in the simulation are listed in Table 4.3. A 5000 ms simulation time was used in Table 4.3 for consistency with Table 4.2.

Table 4.3: Simulation Parameters for Capacity Based CoMP Handover Algorithm and CoMP Handover Algorithm

Parameters	**Values**
Cellular layout	Hexagonal grid, wrap around (reflect), 7 cells
Radius	100 m
Carrier Frequency	2 GHz
Bandwidth	5 MHz
Number of RBs	25
Number of sub-carriers per RB	12
Sub-carrier Spacing	15 kHz
Slot Duration	0.5 ms
Number of OFDM Symbols / Slot	7
Path Loss	Cost 231 Hata model
Shadow fading	Gaussian distribution
Multi-path	Rayleigh fading
Modulation and Coding Scheme	QPSK, 16QAM, and 64QAM
HARQ / Retransmission	Enable / 3 times
Packet Scheduler	Round Robin
Scheduling Time (TTI)	1 ms
Data Traffic	1 Mbps Constant Rate
User	15, 30, 50, 80, 100
User's position	Fixed uniform distributed
User's direction	Randomly choose from $[0,2\pi]$, constantly at all time
User's velocity	120 km/hr
Simulation time	5000 ms
RSRP sampling timer interval	10 ms
Handover Margin	5 dB
Time to Trigger (TTT)	5 ms
Size of CCS	2
Size of CTP	2

Figure 4.20 shows the comparison of the system throughput of Capacity Based CoMP Handover Algorithm and the CoMP Handover Algorithm in LTE-A. The Capacity Based CoMP Handover Algorithm provides higher system throughputs (14.53 Mbps, 28.96 Mbps, 41.67 Mbps, 51.30 Mbps, and 55.29 Mbps) than the CoMP Handover Algorithm (13.16 Mbps, 24.62 Mbps, 38.01Mbps, 48.90 Mbps, and 54.23Mbps) in scenarios of 15, 30, 50, 80, and 100 UEs, respectively. Furthermore, the Capacity Based CoMP Handover Algorithm offers 10.40%, 17.62%, 9.64%, 4.91%, and 1.95% system throughput improvement when compared to the CoMP Handover Algorithm in scenarios of 15, 30, 50, 80, and 100 UEs, respectively. It is shown that the Capacity Based CoMP Handover Algorithm has better system throughputs because it arranges UEs in a capacity priority manner when making the handover decision. A target cell with a lower RB utilization value indicates that the radio resources in the target cell can be fully utilized (by the lower *PRBuse* in Equation (4.4)). The target cell with a higher RSRP indicates a higher SINR which implies a higher data rate of the transmission (by the higher efficiency value in Equation (2.13)). Therefore the radio resources in the system are more efficiently utilized which leads to a higher system throughput result.

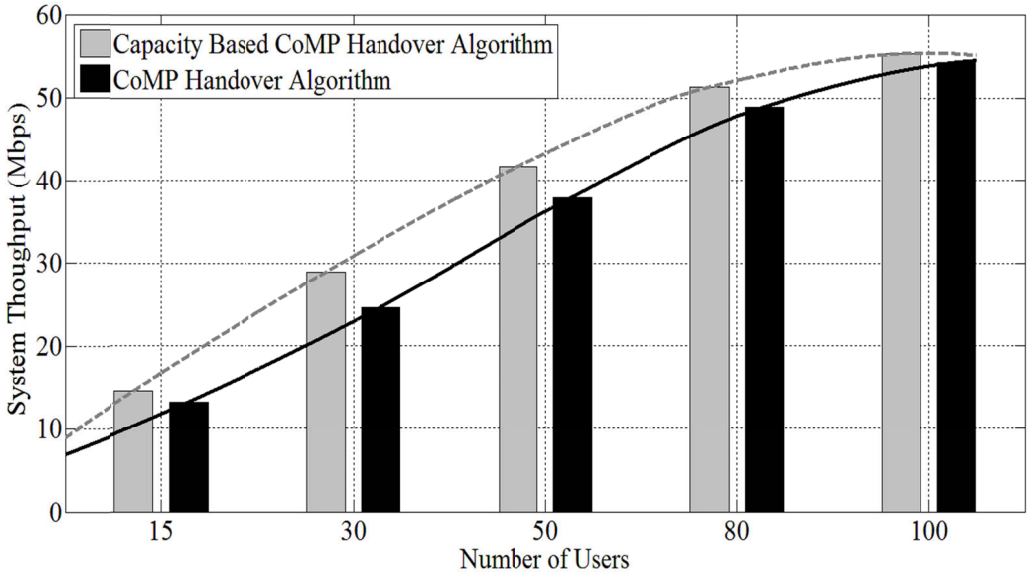

Figure 4.20: System Throughput of Capacity Based CoMP Handover Algorithm vs CoMP Handover Algorithm in LTE-A

Figure 4.21 shows the comparison of system delays of the Capacity Based CoMP Handover Algorithm and the CoMP Handover Algorithm in LTE-A. The Capacity Based CoMP Handover Algorithm provides lower system delay (3819.03ms, 4696.28ms, 5493.13ms, 6621.36ms, and 7238.82ms) than the CoMP Handover Algorithm (4518.98ms, 5576.88ms, 6839.04ms, 9115.71ms, and 9850.31ms) in the scenarios of 15, 30, 50, 80, and 100 UEs, respectively. Furthermore, the Capacity Based CoMP Handover Algorithm has 15.49%, 15.79%, 19.68%, 27.36%, and 26.51% lower system delay than the CoMP Handover Algorithm in scenarios of 15, 30, 50, 80, and 100 UEs, respectively. It is shown that the Capacity Based CoMP Handover Algorithm effectively minimized the system delay by arranging UEs to be handed over to a lower loaded cell when making a handover decision. This mechanism avoids the congestion in the system which leads to a lower system delay.

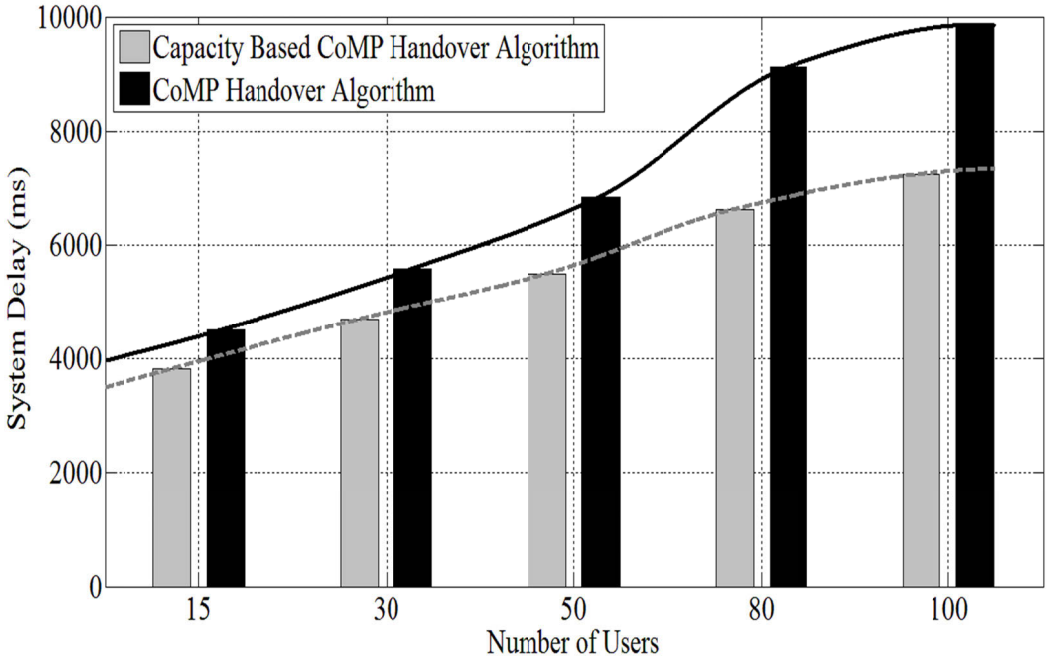

Figure 4.21: System Delay of Capacity Based CoMP Handover Algorithm vs CoMP Handover Algorithm in LTE-A

Figure 4.22 shows the total number of handovers of the Capacity Based CoMP Handover Algorithm and CoMP Handover Algorithm in LTE-A. Both algorithms have the same total number of handovers (12) in the 15 UEs scenario. In the 30, 50, 80, 100

UEs scenarios, the Capacity Based CoMP Handover Algorithm has more total numbers of handover (26, 36, 57, and 72 times) when compared to the CoMP Handover Algorithm (23, 33, 52, and 64 times). Furthermore, the Capacity Based CoMP Handover Algorithm has 13.04%, 9.09%, 9.62% and 12.5% increases in total number of handovers than the CoMP Handover Algorithm in 30, 50, 80, and 100 UEs scenarios respectively. The simulation result shows that the Capacity Based CoMP Handover Algorithm has more total number of handovers than the CoMP Handover Algorithm by arranging UEs to be handed over to a lower loaded cell. This arrangement limits the chance that UEs camp on the most appropriate cell with the best radio signal quality when making a handover decision. Therefore UEs are going to have a higher chance to encounter more handover triggering condition satisfaction (Equation (4.5)) in the system, which leads to more number of handovers in the result.

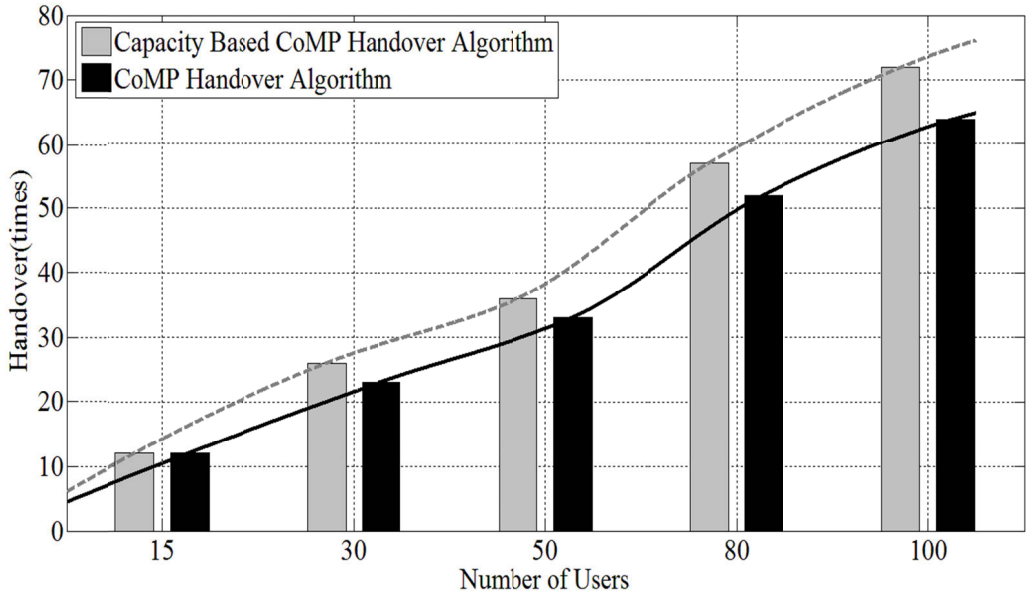

Figure 4.22: Total Number of Handover of Capacity Based CoMP Handover Algorithm vs CoMP Handover Algorithm in LTE-A

A Capacity Based CoMP Handover Algorithmin LTE-A is proposed, evaluated and compared with the open literature handover algorithm in this section. The Capacity Based CoMP Handover Algorithm aims to enhance the system capacity as well as ensure that the radio resources are efficiently used in the system. Simulation results show that the Capacity Based CoMP Handover Algorithm can maximize the system

throughput and minimize the system delay when compared to the CoMP Handover Algorithm. However, a side effect of having higher total numbers of handovers needs to be resolved to improve the Capacity Based CoMP Handover Algorithm.

4.2.3 Capacity Integrated CoMP Handover Algorithm

A Capacity Integrated CoMP Handover Algorithm is proposed based on the Capacity Based CoMP Handover Algorithm with an additional mechanism whereby instantaneous and historical RB utilization values are taken into consideration when making the handover decision.

The Capacity Integrated CoMP Handover Algorithm has four concepts: serving cell, measurement set, CoMP coordinating set (CCS), and CoMP transmission points (CTP).

A historical RB utilize value can be mathematically expressed as:

$$HisRButilize_c(t) = \frac{\sum_{t=1}^{T} RButilize_c(t)}{T} \tag{4.6}$$

where T is the total simulation time, $RButilize_c(t)$ denotes the RB utilize value of cell c at time t obtained from Equation (4.4), and $HisRButilize_c(t)$ is the historical RB utilize value of cell c at time t.

A new handover parameter (called the capacity indicator) is introduced in the Capacity Integrated CoMP Handover Algorithm. The capacity indicator represents the proportional combination of historical RB utilization values and RB utilization values and is expressed as:

$$Capacity_C(t) = (1-\gamma) * HisRButilize_C(t-1) + \gamma * RButilize_C(t) \tag{4.7}$$

where γ is a factor between 0 and 1. When γ approaches 1, the capacity indicator is weighted more to the RB utilization value. Conversely, when γ approaches 0, the capacity indicator will be biased more to the historical RB utilization values at the previous time instant. A cell's capacity condition is expressed as follows:

$$Capacity_c(t) \leq Capacity\ Threshold \tag{4.8}$$

where $Capacity_C(t)$ is the capacity indicator of cell c at time t. *Capacity Threshold* is a factor between 0 and 1. A *Capacity Threshold* value is used for determining appropriate target cells whose current and historical capacities are able to accommodate the incoming UE. A flowchart of the Capacity Integrated CoMP Handover Algorithm is given in Figure 4.23.

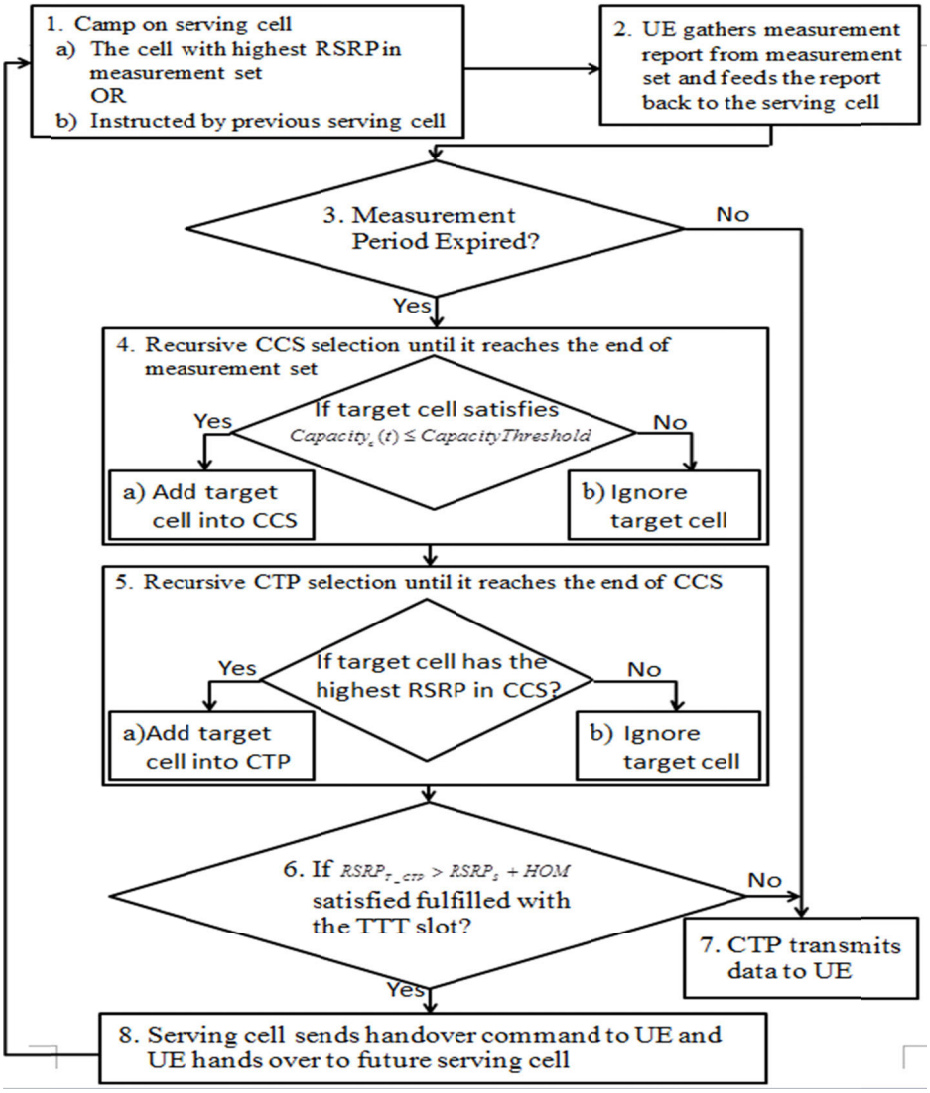

Figure 4.23: Flowchart of Capacity Integrated CoMP Handover Algorithm in LTE-A

The first three steps in the Capacity Integrated CoMP Handover Algorithm (Step 1, Step 2, and Step 3 in Figure 4.23) are the same as the first three steps in Capacity Based

CoMP Handover Algorithm (Step 1, Step 2, and Step 3 in Figure 4.19) and have been described in Section 4.2.2.

The target cells within the measurement set which satisfy Equation (4.8) will be selected as CCS by the serving cell after the measurement period expiration. The CCS selection will be repeated until it reaches the end of the measurement set. Moreover, the CTP selection will be based on selecting a cell with the highest RSRP from CCS. The CTP selection will be repeated until it reaches the end of the CCS. The size of CCS and CTP can be adjusted but the size of CTP cannot be greater than the size of CCS.

A handover will be triggered when Equation (4.8) is satisfied during the entire TTT duration; otherwise the CTP transmits data to the UE and waits for the next measurement period expiration. Once a handover is triggered, a handover command is sent by the serving cell to instruct the UE to be handed over to the future serving cell..

The key features of the Capacity Integrated CoMP Handover Algorithm are: (a) a historical capacity of each eNB in the system is tracked, (b) the capacity indicator takes both the instantaneous and the historical capacities of each eNB in the system into consideration, (c) an adjustable parameter γ is used in the capacity indicator for customizing the proportion between instantaneous and the historical capacities of each eNB, and (d) the capacity threshold can be customized by operators based on different policies.

The use of double filtering in the Capacity Integrated CoMP Handover Algorithm (Step 4 and Step 5 in Figure 4.23) emphasises the quality of target cells in both capacity and channel quality domains and ensures that the radio resources are efficiently used in the system while reducing unnecessary feedback of RSRP measurements from a large cell set for each UE.

The performance of the Capacity Integrated CoMP Handover Algorithm and CoMP Handover Algorithm in LTE-A is evaluated using the simulation tool described in Chapter 2 and is based on four metrics: system throughput, system delay, PLR, and total number of handovers. The system parameters used in the simulation are listed in Table 4.4. A 5000 ms simulation time was used in Table 4.4 for consistency with Table 4.2.

Table 4.4: Simulation Parameters for Capacity Integrated CoMP Handover Algorithm and CoMP Handover Algorithm

Parameters	**Values**
Cellular layout	Hexagonal grid, wrap around (reflect), 7 cells
Radius	100 m
Carrier Frequency	2 GHz
Bandwidth	5 MHz
Number of RBs	25
Number of sub-carriers per RB	12
Sub-carrier Spacing	15 kHz
Slot Duration	0.5 ms
Number of OFDM Symbols / Slot	7
Path Loss	Cost 231 Hata model
Shadow fading	Gaussian distribution
Multi-path	Rayleigh fading
Modulation and Coding Scheme	QPSK, 16QAM, and 64QAM
HARQ / Retransmission	Enable / 3 times
Packet Scheduler	Round Robin
Scheduling Time (TTI)	1 ms
Data Traffic	1 Mbps Constant Rate
User	15, 30, 50, 80, 100
User's position	Fixed uniform distributed
User's direction	Randomly choose from $[0,2\pi]$, constantly at all time
User's velocity	120 km/hr
Simulation time	5000 ms
RSRP sampling timer interval	10 ms
Handover Margin	5 dB
Time to Trigger (TTT)	5 ms
Size of CCS and CTP	2
γ	0.5
Capacity Threshold	0.8

The simulation results of Capacity Integrated CoMP Handover Algorithm are presented and compared with the results of the CoMP handover algorithm in the LTE-A system.

Figure 4.24 shows the comparison of the system throughputs of the Capacity Integrated CoMP Handover Algorithm and the CoMP Handover Algorithm in LTE-A. The Capacity Integrated CoMP Handover Algorithm offers system throughput improvements of 8.58%, 20.64%, 6.24%, and 1.12% when compared to the CoMP Handover Algorithm in scenarios of 15, 30, 50, and 80 UEs, respectively. It is shown that the Capacity Integrated CoMP Handover Algorithm has better system throughputs because it arranges UEs in a capacity priority manner when making the handover decision. The Capacity Integrated CoMP Handover Algorithm prioritizes the target eNB with the lowest system capacity (combined with instantaneous and historical system capacities) to be the target cell in CCS and selects the target eNB with the highest RSRP in CCS to be the target eNB in CTP. A target eNB with a lower RB utilization value indicates that the radio resources in the target cell can be fully utilized (by the lower *PRBuse* in Equation (4.4)). The target eNB with a higher RSRP indicates a higher SINR which implies a higher data rate of the transmission (by the higher efficiency value in Equation (2.13)). Therefore the radio resources in the system are more efficiently utilized which leads to a higher system throughput result

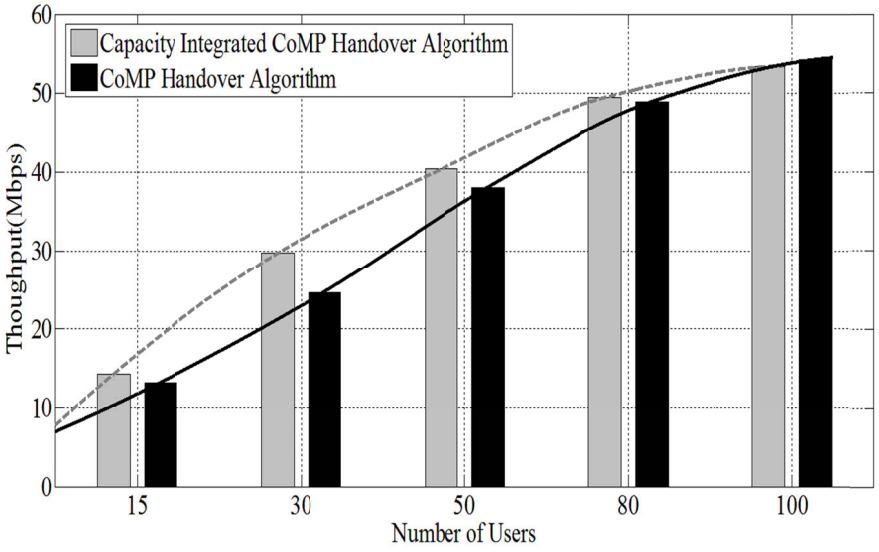

Figure 4.24: System Throughput of Capacity Integrated CoMP Handover Algorithm vs CoMP Handover Algorithm in LTE-A

Figure 4.25 shows the comparison of system delay of the Capacity Integrated CoMP Handover Algorithm and the CoMP Handover Algorithm in LTE-A.

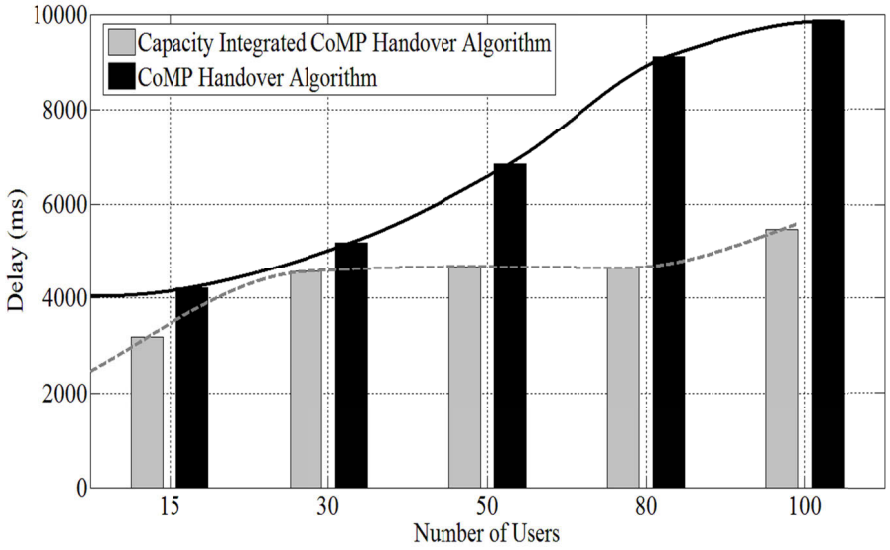

Figure 4.25: System Delay of Capacity Integrated CoMP Handover Algorithm vs CoMP Handover Algorithm in LTE-A

The Capacity Integrated CoMP Handover Algorithm has 24.81%, 11.89%, 31.75%, 49.07%, and 44.54% lower system delay compared to the CoMP Handover Algorithm in scenarios of 15, 30, 50, 80, and 100 UEs, respectively. It is shown that the Capacity Integrated CoMP Handover Algorithm effectively minimized an average of 32.41% system delay than the CoMP handover algorithm among all scenarios. The Capacity Integrated CoMP Handover Algorithm arranges UEs to be handed over to a lower loaded cell when making the handover decision. This mechanism avoids the congestion in the system which leads to a lower system delay result.

The PLR of the Capacity Integrated CoMP Handover Algorithm and the CoMP Handover Algorithm in LTE-A is shown in Figure 4.26. The Capacity Integrated CoMP Handover Algorithm has 67.30%, 60.96%, 53.30%, and 51.12% lower PLR when compared to the CoMP Handover Algorithm in 30, 50, 80, and 100 UEs scenarios, respectively. It is shown that the Capacity Integrated CoMP Handover Algorithm achieves an average of 46.54% lower PLR when compared to the CoMP Handover Algorithm in all scenarios. The CoMP Handover Algorithm always maintains two

transmission points at any time in the simulation which doubles the number of packets received at the UE. This behaviour affects the total discarded packet size and total number of packet size in Equation (2.27), therefore the PLRs of CoMP Handover Algorithm is higher than the PLRs of the Capacity Integrated CoMP Handover Algorithm in 30, 50, 80, and 100 UEs scenarios.

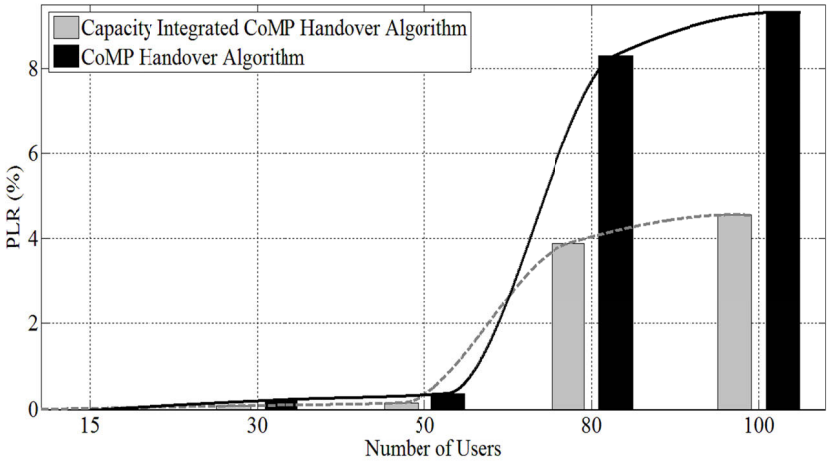

Figure 4.26: PLR of Capacity Integrated CoMP Handover Algorithm vs CoMP Handover Algorithm in LTE-A

The total number of handovers of the Capacity Integrated CoMP Handover Algorithm and the CoMP Handover Algorithm in LTE-A are shown in Figure 4.27.

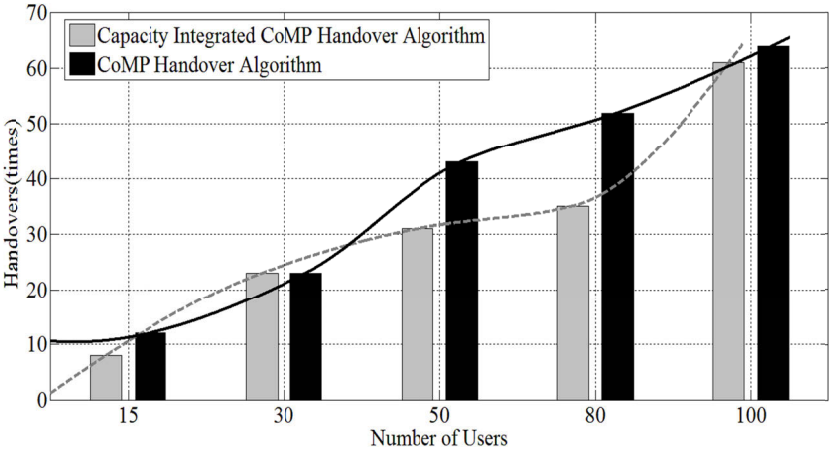

Figure 4.27: Total Number of Handovers of Capacity Integrated CoMP Handover Algorithm vs CoMP Handover Algorithm in LTE-A

The Capacity Integrated CoMP Handover Algorithm has 33.33%, 27.91%, 32.69%, and 4.69% lower total number of handovers than the CoMP Handover Algorithm in 15, 50, 80, and 100 UEs scenarios, respectively. It is shown that the Capacity Integrated CoMP Handover Algorithm has a lower or equivalent total number of handovers than the CoMP Handover Algorithm in all scenarios.

In this section, the Capacity Integrated CoMP Handover Algorithm in LTE-A is proposed, evaluated and compared with an open literature handover algorithm. The Capacity Integrated CoMP Handover Algorithm aims to ensure that the radio resources are efficiently used in the system in both capacity and channel quality domains while reducing unnecessary feedbacks. Simulation results show that the Capacity Integrated CoMP Handover Algorithm can improve the system throughput, minimize system delay, provide lower PLR and a lower or equivalent total number of handovers than the CoMP Handover Algorithm among all scenarios.

4.3 Summary

This chapter describes the CoMP technology mechanism in a LTE-A system and several open literature CoMP handover algorithms for the LTE system. Based on the research work, the JP in CoMP technology enhances the LTE-A system throughput and reduces the PLR when compared to the LTE system. Furthermore, the existing hard handover algorithms in LTE network are not applicable for CoMP networks in the LTE-A system and JP in CoMP technology could lead to system capacity overload and saturated system throughput issues within a highly congested network. To address this situation, three CoMP handover algorithms are proposed for the LTE-A system. These algorithms take into consideration one or more decision criteria to overcome the loaded system throughput problem and maximize the system capacity. The system performance of each proposed CoMP handover algorithm is evaluated and compared with open literature handover algorithm via simulation tools described in Chapter 2.

Chapter 5

PERFORMANCE EVALUATION OF COMP HANDOVER ALGORITHMS

A performance evaluation of selected CoMP handover algorithms with various type of traffic in the LTE-A system is discussed in this chapter. The CoMP Handover Algorithm, the Limited CoMP Handover Algorithm, the Capacity Based CoMP Handover Algorithm, and the Capacity Integrated CoMP Handover Algorithm are selected for performance evaluation and comparison. The handover parameters of each CoMP handover algorithm are optimized by the optimization method purposed in Section 3.6.1. The simulation results of the performance testing of all CoMP handover algorithms for RT, NRT and mixed RT and NRT traffics are shown in this chapter.

The radio resources in the performance testing of the RT traffic are assumed to be fully utilized in a high system load scenario because the RT traffic is a CBR traffic. The radio resources in the performance testing of NRT traffic is assumed to be utilized in a lower system load scenario because the web browsing model in the NRT traffic does not constantly provide packets to the UEs throughout the simulation. Furthermore, the radio resources in the performance testing of the mixed RT and NRT traffic is assumed to be a medium to high system load scenario due to the equal divided for the RT traffic and NRT traffic.

Based on the simulation result obtained from Figure 4.16, around 150 UEs leads to a full loaded state in the seven cells scenario. Therefore a total number of 150 UEs is selected for both parameters optimization and performance testing in RT, NRT, and mixed RT and NRT traffics. The PF packet scheduling algorithm was selected in both parameters optimization and performance testing because PF provides a better trade-off between fairness and throughput when compared to the MR and RR packet scheduling algorithms.

This chapter is organised as follows: Section 5.1 gives the handover parameters optimization of each selected CoMP handover algorithm for performance testing. Section 5.2, Section 5.3, and Section 5.4 discuss the performance testing of selected CoMP handover algorithms for RT traffic, NRT traffic, and mixed RT and NRT traffic in the LTE-A system, respectively. Finally, a summary of this chapter is given in Section 5.5.

5.1 Parameters Optimization

Parameters optimization under three speed scenarios of four CoMP handover algorithms is discussed in this section. The optimization method based on Section 3.6.1 is used to optimize the performance of all CoMP handover algorithms for performance evaluation in the following sections. The common parameters and parameters for optimization in the simulation are listed in Table 5.1 and Table 5.2, respectively. The simulation time for parameters optimization in Table 5.1 was intentionally set to 1000 ms in order to be consistent with the simulation time for optimization in Table 3.1 in Chapter 3.

Table 5.1: The Common Simulation Parameters for Parameters Optimization

Parameters	**Values**
Cellular layout	Hexagonal grid, wrap around (reflect), 7 cells
Radius	100 m
Carrier Frequency	2 GHz
Bandwidth	5 MHz
Number of RBs	25
Number of sub-carriers per RB	12
Sub-carrier Spacing	15 kHz
Slot Duration	0.5 ms
Number of OFDM Symbols / Slot	7
Path Loss	Cost 231 Hata model
Shadow fading	Gaussian distribution
Multi-path	Rayleigh fading
Modulation and Coding Scheme	QPSK, 16QAM, and 64QAM
HARQ / Retransmission	Enable / 3 times
Packet Scheduler	Proportional Fair
Scheduling Time (TTI)	1 ms
Data Traffic	1 Mbps Constant Rate
User	150
User's position	Fixed uniform distributed
User's direction	Randomly choose from [0,2π]
Simulation time	1000 ms
Simulation run	3 times
RSRP sampling timer interval	10 ms
Size of CCS	3
Size of CTP	2
γ	0.75
Capacity Threshold	0.9

Table 5.2: Simulation Parameters Optimization for CoMP Handover Algorithms

Parameters	Values
HOA	5: CoMP Handover Algorithm 6: Limited CoMP Handover Algorithm 7: Capacity Based CoMP Handover Algorithm 8: Capacity Integrated CoMP Handover Algorithm
TTT	(0, 1, 2, 3, 4, 5) millisecond
HOM	(0, 1, 2, 3, 4, 5) dB
UE Speed	(3, 30, 120) km/hr

An average system throughput and ANOH are calculated from the three simulations of the same HOM, TTT, HOA, and UE speed. Furthermore, the average system throughput and ANOM from the three simulations are applied to the optimization method based on Equation (3.14) to find out the *OptimizeRatio* value. A log scale of *OptimizeRatio* value was added for refined comparison. The highest $\log_{10}$(*OptimizeRatio*) value in each speed scenario leads to an optimized set of HOM and TTT of the HOA.

The $\log_{10}$(*OptimizeRatio*) of HOA5 results in Figure 5.1 are calculated using Equation (3.14) under 3, 30, and 120 km/hr scenarios with an input set of HOM and TTT increasing from 0 to 5 dB and 0 to 5 ms, respectively. The highest bar graph in each speed scenario in Figure 5.1 indicates the highest $\log_{10}$(*OptimizeRatio*) value in each speed and it refers to HOM and TTT equivalent to 4 and 5, 4 and 5, 5 and 4, in 3 km/hr, 30km/hr, and 120 km/hr scenarios, respectively.

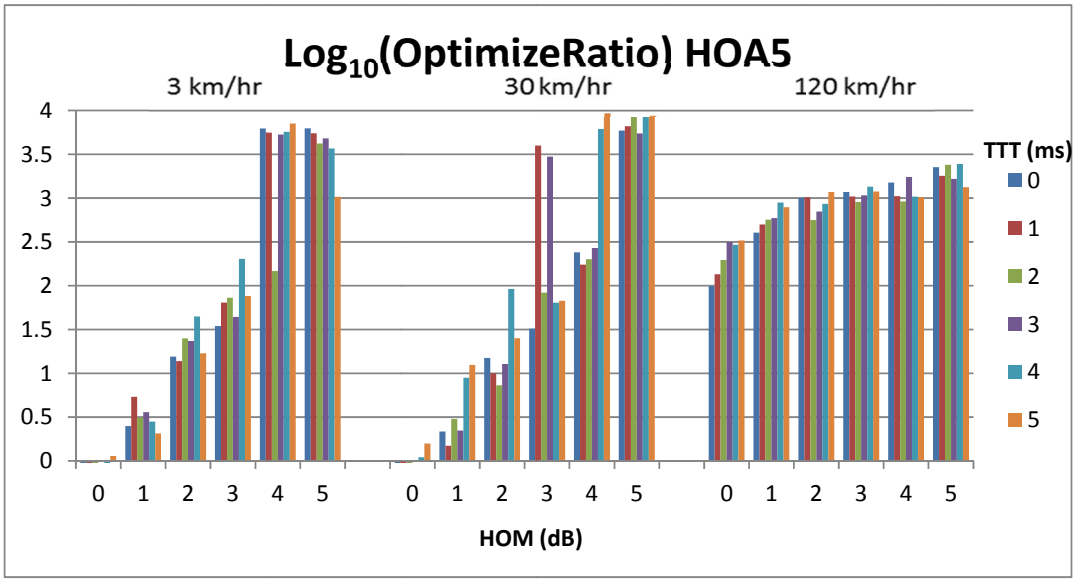

Figure 5.1: $\log_{10}(OptimizeRatio)$ of HOA5 in LTE-A

The $\log_{10}(OptimizeRatio)$ of HOA6 results in Figure 5.2 are calculated using Equation (3.14) under 3, 30, and 120 km/hr scenarios with an input set of HOM and TTT increasing from 0 to 5 dB and 0 to 5 ms, respectively. The highest bar graph in each speed scenario in Figure 5.2 indicates the highest $\log_{10}(OptimizeRatio)$ value in each speed and it refers to HOM and TTT equivalent to 4 and 4, 5 and 4, 5 and 3, in 3 km/hr, 30km/hr, and 120 km/hr scenarios, respectively.

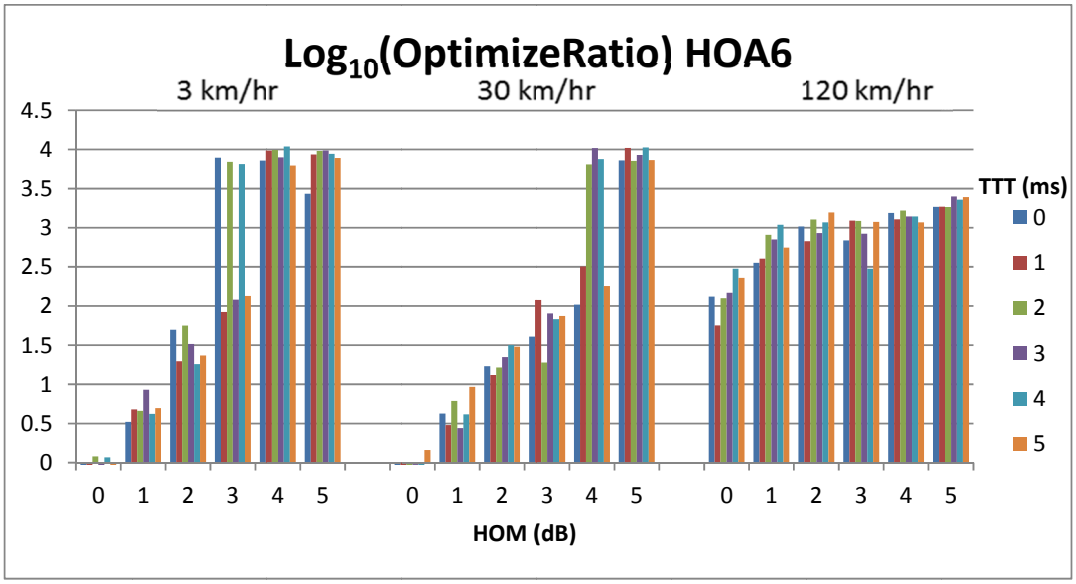

Figure 5.2: $\log_{10}(OptimizeRatio)$ of HOA6 in LTE-A

Figure 5.3 shows the $\log_{10}(OptimizeRatio)$ of HOA 7 under 3, 30, and 120 km/hr scenarios with an input set of HOM and TTT increasing from 0 to 5 dB and 0 to 5 ms, respectively. The highest $\log_{10}(OptimizeRatio)$ value in Figure 5.3 indicates the optimized set of HOM and TTT equivalent to 5 and 3, 4 and 1, 5 and 5, in 3 km/hr, 30km/hr, and 120 km/hr scenarios, respectively.

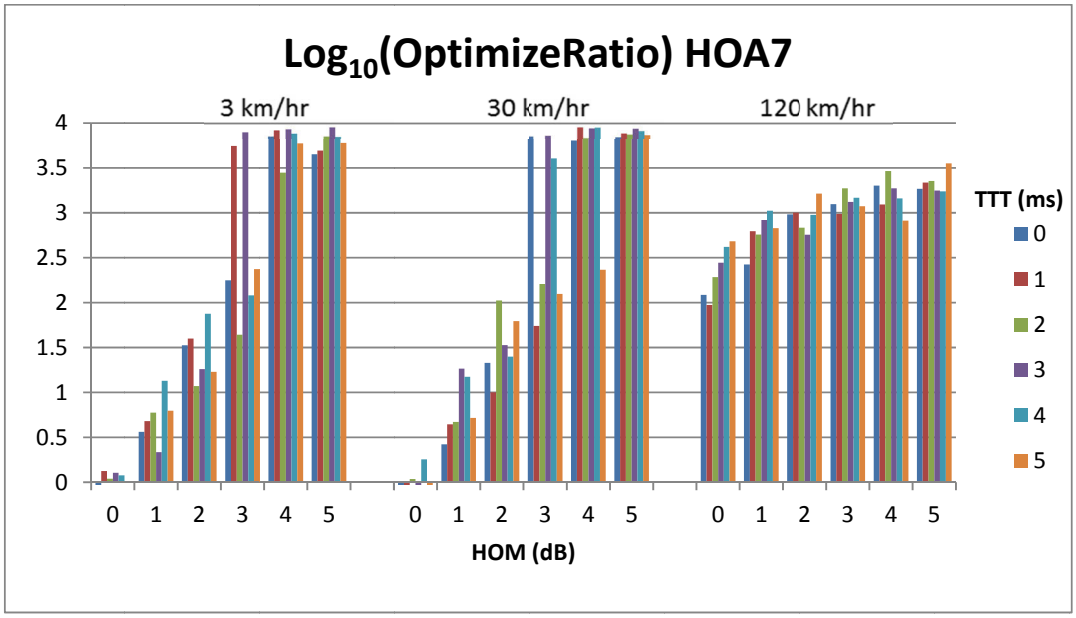

Figure 5.3: $\log_{10}(OptimizeRatio)$ of HOA7 in LTE-A

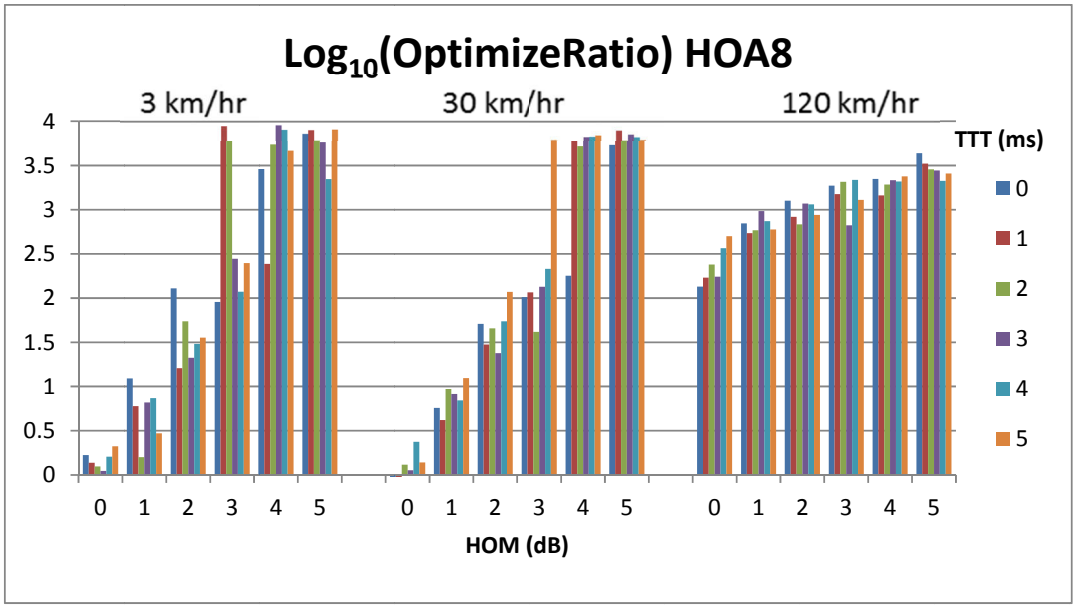

Figure 5.4: $\log_{10}(OptimizeRatio)$ of HOA8 in LTE-A

Figure 5.4 shows the $\log_{10}(OptimizeRatio)$ of HOA 8 under 3, 30, and 120 km/hr scenarios with an input set of HOM and TTT increasing from 0 to 5 dB and 0 to 5 ms, respectively. The highest $\log_{10}(OptimizeRatio)$ value in Figure 5.4 indicates the optimized set of HOM and TTT equivalent to 4 and 3, 5 and 1, 5 and 0, in 3 km/hr, 30km/hr, and 120 km/hr scenarios, respectively.

The results in Table 5.3 are used to evaluate and compare the system performance of all four CoMP handover algorithms in the following sections of performance testing with RT, NRT, and mixed RT and NRT traffic models.

Table 5.3: Optimized Parameters of four CoMP handover algorithms

Speed [km/hr]	HOA 5: CoMP Handover Algorithm	HOA 6: Limited CoMP Handover Algorithm	HOA 7: Capacity Based CoMP Handover Algorithm	HOA 8: Capacity Integrated CoMP Handver Algorithm
3	[HOM, TTT] = [4, 5]	[HOM,TTT] = [4, 4]	[HOM, TTT] = [5, 3]	[HOM, TTT] = [4, 3]
30	[HOM, TTT] = [4, 5]	[HOM,TTT] = [5, 4]	[HOM,TTT] = [4, 1]	[HOM, TTT] = [5, 1]
120	[HOM, TTT] = [5, 4]	[HOM,TTT] = [5, 3]	[HOM,TTT] = [5, 5]	[HOM, TTT] = [5, 0]

5.2 Performance of CoMP Handover Algorithms for RT Traffic

In this section the performance of four selected CoMP Handover Algorithms discussed in Chapter 4 are evaluated and compared (using the simulation tool described in Chapter 2) for RT traffic. The performance is evaluated based on three metrics: system throughput, system delay, and the number of handovers. The system performance of each CoMP handover algorithm under each user speed is optimized by applying the optimized parameters in Table 5.3. The system parameters used in the performance testing for RT traffic are listed Table 5.4. The simulation time for performance evaluation in Table 5.4 was intentionally set to 10000 ms in order to be consistent with the simulation time for performance evaluation in Table 3.1 in Chapter 3.

Table 5.4: Simulation Parameters for Capacity Integrated CoMP Handover Algorithm and CoMP Handover Algorithm

Parameters	**Values**
Cellular layout	Hexagonal grid, wrap around (reflect), 7 cells
Radius	100 m
Carrier Frequency	2 GHz
Bandwidth	5 MHz
Number of RBs	25
Number of sub-carriers per RB	12
Sub-carrier Spacing	15 kHz
Slot Duration	0.5 ms
Number of OFDM Symbols / Slot	7
Path Loss	Cost 231 Hata model
Shadow fading	Gaussian distribution
Multi-path	Rayleigh fading
Modulation and Coding Scheme	QPSK, 16QAM, and 64QAM
HARQ / Retransmission	Enable / 3 times
Packet Scheduler	Proportional Fair
Scheduling Time (TTI)	1 ms
Data Traffic	Real Time1 Mbps Constant Rate
User	150
User's position	Fixed uniform distributed
User's direction	Randomly choose from $[0,2\pi]$, constantly at all time
User's velocity	3 km/hr, 30 km/hr, 120 km/hr
Simulation time	10000 ms
RSRP sampling timer interval	10 ms
Handover Margin	5 dB
Time to Trigger (TTT)	5 ms
Size of CCS	3
Size of CTP	2
γ	0.75
Capacity Threshold	0.9

Figure 5.5 shows the system throughputs of four CoMP handover algorithms with RT CBR traffic under three user speeds in LTE-A simulation. A higher system throughput value indicates a better system performance by a CoMP handover algorithm. The trend of the system throughput of all CoMP handover algorithms decreases when the speed increases due to the radio channel quality decreasing caused by Doppler effect [140]. The Limited CoMP Handover Algorithm has the highest RT system throughput of 109.855 Mbps at a user speed of 3 km/hr followed by the Capacity Based CoMP Handover algorithm, the Capacity Integrated CoMP Handover Algorithm, and the CoMP Handover Algorithm (95.8714 Mbps, 91.9673Mbps, and 82.7185 Mbps, respectively).

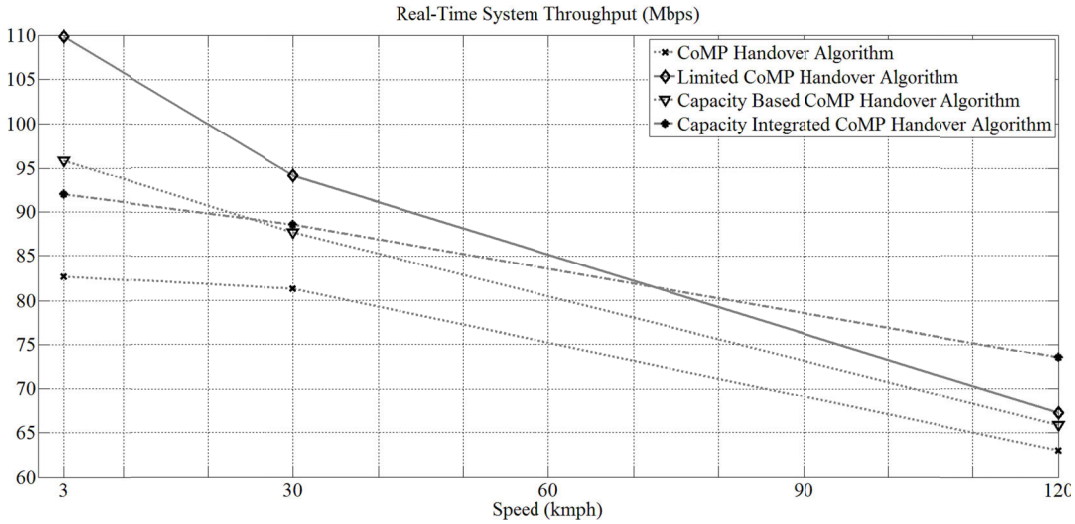

Figure 5.5: System Throughput of Four CoMP Handover Algorithms for RT Traffic

The Limited CoMP Handover Algorithm outperforms other CoMP handover Algorithms in a low speed scenario because the radio channel quality does not vary much in a low speed scenario. All CoMP handover algorithms other than the Limited CoMP Handover Algorithm do not have the chance to update the target cells in CCS and CTP before the next measurement period expires, restricting full utilization of the radio resources in the simulation. On the other hand, the Limited CoMP Handover Algorithm constantly checks the RSRP of the target cells in CCS to filter out target cells that are not to be added into the CTP. This leads to better system throughput in a low speed scenario than the other three CoMP Handover Algorithms. The Capacity Based

CoMP Handover Algorithm outperforms Capacity Integrated CoMP Handover Algorithm in a low speed scenario because the Capacity Threshold factor in the Capacity Integrated CoMP Handover Algorithm could filter out most of the target cells during the filtering in the high system load scenario. Therefore the Capacity Based CoMP Handover Algorithm has a higher chance to provide multiple transmission points in a high system load scenario which leads to a slightly higher system throughput. Finally, the CoMP Handover Algorithm has the lowest system throughput (82.7185 Mbps) in the high system load scenario as discussed in Section 4.1.3.

In the scenario of 30 km/hr, the Limited CoMP Handover Algorithm offers the highest RT system throughput of 94.1135 Mbps followed by the Capacity Integrated CoMP Handover algorithm, the Capacity Based CoMP Handover Algorithm, and the CoMP Handover Algorithm (88.5998 Mbps, 87.7103 Mbps, and 81.2869 Mbps, respectively). The Limited CoMP Handover Algorithm outperforms all other CoMP handover algorithms in the scenario of 30 km/hr with a system throughput increase of 14.33% when compared to the scenario of 3 km/hr. The Capacity Integrated CoMP Handover Algorithm outperforms the Capacity Based CoMP Handover Algorithm in the scenario of 30 km/hr due to the assistance of the Capacity Threshold factor which restricts the cells in the measurement set to be the target cells in the CCS of each UE. Therefore the available radio resources in the target cells in the CCS can be further utilized by other UEs. The system throughput is enhanced and the number of handovers is reduced (Figure 5.7). The CoMP Handover Algorithm has the lowest system throughput (81.2869 Mbps) in the scenario of 30 km/hr in the high system load scenario.

In the scenario of 120 km/hr, the Capacity Integrated CoMP Handover Algorithm overcomes the Limited CoMP Handover Algorithm (system throughput of 73.4635 Mbps and 67.2567 Mbps, respectively). The Limited CoMP Handover Algorithm has a lower system throughput in the scenario of 120 km/hr because the Step 6 in Figure 4.15 constantly checks the RSRP of the target cells in CCS. However, the feedback messages required from UEs at any time instant for checking the RSRP are heavily affected by the high speed and the radio propagation in the scenario. This situation affected the handover decisions, therefore the Limited CoMP Handover Algorithm offers a lower system throughput in the 120 km/hr scenario than other speed scenarios. On the other

hand, the RB utilization value used in the Capacity Integrated CoMP Handover Algorithm is calculated by each eNodeB and exchanged via X2 interfaces in the system. The RB utilization value is not affected by the speed and the radio propagation. Therefore the Capacity Integrated CoMP Handover Algorithm can provide higher system throughput than the Limited CoMP Handover Algorithm in a high speed scenario.

The Capacity Based CoMP Handover Algorithm and the CoMP Handover Algorithm have 65.8869 Mbps and 63.0107 Mbps throughput in the scenario of 120 km/hr, respectively. The RB utilization value in the Capacity Based CoMP Handover Algorithm is less affected by the speed and the radio propagation. However, the Capacity Based CoMP Handover Algorithm has a higher number of handovers as discussed in Section 4.2.2. This issue could cause signalling overhead and waste of radio resources which leads to a lower system throughput. Finally, the CoMP Handover Algorithm provides the lowest system throughput performance in the scenario of 120 km/hr when compared to other CoMP handover algorithms in the high system load scenario.

Figure 5.6 shows the system delay of four CoMP handover algorithms for RT traffic in the simulation. A lower system delay value indicates a better system performance under a CoMP handover algorithm. The trend of the system delay of all CoMP handover algorithms increases when the speed increases due to the rapid variation in the radio channel in the simulation.

The Capacity Integrated CoMP Handover Algorithm offers the lowest system delay of 11645.5 ms, 13237.1 ms, and 23176.7 ms in 3 km/hr, 30 km/hr, and 120 km/hr scenarios, respectively. The Capacity Integrated CoMP Handover Algorithm outperforms all other CoMP Handover Algorithms among all speed scenarios in the simulation due to the assistance of the Capacity Threshold factor. The number of data connection of each UE can be minimized and the number of incoming traffic packets in target cells in CTP are reduced by the Capacity Threshold factor. Due to the lower number of incoming traffic packets in target cells in CTP, the queuing delay of each cell in the simulation can be shortened, therefore the Capacity Integrated CoMP Handover

Algorithm offers the lowest system delay among all speed scenarios when compared to other CoMP handover algorithms.

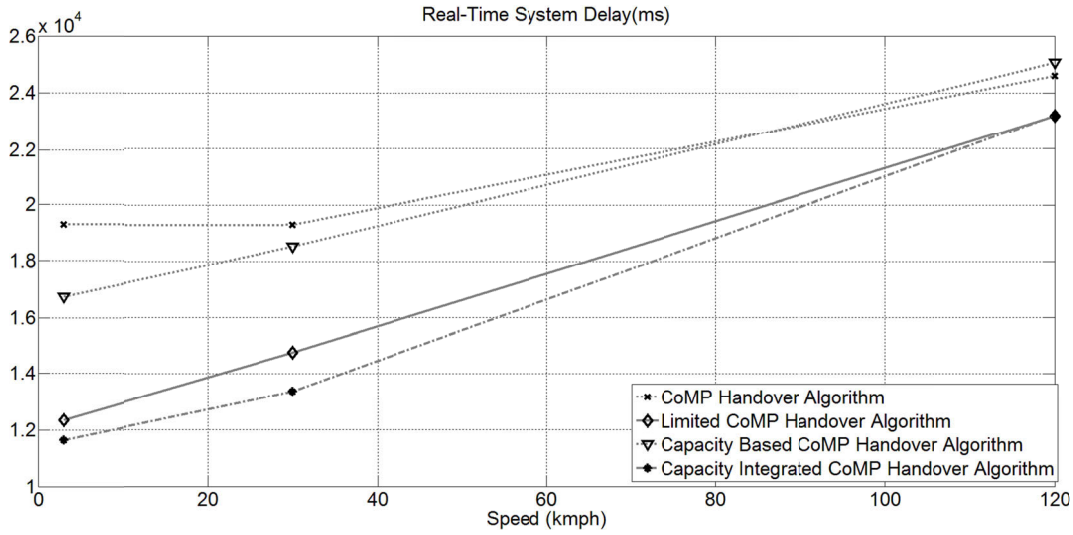

Figure 5.6: System Delay of Four CoMP Handover Algorithms for RT Traffic

The Limited CoMP Handover Algorithm offers the second lowest system delay of 12366.3 ms, 15377.2 ms, and 23196.9 ms in 3 km/hr, 30 km/hr, and 120 km/hr scenarios, respectively. The Limited CoMP Handover Algorithm constantly checks the RSRP of the target cells in CCS which increases the signalling overhead and delay the data transmissions of the target cells in CTP, therefore the Limited CoMP Handover Algorithm offers a slightly higher system delay than the Capacity Integrated CoMP Handover Algorithm.

The CoMP Handover Algorithm and the Capacity Based CoMP Handover Algorithm offer 19289 ms and 16757.5 ms, 19314.7 ms and 18532.5 ms, 24596.4 ms and 25069.3 ms, in 3 km/hr, 30 km/hr, 120 km/hr scenarios, respectively. The CoMP Handover Algorithm is expected to have higher system delay than the Capacity Based CoMP Handover Algorithm in the 120 km/hr scenario. However, the Capacity Based CoMP Handover Algorithm has the higher number of handovers issue (in Figure 5.7) as discussed in Section 4.2.2 which causes a lower system throughput and higher system delay.

Figure 5.7 shows the number of handovers of four CoMP handover algorithms for RT traffic in the simulation. A lower number of handover indicates a better system performance under a CoMP handover algorithm. A higher number of handovers is expected when the speed increases due to more cell changes in the simulation. When the speed is as low as 3 km/hr, all four CoMP handover algorithms have 0 handovers. The Capacity Integrated CoMP Handover Algorithm outperforms other CoMP handover algorithms with the help of the Capacity Threshold factor (35 and 205 handovers in 30 km/hr and 120 km/hr, respectively). The Limited CoMP Handover Algorithm offers the second lowest number of handovers of 42 and 209 times in 30 km/hr and 120 km/hr scenarios, respectively. Based on the assistance of the optimized parameters to limit handover occurrences, the Capacity Based CoMP Handover Algorithm has 45 handovers, which is the same as the CoMP Handover Algorithm in the 30 km/hr scenario. The CoMP handover Algorithm and the Capacity Based CoMP Handover Algorithm have 210 and 211 handovers in 120 km/hr scenario, respectively. Furthermore, the Capacity Based CoMP Handover Algorithm has the highest number of handovers due to handing over UEs to a lower loaded cell. This arrangement limits the possibility that UEs camp on the cell with the best radio signal quality when making the handover decision.

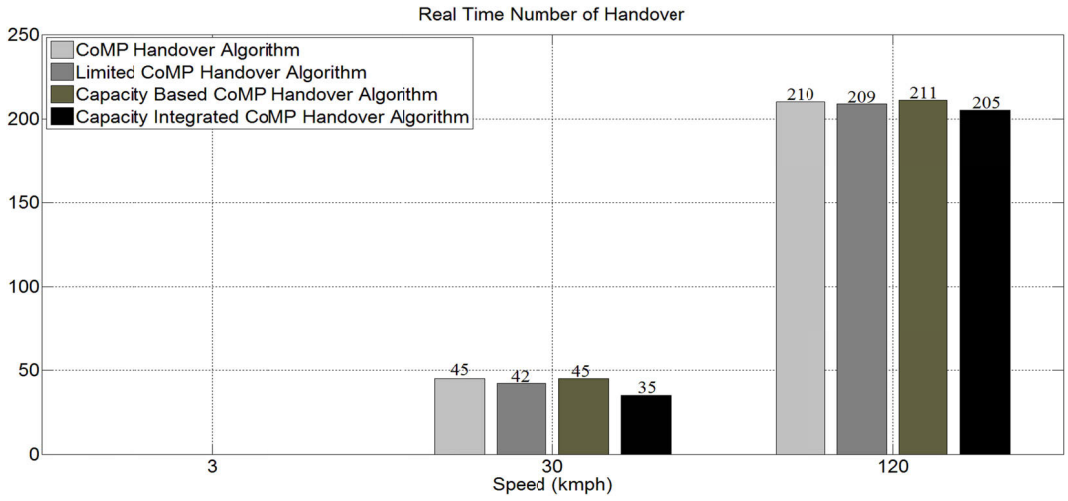

Figure 5.7: Number of Handovers of Four CoMP Handover Algorithms for RT Traffic

5.3 Performance of CoMP Handover Algorithms for NRT Traffic

In this section, the performance evaluation of four CoMP Handover Algorithms is compared with the NRT web browsing traffic discussed in Section 2.10.1 with D_{pc} equivalent to 30 ms. The system throughput of the NRT web browsing traffic is expected to be lower than the system throughput of the RT traffic because the packets in are not constantly provided throughout the simulation. The NRT web browsing traffic has the period of empty incoming packet in an ongoing session between the main objects and the embedded objects and between the packet calls (in Figure 2.11). Therefore the simulation of performance testing in this section is assumed as a low system load scenario.

The performance is compared based on three metrics: system throughput, system delay, and the number of handovers. The parameters of each CoMP handover algorithm under each user speed are optimized as shown in Table 5.3 and the system parameters used in the performance testing for NRT web browsing traffic are listed in Table 5.5. The simulation time for performance evaluation in Table 5.5 was intentionally set to 10000 ms in order to be consistent with the simulation time for performance evaluation in Table 3.1 in Chapter 3.

Table 5.5: Simulation Parameters for Capacity Integrated CoMP Handover Algorithm and CoMP Handover Algorithm

Parameters	**Values**
Cellular layout	Hexagonal grid, wrap around (reflect), 7 cells
Radius	100 m
Carrier Frequency	2 GHz
Bandwidth	5 MHz
Number of RBs	25
Number of sub-carriers per RB	12
Sub-carrier Spacing	15 kHz
Slot Duration	0.5 ms
Number of OFDM Symbols / Slot	7
Path Loss	Cost 231 Hata model
Shadow fading	Gaussian distribution
Multi-path	Rayleigh fading
Modulation and Coding Scheme	QPSK, 16QAM, and 64QAM
HARQ / Retransmission	Enable / 3 times
Packet Scheduler	Proportional Fair
Scheduling Time (TTI)	1 ms
Data Traffic	Non-Real Time Web Browsing Traffic D_{pc}=30 ms
User	150
User's position	Fixed uniform distributed
User's direction	Randomly choose from [0,2π], constantly at all time
User's velocity	3 km/hr, 30 km/hr, 120 km/hr
Simulation time	10000 ms
RSRP sampling timer interval	10 ms
Handover Margin	5 dB
Time to Trigger (TTT)	5 ms
Size of CCS	3
Size of CTP	2
γ	0.75
Capacity Threshold	0.9

Figure 5.8 shows the system throughput of four CoMP handover algorithms with NRT web browsing traffic under three user speeds in LTE-A simulation. This is similar to the RT traffic scenario, where a higher system throughput value indicates better system performance. The trends of the system throughputs of all CoMP handover algorithms decrease when the speed increases due to the radio channel quality decreasing.

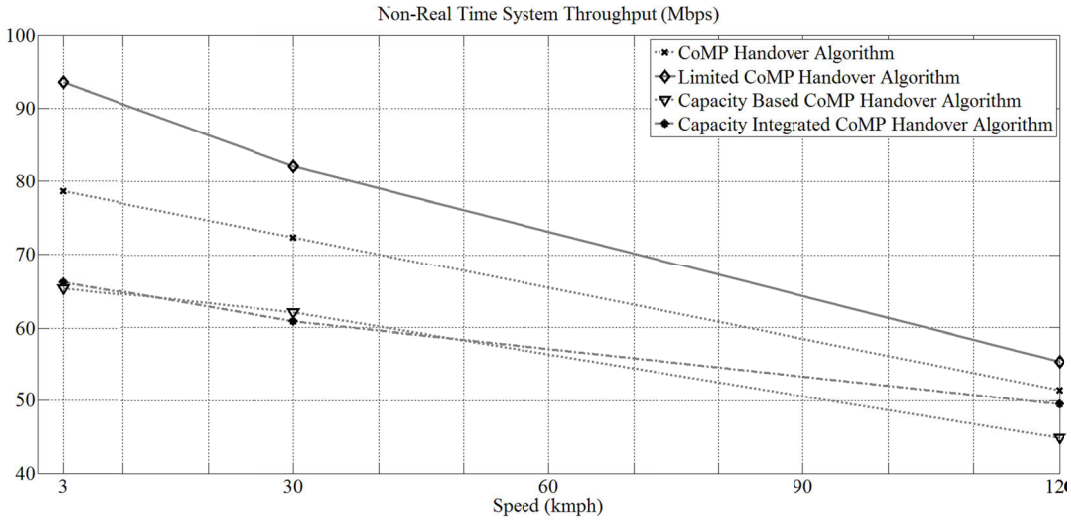

Figure 5.8: System Throughput of Four CoMP Handover Algorithms for NRT Traffic

Based on the help of constantly checking the RSRP of the target cells in CCS, the Limited CoMP Handover Algorithm offers the highest NRT system throughput of 93.6004 Mbps, 82.0607 Mbps, and 55.3347 Mbps in 3 km/hr, 30 km/hr, and 120 km/hr scenarios, respectively. The Limited CoMP Handover Algorithm has the highest system throughput at 120 km/hr because the web browsing model in the NRT traffic does not constantly provide packets to the UEs throughout the simulation. The handover decisions with high UE mobility and consequent fluctuations in SINR levels in the NRT traffic are not as many as required compared to the same situation in the RT traffic. Therefore the Limited CoMP Handover Algorithm maintains the highest system throughput among other CoMP handover algorithms at 120 km/hr scenario.

The CoMP Handover Algorithm offers the second highest NRT system throughputs of 78.6486 Mbps, 72.3635 Mbps, and 52.5902 Mbps at user speeds of 3 km/hr, 30 km/hr, and 120 km/hr, respectively. The CoMP Handover Algorithm outperforms the Capacity

Integrated CoMP Handover Algorithm and Capacity Based CoMP Handover Algorithm in a low system load scenario in every speed scenario. This result directly confirms that the CoMP Handover Algorithm increases the system throughput among 3 km/hr, 30, km/hr, and 120 km/hr cases in a low system load scenario.

The Capacity Integrated CoMP Handover Algorithm and Capacity Based CoMP Handover Algorithm have the system throughputs of 66.318 Mbps and 65.4891 Mbps, 60.8015 Mbps and 62.0797 Mbps, and 49.4818 Mbps and 44.8897 Mbps in 3 km/hr, 30 km/hr, and 120 km/hr scenarios, respectively. The Capacity Integrated CoMP Handover Algorithm produces very similar results to the Capacity Based CoMP Handover Algorithm in 3 km/hr and 30 km/hr scenarios because the γ factor is close to 1 which makes the behaviour of the Capacity Integrated CoMP Handover Algorithm similar to the Capacity Based CoMP Handover Algorithm. However, the Capacity Integrated CoMP Handover Algorithm makes more accurate handover decisions due to the mechanism of tracking historical capacity of each individual eNB in the system. This mechanism enhances the system throughput and minimizes the number of handovers (in Figure 5.10) compared to the Capacity Based CoMP Handover Algorithm in the 120 km/hr scenario.

Figure 5.9 shows the system delay of four CoMP handover algorithms with NRT web browsing traffic under three user speeds in the LTE-A simulation. Similar to RT traffic scenario, a lower system delay indicates a better system performance under a CoMP handover algorithm and the trends of the system delay of all CoMP handover algorithms increase when the UE speed increases due to the rapid variation of radio channel quality.

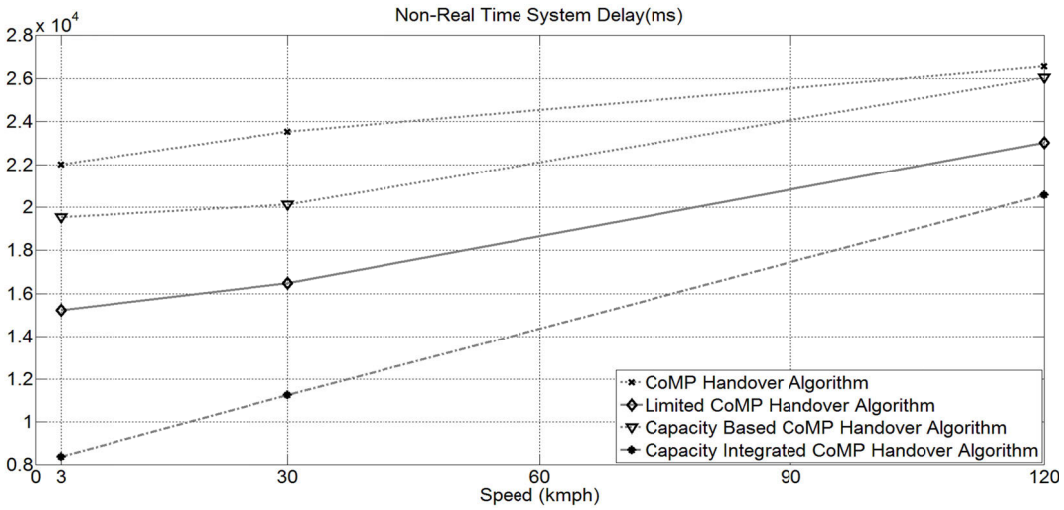

Figure 5.9: System Delay of Four CoMP Handover Algorithms for NRT Traffic

The Capacity Integrated CoMP Handover Algorithm achieves the lowest system delay of 8367.19 ms, 11257.8 ms, and 20587.8 ms in 3 km/hr, 30 km/hr, and 120 km/hr scenarios, respectively. The Capacity Integrated CoMP Handover Algorithm effectively minimizes the system delay in all speed scenarios and the number of handovers (Figure 5.10). The Limited CoMP Handover Algorithm has the system delay of 15232 ms, 16480.1 ms, and 23020.1 ms in 3 km/hr, 30 km/hr, and 120 km/hr scenarios. The Limited CoMP Handover Algorithm minimizes the amount of multiple transmissions acquired by the UEs by separating the cell-center UEs and cell-edge UEs. Therefore, the queuing delay of the incoming packets can be shortened due to fewer incoming packets buffered in the eNodeBs in the system. Thus the system delay is minimized.

The Capacity Based CoMP Handover Algorithm and CoMP Handover Algorithm have the system delays of 19552.8 ms and 22001.9 ms, 20126.9 ms and 23551.8 ms, and 26067.3 ms and 26581.2 ms in 3 km/hr, 30 km/hr, and 120 km/hr scenarios, respectively. The Capacity Based CoMP Handover Algorithm outperforms the CoMP Handover Algorithm by choosing the target cell which has the lowest system capacity and the highest RSRP when making the handover decision. This mechanism limits the possibility of a target cell to become a CTP in the CCS selection and reduces the number of transmissions (from two to one) of each UE. The queuing delay of the incoming packets can be shortened due to fewer incoming packets buffered in the eNodeBs in the system. Thus the system delay can be minimized. However, the

Capacity Based CoMP Handover Algorithm has the side effect of having a higher number of handovers especially in the high speed scenario. This side effect gradually increases the system delay in the 120 km/hr scenario. Therefore the system delay of the Capacity Based CoMP Handover Algorithm in the 120 km/hr scenario converges to the system delay of the CoMP Handover Algorithm.

Figure 5.10 shows the number of handovers of four CoMP handover algorithms for NRT traffic in the simulation.

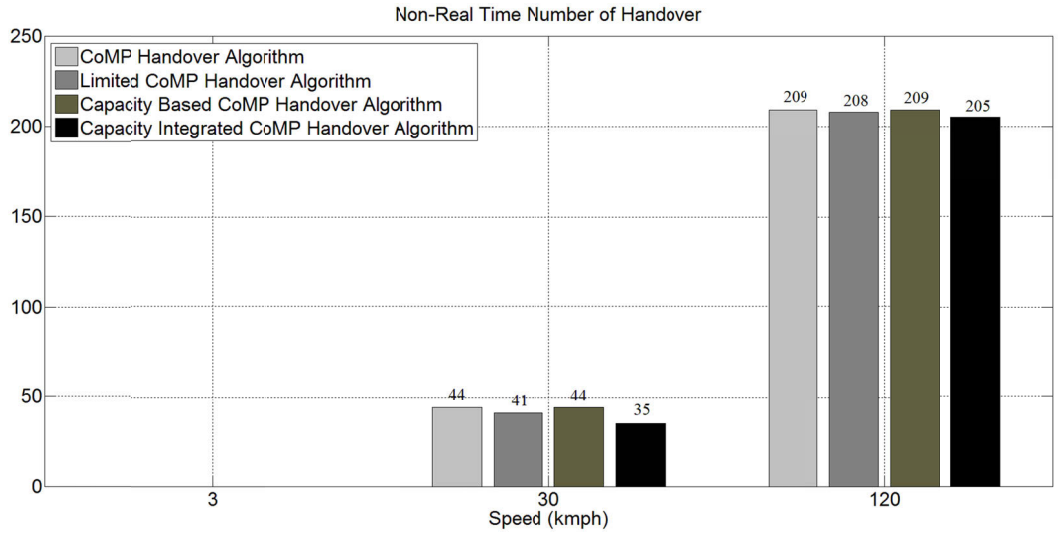

Figure 5.10: Number of Handovers of Four CoMP Handover Algorithms for NRT Traffic

The total number of handovers of all CoMP handover algorithms for NRT traffic is slightly lower than the total number of handovers of all CoMP handover algorithms in RT traffic due to the definition of a handover: a handover only occurs when a UE has an on-going call or data session. The NRT web browsing traffic has the period of empty incoming packet in an on-going session; therefore a handover is not performed if a UE changes cells during the period of empty incoming packet in an on-going session. Thus, the total number of handovers of all CoMP handover algorithms in NRT traffic is slightly lower when compared to the ones in RT traffic.

When the speed is as low as 3 km/hr, all CoMP handover algorithms have 0 handovers by the assistance of the optimized parameters in Table 5.3. The Capacity Integrated

CoMP Handover Algorithm outperforms other CoMP handover algorithms (35 and 205 handovers in 30 km/hr and 120 km/hr, respectively). The Limited CoMP Handover Algorithm has the second lowest number of handovers of 41 and 209 handovers in 30 km/hr and 120 km/hr scenarios, respectively. Based on the assistance of the optimized parameters to limit handover occurring, the Capacity Based CoMP Handover Algorithm and the CoMP Handover Algorithm have the same number of handovers as 44 and 209 in 30 km/hr and 120 km/hr scenarios, respectively. Furthermore, the CoMP Handover Algorithm has the highest number of handovers due to searching the corresponding target cell with the highest RSRP for each UE. The Capacity Based CoMP Handover Algorithm has the highest number of handovers due to handing over UEs to a lower loaded cell. This arrangement limits the chance that UEs camp on the most appropriate cell with the best radio signal quality when making the handover decision. Therefore the Capacity Based CoMP Handover Algorithm finds the most appropriate cell for each UE by having higher number of handovers.

5.4 Performance of CoMP Handover Algorithms for Mixed RT and NRT Traffic

In this section, the performance evaluation of four CoMP Handover Algorithms is carried out with mixed RT and NRT traffic. The performance evaluation is compared based on three metrics: system throughput, system delay, and number of handovers. The total number of users in the simulation is 150 and is equally divided for the RT constant traffic and the NRT web browsing traffic.

The system load of the mixed RT and NRT traffic is expected to be a medium to high load scenario due to the equal divided for the RT traffic and NRT traffic. The parameters of each CoMP handover algorithm under each user speed are optimized as shown in Table 5.3 and the system parameters used in the performance testing for NRT web browsing traffic are listed in Table 5.6. The simulation time for performance evaluation in Table 5.6 was intentionally set to 10000 ms in order to be consistent with the simulation time for performance evaluation in Table 3.1 in Chapter 3.

Table 5.6: Simulation Parameters for Capacity Integrated CoMP Handover Algorithm and CoMP Handover Algorithm

Parameters	**Values**
Cellular layout	Hexagonal grid, wrap around (reflect), 7 cells
Radius	100 m
Carrier Frequency	2 GHz
Bandwidth	5 MHz
Number of RBs	25
Number of sub-carriers per RB	12
Sub-carrier Spacing	15 kHz
Slot Duration	0.5 ms
Number of OFDM Symbols / Slot	7
Path Loss	Cost 231 Hata model
Shadow fading	Gaussian distribution
Multi-path	Rayleigh fading
Modulation and Coding Scheme	QPSK, 16QAM, and 64QAM
HARQ / Retransmission	Enable / 3 times
Packet Scheduler	Proportional Fair
Scheduling Time (TTI)	1 ms
Data Traffic	Non-Real Time Web Browsing Traffic with D_{pc}= 30 ms Real Time Constant Stream Traffic
User	Total 150 Users 75 Users: NRT Web Browsing Traffic 75 Users: RT Constant Stream Traffic
User's position	Fixed uniform distributed
User's direction	Randomly choose from [0,2π], constantly at all time
User's velocity	3 km/hr, 30 km/hr, 120 km/hr
Simulation time	10000 ms
RSRP sampling timer interval	10 ms
Handover Margin	5 dB
Time to Trigger (TTT)	5 ms
Size of CCS	3
Size of CTP	2
γ	0.75
Capacity Threshold	0.9

Figure 5.11 shows the system throughput of four CoMP handover algorithms with mixed RT and NRT traffic under three user speeds in the LTE-A simulation.

The Limited CoMP Handover Algorithm has the highest system throughputs of 106.374 Mbps and 91.4014 Mbps in 3 and 30 km/hr scenarios, respectively. The Limited CoMP Handover Algorithm has the second highest system throughput (63.641 Mbps) when compared to the Capacity Integrated CoMP Handover Algorithm (64.782 Mbps) in the 120 km/hr scenario. The Limited CoMP Handover Algorithm results in lower system throughput for the 120 km/hr scenario for the same reasons discussed in Section 5.2.

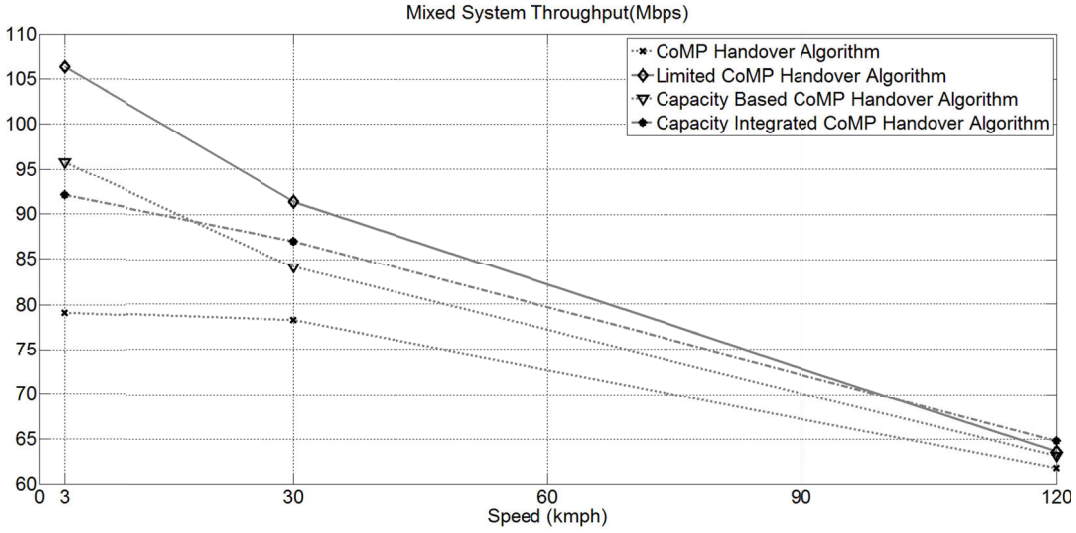

Figure 5.11: System Throughput of Four CoMP Handover Algorithms for Mixed RT and NRT Traffic

The Capacity Based CoMP Handover Algorithm and the Capacity Integrated CoMP Handover Algorithm have the system throughputs of 95.8426 Mbps and 92.1148 Mbps in the 3 km/hr scenario, respectively. The Capacity Based CoMP Handover Algorithm outperforms the Capacity Integrated CoMP Handover Algorithm in a low speed scenario due to the reason discussed in Section 5.2. The Capacity Integrated CoMP Handover Algorithm and the Capacity Based CoMP Handover Algorithm have throughputs of 87.0644 Mbps and 84.1339 Mbps, and 64.782 Mbps and 63.1392 Mbps in the 30 km/hr and 120 km/hr scenarios, respectively. The Capacity Integrated CoMP Handover Algorithm outperforms the Capacity Based CoMP Handover Algorithm in

the scenarios of 30 km/hr and 120 km/hr due to the assistance of the Capacity Threshold factor which restricts the cells in the measurement set to be the target cells in the CCS of each UE. Therefore the available radio resources in the target cells in the CCS can be further utilized by other UEs and the system throughput is enhanced.

The CoMP Handover Algorithm has the lowest system throughputs of 79.1266 Mbps, 78.2245 Mbps, and 61.7326 Mbps in 3 km/hr, 30 km/hr, and 120 km/hr scenarios, respectively. The CoMP Handover Algorithm fully uses the multiple transmission points of each user in the system which makes each eNB loaded and hence results in the lowest system throughput in every speed scenario.

Figure 5.12 shows the system delay of four CoMP handover algorithms for Mixed RT and NRT traffic in the simulation.

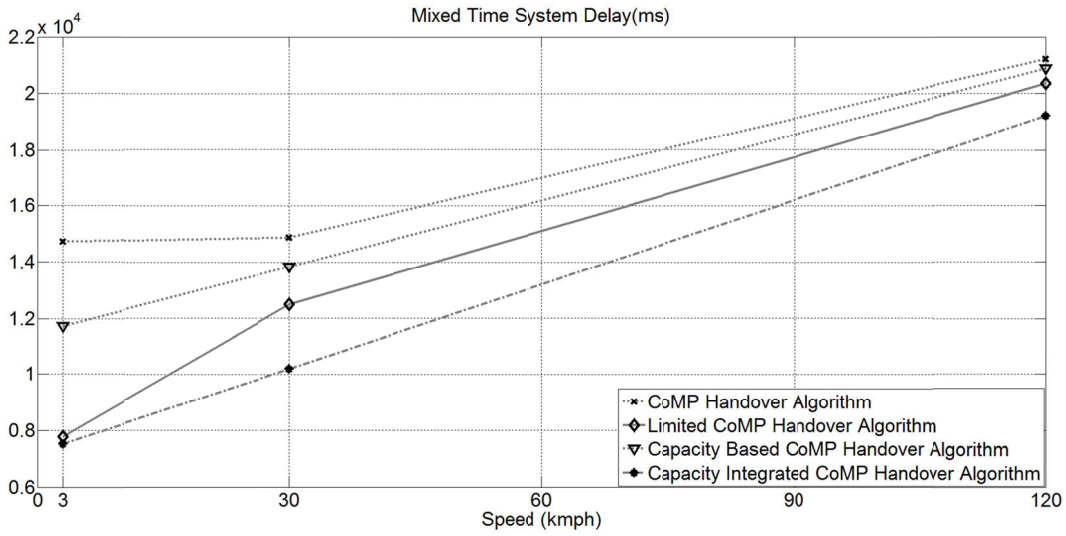

Figure 5.12: System Delay of Four CoMP Handover Algorithms for Mixed RT and NRT Traffic

The Capacity Integrated CoMP Handover Algorithm offers the lowest system delay of 7526.81 ms, 10205 ms, and 19202.1 ms in 3 km/hr, 30 km/hr, and 120 km/hr scenarios, respectively. The Capacity Integrated CoMP Handover Algorithm outperforms all other CoMP handover algorithms among all speed scenarios in the simulation due to the assistance of the Capacity Threshold factor. The Capacity Threshold factor minimizes the number of transmission points of each UE and reduces the number of incoming

traffic packets in target cells in CTP. Due to fewer incoming traffic packets in target cells in CTP, the queuing delay of each target cell in the simulation can be shortened, therefore the Capacity Integrated CoMP Handover Algorithm has the lowest system delay among all speed scenarios when compared to other CoMP handover algorithms.

The Limited CoMP Handover Algorithm has the system delay of 7781.29 ms, 12480.1 ms, and 20357.1 ms in 3 km/hr, 30 km/hr, and 120 km/hr scenarios, respectively. The Limited CoMP Handover Algorithm utilizes the separation between cell-center users and cell-edge users and minimizes the multiple transmission points of cell-center users. The packets within the transmission points are reduced due to the lower number of multiple transmission points. Therefore the queuing delay of the buffered packets in the eNodeBs are shortened which minimizes the system delay. However, the separation mechanism in the Limited CoMP Handover Algorithm involves the constant RSRP feedback from the UEs at any time instant, which increases the feedback messages, signalling overhead, and system delay. Unlike the Limited CoMP Handover Algorithm, the Capacity Integrated CoMP Handover Algorithm checks the capacity indicator in each eNB via X2-interfaces in the system, therefore the system delay can be minimized.

The Capacity Based CoMP Handover Algorithm and the CoMP Handover Algorithm have the system delay of 11741 ms and 14719.1 ms, 13832.5 ms and 14886.3 ms, 20891.5 ms and 21223.8 ms in 3 km/hr, 30 km/hr, and 120 km/hr scenarios, respectively. The Capacity Based CoMP Handover Algorithm outperforms the CoMP Handover Algorithm by using the double filtering discussed in Section 4.2.2 to choose the target cell with the lowest system capacity and highest RSRP when making the handover decision. This mechanism minimizes the system delay by minimizing the multiple transmission points to a single transmission point which minimises the time spent by the incoming packets in the eNodeB buffer. However, the Capacity Based CoMP Handover Algorithm has the side effect of having a higher number of handovers especially in a high speed scenario; therefore the system delay of the Capacity Based CoMP Handover Algorithm in 120 km/hr scenario converges to the system delay of the CoMP Handover Algorithm.

The CoMP Handover Algorithm has the highest system delay because 150 UEs leads to a full loaded state for the CoMP Handover Algorithm in the simulation (refer to Figure

4.16). The radio resources are fully used in a full loaded state and the incoming packets for the UEs have to be queued in the eNodeBs for transmission. Therefore the queuing delay of the buffered packets in the eNodeBs are increased which increases the system delay.

Figure 5.13 shows the number of handovers of four CoMP handover algorithms for mixed RT and NRT traffic. All four CoMP handover algorithms have 0 handovers at 3 km/hr by the assistance of the optimized parameters listed in Table 5.3.

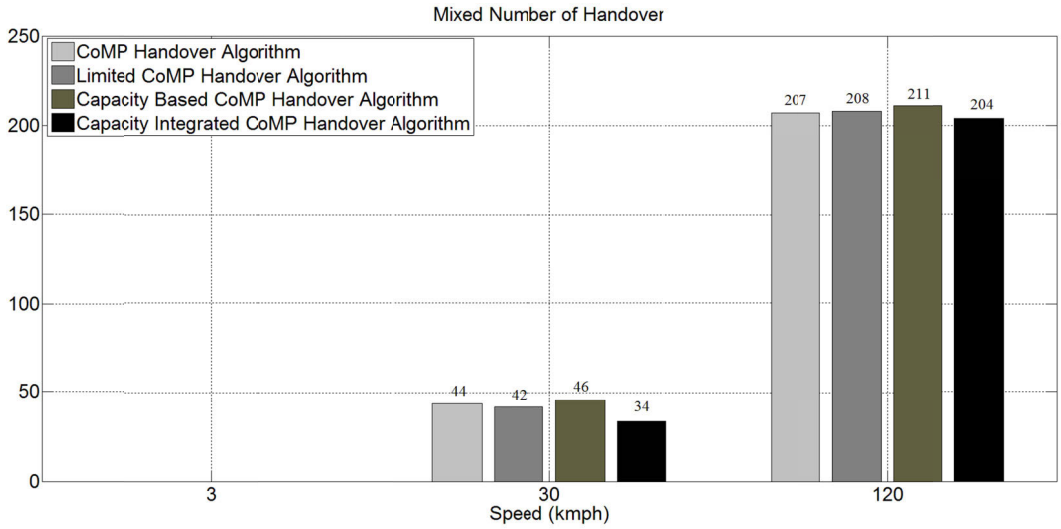

Figure 5.13: Number of Handovers of Four CoMP Handover Algorithms for Mixed RT and NRT Traffic

The Capacity Integrated CoMP Handover Algorithm outperforms other CoMP handover algorithms with lower number of handovers (34 and 204) in 30 km/hr and 120 km/hr scenarios, respectively. The Limited CoMP Handover Algorithm has the second lowest number of handovers of 42 and 208 handovers in 30 km/hr and 120 km/hr scenarios, respectively. The CoMP Handover Algorithm and the Capacity Based CoMP Handover Algorithm have 44 and 46 handovers and 207 and 211 handovers in 30 km/hr and 120 km/hr scenarios, respectively. The Capacity Based CoMP Handover Algorithm has the highest number of handovers as expected due to the arrangement limiting the chance that UEs camp on the most appropriate cell with the best radio signal quality when making the handover decision. Therefore the Capacity Based CoMP Handover

Algorithm finds the most appropriate cell for each UE by having higher number of handovers.

5.5 Summary

Simulation results have shown that the Capacity Integrated CoMP Handover Algorithm can effectively minimize the system delay and the number of handovers with RT traffic, NRT traffic, and Mixed RT and NRT traffic in 3 km/hr, 30 km/hr, and 120 km/hr scenarios. Furthermore, the Capacity Integrated CoMP Handover Algorithm provides the highest system throughput with most of the traffic models at 120 km/hr except for the NRT traffic. For the NRT traffic model, the Limited CoMP Handover Algorithm provides the highest system throughput among all speed scenarios.

Chapter 6

COMPARATIVE STUDY OF COMP HANDOVER ALGORITHMS UNDER CHANNEL IMPAIRMENTS

The works in the earlier chapters mostly assume that all channel feedbacks were correctly received at the eNodeB and UEs immediately perform a handover action after receiving the HANDOVER COMMAND message from the eNodeBs. These assumptions are applicable for preliminary research work, but they are not appropriate for a practical mobile cellular system as the channels are subject to various impairments, such as interference, multi-path fading, shadowing, and imperfect channel feedback reports (including delayed channel feedback and missing channel feedback). These impairments may cause severe performance degradation (in terms of system throughput and delay) especially for handover algorithms that strongly rely on an accurate RSRP report.

To study and analyse the impacts from these impairments, a practical LTE-A cellular system with mobile cellular channel impairments is considered in this chapter. Two impairment environments are assumed for the practical LTE-A system: outdated feedback and missing feedback scenarios. A constantly feedback delayed channel is assumed in the outdated feedback scenario while a missing feedback channel is assumed in the missing feedback scenario. The performance of each CoMP handover algorithm for perfect feedback scenario, outdated feedback scenario, and missing feedback scenario in a practical LTE-A system is evaluated and discussed in this chapter, respectively.

This chapter is structured as follows: Section 6.1 provides a thorough description on the related works including the 3GPP standards of handover parameters in a practical LTE-A system and the performance impact due to imperfect channel feedback reports in a practical LTE-A system. Section 6.2 describes the simulation environments for a

practical LTE-A System. Section 6.3 evaluates and discusses the performance of each CoMP handover algorithm for perfect feedback scenario, outdated feedback scenario, and missing feedback scenario in a practical LTE-A system. The summary of this chapter is given in Section 6.4.

6.1 Related Works

The imperfect channel feedback reports in a practical LTE-A system are categorized into two feedback reports: CQI reports and RSRP reports. Each of these imperfect channel feedback reports is discussed after the 3GPP standards of handover parameters in a practical LTE-A system.

6.1.1 The 3GPP Standards of Handover Parameters in a Practical LTE-A System

The handover parameters in a practical LTE-A system including the report interval values, the range of the TTT values, the range of RSRP values, and the Hysteresis values are specified in the 3GPP Technical Report 36.331 [93, 141].

The report interval is applicable if the UE performs periodical reporting and indicates the time interval between each periodical report. Thirteen values are considered as the report interval in a practical LTE-A system. The values are enumerated (120, 240, 480, 640, 1024, 2048, 5120, and 10240) in millisecond and (1, 6, 12, 30, and 60) in minute.

The value range used for TTT parameter is the time interval which the HOM condition is satisfied in order to trigger a handover. Sixteen values are considered as the TTT parameter in a practical LTE-A system. The values are enumerated (0, 40, 64, 80, 100, 128, 160, 256, 320, 480, 512, 640, 1024, 1280, 2560, and 5120) in millisecond.

The range of the RSRP values specifies the value range used in RSRP measurements. The range of the RSRP values was specified as an integer (in 3GPP Technical Specification 36.133 [142]) with the range between 0 and 97 dBm.

The Hysteresis is a parameter used within the entry and leave condition of an event triggered reporting condition. The range of the Hysteresis value is specified as an integer with the range between 0 and 30 dB.

Given that a practical LTE-A system is studied in this chapter, it is important to follow the 3GPP standards for performance testing and evaluation. The report interval values, the range of the TTT values, the range of RSRP values, and the Hysteresis values specified by the 3GPP standards described in this section are used in the performance testing sections.

6.1.2 Performance Impact due to Imperfect CQI Reports

The impact on HSDPA performance due to outdated CQI reports was investigated in [143]. It is shown in [143] that the outdated CQI reports lead to degradation on HSDPA performance as the inaccuracy CQI experienced by a user due to the delay in the acquisition and processing of the CQI reports. Furthermore, this degradation depends on the speed of the UE and the system load situations or the resource allocating scheme. Simulation results in [143] show that the Max-Rate algorithm has a 7% throughput degradation in the 50 km/hr scenario compared to the 3 km/hr scenario when a 2 ms delayed CQI report is available at the base station.

The performance impact due to channel estimation errors, outdated and erroneous CQI reports over a multi-carrier mobile cellular system for different user speeds has been studied in [90]. It was shown in [90] that the maximum tolerable CQI delay is related to the user speed in the simulation. If the BLER is to be kept below 10^{-3} threshold, (a) a maximum of 5 ms CQI delay is tolerable for a 5 km/hr user speed scenario, (b) a maximum of 1 ms CQI delay is tolerable for a 30 km/hr user speed scenario, and (c) a maximum of -15 dB in Mean Square Error (MSE) of the channel estimation when the average SINR is fixed at 10 dB. Moreover, Simulation results have shown that the system performance is very sensitive against outdated CQI (which may cause a wrong selection of the instantaneous modulation scheme) when compared to other CQI imperfectness.

The performance impact due to three different CQI errors (CQI errors caused by user speed, interference variation, and channel estimation error) on the throughput within AMC/HARQ systems is discussed in [144]. The simulation results have shown that CQI errors caused by the user speed can significantly degrade the system performance in a pure AMC system and the CQI errors caused by the channel estimation error is the most difficult one to be recovered. Furthermore, ignoring CQI errors in rate adaptation could result in a very high average BLER in the user mobility case.

6.1.3 Performance Impact due to Imperfect Measurement Reports

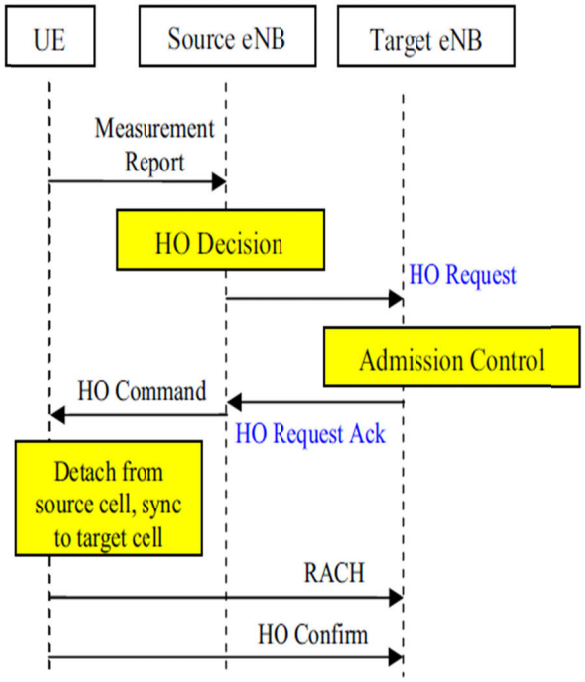

Figure 6.1: LTE Handover Message Sequence [145]

Figure 6.1 shows the handover message sequence of a successful handover procedure in a LTE / LTE-A system. A successful handover requires (i) a correct measurement report delivered from the UE to the source eNodeB, (ii) the right handover decision made at the source eNodeB, (iii) communication over the X2 between the source and target eNodeBs (resource preparation), (iv) successful delivery of a handover command message from the source eNodeB to the UE, (v) a successful random access and delivery of a handover confirmation message to the target eNodeB. A handover failure could be caused by inappropriate measurement reports [146] and occur at any of these

above stages [145]. A handover failure caused by an inappropriate measurement report can be categorized into the following three types: too late handover, too early handover, and handover to a wrong cell [147].

A too late handover occurs when a measurement report feedback failure between a UE and the serving cell during a handover procedure or before a handover is triggered. The RSRP of the serving cell is too low when the too late handover is triggered; therefore the performance impact of a too late handover increases the system delay and decreases the system throughput (due to the poor radio channel condition). Figure 6.2 shows a too late handover scenario in which RLF occurs in the serving Cell A before a successful handover procedure [148].

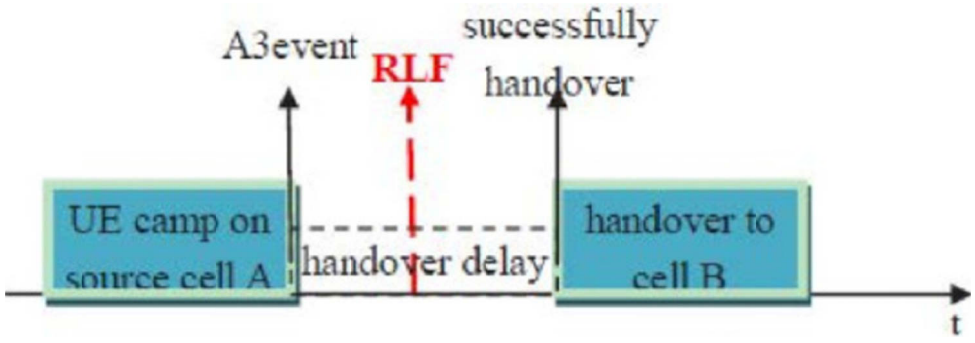

Figure 6.2: Too Late Handover [148]

A too early handover occurs when a handover is successfully triggered by the serving cell based on the inappropriate measurement report sent by the UE. The RSRP of the serving cell is not low enough when the too early handover is triggered. Therefore the performance impact of a too early handover increases the number of unnecessary handovers which demand additional resources in the network and have the potential to significantly degrade the quality of service of ongoing connections [149].

Figure 6.3 shows a too early handover scenario where RLF occurs in the target Cell B after a successful handover and the UE reconnects to the source Cell A after the RLF. A too early handover usually occurs when the UE enters an unintended coverage of a target cell which is inside the coverage area of the serving cell. This is a typical scenario for areas where fragmented cell coverage is inherent to the radio propagation environment, such as dense urban areas [150].

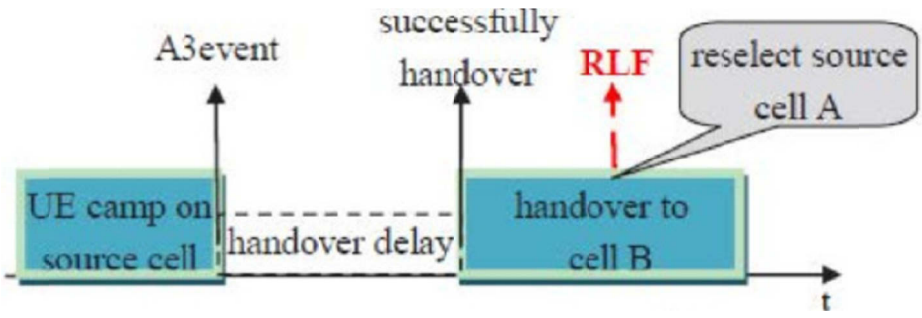

Figure 6.3: Too Early Handover [148]

Figure 6.4 shows a handover to a wrong cell scenario where RLF occurs in the target Cell B after a successful handover performed and the UE reconnects to a cell that is neither the serving cell nor the target cell [146]. The performance impact of handover to a wrong cell also increases the number of unnecessary handovers which requires additional resources in the network and has the potential to significantly degrade the system performance.

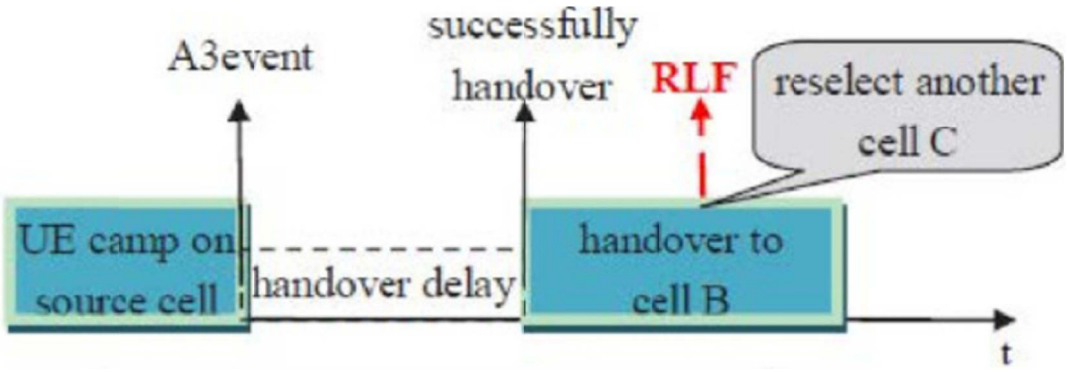

Figure 6.4: Handover to a wrong cell [148]

6.2 Simulation Environments for a Practical LTE-A System

The simulation environments of a perfect feedback scenario, an outdated feedback scenario, and a missing feedback scenario in a practical LTE-A system are introduced in this section.

Figure 6.5 shows the simulation environment for a perfect feedback scenario and an outdated feedback scenario in a practical LTE-A system. The simulation environment consists of 7 hexagonal cells with a 500 m radius and each eNodeB is located at the

centre of each cell. A total number of 100 UEs are uniformly distributed within the red rectangle area in Figure 6.5 and reflected wrap-around if reaches the boundary. It is assumed that the CQI report and the measurement report is performed without any channel delay in a perfect feedback scenario whereas the CQI report and the measurement report feedback by the UE to the serving cell is delayed by 3 ms in an outdated feedback scenario.

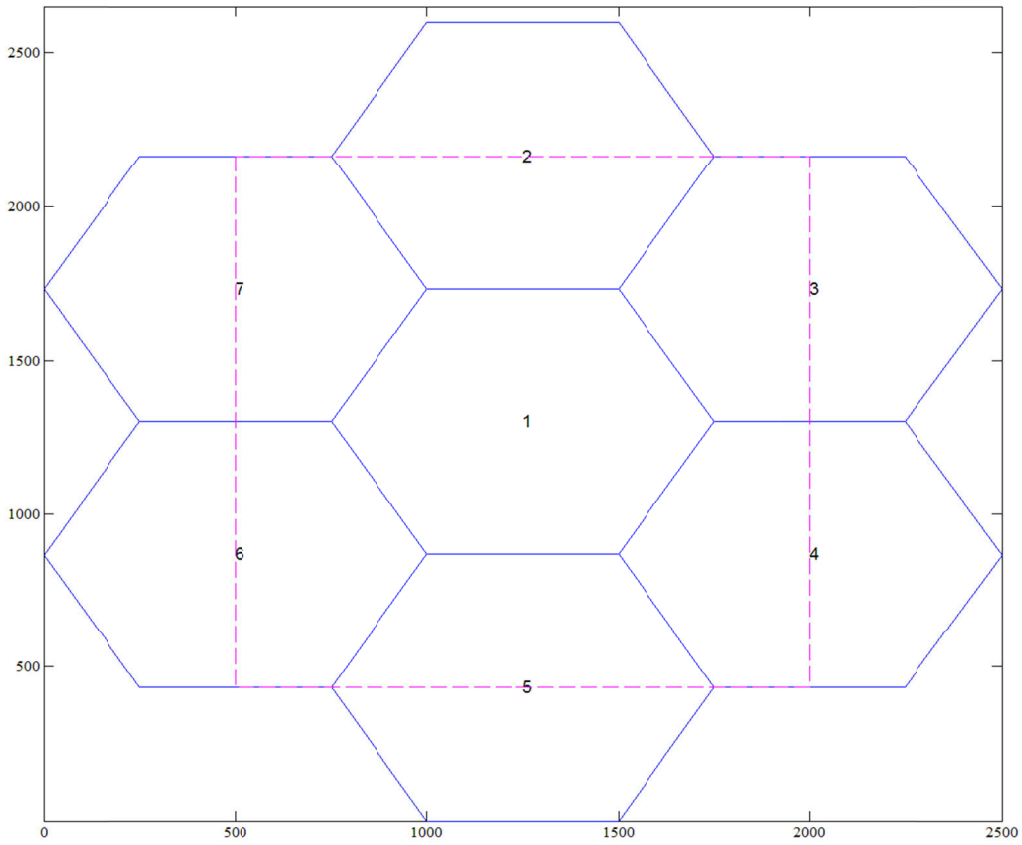

Figure 6.5: Perfect / Outdated Feedback Environment for a Practical LTE-A System

Figure 6.6 shows the simulation environment for a missing feedback scenario in a practical LTE-A system. Two tunnels are assumed in the missing feedback scenario where each tunnel is assumed with a width of 100 m and a length across the whole environment (as shown in Figure 6.6). A missing feedback is assumed only if a UE is in the tunnel areas. It is assumed that the CQI report and the measurement report fed back by a UE to the serving cell is delayed by 3 ms in a missing feedback scenario when the UE is not in the tunnel areas.

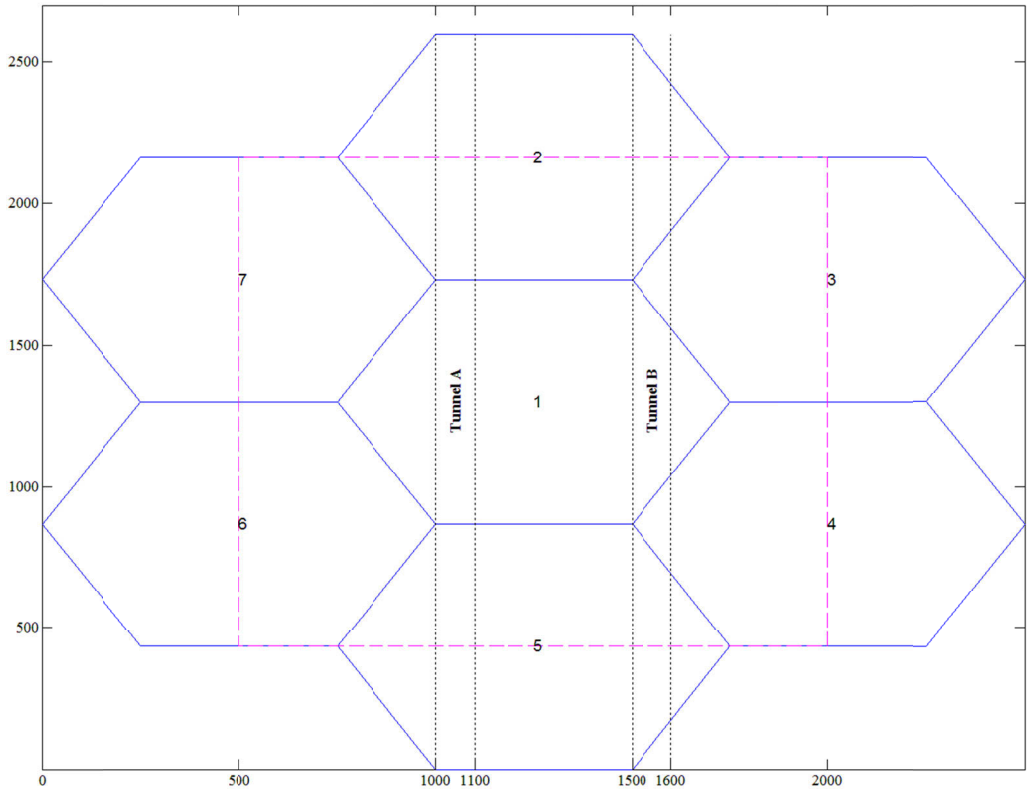

Figure 6.6: Missing Feedback Environment for a Practical LTE-A System

The system parameters used in the simulation are listed in Table 6.1. The maximum number of error packet retransmissions is limited to 3. A PF packet scheduler is chosen to provide a better trade-off between throughput maximization and fairness guarantee for all UEs. A RT traffic of 1 Mbps CBR stream is selected for observing the handover behaviour. Three UE speeds are simulated: 3 km/hr, 30 km/hr, and 120 km/hr. The CoMP Handover Algorithm, the Limited CoMP Handover Algorithm, the Capacity Based CoMP Handover Algorithm, and the Capacity Integrated CoMP Handover Algorithm referred as HOA 5, HOA 6, HOA 7, and HOA 8, respectively, are selected for the performance evaluation of a perfect feedback scenario, an outdated feedback scenario, and a missing feedback scenario in a practical LTE-A system. The values of the TTT, the HOM, and the measurement report interval are selected from the 3GPP standards discussed in section 6.1.1 as 0 ms, 0 dB, and 120 ms, respectively. In order to maintain the consistency, the value used for the size of CCS and CTP, the γ, and the capacity threshold are the same as in Section 5.1, respectively.

Table 6.1: The Simulation Parameters for a Practical LTE-A System

Parameters	Values
Cellular layout	Hexagonal grid, wrap around (reflect), 7 cells
Radius	500 m
Carrier Frequency	2 GHz
Bandwidth	5 MHz
Number of PRBs	25
Number of sub-carriers per PRB	12
Sub-carrier Spacing	15 kHz
Slot Duration	0.5 ms
Number of OFDM Symbols / Slot	7
Path Loss	Cost 231 Hata model
Shadow fading	Gaussian distribution
Multi-path	Rayleigh fading
Modulation and Coding Scheme	QPSK, 16QAM, and 64QAM
HARQ / Retransmission	Enable / 3 times
Packet Scheduler	Proportional Fair
Scheduling Time (TTI)	1 ms
Data Traffic	RT Traffic: 1 Mbps CBR
User	100
UE position	Fixed uniform distributed
UE direction	Randomly choose from $[0,2\pi]$
UE speed	3, 30, 120 km/hr
Simulation time	1000 ms
HOA	5: CoMP Handover Algorithm 6: Limited CoMP Handover Algorithm 7: Capacity Based CoMP Handover Algorithm 8: Capacity Integrated CoMP Handover Algorithm
TTT	0 ms
HOM	0 dB
Measurement report interval	120 ms
Size of CCS	3
Size of CTP	2
γ	0.75
Capacity Threshold	0.9

6.3 Performance Impact of CoMP Handover Algorithms in a Practical LTE-A System

The performance impacts of selected CoMP handover algorithms due to impairment environments in a practical LTE-A system are evaluated in terms of system throughput, system delay, and the number of handovers in this section. The performance evaluation of each selected CoMP handover algorithm in impairment environments is discussed individually in the following sub-sections.

6.3.1 CoMP Handover Algorithm

Figure 6.7 shows the system throughputs of HOA5 in a perfect feedback scenario, an outdated feedback scenario, and a missing feedback scenario in a practical LTE-A system.

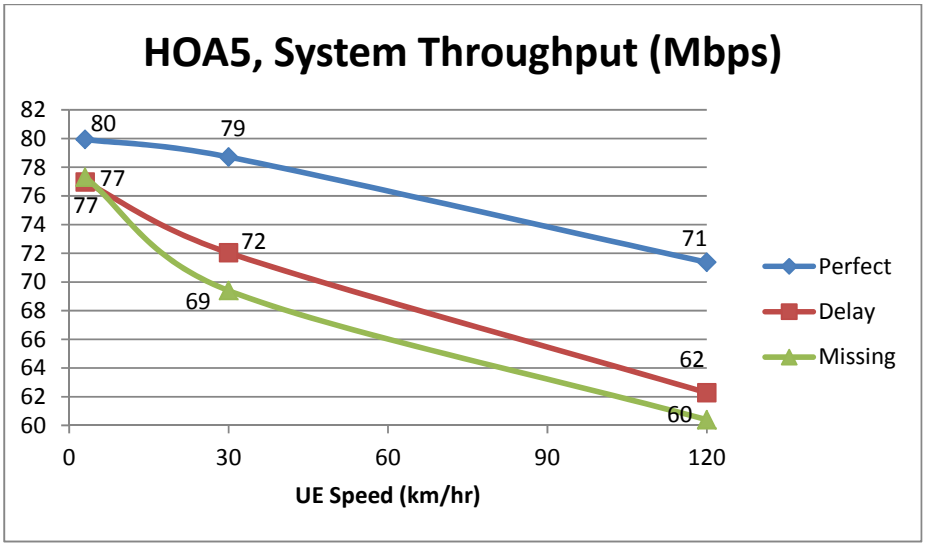

Figure 6.7: System Throughput of HOA5 in a Practical LTE-A System

There is a 3.3% and 3.7% performance degradation in the system throughput due to the outdated feedback and the missing feedback scenarios compared to the perfect feedback scenario at 3 km/hr, respectively. These performance degradations are not significant when compared to the perfect feedback scenario due to the slow UE speed.

The performance in the system throughput due to the outdated feedback and the missing feedback scenarios has an 8.5% and 11.8% degradation compared to the perfect feedback scenario at 30 km/hr, respectively. As the UE speed increases from 3 km/hr to 30 km/hr, the performance degradation due to the outdated feedback and the missing feedback scenarios compared to the perfect feedback scenario increases 5.2% and 8.1%, respectively. The performance in the system throughput due to the outdated feedback and the missing feedback scenarios has a 12.75% and 15.38% degradation compared to the perfect feedback scenario at 120 km/hr, respectively. As the UE speed increases from 3 km/hr to 120 km/hr, the performance degradation due to the outdated feedback and the missing feedback scenarios compared to the perfect feedback scenario increases 9.45% and 11.68%, respectively.

A 3 ms CQI delay in the outdated feedback scenario causes a wrong selection of the instantaneous modulation scheme and a significant performance degradation occurs with increasing UE speed. Moreover, the tunnels and the 3 ms CQI delay in the missing feedback scenario causes (a) a wrong selection of the instantaneous modulation scheme for all UEs and (b) unreachable data transmissions for UEs in the tunnel areas. These conditions significantly decrease the system throughput for having lower number of correctly transmitted and received packets.

Figure 6.7 shows the system delay of HOA5 in a perfect feedback scenario, an outdated feedback scenario, and a missing feedback scenario in a practical LTE-A system. The performance in the system delay due to the outdated feedback scenario has 4.66%, 36.33%, and 47.3% degradations compared to the perfect feedback scenario at UE speeds of 3 km/hr, 30 km/hr, and 120 km/hr, respectively. The performance in the system delay due to the missing feedback scenario has 12.76%, and 44.76%, and 53.7% degradations compared to the perfect feedback scenario at 3 km/hr, 30 km/hr, and 120 km/hr, respectively.

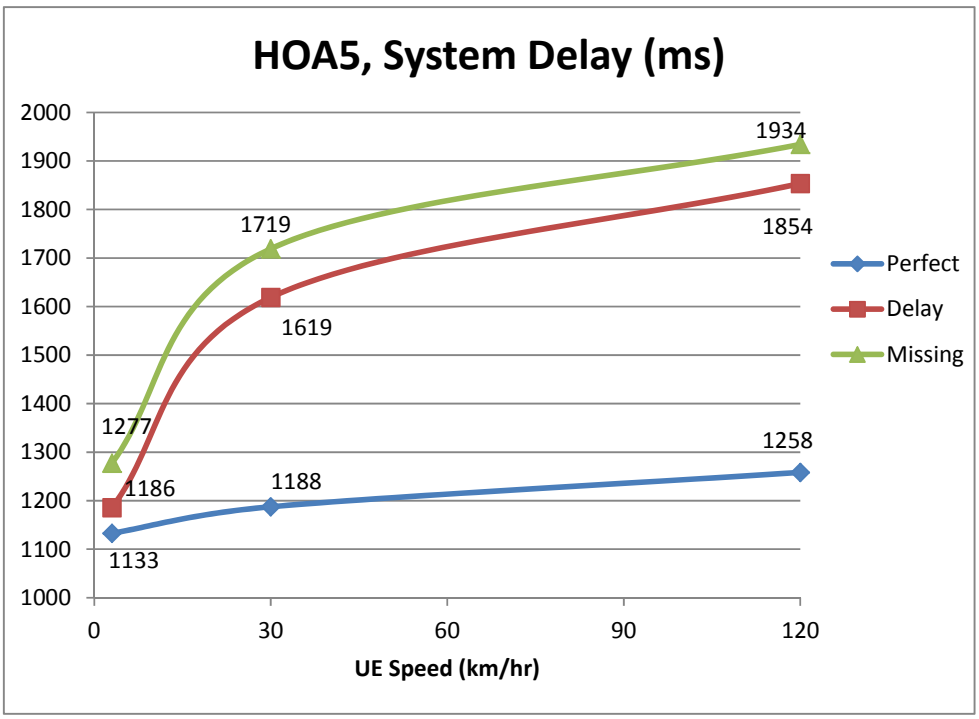

Figure 6.8: System Delay of HOA5 in a Practical LTE-A System

A 0 ms CQI delay is assumed in the perfect feedback scenario whereas a 3 ms CQI delay in the outdated feedback scenario causes a total of 6 ms system delay for a single TB of all UEs. A 3 ms delay duration used by the UE to decode the received TB and perform a CRC check followed by another 3 ms delay duration is used by the serving cell to decode the HARQ feedback and constructs a new encoded TB based on the feedback (which is outdated already). Therefore, the system delay is significantly higher in the outdated feedback scenario than in the perfect feedback scenario for all speed scenarios. Moreover, the missing feedback scenario causes a total system delay of 6 ms for a single TB of all UEs and an increased queuing delay for the buffered packets in the serving cell waiting to be transmitted to the unreachable UEs in the tunnel areas. Thus, the system delay of a missing feedback scenario is higher than an outdated feedback scenario for all speed scenarios.

Figure 6.9 shows the number of handovers of HOA5 in a perfect feedback scenario, an outdated feedback scenario, and a missing feedback scenario in a practical LTE-A system.

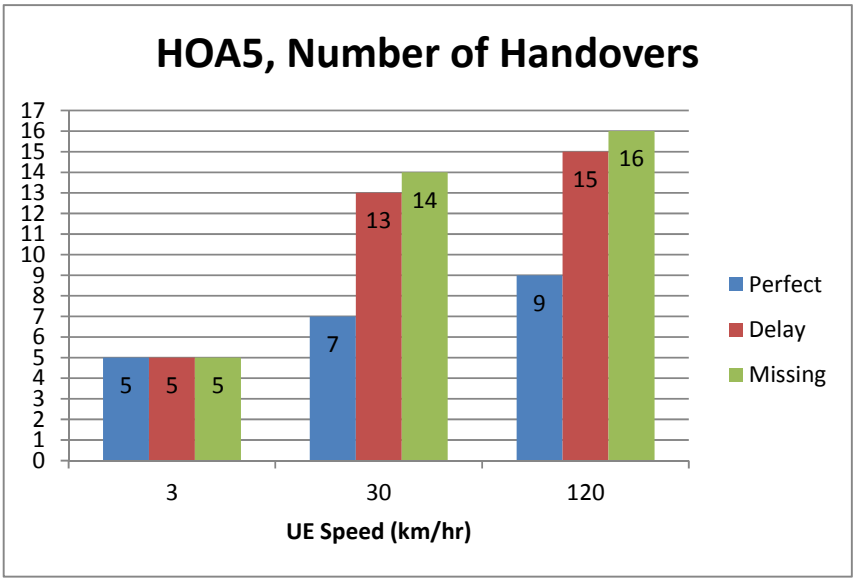

Figure 6.9: Number of Handovers of HOA5 in a Practical LTE-A System

There are 5 handovers for all speed scenarios in HOA5 at 3 km/hr. The number of handovers is equivalent in the perfect feedback, the outdated feedback, and the missing feedback scenarios due to the slow UE speed. The performance in the number of handovers due to the outdated feedback scenario has 6 more handovers compared to the perfect feedback scenario at UE speeds of 30 km/hr and 120 km/hr. The serving cell in the outdated feedback scenario makes the handover decision based on the outdated measurement report where the RSRP of the serving cell will be too low when a handover is triggered. Thus a too late handover occurs in the outdated feedback scenario. In order to maintain the received signal quality for the UE in the outdated feedback scenario, the serving cell keeps handing over the UE to a target cell whether it has a better received signal strength or not. However, due to the outdated measurement reports, the signal strengths of the target cells are always outdated (inaccurate) and therefore the number of handovers at user speeds at 30 km/hr and 120 km/hr are increased in the outdated feedback scenario compared to the perfect feedback scenario.

The performance in the number of handovers due to the missing feedback scenario has 7 more handovers compared to the perfect feedback scenario at UE speeds of 30 km/hr and 120 km/hr. A too early handover and a handover to a wrong cell could possibly occur when the UEs travel through the tunnel areas in the missing feedback scenario.

Due to the obstruction of the tunnels, a RLF could possibly occur in the target cell after a successful handover triggered by the serving cell when the UE enters the tunnel areas. Therefore (a) if the UE reconnects to the serving cell after the RLF occurred, then a too early handover occurs or (b) if the UE reconnects to a cell which is neither the serving cell nor the target cell after the RLF occurred, then a handover to a wrong cell occurs. The number of unnecessary handovers is increased due to the situations described above in the missing feedback scenario which results in a higher number of handovers compared to the perfect feedback and the outdated feedback scenarios for user speeds of 30 km/hr and 120 km/hr.

6.3.2 Limited CoMP Handover Algorithm

Figure 6.10 shows the system throughputs of HOA6 in a perfect feedback scenario, an outdated feedback scenario, and a missing feedback scenario in a practical LTE-A system.

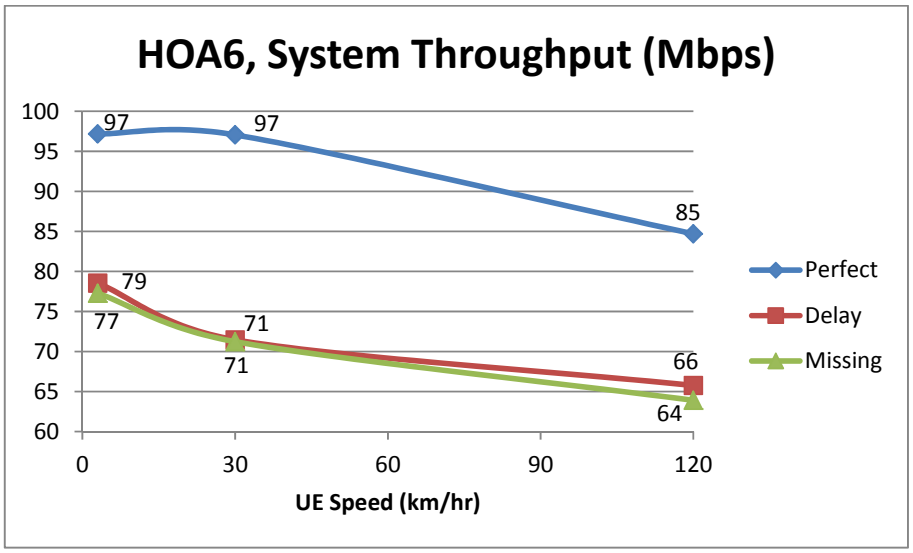

Figure 6.10: System Throughput of HOA6 in a Practical LTE-A System

The performance in the system throughput in the outdated feedback scenario has 19.16%, 26.37%, and 26.61% degradations compared to the perfect feedback scenario at UE speeds of 3 km/hr, 30 km/hr, and 120 km/hr, respectively. The performance

degradation in the system throughput from a UE speed of 3 km/hr to 30 km/hr and from 3 km/hr to 120 km/hr increases 9.02% and 16.28%, respectively.

The performance in the system throughput due to the missing feedback scenario has 20.46%, and 22.4%, and 24.54% degradation compared to the perfect feedback scenario at UE speeds of 3 km/hr, 30 km/hr, and 120 km/hr, respectively. The performance degradation in the system throughput from a UE speed of 3 km/hr to 30 km/hr and from 3 km/hr to 120 km/hr increases 7.84% and 17.31%, respectively.

The overall system throughputs of HOA6 among all speed scenarios are higher than the overall system throughputs of HOA5 among all speed scenarios; however the performance degradations in the outdated feedback and the missing feedback scenarios are significantly higher than those for HOA5. HOA6 heavily relies on the measurement report at each TTI to add or remove a target cell in the CCS by constantly checking the RSRP from the CCS. The outdated and missing measurement reports in the outdated feedback and the missing feedback scenarios mislead the handover decision of HOA6, therefore the system throughputs of HOA6 decrease sharply for all speed scenarios in these two impairment environments.

Figure 6.11 shows the system delay of HOA6 in a perfect feedback scenario, an outdated feedback scenario, and a missing feedback scenario in a practical LTE-A system.

The performance in the system delay due to the outdated feedback scenario has 47.16%, 87.70%, and 66.47% degradations compared to the perfect feedback scenario at 3 km/hr, 30 km/hr, and 120 km/hr, respectively. The performance in the system delay due to the missing feedback scenario has 57.58%, and 97.99%, and 71.63% degradations compared to the perfect feedback scenario at 3 km/hr, 30 km/hr, and 120 km/hr, respectively.

A 0 ms CQI delay is assumed in the perfect feedback scenario whereas a total system delay of 6 ms for a single TB for all UEs is assumed in the outdated feedback scenario causes. Therefore the system delay is significantly higher in the outdated feedback scenario than in the perfect feedback scenario for all speed scenarios. Moreover, the

missing feedback scenario causes a total system delay of 6 ms for a single TB for all UEs and an increased queuing delay for the buffered packets in the serving cell waiting to be transmitted to the unreachable UEs in the tunnel areas. Thus, the system delay of the missing feedback scenario is higher than the outdated feedback scenario for all speed scenarios.

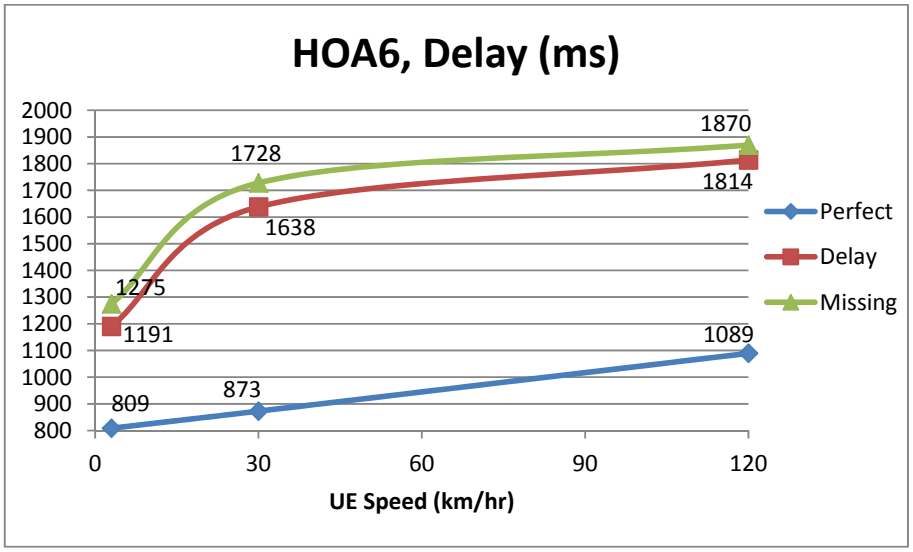

Figure 6.11: System Delay of HOA6 in a Practical LTE-A System

Figure 6.12 shows the number of handovers of HOA6 in a perfect feedback scenario, an outdated feedback scenario, and a missing feedback scenario in a practical LTE-A system.

The performance in the number of handovers due to the outdated feedback scenario has 4, 3, and 1 more handovers compared to the perfect feedback scenario at UE speeds of 3 km/hr, 30 km/hr and 120 km/hr, respectively. The performance in the number of handovers due to the missing feedback scenario has 4, 3, and 2 more handovers compared to the perfect feedback scenario at UE speeds of 3 km/hr, 30 km/hr and 120 km/hr, respectively.

Simulation results have shown that HOA6 is less tolerable to an outdated feedback scenario than a missing feedback scenario because an accurate measurement report at each TTI is needed for the HOA6 to perform the correct handover decision. A too late handover occurred in the outdated feedback scenario whereas a too early handover and

a handover to a wrong cell could both possibly occur in the missing feedback scenario; therefore the number of handovers in the missing feedback scenario is higher than the one in the outdated feedback scenario at 120 km/hr.

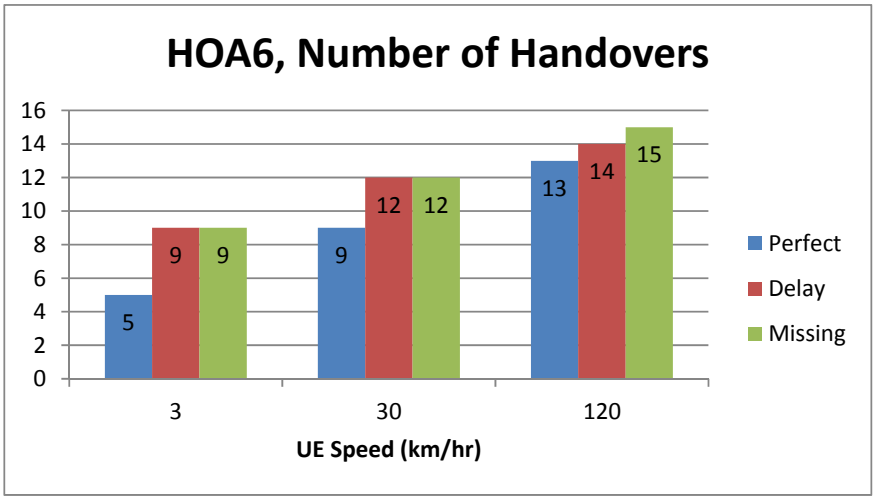

Figure 6.12: Number of Handovers of HOA6 in a Practical LTE-A System

6.3.3 Capacity Based CoMP Handover Algorithm

Figure 6.13 shows the system throughput of HOA7 in a perfect feedback scenario, an outdated feedback scenario, and a missing feedback scenario in a practical LTE-A system.

The performance in the system throughput due to the outdated feedback scenario has 2.24%, 12.12%, and 12.34% degradations compared to the perfect feedback scenario at UE speeds of 3 km/hr, 30 km/hr, and 120 km/hr, respectively. The performance degradation in the system throughput of the outdated feedback scenario from a UE speed of 3 km/hr to 30 km/hr and from 3 km/hr to 120 km/hr increases 11.22% and 22.35%, respectively.

The performance in the system throughput due to the missing feedback scenario has 8.02%, and 12.95%, and 13.82% degradations compared to the perfect feedback scenario at 3 km/hr, 30 km/hr, and 120 km/hr, respectively. The performance degradation in the system throughput at a UE speed from 3 km/hr to 30 km/hr and from 3 km/hr to 120 km/hr increases 6.5% and 18.87%, respectively.

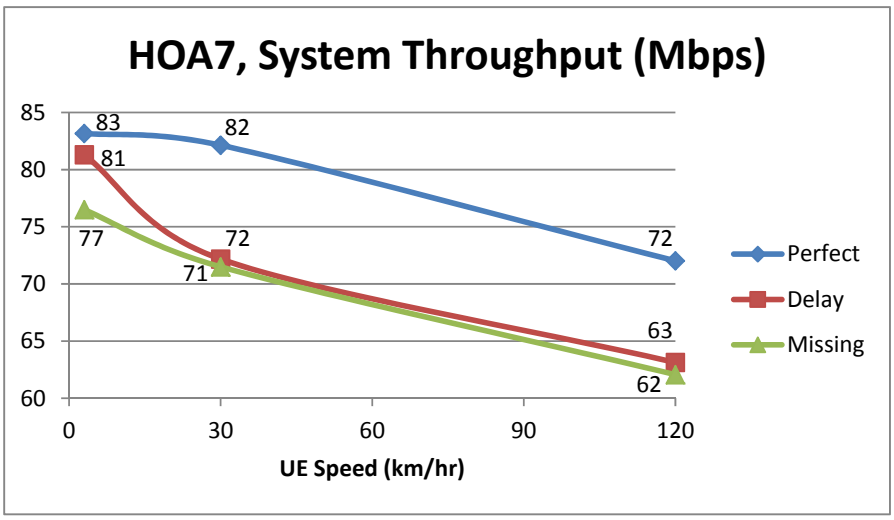

Figure 6.13: System Throughput of HOA7 in a Practical LTE-A System

Simulation results have shown that HOA7 is slightly more robust against the performance degradation in terms of the system throughput from 3 km/hr to 120 km/hr UE speeds in the outdated feedback and the missing feedback scenarios compared to the HOA6. It is because the RB utilization value used in the HOA7 is calculated by each eNodeB and exchanged via X2 interfaces in the system. The RB utilization value is less subjected to the delay and missing impairments in the radio channels in the outdated and missing feedback scenarios.

Figure 6.14 shows the system delay of HOA7 in a practical LTE-A system with a perfect feedback scenario, an outdated feedback scenario, and a missing feedback scenario.

The performance in the system delay due to the outdated feedback scenario has 7.24%, 49.17%, and 40% degradations compared to the perfect feedback scenario at UE speeds of 3 km/hr, 30 km/hr, and 120 km/hr, respectively. The performance degradation in the system delay due to the outdated feedback scenario increases 44.40% and 79.92% from 3 km/hr to 30 km/hr and from 3 km/hr to 120 km/hr UE speeds, respectively.

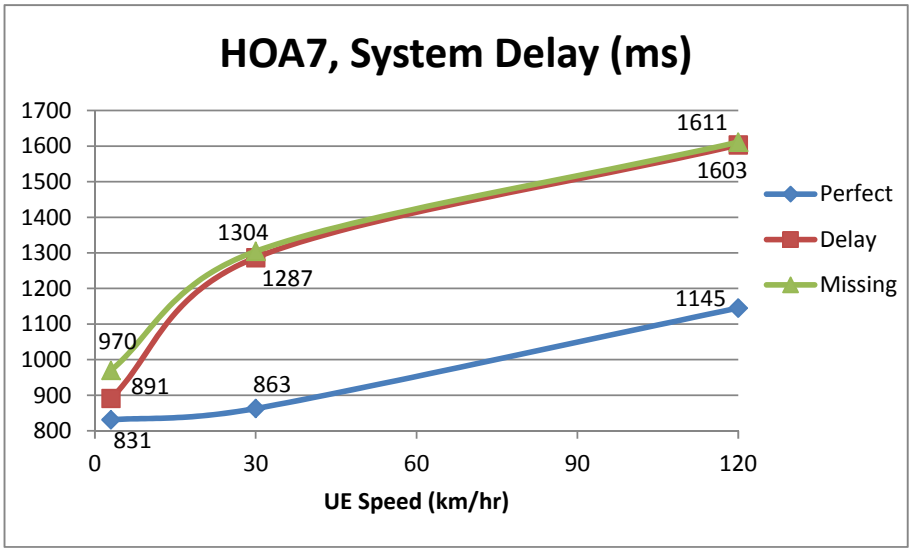

Figure 6.14: System Delay of HOA7 in a Practical LTE-A System

The performance in the system delay due to the missing feedback scenario has 16.73%, and 51.20%, and 40.71% degradation compared to the perfect feedback scenario at UE speeds of 3 km/hr, 30 km/hr, and 120 km/hr, respectively. The performance degradation in the system delay due to the missing feedback scenario increases 34.47% and 66.11% from 3 km/hr to 30 km/hr and from 3 km/hr to 120 km/hr UE speeds, respectively.

A 0ms CQI delay is assumed in the perfect feedback scenario whereas a total system delay of 6 ms for a single TB for all UEs is assumed in the outdated feedback scenario. Therefore the system delay is significantly higher in the outdated feedback scenario than in the perfect feedback scenario for all speed scenarios. Moreover, the missing feedback scenario causes a total system delay of 6 ms for a single TB for all UEs and an increased queuing delay for the buffered packets in the serving cell waiting to be transmitted to the unreachable UEs in the tunnel areas. Thus, the system delay of the missing feedback scenario is higher than the outdated feedback scenario for all speed scenarios.

The performance degradation in the system delay for the outdated feedback scenario is caused by (a) a total of 6 ms system delay for a single TB for all UEs and (b) an increased queuing delay of the buffered packets in the serving cell for the unreachable UEs in the tunnel areas. However, HOA7 has the robustness to tolerate the missing

measurement reports and is able to minimize the system delay difference between the outdated feedback scenario and the missing feedback scenario for all speed scenarios.

Figure 6.15 shows the number of handovers of HOA7 with a perfect feedback scenario, an outdated feedback scenario, and a missing feedback scenario in a practical LTE-A system.

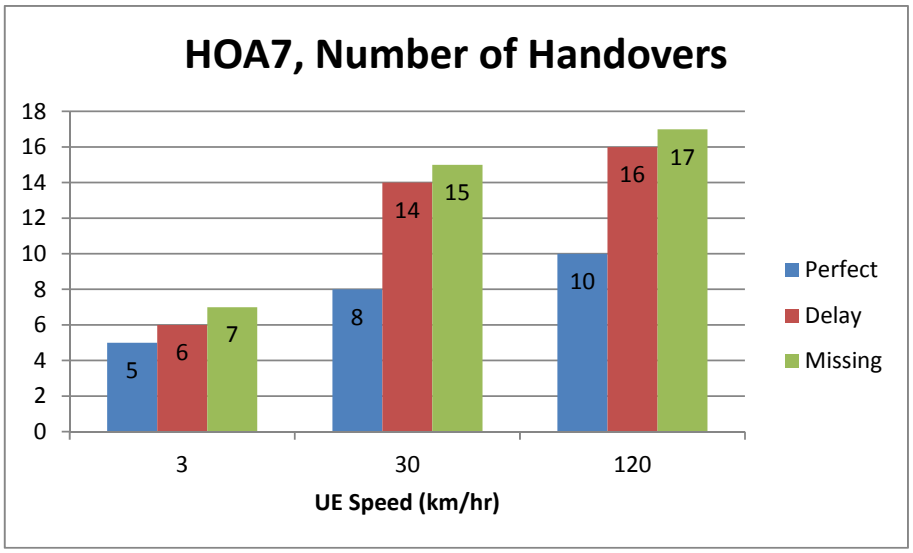

Figure 6.15: Number of Handovers of HOA7 in a Practical LTE-A System

The performance in the number of handovers in the outdated feedback scenario has 1, 6, and 6 more handovers compared to the perfect feedback scenario at UE speeds of 3 km/hr, 30 km/hr and 120 km/hr, respectively. The performance in the number of handovers due to the missing feedback scenario has 2, 7, and 7 more handovers compared to the perfect feedback scenario at UE speeds of 3 km/hr, 30 km/hr and 120 km/hr, respectively.

A too late handover occurs in the outdated feedback scenario whereas a too early handover and a handover to a wrong cell can possibly both occur in the missing feedback scenario; therefore the number of handovers in the missing feedback scenario is higher than the outdated feedback scenario for all speed scenarios.

HOA7 has a higher total number of handovers compared to HOA5 and HOA6 because HOA7 tries to arrange UEs to be handed over to a target cell which has a better received

signal strength especially in the outdated and missing feedback scenarios. However, the arrangement based on an inaccurate measurement report (outdated or missing) directs the UEs to inappropriate target cells. Therefore UEs have a higher chance of more handovers which leads to a higher handover count.

6.3.4 Capacity Integrated CoMP Handover Algorithm

Figure 6.16 shows the system throughputs of HOA8 in a perfect feedback scenario, an outdated feedback scenario, and a missing feedback scenario in a practical LTE-A system.

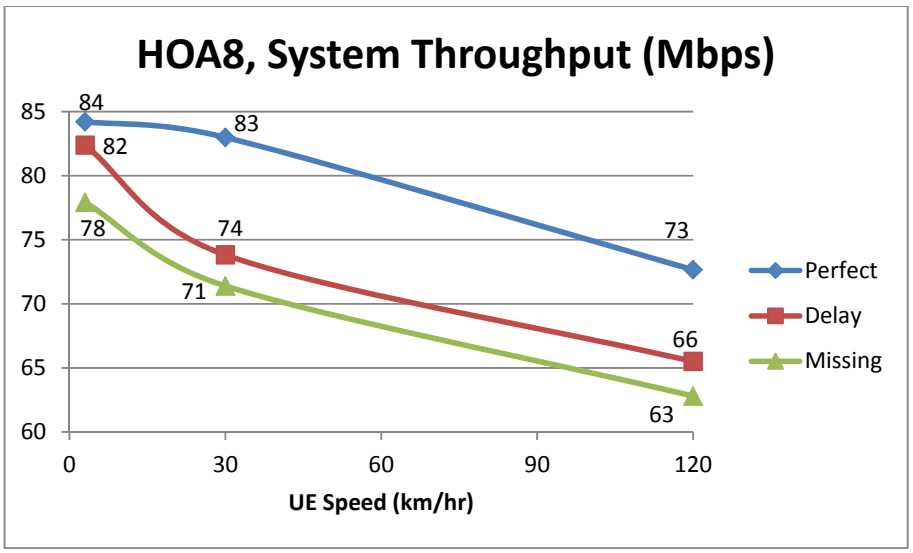

Figure 6.16: System Throughput of HOA8 in a Practical LTE-A System

The performance of the system throughput in the outdated feedback scenario has 2.17%, 11.05%, and 9.85% degradations compared to the perfect feedback scenario at UE speeds of 3 km/hr, 30 km/hr, and 120 km/hr, respectively. The performance degradation of system throughput for the outdated feedback scenario increases 10.4% and 20.49% from 3 km/hr to 30 km/hr and from 3 km/hr to 120 km/hr UE speeds, respectively.

The performance in the system throughput due to the missing feedback scenario has 7.46%, and 13.97%, and 13.57% degradations compared to the perfect feedback scenario at 3 km/hr, 30 km/hr, and 120 km/hr, respectively. The performance degradation in the system throughput due to the missing feedback scenario increases

8.38% and 19.40% from 3 km/hr to 30 km/hr and from 3 km/hr to 120 km/hr UE speeds, respectively.

HOA8 checks the RB utilization value which is calculated by each eNodeB and exchanged via X2 interfaces in the network. The RB utilize value and the capacity indicator are less subjected to the delay and missing impairments in the outdated and missing feedback scenarios. In terms of the degradation of system throughput in the outdated feedback and the missing feedback scenarios (for all speed scenarios), HOA8 is more robust than HOA6 and HOA7.

Figure 6.17 shows the system delay of HOA8 in a perfect feedback scenario, an outdated feedback scenario, and a missing feedback scenario in a practical LTE-A system.

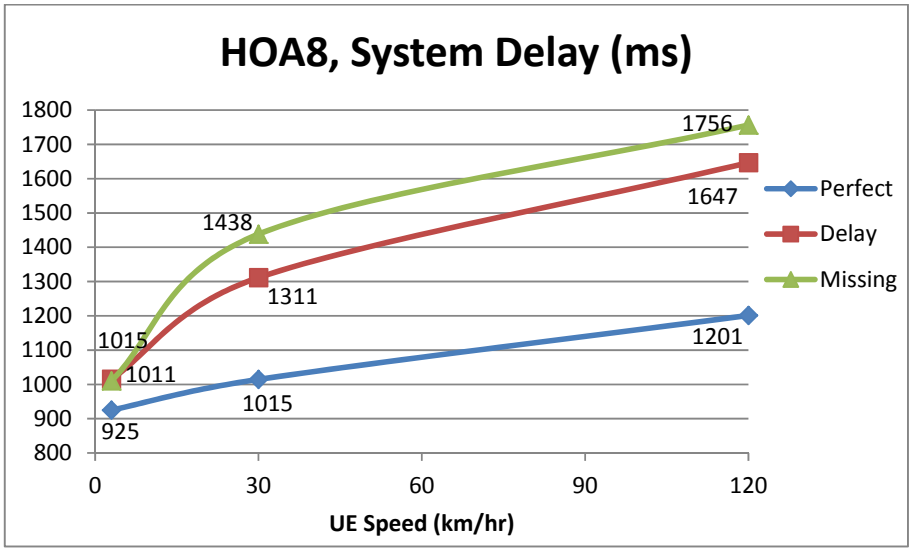

Figure 6.17: System Delay of HOA8 in a Practical LTE-A System

The performance in the system delay due to the outdated feedback scenario has 9.71%, 29.26%, and 37.09% degradations compared to the perfect feedback scenario at UE speeds of 3 km/hr, 30 km/hr, and 120 km/hr, respectively. The performance degradations in the system delay due to the outdated feedback scenario increase 29.78% and 62.95% from 3 km/hr to 30 km/hr and from 3 km/hr to 120 km/hr UE speeds, respectively.

The performance in the system delay due to the missing feedback scenario has 9.24%, 41.75%, and 46.23% degradations compared to the perfect feedback scenario at UE speeds of 3 km/hr, 30 km/hr, and 120 km/hr, respectively. The performance degradations in the system delay due to the missing feedback scenario increase 41.71% and 73.07% from 3 km/hr to 30 km/hr and from 3 km/hr to 120 km/hr UE speeds, respectively.

Simulation results show that HOA8 is more robust when missing measurement reports are considered. This minimizes the system delay difference between the outdated feedback and the missing feedback scenarios for all speed scenarios. The RB utilize value and the capacity indicator used in the HOA8 are less subjected to the delay and missing impairments in the radio channels in the outdated and missing feedback scenarios.

Figure 6.18 shows the number of handovers of HOA8 in a perfect feedback scenario, an outdated feedback scenario, and a missing feedback scenario in a practical LTE-A system.

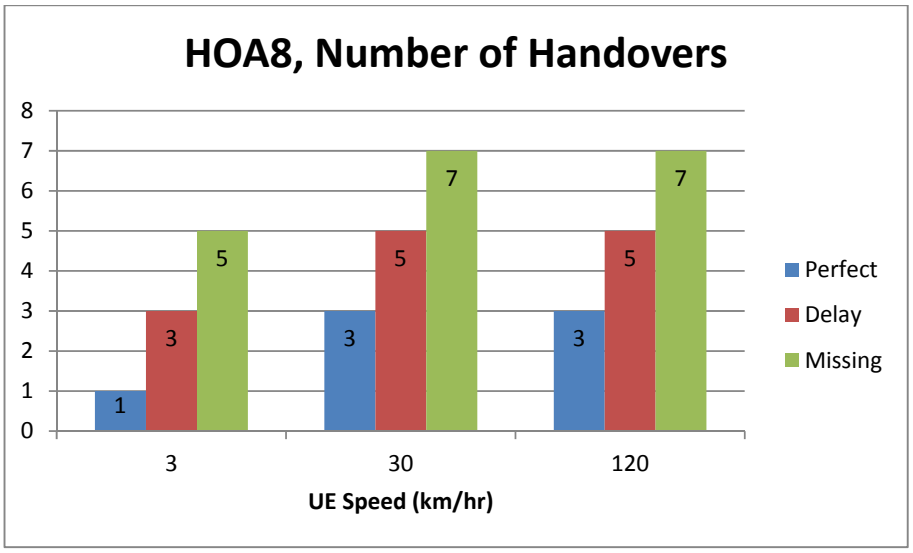

Figure 6.18: Number of Handovers of HOA8 in a Practical LTE-A System

The performance in the number of handovers due to the outdated feedback and missing feedback scenarios has 2 and 4 more handovers compared to the perfect feedback scenario for all speed scenarios, respectively.

Simulation results have shown HOA8 can minimize the number of (unnecessary) handovers in the perfect feedback, the outdated feedback, and the missing feedback scenarios compared to HOA5, HOA6, and HOA7 for all speed scenarios because HOA8 limits the UEs to be handed over to a target cell. However, a too late handover occurs in the outdated feedback scenario whereas a too early handover and a handover to a wrong cell can possibly both occur in the missing feedback scenario; therefore the number of handovers in the missing feedback scenario is higher than the outdated feedback scenario among all speed scenarios.

6.4 Summary

The performance impact of selected CoMP handover algorithms due to mobile cellular channel impairments in a practical LTE-A cellular system is considered in this chapter. This chapter initially studied the related works including the 3GPP standards of handover parameters in a practical LTE-A system and the performance impact due to imperfect channel feedbacks in a practical LTE-A system. The impairments for a practical LTE-A system are assumed to be in two scenarios: outdated feedback scenario and missing feedback scenario. The simulation environments for each scenario in a practical LTE-A are individually discussed. The performances of each CoMP handover algorithm for a perfect feedback scenario, an outdated feedback scenario, and a missing feedback scenario in a practical LTE-A system are individually evaluated and discussed in this chapter.

Simulation results show that the system performance (in terms of system throughput and system delay) is very sensitive against outdated CQI feedback and missing CQI feedback. A handover failure (too late handover, too early handover, or handover to a wrong cell) increases the number of unnecessary handovers which requires additional resources in the network and may significantly degrade the system performance.

Chapter 7

CONCLUSIONS AND FUTURE RESEARCH DIRECTIONS

This chapter summarises a number of challenges in handover algorithms studied in this thesis and contributions made to improve the system performance in the LTE and LTE-A systems followed by some discussions for the future research. Section 7.1 summarises the original contributions of this thesis. Section 7.2 and Section 7.3 discuss the system implications and limitations and future research directions, respectively.

7.1 Summary of Thesis Contributions

The original contributions of this thesis are divided into three major areas described as follows:

7.1.1 Handover Parameters Optimization Method

Given the scarcity of the radio resources, the dynamic nature of the propagation environment and the variety of user mobility, maximizing the possible system throughput and minimizing the system delay are the major challenges that need to be addressed in the handover mechanisms in LTE and LTE-A systems. A handover parameters optimization method was proposed to address the research question: "Given the current handover algorithms in multi-carrier systems, can one improve the performance of the current algorithms by minimizing system delay and maximizing the system throughput in a multi-cell scenario"?

The handover parameters optimization method was proposed based on a ratio of total system throughput to the average number of handovers across a number of HOM and TTT values. The handover parameters optimization method can minimize the

unnecessary number of handovers while maximizing the system throughput (see Section 3.6.1 and Section 5.1).

7.1.2 Handover Algorithm in LTE

A handover algorithm in LTE, namely LTE Hard Handover Algorithm with Average RSRP Constraint (LHHAARC) is proposed for better handover performance. LHHAARC was proposed to address the research question: "Given a set of handover algorithms in LTE, can one evaluate these algorithms based on the simulation performance analysis"?

Under the assumption of an ideal channel conditions and optimized handover parameters, it was shown via computer simulation that the proposed LHHAARC has reduced (by up to 35.56%) the average number of handovers compared to the LTE Integrator Handover Algorithm. LHHAARC has 3.55%, 25%, and 1.302% higher total system throughputs compared to the other three well known handover algorithms respectively (see Section 3.6.2). The proposed handover algorithm is able to maintain a lower system delay compared to the other three well known handover algorithms (i.e. 17.93%, 22.77%, and 47.58% reductions in delay when compared to LTE Hard Handover Algorithm, RSS Based TTT Window Algorithm and LTE Integrator Handover Algorithms, respectively).

Given that a LTE-A system is a major enhancement of the LTE system, the feasibility of the LTE handover mechanisms on LTE-A system needs to be studied. The CoMP technology is expected to improve the cell-edge throughput and/or system throughput with multiple data transmissions in LTE-A compared to the throughput(s) in the LTE system. Therefore, the current existing handover algorithms in the LTE network are not applicable for CoMP networks. A computer simulation was developed to address the research question: "How suitable are LTE handover mechanisms for LTE Advanced"? Based on the discussion (see Section 4.1.3), the computer simulation results show that, when compared to the standard LTE Hard Handover Algorithm in the LTE system, the CoMP Handover Algorithm in LTE-A is able to improve the system throughput and minimize PLR effectively. However, this algorithm could lead to system capacity overload and saturated system throughput issues within a highly congested network.

7.1.3 CoMP Handover Algorithms in LTE-A

Three CoMP handover algorithms are proposed for the LTE-A system in this thesis: Limited CoMP Handover Algorithm, Capacity Based CoMP Handover Algorithm, and Capacity Integrated CoMP Handover Algorithm. These algorithms take into consideration one or more decision criteria to overcome the loaded system throughput and maximize the system capacity usage. These algorithms are proposed to address the research question: "Given that existing handover algorithms in the LTE network are not applicable for CoMP networks, can one design a handover algorithm that support CoMP technology and take system capacity into consideration in the LTE-A system"?

Under the assumption of an ideal channel condition and optimized handover parameters, it was shown via computer simulation that the Capacity Integrated CoMP Handover Algorithm can minimize the system delay and the number of handovers with RT traffic, NRT traffic, and mixed RT and NRT traffic in 3 km/hr, 30 km/hr, and 120 km/hr scenarios. Furthermore, the Capacity Integrated CoMP Handover Algorithm provides the highest system throughput at 120 km/hr for the RT traffic and mixed RT and NRT traffic. For the NRT traffic model, the Limited CoMP Handover Algorithm provides the highest system throughput among all speed scenarios.

Chapter 6 studied a practical LTE-A cellular system with realistic mobile cellular channel impairments. These impairments may cause severe performance degradations especially for handover algorithms that strongly rely on an accurate RSRP report. This chapter aimed to address the research questions: "Given that handover algorithms rely on an accurate RSRP report to perform optimized performance, what is the performance impact of CoMP handover algorithms due to impairment environments in a practical LTE-A cellular network"?

The performance impact of selected CoMP handover algorithms due to mobile cellular channel impairments in a practical LTE-A cellular system is considered in Chapter 6. The impairments for a practical LTE-A system are assumed to be in two scenarios: outdated feedback scenario and missing feedback scenario. It is shown via computer simulation that the system throughput and system delay are very sensitive to outdated CQI feedback and missing CQI feedback. A handover failure (too late handover, too

early handover, or handover to a wrong cell) caused by an inaccurate measurement report increases the number of unnecessary handovers which requires additional resources in the network and may significantly degrade the system performance.

7.2 System Implications and Limitations

This thesis proposed five novel contributions (a handover parameters optimization method, a handover algorithm in the LTE system, and three CoMP handover algorithms in the LTE-A system) are needed to be addressed the research challenges of: (i) why the new handover techniques for downlink LTE-A are designed and evaluated, (ii) what a system planner needs to do to use the system, and (iii) how system planners can be benefitted from this research.

(i) During the research on the literature, the CoMP Handover Algorithm enhances the LTE-A system throughput and reduces the PLR when compared with the LTE system. However, system capacity overload and saturated system throughput issues are found based on the simulation results. The new handover techniques for downlink LTE-A are designed for supporting CoMP technology and taking the system capacity and the system load into consideration. Limited CoMP handover algorithm enhances the system capacity by accommodating as many users as possible in the system. Capacity Based CoMP Handover Algorithm and Capacity Integrated CoMP Handover Algorithm enhance the system capacity by giving the available radio resources to the users based on the current and historical available radio resources, respecitvely.

(ii) A system planner can use the proposed three CoMP handover algorithms in an urban density area where CoMP technology and LTE-A are deployed. These three CoMP handover algorithms are designed and evaluated for enhancing the system capacity, maximizing the system throughput, and minimizing the system delay.

(iii) The system planners can be benefitted from this research for less equipment expansive. The system planners could also be benefitted for better user experience from their customers based on the higher system throughput and less system delay their system provides.

This thesis is limited to a seven hexagonal cells scenario which supports multiple users with one active application (RT, NRT, or RT and NRT traffic) at a time in the performance evaluation. Moreover, a number of assumptions were made in this thesis due to the time constraint as well as to further reduce complexity of the system simulation. The limitations of this thesis are addressed in Section 2.12.

7.3 Future Research Directions

Based on the study of handover challenges in LTE and LTE-A systems, a number of important issues have been identified for future research. Some of the issues are briefly discussed as follows:

(i) The majority of works discussed in this thesis focus on the total number of handovers in the simulation. One of the major problems with handover is the ping-pong effect. Ping-pong effect results in a wastage of network resources. However, handovers are essential to provide a satisfactory user experience. The development of necessary and unnecessary (ping-pong) handovers detection in the simulation is a subject for future study.

(ii) RLF is one of the major issues that occur in a handover failure and is related to the PHY layer aspects. The majority of works discussed in this thesis focus on the effects caused by the RLF. A detailed research on the relationship between RLF in the PHY layer and handover failure is a subject for future study.

(iii) The performance impact due to outdated and missing feedbacks towards handover performance has been studied in Chapter 6. The simulation results in Chapter 6 have shown that the outdated and missing feedbacks significantly degrade the system performance. A handover mechanism with handover failure rescue in the imperfect feedback scenarios in the LTE-A system will be included in future studies.

REFERENCES

[1] ITU. (2013, 22/04/2013). *Global mobile-cellular subscriptions, total and per 100 inhabitants, 2001-2013*. Available: http://www.itu.int/en/ITU-D/Statistics/Documents/statistics/2012/stat_page_all_charts.xls

[2] 4GAmericas. (2013, 22/04/2013). *LTE: Long Term Evolution*. Available: http://www.3gamericas.org/index.cfm?fuseaction=page&sectionid=249

[3] E. Dahlman, S. Parkvall, J. Skold, and P. Beming, *3G Evolution: HSPA and LTE for Mobile Broadband*, First ed.: Elsevier Ltd., 2007.

[4] R. Ramachandran, "Evolution to 3G Mobile Communication: Second Generation Cellular Systems," *RESONANCE,* vol. 8, no. 9, pp. 60-72, 2003.

[5] E. Dahlman, "3G Long Term Evolution," Ericsson Research2007.

[6] F. Ivanek, "Mobile Backhaul [From the Guest Editor's Desk]," *Microwave Magazine, IEEE,* vol. 10, no. 5, pp. 10-20, 2009.

[7] R. Ramachandran, "Evolution to 3G Mobile Communication: Development Towards Third Generation Systems," *RESONANCE,* vol. 8, no. 11, pp. 37-51, 2003.

[8] D. E. Dilger. (2012, 22/04/2013). *NPD ranks iPhone 4S as America's most popular 4G phone due to HSPA+*. Available: http://appleinsider.com/articles/12/03/13/npd_ranks_iphone_4s_as_americas_most_popular_4g_phone_due_to_hspa

[9] T. Seymour and A. Shaheen, "History of Wireless Communication," *Review of Bussiness Information Systems - Second Quarter 2011,* vol. 15, no. 2, pp. 1-6, 2011.

[10] S. Sesia, I. Toufik, and M. Baker, *LTE: The UMTS Long Term Evolution - From Theory To Practice*, First ed.: John Wiley & Sons Ltd., 2009.

[11] H. Holma and A. Toskala, *LTE for UMTS: OFDMA and SC-FDMA Based Radio Access*, First ed.: John Wiley & Sons Ltd., 2009.

[12] GSA, "GSM/3G market/Technology update, Evolution to LTE Report," May 10, 2013.

[13] D. McQueen, "The Momentum behind LTE Adoption," *IEEE Communications Magazine,* vol. 47, no. 2 pp. 44–45, 2009.

[14] ITU-R and M.2134, "Requirements related to technical performance for IMT-Advanced radio interface(s)," 2008.

[15] GSA. (2013, 14/07/2013). *GSA Evolution to LTE report: 163 commercial networks launched; 415 operators investing in LTE*. Available: http://www.gsacom.com/news/gsa_375.php

[16] YOTA. (2012, 30/04/2013). Yota Networks has launched the world's first mobile communication technology LTE Advanced. Available: http://www.yota.ru/ru/news/details/?ID=316537

[17] 3GPP TR25.913 version 7.3.0, "Requirements for Evolved UTRA (E-UTRA) and Evolved UTRAN (E-UTRAN) (Release 7)," March 2006.
[18] T. Saito, Y. Tanaka, and T. Kato, "Trends in LTE/WiMAX Systems," *Fujitsu Sci. Tech.,* vol. 45, October 2009.
[19] A. M. Rao, A. Weber, S. Gollamudi, and R. Soni, "LTE and HSPA+:Revolutionary and Evolutionary Solutions for Global Mobile Broadband," *Bell Labs Technical Journal,* vol. 13, 2009.
[20] Ericsson. (June 2009). *LTE – an introduction*.
[21] R. Divya and A. Hüseyin, "3GPP – Long Term Evolution – A Technical Study," ed, Spring 2009.
[22] M. Kottkamp, "LTE-Advanced Technology Introduction White Paper," Rohde & Schwarz GmbH & Co. KG 07-2010.
[23] A. Krishnarajah and K. Sandrasegaran, "Lecture Notes: Mobile Communication Systems - Long Term Evolution," University of Technology, Sydney 2008.
[24] A. Hadden, "Mobile Broadband - Where the Next Generation Leads Us," *IEEE Wireless Communications,* pp. 6-9, 2009.
[25] Alcatel-Lucent. (2013). *42890 4G Mobile Technologies*.
[26] 3GPP TS36.300 version 9.2.0, "Evolved Universal Terrestrial Radio Access (E-UTRA) and Evolved Universal Terrestrial Radio Access Network (E-UTRAN); Overall Description; Stage 2 (Release 9)," December 2009.
[27] 3GPP TS23.401 version 9.3.0, "General Packet Radio Service (GPRS) Enhancements for Evolved Universal Terrestrial Radio Access Network (E-UTRAN) Access (Release 9)," December 2009.
[28] M. Rumney, *LTE and the Evolution to 4G Wireless*: John Wiley & Sons Ltd., 2009.
[29] A. Larmo, M. Lindstrom, M. Meyer, G. Pelletier, J. Torsner, and H. Wiemann, "The LTE Link-Layer Design," *IEEE Communications Magazine,* vol. 47, no. 4, pp. 52-59, 2009.
[30] 3GPP TR25.814 version 7.1.0, "Physical Layer Aspects for Evolved Universal Terrestrial Radio Access (UTRA) (Release 7)," September 2006.
[31] Agilent, "3GPP Long Term Evolution: System Overview, Product Development, and Test Challenges Application Note," 2009.
[32] IXIA, "SC-FDMA Single Carrier FDMA in LTE," November 2009.
[33] 3GPP TR25.892 version 6.0.0, "Feasibility Study for Orthogonal Frequency Division Multiplexing (OFDM) for UTRAN Enhancement (Release 6)," June 2004.
[34] A. Omri, R. Bouallegue, R. Hamila, and M. Hasna, "Channel Estimation for LTE Uplink System by Perceptron Neural Network," *International Journal of Wireless & Mobile Networks (IJWMN),* vol. 2, pp. 155-165, 2010.
[35] 3GPPHelp. (2011, 14/07/2013). *Resource Element in LTE* Available: http://3gpphelp.blogspot.com.au/2011/10/resource-element-in-lte.html
[36] J. Zyren, "White Paper Overview of the 3GPP Long Term Evolution Physical Layer," Freescale, semiconductor July 2007.
[37] G. Piro, L. A. Grieco, G. Boggia, F. Capozzi, and P. Camarda, "Simulating LTE Cellular Systems: An Open-Source Framework," *IEEE Transactions on Vehicular Technology,* vol. 60, no. 2, pp. 498-513, 2011.
[38] 3GPP TS23.203 version 9.3.0, "Policy and Charging Control Architecture (Release 9)," December 2009.

[39] S. Redana and B. Raaf, "LTE-A Relaying Tutorial," in *IEEE Wireless Communications and Networking Conference (WCNC)*, Maxico, 2011, p. 38.
[40] Y. Guangxiang, Z. Xiang, W. Wenbo, and Y. Yang, "Carrier aggregation for LTE-advanced mobile communication systems," *Communications Magazine, IEEE,* vol. 48, pp. 88-93, 2010.
[41] A. Ghosh, R. Ratasuk, B. Mondal, N. Mangalvedhe, and T. Thomas, "LTE-advanced: next-generation wireless broadband technology [Invited Paper]," *IEEE Wireless Communications,* vol. 17, pp. 10-22, 2010.
[42] S. Georgoulis. (2012, 14/07/2013). Testing Carrier Aggregation in LTE-Advanced Network Infrastructure. Available: http://www.techonlineindia.com/techonline/design_centers/170955/testing-carrier-aggregation-lte-advanced-network-infrastructure
[43] J. Whitacre. (14/07/2013). *LTE-Advanced… Already? (OSP Magazine ed.)*. Available: http://www.ospmag.com/issue/article/LTE-Advanced-Already
[44] I. Poole. (14/07/2013). *4G LTE CoMP, Coordinated Multipoint Tutorial*. Available: http://www.radio-electronics.com/info/cellulartelecomms/lte-long-term-evolution/4g-lte-advanced-comp-coordinated-multipoint.php
[45] H. Du, L. Fan, and B. G. Evans, "Optimization of Packet Scheduling Schemes," *Handbook of Mobile Broadcasting: DVB-H, DMB, ISDB-T, and MediaFLO,* pp. 481-506, 2008.
[46] K. Dongmyoung, C. Youngkyu, J. Sunggeun, H. Kwanghun, and C. Sunghyun, "A MAC/PHY Cross-Layer Design for Efficient ARQ Protocols," *IEEE Communications Letters,* vol. 12, no.12, pp. 909-911, 2008.
[47] Z. Nan, Z. Xu, H. Yi, and L. Hai, "Low Complexity Cross-Layer Design with Packet Dependent Scheduling for Heterogeneous Traffic in Multiuser OFDM Systems," *IEEE Transactions on Wireless Communications,* vol. 9, no. 6, pp. 1912-1923, 2010.
[48] N. Mokari, M. R. Javan, and K. Navaie, "Cross-Layer Resource Allocation in OFDMA Systems for Heterogeneous Traffic With Imperfect CSI," *IEEE Transactions on Vehicular Technology,* vol. 59, no. 2, pp. 1011-1017, 2010.
[49] M. Torabzadeh and W. Ajib, "Packet Scheduling and Fairness for Multiuser MIMO Systems," *IEEE Transactions on Vehicular Technology,* vol. 59, no. 3, pp. 1330-1340, 2010.
[50] Y. J. Zhang and S. C. Liew, "Link-Adaptive Largest-Weighted-Throughput Packet Scheduling for Real-Time Traffics in Wireless OFDM Networks," in *IEEE Global Telecommunications Conference*, 2005, pp. 2490-2494.
[51] S. Ryu, B. Ryu, H. Seo, and M. Shin, "Urgency and Efficiency based Packet Scheduling Algorithm for OFDMA Wireless System," in *IEEE International Conference on Communications*, pp. 2779 - 2785, 2005.
[52] A. Gyasi-Agyei and S.-L. Kim, "Comparison of Opportunistic Scheduling Policies in Time-Slotted AMC Wireless Networks," in *1st International Symposium on Wireless Pervasive Computing*, 2006.
[53] T.-Y. Tsai, Y.-L. Chung, and Z. Tsai, "Introduction to Packet Scheduling Algorithms for Communication Networks," *Communications and Networking,* pp. 263-288, 2011.
[54] D. L. Ruyet and B. Ozbek, "Resource Management Techniques for OFDMA," *Orthogonal Frequency Division Multiple Access Fundamentals and Applications,* pp. 101-129, 2010.

[55] H. A. M. Ramli, "Performance Analysis of Packet Scheduling in Long Term Evolution (LTE)," Doctor of Philosophy, Faculty of Engineering and Information Technology, University of Technology, Sydney, New South Wales, Australia, 2011.

[56] A. Basir. (2012, 14/07/2013). *Transport Block Size and Code rate* Available: http://4g-lte-world.blogspot.com.au/2012/12/transport-block-size-code-rate-protocol.html

[57] Y.-G. Jan, Y.-H. Lee, M.-H. Chuang, H.-W. Tseng, W.-C. Tseng, P.-J. Lin, T.-C. Wang, S.-T. Sheu, and W.-E. Chen, "IEEE 802.16 Presentation Submission Template (Rev. 9) Multi-carrier Handover Method," 2008.

[58] R. Y. Kim, J. Inuk, Y. Xiangying, and C. Chao-Chin, "Advanced handover schemes in IMT-advanced systems [WiMAX/LTE Update]," *IEEE Communications Magazine,* vol. 48, pp. 78-85, 2010.

[59] A. Sgora and D. D. Vergados, "Handoff prioritization and decision schemes in wireless cellular networks: a survey," *IEEE Communications Surveys & Tutorials,* vol. 11, pp. 57-77, 2009.

[60] J. Namakoye and R. Van Olst, "Performance evaluation of a voice call handover scheme between LTE and UMTS," in *AFRICON 2011*, pp. 1-5, 2011.

[61] A. K. Salkintzis, M. Hammer, I. Tanaka, and C. Wong. (Feburary, 2009) Voice Call Handover Mechanisms in Next-Generation 3GPP Systems. *IEEE Communications Magazine*.

[62] Y. Ji-Hoon, L. Myoungwon, C. Suhan, and C. Hwajin. (2008, Comparison of Handover Schemes for 3GPP Long Term Evolution and 3GPP2 Ultra Mobile Broadband.

[63] F. Torsten. (2012, 09290959.7). *Handover procedure in a coordinated multipoint (CoMP) transmission network.* Available: https://data.epo.org/publication-server/rest/v1.0/publication-dates/20120418/patents/EP2337400NWB1/document.pdf

[64] Emulab. (2000, 04/08/2013). *Emulab - Network Emulation Testbed Home*. Available: http://www.emulab.net/

[65] V. Jungnickel, L. Thiele, T. Wirth, T. Haustein, S. Schiffermuller, A. Forck, S. Wahls, S. Jaeckel, S. Schubert, H. Gabler, C. Juchems, F. Luhn, R. Zavrtak, H. Droste, G. Kadel, W. Kreher, J. Mueller, W. Stoermer, and G. Wannemacher, "Coordinated Multipoint Trials in the Downlink," in *2009 IEEE GLOBECOM Workshops*, pp. 1-7, 2009.

[66] T. Jansen, I. Balan, J. Turk, I. Moerman, Ku, x, and T. rner, "Handover Parameter Optimization in LTE Self-Organizing Networks," in *2010 IEEE 72nd Vehicular Technology Conference Fall (VTC 2010-Fall)*, pp. 1-5, 2010.

[67] K. Tan, D. Wu, A. Chan, and P. Mohapatra, "Comparing Simulation Tools and Experimental Testbeds for Wireless Mesh Networks," in *2010 IEEE International Symposium on a World of Wireless Mobile and Multimedia Networks (WoWMoM)*, pp. 1-9, 2010.

[68] Y.-F. C. Chao. (2010, 04/08/2013). *990526 Theory analysis and evaluation*. Available: http://xms.tmu.edu.tw/xms/read_attach.php?id=1614

[69] L. Bononi, M. Bracuto, G. D'Angelo, and L. Donatiello, "Performance Analysis of a Parallel and Distributed Simulation Framework for Large Scale Wireless Systems," 2004.

[70] C. Melfuhrer, M. Wrulich, J. C. Ikuno, D. Bosanska, and M. Rupp, "Simulating the Long Term Evolution Physical Layer," in *17th European Signal Processing Conference*, pp. 1471-1478, 2009.

[71] J. J. Sanchez, G. Gomez, D. Morales-Jimenez, and J. T. Entrambasaguas, "Performance Evaluation of OFDMA Wireless Systems using WM-SIM Platform," in *ACM International workshop Mobiwac*, pp. 131-134, 2006.

[72] S. Ascent. (04/08/2013). *4G Evolution Lab - LTE Toolbox and Blockset [Online]*. Available: http://www.steepestascent.com/content/default.asp?page=s2_10

[73] Aricent. (04/08/2013). *LTE eNodeB Software Framework [Online]*. Available: http://www.aricent.com/software/lte-enodeb-software-framework.html

[74] J. C. Ikuno, M. Wrulich, and M. Rupp, "System Level Simulation of LTE Networks," in *IEEE 71st Vehicular Technology Conference*, pp. 1-5, 2010.

[75] G. Piro, L. A. Grieco, G. Boggia, F. Capozzi, and P. Camarda, "Simulating LTE Cellular Systems: An Open-Source Framework," *IEEE Transactions on Vehicular Technology,* vol. 60, pp. 498-513, 2011.

[76] J. C. Ikuno, M. Wrulich, and M. Rupp, "System Level Simulation of LTE Networks," in *IEEE 71st Vehicular Technology Conference (VTC 2010-Spring)*, pp. 1-5, 2010.

[77] H. A. M. Ramli, K. Sandrasegaran, R. Basukala, and W. Leijia, "Modeling and Simulation of Packet Scheduling in the Downlink Long Term Evolution System," in *15th Asia-Pacific Conference on Communications*, pp. 68-71, 2009.

[78] A. G. Orozco-Lugo, F. A. Cruz Prez, and G. Hernandez Valdez, "Investigating the boundary effect of a multimedia TDMA personal mobile communication network simulation," in *IEEE 54th Vehicular Technology Conference (VTC 2001-Fall)*, pp. 2740-2744 vol.4, 2001.

[79] B. G. Lee and S. Choi, *Broadband Wireless Access and Local Networks: Mobile WiMAX and WiFi*. Norwood, MA: Artech House, Inc., 2008.

[80] H. Holma and A. Toskala, *WCDMA for UMTS: HSPA Evolution and LTE*, Fourth ed.: John Wiley & Sons Ltd., 2007.

[81] A. Medeisis and A. Kajackas, "On the use of the universal Okumura-Hata propagation prediction model in rural areas," in *IEEE 51st Vehicular Technology Conference Proceeding (VTC 2000-Spring) Tokyo*, pp. 1815-1818 vol.3, 2000.

[82] D. T. Paris and F. K. Hurd, *Basic Electromagnetic Theory*. New York: McGraw Hill, 1969.

[83] M. Gudmundson, "Correlation Model for Shadow Fading in Mobile Radio Systems," in *Electronics Letters*, pp. 2145-2146, 1991.

[84] M. Patzold, U. Killat, and F. Laue, "A Deterministic Digital Simulation Model for Suzuki Processes with Application to a Shadowed Rayleigh Land mobile Radio Channel," *IEEE Transactions on Vehicular Technology,* vol. 45, no. 2, pp. 318-331, 1996.

[85] A. K. F. Khattab and K. M. F. Elsayed, "Opportunistic Scheduling of Delay Sensitive Traffic in OFDMA-based Wireless Networks," in *International Symposium on a World of Wireless, Mobile and Multimedia Networks*, pp. 288-297, 2006.

[86] K. Kim, G.-M. Yeo, B.-H. Ryu, and K. Chang, "Interference Analysis and Subchannel Allocation Schemes in Tri-Sectored OFDMA Systems," in *IEEE 66th Vehicular Technology Conference*, pp. 1857-1861, 2007.

[87] 3GPP TR36.213 version 10.1.0, "Physical Layer Procedures (Release 10)," March 2011.

[88] K. I. Pedersen, T. E. Kolding, I. Z. Kovacs, G. Monghal, F. Frederiksen, and P. Mogensen, "Performance Analysis of Simple Channel Feedback Schemes for a Practical OFDMA System," *IEEE Transactions on Vehicular Technology,* vol. 58, no. 9, pp. 5309-5314, 2009.

[89] R. Basukala, H. A. M. Ramli, K. Sandrasegaran, and L. Chen, "Impact of CQI Feedback Rate/Delay on Scheduling Video Streaming Services in LTE Downlink," in *12th IEEE International Conference on Communication Technology*, pp. 1349-1352, 2010.

[90] D. Morales-Jimenez, J. J. Sanchez, G. Gomez, M. C. Aguayo-Torres, and J. T. Entrambasaguas, "Imperfect Adaptation in Next Generation OFDMA Cellular Systems," *Journal of Internet Engineering,* vol. 3, no. 1, pp. 202-209, 2009.

[91] K. Kim, G.-M. Yeo, B.-H. Ryu, and K. Chang, "Interference Analysis and Subchannel Allocation Schemes in Tri-Sectored OFDMA Systems," in *IEEE 66th Vehicular Technology Conference*, 2007.

[92] 3GPP TS36.300 version 8.2.0, "3rd Generation Partnership Project; Technical Specification Group Radio Access Network; Evolved Universal Terrestrial Radio Access (E-UTRA) and Evolved Universal Terrestrial Radio Access Network (E-UTRAN); Overall description; Stage 2 (Release 8)," September 2007.

[93] 3GPP TR36.331 version 8.5.0, "Evolved Universal Terrestrial Radio Access (E-UTRA); Radio Resource Control (RRC); Protocol specification (3GPP TS 36.331 version 8.5.0 Release 8) " March 2009.

[94] H. Shirani-Mehr, H. Papadopoulos, S. Ramprashad, and G. Caire, "Joint Scheduling and ARQ for MU-MIMO Downlink in the Presence of Inter-Cell Interference," *IEEE Transactions on Communications,* vol. PP, no. 99, pp. 1-12, 2010.

[95] X. Liu, Z. Huiling, and W. Jiangzhou, "Packet Retransmission using Frequency Diversity in OFDMA," in *IEEE 21st International Symposium on Personal Indoor Mobile Radio Communications*, 2010, pp. 1190-1194.

[96] C. Yao-Liang and T. Zsehong, "Performance Analysis of Two Multichannel Fast Retransmission Schemes for Delay-Sensitive Flows " *IEEE Transactions on Vehicular Technology*, vol. 59, no. 7, pp. 3468-3479, 2010.

[97] B. S. Tsybakov, "File Transmission over Wireless Fast Fading Downlink," *IEEE Transactions on Information Theory,* vol. 48, no. 8, pp. 2323-2337, 2002.

[98] A. Jalali, R. Padovani, and R. Pankaj, "Data Throughput of CDMA-HDR a High Efficiency-High Data Rate Personal Communication Wireless System," in *IEEE 51st Vehicular Technology Conference Proceedings*, pp. 1854-1858, 2000.

[99] 3GPP TS36.212 version 10.2.0, "Multiplexing and Channel Coding (Release 10)," June 2011.

[100] D. Chase, "Code Combining - A Maximum-Likelihood Decoding Approach for Combining an Arbitrary Number of Noisy Packets," *IEEE Transactions on Communications,* vol. 33, no. 5, pp. 385-393, 1985.

[101] M. B. Pursley and S. D. Sandberg, "Incremental-Redundancy Transmission for Meteor-Burst Communications," *IEEE Transactions on Wireless Communications,* vol. 39, pp. 689-702, 1991.

[102] S. Sesia, I. Toufik, and M. Baker, *LTE – The UMTS Long Term Evolution From Theory to Practice*: John Wiley & Sons Ltd, 2009.
[103] M. Stambaugh, "HARQ Process Boosts LTE Communications," AgilentSeptember 2008.
[104] L.-N. Pouchet, "Writing Algorithms," Dept. of Computer Science and Engineering, the Ohio State UniversitySeptember 2010.
[105] Y. Chen and L. G. Cuthbert, "Joint Performance of Cell Selection/Reselection and Soft Handover in the Downlink Direction of 3G WCDMA Systems," 2003.
[106] 3GPP TR25.936 version 4.0.1, "3rd Generation Partnership Project; Technical Specification Group (TSG) RAN 3; Handovers for real-time services from PS domain; (Release 4)," December 2001.
[107] 3GPP TR25.931 version 9.0.0, "3rd Generation Partnership Project; Technical Specification Group Radio Access Network; UTRAN functions, examples on signalling procedures (Release 9)," December 2009.
[108] 3GPP TR21.905 version 8.4.0, "3rd Generation Partnership Project; Technical Specification Group Services and System Aspects; Vocabulary for 3GPP Specifications (Release 8)," March 2008.
[109] Y.-B. Lin, A.-C. Pang, and H. C.-H. Rao, "Impact of Mobility on Mobile Telecommunications Networks," May 2010.
[110] Z. Ghadialy. (2012, 25/07/2013). *Handover principle and concepts*. Available: http://brucekim.egloos.com/3376166
[111] L. Bajzik, P. Horváth, L. Krössy, and C. Vulkán. (July 2007, Impact of Intra-LTE Handover with Forwarding on the User Connections.
[112] E. Dahlman, S. Parkvall, J. Sköld, and P. Beming, *3G Evolution: HSPA and LTE for Mobile Broadband*, 2007.
[113] 3GPP TS23.401 version 8.7.0, "Technical Specification Group Services and System Aspects; General Packet Radio Service (GPRS) enhancements for Evolved Universal Terrestrial Radio Access Network (E-UTRAN) access (Release 8)," September 2009.
[114] 3GPP TS36.300 version 8.5.0, "Technical Specification Group Radio Access Network; Evolved Universal Terrestrial Radio Access (E-UTRA) and Evolved Universal Terrestrial Radio Access Network (E-UTRAN); Overall description; Stage 2 (Release 8)," May 2008.
[115] A. Racz, A. Temesvary, and N. Reider, "Handover Performance in 3GPP Long Term Evolution (LTE) Systems," in *16th IST Mobile and Wireless Communications Summit*, pp. 1-5, 2007.
[116] L. Bajzik, P. Horvath, L. Korossy, and C. Vulkan, "Impact of Intra-LTE Handover with Forwarding on the User Connections," in *16th IST Mobile and Wireless Communications Summit*, pp. 1-5, 2007.
[117] K. Dimou, W. Min, Y. Yu, M. Kazmi, A. Larmo, J. Pettersson, W. Muller, and Y. Timner, "Handover within 3GPP LTE: Design Principles and Performance," in *IEEE 70th Vehicular Technology Conference (VTC 2009-Fall)*, pp. 1-5, 2009.
[118] D. Aziz and R. Sigle, "Improvement of LTE Handover Performance through Interference Coordination," in *IEEE 69th Vehicular Technology Conference Spring (VTC Spring 2009)*, pp. 1-5, 2009.
[119] M. Anas, F. D. Calabrese, P. E. Mogensen, C. Rosa, and K. I. Pedersen, "Performance Evaluation of Received Signal Strength Based Hard Handover for

UTRAN LTE," in *IEEE 65th Vehicular Technology Conference (VTC2007-Spring)*, pp. 1046-1050, 2007.
[120] N. Zheng and J. Wigard, "On the Performance of Integrator Handover Algorithm in LTE Networks," in *IEEE 68th Vehicular Technology Conference (VTC 2008-Fall)*, pp. 1-5, 2008.
[121] H. Lee, H. Son, and S. Lee, "Semisoft Handover Gain Analysis Over OFDM-Based Broadband Systems," *IEEE Transactions on Vehicular Technology,* vol. 58, pp. 1443-1453, 2009.
[122] 3GPP TSGR1#3(99)187, "Improvements to Site Selection Diversity Transmission (SSDT)," March 1999.
[123] Q. Wang, G. Ren, and J. Tu, "A soft handover algorithm for TD-LTE system in high-speed railway scenario," in *IEEE International Conference on Signal Processing, Communications and Computing (ICSPCC)*, pp. 1-4, 2011.
[124] C.-C. Lin, K. Sandrasegaran, H. A. M. Ramli, and R. Basukala, "Optimized Performance Evaluation of LTE Hard Handover Algorithm with Average RSRP Constraint," *International Journal of Wireless & Mobile Networks (IJWMN),* April 2011.
[125] J. C. Ikuno, M. Wrulich, and M. Rupp, "PERFORMANCE AND MODELING OF LTE H-ARQ," presented at the International ITG Workshop on Smart Antennas (WSA) Fraunhofer Heinrich-Hertz-Institut, Berlin, Germany, 2009.
[126] C.-C. Lin, K. Sandrasegaran, H. A. M. Ramli, R. Basukala, R. Patachaianand, L. Chen, and T. S. Afrin, "Optimization of handover algorithms in 3GPP long term evolution system," in *4th International Conference on Modeling, Simulation and Applied Optimization (ICMSAO)*, pp. 1-5, 2011.
[127] T. Jansen, I. Balan, S. Stefanski, I. Moerman, and T. Kurner, "Weighted Performance Based Handover Parameter Optimization in LTE," in *IEEE 73rd Vehicular Technology Conference (VTC Spring 2011)*, pp. 1-5, 2011.
[128] 3GPP TR36.912 version 10.0.0, "3rd Generation Partnership Project; Technical Specification Group Radio Access Network; Feasibility study for Further Advancements for E-UTRA (LTE-Advanced) (Release 10)," March 2011.
[129] 3GPP TR36.913 version 10.0.0, "3rd Generation Partnership Project; Technical Specification Group Radio Access Network; Requirements for further advancements for Evolved Universal Terrestrial Radio Access (E-UTRA) (LTE-Advanced) (Release 10)," March 2011.
[130] E. Seidel, "3GPP LTE-A Standardisation in Release 12 and Beyond," 2013.
[131] Z. Ghadialy, "Small cell standardization in 3GPP Release 12," Dongjoo Park, 18 October 2012.
[132] R. Shrivastava and M. C. Aguayo-Torres, "Analysis and evaluation of Cooperative Multi-Point transmission/reception and soft handover for LTE-Advanced," in *World Congress on Information and Communication Technologies (WICT)*, pp. 826-830, 2012.
[133] X. Xu, X. Chen, and J. Li. (2010, 2010-03-21) Handover Mechanism in Coordinated Multi-Point Transmission/Reception System. *ZTE Communications*. 5.
[134] P. Marsch and G. P. Fettweis, *Coordinated Multi-Point in Mobile Communications: From Theory to Practice*: Cambridge University Press, 2011.
[135] L. Daewon, S. Hanbyul, B. Clerckx, E. Hardouin, D. Mazzarese, S. Nagata, and K. Sayana, "Coordinated multipoint transmission and reception in LTE-

advanced: deployment scenarios and operational challenges," *IEEE Communications Magazine,* vol. 50, pp. 148-155, 2012.
[136] T.-T. Tran, Y. Shin, and O.-S. Shin, "Overview of enabling technologies for 3GPP LTE-advanced," *EURASIP Journal on Wireless Communications and Networking,* vol. 2012, 12-01 2012.
[137] C. Cox. (2012). *An introduction to LTE*.
[138] C. Junren, L. Yajuan, F. Shulan, W. Haiguang, S. Chengzhen, and P. Zhang, "A Fractional Soft Handover Scheme for 3GPP LTE-Advanced System," in *IEEE International Conference on Communications Workshops (ICC Workshops 2009)*, pp. 1-5, 2009.
[139] W. Luo, R. Zhang, and X. Fang, "A CoMP soft handover scheme for LTE systems in high speed railway," *EURASIP Journal on Wireless Communications and Networking,* 13 June 2012.
[140] W. C. Jakes, *Microwave Mobile Communications*: John Wiley & Sons, Inc., 1994.
[141] 3GPP TR36.331 version 10.5.0, "Evolved Universal Terrestrial Radio Access (E-UTRA); Radio Resource Control (RRC); Protocol specification (Release 10) " March 2012.
[142] 3GPP TS36.133 version 10.5.0, "3rd Generation Partnership Project; Technical Specification Group Radio Access Network; Evolved Universal Terrestrial Radio Access (E-UTRA); Requirements for support of radio resource management (Release 10) " January 2012.
[143] D. Martin-Sacristan, J. F. Monserrat, J. Gozalvez, and N. Cardona, "Effect of Channel-Quality Indicator Delay on HSDPA Performance," in *IEEE 65th Vehicular Technology Conference (VTC2007-Spring)*, pp. 804-808, 2007.
[144] C.-H. Yu, A. Hellsten, and O. Tirkkonen, "Rate Adaptation of AMC/HARQ Systems with CQI Errors," in *IEEE 71st Vehicular Technology Conference (VTC 2010-Spring)*, pp. 1-5, 2010.
[145] P. Legg, H. Gao, and J. Johansson, "A Simulation Study of LTE Intra-Frequency Handover Performance," in *2010 IEEE 72nd Vehicular Technology Conference Fall (VTC 2010-Fall)*, pp. 1-5, 2010.
[146] K. Kitagawa, T. Komine, T. Yamamoto, and S. Konishi, "A handover optimization algorithm with mobility robustness for LTE systems," in *2011 IEEE 22nd International Symposium on Personal Indoor and Mobile Radio Communications (PIMRC)*, pp. 1647-1651, 2011.
[147] 3GPP TR36.902 version 9.3.1, "3rd Generation Partnership Project; Technical Specification Group Radio Access Network; Evolved Universal Terrestrial Radio Access Network (E-UTRAN); Self-configuring and self-optimizing network (SON) use cases and solutions (Release 9)," March 2011.
[148] W. Zheng, H. Zhang, X. Chu, and X. Wen, "Mobility robustness optimization in self-organizing LTE femtocell networks," *EURASIP Journal on Wireless Communications and Networking,* 12 February 2013.
[149] N. Sinclair, D. Harle, I. A. Glover, J. Irvine, and R. C. Atkinson, "An Advanced SOM Algorithm Applied to Handover Management Within LTE," *IEEE Transactions on Vehicular Technology, ,* vol. 62, pp. 1883-1894, 2013.
[150] 4GAmericas, "Self Optimizing Networks : Benefits of SON in LTE," July 2011.
[151] MATLAB. (2012, 14/07/2013). *rand - Uniformly distributed pseudorandom numbers*. Available: http://www.mathworks.com.au/help/matlab/ref/rand.html

APPENDIX

This appendix gives validations of the system level simulator used in this research work and the validated simulation results are discussed. Validation of simulation results is to ensure the results obtained via simulation are correct and reliable. Two validations were used to validate the simulation results that are in-line with other works in the literature.

Validation 1:

A simple validation of the behaviour of the uniform distribution of the users' positions in one simulation is given in Figure A.1 which shows the X, Y coordinates of users in one simulation. The validation was set to compare the probability density function (PDF) and cumulative distribution function (CDF) of the X, Y coordinates of all users in the simulation and the uniformly distributed random numbers from MATLAB [151].

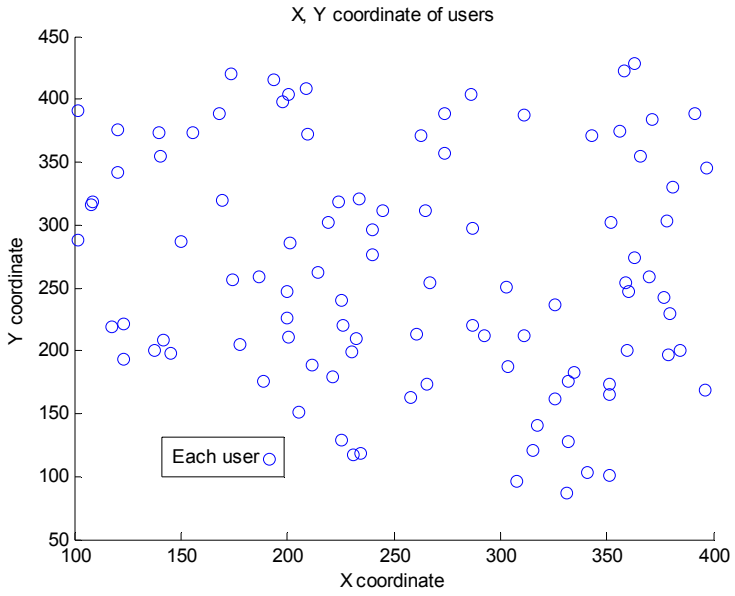

Figure A.1: X, Y coordinates of all users in one simulation

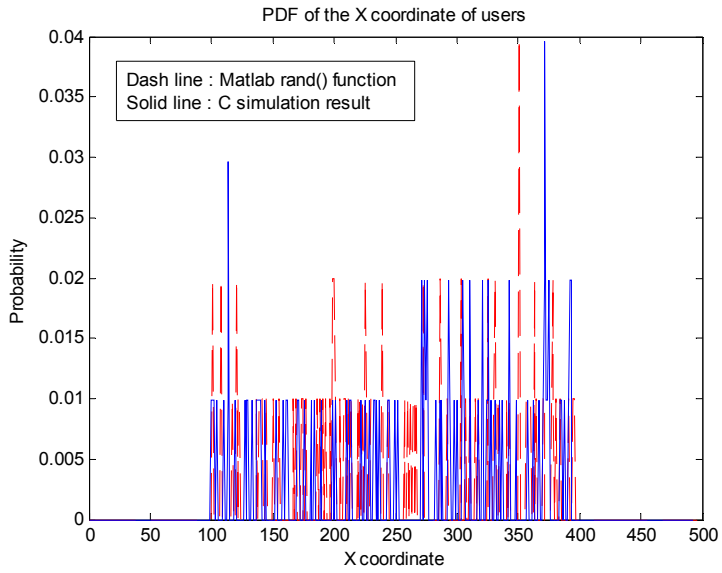

Figure A.2: PDF of the X coordinate of all users in one simulation

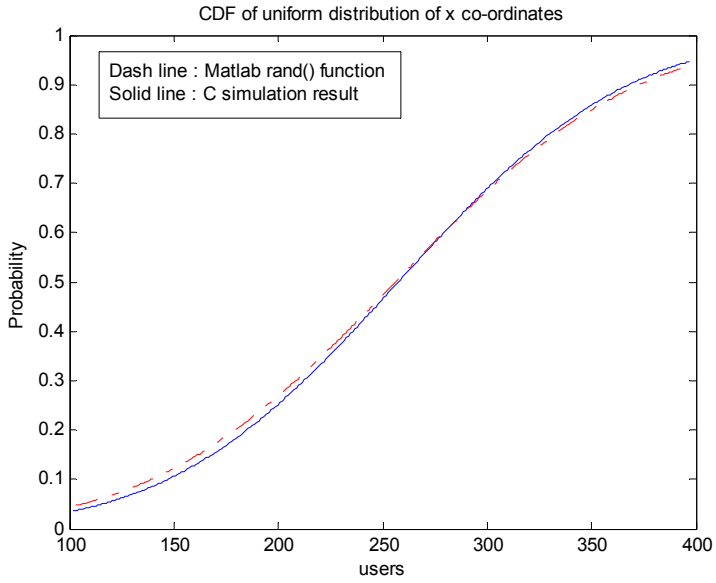

Figure A.3: CDF of the X coordinate of all users in one simulation

Figure A.2 and Figure A.3 show the PDF and CDF of the X coordinate of all users in one simulation, respectively. The comparison shows the similarity of the simulation result and the random function result in MATLAB. The closer the dash and solid lines in Figure A.2 and Figure A.3, the higher the similarity these two scenarios are.

The probability of the X coordinate of all users is distributed between 100 and 400 in Figure A.2 for both dash and solid lines. This can validate that X coordinates of all users are distributed in the manner as expected as shown in Figure A.1. In Figure A.3, the solid line is mostly overlapping the dash line which means the initial position and the distribution of the x coordinates of all users in the simulation follows the random distribution function in MATLAB. Figure A.4 and Figure A.5 show the PDF and CDF of the Y coordinate of all users in one simulation, respectively.

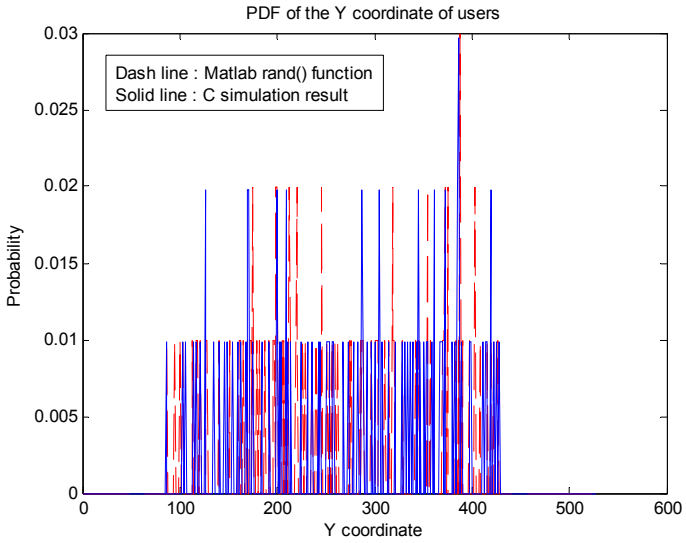

Figure A.4: PDF of the Y coordinate of all users in one simulation

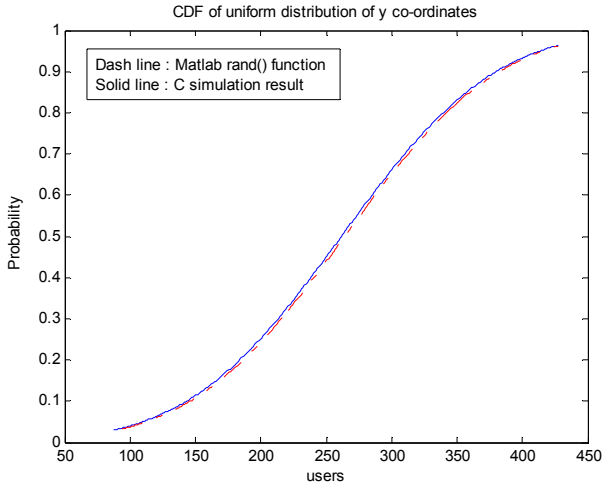

Figure A.5: CDF of the Y coordinate of all users in one simulation

The probability of the Y coordinate of all users is distributed between 50 and 450 in Figure A.4 for both dash and solid lines. This can validate that Y coordinates of all users are distributed in the manner as expected as shown in Figure A.1. In Figure A.5, the solid line is mostly overlapping the dash line which means the initial position and the distribution of the Y coordinates of all users in the simulation follows the random distribution function in MATLAB.

Validation 2:

In this validation, the simulation results were compared with the result in the literature [77]. The simulation results provided by the simulator in this thesis should be the same or similar to the results provided in the literature [77] when similar input was considered for each simulation run. A simulation time of 1000 milliseconds was used for validation. System parameters used in the simulation are given in Table A.1. Note that the cellular layout in the simulator in this validation was changed to single cell in order to be consistent with the simulator used in the literature [77].

Table A.1: The Common Simulation Parameters for Validation

Parameters	**Values**
Cellular layout	Hexagonal grid, wrap around (reflect) Cell = 1
Cell radius	100 m
Path Loss	Hata model
Shadow fading	Gaussian model
Multi path	Rayleigh model
Carrier Frequency	2 GHz
Bandwidth	5 MHz
Number of sub-carriers	300
Resource Block	25
Number of sub-carriers per RB	12
Sub-Carrier Spacing	15 kHz
Scheduling Time (TTI)	1 ms
Packet Scheduling Algorithm	Round Robin
Number of PFDM Symbols per Slot	7
User	50
User's direction	Uniform distributed, [0,2π]
User's Speed	[0, 30, 65, 100]
Simulation time	1000 ms
RSRP sampling timer interval	50 ms
Handover Margin, RSRP unit	5 dB
Handover Time to Trigger (TTT)	5 ms
Data Traffic	1 Mbps Constant Rate

Figure A.6 and Figure A.7 show the average user throughput and average system delay in multi-cells simulator and single cell simulator, respectively.

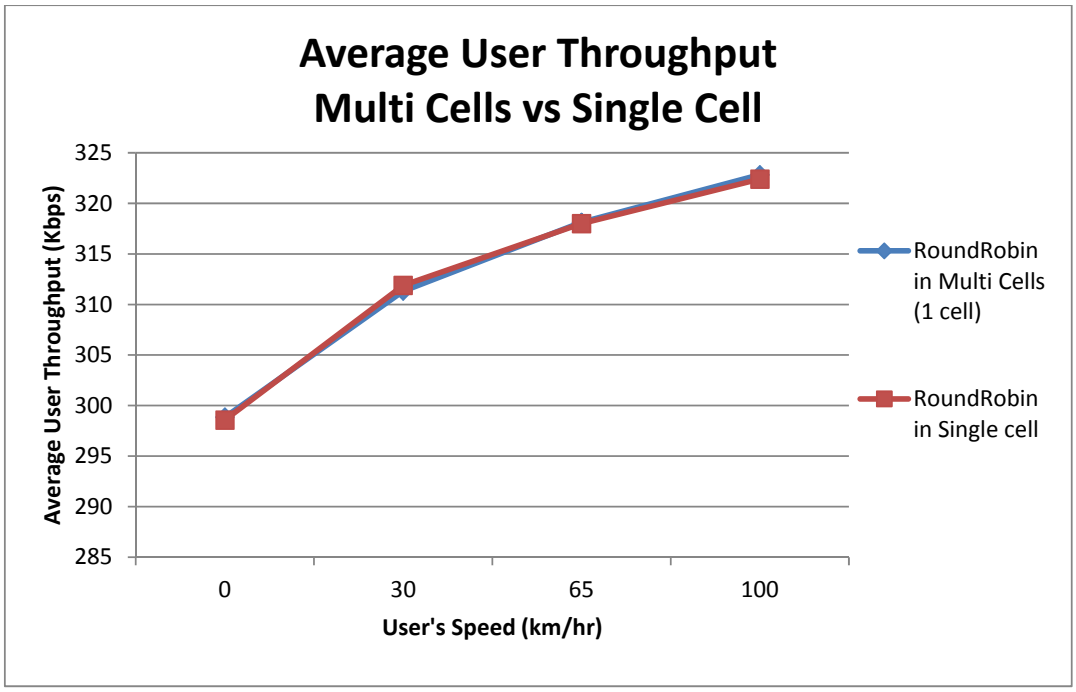

Figure A.6: Average User Throughput Multi-Cells (1 cell) vs Single Cell

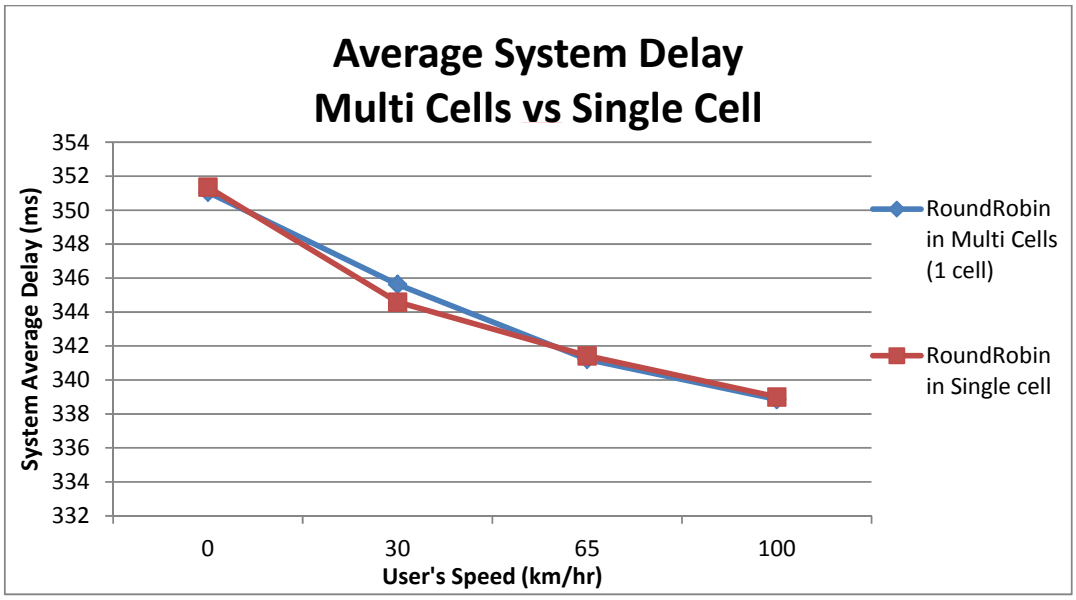

Figure A.7: Average System Delay Multi-Cells (1 cell) vs Single Cell

It can be observed in the figures that the simulator used in this thesis provided valid results as the simulation results are the same or similar to the results provided from the simulator in the literature [77] for both Figure A.6 and Figure A.7.